THÈSE

PRÉSENTÉE A

L'UNIVERSITÉ BORDEAUX 1

ÉCOLE DOCTORALE DES SCIENCES CHIMIQUES

Par Thomas, LEBARBÉ

POUR OBTENIR LE GRADE DE

DOCTEUR

SPÉCIALITÉ : POLYMÈRES

Synthèse de nouveaux polyesters "verts" issus de ressources oléagineuses. Application au renfort au choc du poly(L-lactide).

Synthesis of novel "green" polyesters from plant oils. Application to the rubber-toughening of poly(L-lactide).

Directeur de recherche : Pr Henri CRAMAIL

Soutenue le : 06 décembre 2013

Devant la commission d'examen formée de :

M. C. THOMAS	Professeur, Université Paris	*Rapporteur*
Mme. C. JEROME	Professeur, Université Liège	*Rapporteur*
M. L. AVEROUS	Professeur, Université Strasbourg	*Examinateur*
M. C. NAVARRO	Docteur, ARKEMA	*Examinateur*
M. S. CARLOTTI	Professeur, Université Bordeaux	*Examinateur*
M. H. CRAMAIL	Professeur, Université Bordeaux	*Directeur de thèse*
M. E. GRAU	Docteur, Université Bordeaux	*Invité*
Mme. C. ALFOS	Directrice Innovation, ITERG	*Invitée*
Mme. A. GUEUDET	Service Bioressources, ADEME	*Invitée*

SCIENTIFIC PRODUCTION

Peer review articles :

T.Lebarbé, M.Neqal, E.Grau, C.Alfos, H.Cramail, *Branched polyethylene mimicry by metathesis copolymerization of fatty acid-based α,ω-dienes*, **2013**, Green Chemistry, accepted

T.Lebarbé, A.S.More, P.S.Sane, E.Grau, C.Alfos, H.Cramail, *Bio-based aliphatic polyurethanes through ADMET polymerization in bulk and green solvent*, **2013**, Macromolecular Rapid Communications, accepted

H.Cramail, T.Lebarbé, L.Maisonneuve, E.Grau, *Structure-properties relationship of fatty acid-based thermoplastics as synthetic polymer mimics*, **2013**, Polymer Chemistry, 4, 5472-5517

T.Lebarbé, E.Ibarboure, B.Gadenne, C.Alfos, H.Cramail, *Fully bio-based poly(L-lactide)-b-poly(ricinoleic acid)-b-poly(L-lactide) triblock copolyesters: investigation of solid-state morphology and thermo-mechanical properties*, **2013**, Polymer Chemistry, 4, 3357-3369

T.Lebarbé, L.Maisonneuve, N.N.Nguyen, B.Gadenne, C.Alfos, H.Cramail, *Methyl 10-undecenoate as a raw material for the synthesis of renewable semi-crystalline polyesters and poly(ester-amide)s*, **2013**, Polymer Chemistry, 3, 2842-2851

L.Maisonneuve, T.Lebarbé, N.N.Nguyen, E.Cloutet, B.Gadenne, C.Alfos, H.Cramail, *Hydroxyl telechelic building blocks from fatty acid methyl esters for the synthesis of poly(ester/amide urethane)s with versatile properties*, **2013**, Polymer Chemistry, 3, 2583-2595

A.S.More, T.Lebarbé, L.Maisonneuve, B.Gadenne, C.Alfos, H.Cramail, *Novel fatty acid-based di-isocyanates towards the synthesis of thermoplastic polyurethanes*, **2013**, European Polymer Journal, 49, 823-833

A.S.More, L.Maisonneuve, T.Lebarbé, B.Gadenne, C.Alfos, H.Cramail, *Vegetable-based building blocks for the synthesis of thermoplastic renewable polyurethanes and polyesters*, **2012**, European Journal of Lipid Science and Technology, 115, 61-75

Patents:

H.Cramail, T.Lebarbé, L.Maisonneuve, E.Cloutet, C.Alfos, B.Gadenne, *New process of preparation of polyols and polyamines, and products as obtained*, **2013**, WO 2013072436 A1 20130523

H.Cramail, T.Lebarbé, C.Alfos, B.Gadenne, *Utilisation de polymères comme additifs dans une matrice de poly(acide lactique)*, **2013**, FR 13 53138

H.Cramail, T.Lebarbé, C.Alfos, B.Gadenne, *Nouveaux pré-polymères biosourcés et leurs utilisations pour la préparation de polymères utiles comme additifs dans une matrice poly(acide lactique)*, **2012**, FR 12 58907

REMERCIEMENTS

C’est avec beaucoup de plaisir que je profite de ces quelques lignes pour remercier toutes les personnes qui ont, d’une manière ou d’une autre, contribué à la bonne réalisation de ma thèse.

Je tiens à exprimer ma profonde reconnaissance à Henri Cramail, Professeur à l’université de Bordeaux, qui a dirigé cette étude, pour ses qualités humaines et sa confiance réconfortante. Je me permets également de souligner sa patience et sa forte disponibilité malgré son emploi du temps très chargé. Ses qualités scientifiques, ainsi que ses conseils avisés m’ont permis de réaliser ce projet dans des conditions tout à fait idéales.

Je tiens à remercier tout particulièrement Dr Etienne Grau, mon encadrant de proximité. Son arrivée au laboratoire lors de ma dernière année de thèse m’a été très bénéfique car elle m’a permis d’apprendre énormément d’un point de vue scientifique. L’intérêt qu’il a manifesté à l’égard de cette étude ainsi que ses conseils avisés ont été un réel soutien.

Je suis très reconnaissant au Pr. Christine Jérôme et au Pr. Christophe Thomas d’avoir accepté d’être les rapporteurs de cette thèse, ainsi qu’au Pr. Luc Avérous, au Pr. Stéphane Carlotti et au Dr Christophe Navarro d’avoir accepté d’examiner ce travail.

Cette étude a été réalisée dans le cadre d’un projet co-financé par l’Agence De l’Environnement et de la Maîtrise de l’Energie (ADEME) et par l’ITERG (Centre technique industriel des huiles et des corps gras). La collaboration autour de ce projet a été un réel plaisir et je tiens à remercier Mr Guillaume Chantre, Mme Carine Alfos, Mr Hilaire Bewa et Mme Alice Gueudet qui m’ont donné l’opportunité de travailler dans le cadre de ce projet de thèse.

Je remercie ici aussi les Drs Benoit Gadenne, Guillaume Chollet et Didier Pintori pour leur intérêt et leur encadrement dans ce projet. Je tiens également à remercier Mr Jérôme Vila, Mr François Foulonneau et Mr Matthieu Barrière pour leur aide lors d’expériences et d’analyses réalisées à l’ITERG.

Je tiens également à remercier le Pr Michel Dumon et Mr Mathieu Pedros de l’IUT SGM de Bordeaux pour leur implication dans la réalisation des essais de chocs IZOD ainsi qu’à Mr Ahmed Bentaleb et Mme Marie-France Achard du laboratoire CRPP pour la réalisation des analyses de diffraction des rayons X et enfin Mr Patrick Garrigues de l’ISM pour l’imagerie MEB.

J’ai également une pensée toute particulière pour les stagiaires Licences, Masters ou Ingénieurs qui ont participé à cette étude et en particulier pour Nga, Clément et Mehdi, pour leur enthousiasme et leur bonne humeur.

Je tiens également à exprimer ma sympathie et mes remerciements à l’ensemble du personnel permanent du LCPO et tout particulièrement à Nico, Anne-Laure, Eric, Frédéric, Catherine, Corinne, Mimi, Bernadette, Loic sans oublier LA DREAM TEAM (Manu, Cédric et Gégé l’amateur d’andouille de Guémené).

Un grand merci également à tous les doctorants, ex-doctorants, post-doc et stagiaires rencontrés et appréciés au LCPO (Chris, Vincent, Katerina, Antoinette, Maréva, Célia, Jules, Paul, Bertrand, Estelle, Blandine, Maud, Olivia, Kévin, Karine, Elise, Chrystilla, Samira, Colin, Romain, Kévin, Julie, Silvia, Charlotte, Camille, Geoffrey, Océane, Thibault, Maité, Floraine, Jun, Na, Feifei, Mathilde, Coraline, Mickaël, Giordano, Romain, Loïc, Edgar, Laurie, Jérémie et bien d’autres encore…). Un clin d’œil tout particulier à Audrey, Lise et Prakash, mes colocs de labo avec qui ces 3 années de thèse furent merveilleuses. Un grand merci également à Arvind (et Deepa pour les bons petits plats indiens), mon mentor scientifique et philosophe qui s’est montré toujours disponible et enthousiaste vis-à-vis de mon étude.

Enfin j’aimerais adresser mes remerciements à plusieurs enseignants croisés au cours de mon cursus ingénieur pour m’avoir inspiré et donner le goût des polymères : Pr Stéphane Carlotti et Pr Henri Cramail (même si je les ai déjà remercié), Pr Alain Soum, Pr Daniel Taton, Pr Eric Papon, Pr Sébastien Lecommandoux, Dr Eric Cloutet, Dr Christophe Schatz, Dr Valérie Héroguez, Dr Jean-François Le Meins et bien d’autres encore…

Je remercie aussi toute ma famille et mes amis et particulièrement mes parents pour leur soutien.

Enfin je souhaite remercier spécialement ma petite femme Sonia, qui m’a soutenu jusqu’au bout avec énormément de patience.

« Un chercheur doit avoir conscience du peu de ce qu'il a trouvé ; mais il a le droit d'estimer que ce peu est immense ». Jean Rostand

« La connaissance s'acquiert par l'expérience, tout le reste n'est que de l'information ».
Albert Einstein

TABLE OF CONTENTS

Table of contents

RÉSUMÉ

L'essor de la pétrochimie dans les années 1950 a permis le développement d'une très grande variété de molécules d'intérêt pour la chimie de commodité, la chimie fine et la chimie des matériaux. Parmi ces molécules, de nombreux monomères ont vu le jour permettant l'émergence des polymères synthétiques. L'exploitation massive des ressources fossiles (pétrole et gaz naturel) a fortement contribué à la baisse du prix de ces matériaux qui sont désormais omniprésents dans notre vie quotidienne. Les plastiques, avec une production globale annuelle d'environ 300 millions de tonnes, contribuent à hauteur de 7% de la consommation pétrolière annuelle mondiale.

Cependant, face à l'épuisement avéré des réserves de pétrole et de l'augmentation des gaz à effet de serre, l'utilisation de ressources renouvelables non fossiles apparaît comme une véritable nécessité. Dans ce but, les ressources renouvelables issues de la biomasse offrent des perspectives prometteuses. En effet, un simple constat concernant le temps de régénération de la source de carbone est sans appel. Le cycle du carbone lors de l'utilisation de la biomasse comme matière première se compte au plus en dizaines d'années alors que dans le cas des ressources fossiles cette valeur est évaluée en millions d'années.

Actuellement, la chimie assiste à une mutation de la pétrochimie vers la chimie bio-sourcée. Le concept de bio-raffinerie est né dans le but de créer une bio-plateforme de molécules permettant le développement de substituts bio-sourcés aux produits actuellement pétro-sourcés. Ceci implique l'application des principes de la chimie verte à toutes les étapes du développement de ces produits (pré-production, production, distribution, usage, fin de vie). Grâce aux nombreuses avancées dans les procédés de transformation de la biomasse, le portefeuille de molécules bio-sourcées se diversifie. Le défi futur pour les chimistes est alors de concevoir de nouveaux produits bio-sourcés utilisant les molécules de cette bio-plateforme.

Les bioplastiques issus des bioraffineries s'installent progressivement dans le paysage économique des produits bio-sourcés avec une production globale en 2011 d'environ 1,1 million de tonnes. Les estimations pour 2016 annoncent une production d'environ 5,8 millions de tonnes. Le poly(acide lactique) ou poly(lactide) (PLA) constitue l'un des plus matures des plastiques bio-sourcés actuellement présents sur le marché avec une production globale d'environ 180 000 tonnes par an (16% de la production globale des plastiques bio-sourcés en 2011). De plus, la production de PLA est estimée à 300 000 tonnes par an pour 2016. Le PLA est un polyester aliphatique compostable produit industriellement à partir de l'acide lactique (plus précisément du lactide), lui-même obtenu par biotransformation de

l'amidon. Les nombreuses avancées technologiques concernant l'efficacité de la biotransformation de l'amidon en acide lactique ainsi que le développement industriel de la synthèse du PLA ont fortement contribué à la baisse du prix de ce polymère. Natureworks (USA), premier producteur mondial de PLA avec une production annuelle de 140 000 tonnes, commercialise le PLA à 1,90€/kg. Bien qu'utilisé initialement dans le domaine biomédical, le PLA est aujourd'hui l'un des candidats les plus sérieux pour substituer partiellement le poly(téréphtalate d'éthylène) (PET) et le polystyrène (PS) dans le domaine de l'emballage, en raison de son faible coût. L'élargissement des applications du PLA aux domaines du transport et des équipements électriques et électroniques constitue une perspective intéressante pour le développement de ce polymère. Cependant, le caractère cassant du PLA (élongation à la rupture d'environ 4% et résilience IZOD de 2,5 $kJ.m^{-2}$) limite actuellement un tel développement.

Le renfort au choc des polymères fragiles par dispersion d'un polymère à faible Tg est une méthode utilisée depuis plusieurs années pour optimiser les propriétés mécaniques des matériaux. Ainsi, le PLA a fait l'objet de nombreuses investigations ces dernières années pour augmenter sa résilience. Cependant, la plupart des additifs actuellement utilisés dans l'industrie sont d'origine pétrochimique. De plus, ces additifs ne sont ni biocompostables ni biodégradables ce qui influe fortement sur le caractère compostable du matériau final. Il apparaît donc comme un enjeu de développer des additifs biodégradables et bio-sourcés.

L'objectif de cette thèse de doctorat concerne le développement d'additifs polymères pour le renfort au choc du PLA en se positionnant en accord avec le concept de bioraffinerie qui vise l'utilisation de matières premières bio-sourcées tout en respectant les principes de la chimie verte. La plateforme oléagineuse a été sélectionnée pour ces travaux de thèse. Cette étude a été financée par l'ADEME et l'ITERG (centre technique industriel des huiles et corps gras), deux acteurs fortement impliqués dans la promotion des bioraffineries en France.

Un état de l'art sur le renfort au choc du PLA a été réalisé afin de cibler les systèmes les plus efficaces. Cette partie bibliographique a fait ressortir deux principaux types de systèmes de renfort.

Dans un premier cas, il s'agit de copolymères à blocs composés de segments PLA et de segments souples à faible Tg. Plusieurs morphologies de copolymères ont été étudiées dans la littérature telles que des morphologies triblocs, multiblocs et greffées. L'étude a notamment permis de différencier les systèmes ou le bloc souple est d'origine pétrochimique et non biodégradable et les systèmes ou le bloc souple est biodégradable (bio-sourcé ou non). Une transition entre un comportement fragile et un comportement ductile est observée dans la

plupart des copolymères à blocs décrits. Cependant, le coût de production de ces systèmes est régulièrement mentionné comme un frein pour leur développement industriel.

Une deuxième approche basée sur le mélange de polymères a été développée dans la partie bibliographique. De façon similaire aux copolymères à blocs, les additifs pétro-sourcés et non biodégradables ont été différenciés des additifs biodégradables. Parmi les additifs non-biodégradables, les polymères oléfiniques (HDPE, LDPE, LLDPE, PE-co-EVA, copolymères éthylène-acrylate), acryliques (PBA) et styrèniques (SBS, SEBS, ABS) ont été les systèmes les plus employés. Cependant, ces additifs ne constituent pas une solution durable au renforcement du PLLA car ils modifient la compostabilité de la matrice. De ce fait, de nouveaux mélanges basés sur l'utilisation de polyesters aliphatiques biodégradables à faible Tg ont été développés. Les principaux additifs décrits dans la littérature sont le PCL (poly(ε-caprolactone)), le PBS (poly(succinate de butylène)), le PBAT (poly(adipate téréphtalate de butylène)) et les PHAs (polyhydroxyalcanoates). La plupart de ces additifs amènent à un renfort au choc significativement accru du PLLA. Cependant, dans la plupart des cas, ces nouvelles performances sont atteintes uniquement par addition d'un troisième composant, appelé promoteur d'adhésion, qui a pour rôle de stabiliser l'interface entre la matrice et la phase dispersée en augmentant significativement l'adhésion à l'interface. Parmi ces additifs biodégradables, aucun exemple ne concerne des polyesters thermoplastiques aliphatiques issus de la plateforme oléagineuse.

Lors de ce projet de thèse, nous avons orienté nos recherches vers la synthèse de nouveaux polyesters issus des acides gras pour le renfort au choc du PLLA. Cette matière première, caractérisée par sa nature aliphatique et son importante fonctionnalité, est en effet parfaitement adaptée à la synthèse de polyesters aliphatiques. Un état de l'art concernant la synthèse de polyesters aliphatiques issus des acides gras a été réalisé afin de juger de la faisabilité de notre démarche de recherche. Cette étude bibliographique a révélé une multitude de polyesters tels que des polymères de type polyéthylène, des élastomères thermoplastiques ou encore des polyesters fonctionnalisés. La grande diversité de structures et de propriétés mécaniques de ces matériaux laisse entrevoir des perspectives prometteuses pour l'application au renfort au choc du PLLA.

La première partie de mon travail de thèse a concerné la synthèse de nouveaux diols issus de l'undécénoate de méthyle pour la formation de polyesters et poly(ester-amide)s. Par une combinaison de réactions de transestérification, amidification et addition thiol-ène, six diols présentant des fonctions ester et/ou amide ont été obtenus avec une pureté suffisante (>92%). La polycondensation de ces diols avec un diester aliphatique linéaire présentant 20 unités

méthylène (synthétisé par métathèse de l'undécénoate de méthyle) a permis d'obtenir des polyesters et poly(ester-amide)s couvrant une large gamme de propriétés thermomécaniques. L'effet notoire de la densité en fonctions amide sur les propriétés finales du matériau a notamment été mis en exergue par une série d'analyses incluant l'analyse enthalpique différentielle (DSC) et les essais mécaniques en traction. Il a été conclu que la présence de fonctions amide joue un rôle prépondérant sur l'augmentation de la température de fusion ainsi que sur le module d'Young du matériau. Le renfort au choc du PLLA implique une faible rigidité de l'additif afin d'observer une absorption optimale de l'énergie d'impact. Afin de diminuer le module élastique du poly(ester-amide) présentant la température de fusion la plus élevée tout en conservant cette dernière caractéristique, le diester en C20 (issu de la métathèse de l'undécénoate de méthyle) a été substitué par un dimère d'acide gras (Pripol® 1009) qui présente des chaînes alkyle pendantes nécessaires pour la diminution de la rigidité du matériau final. Le matériau ainsi formé présente les caractéristiques d'un bon additif pour le renfort au choc du PLLA; à savoir une immiscibilité théorique avec le PLLA, un faible module d'Young, une faible Tg ainsi qu'une bonne stabilité thermique.

Le mélange de ce poly(ester-amide) (PEA) en différentes proportions (5, 10, 15 et 20% en masse) avec du PLLA commercial a ensuite été réalisé par extrusion bi-vis. Les mélanges ont été finement caractérisés dans le but d'évaluer l'influence de l'additif sur les propriétés thermomécaniques et mécaniques. Deux effets principaux ont été observés : dans un premier temps, des études cinétiques de cristallisation de la matrice PLLA ont révélé le caractère d'assistant de nucléation du PEA à la fois lors d'expériences de cristallisation non-isotherme et isotherme ; le deuxième effet notoire du PEA est, comme attendu, une amélioration de la ductilité du matériau formulé comparé au PLLA seul. Ce point a été vérifié à la fois lors d'essais en traction et lors d'essais d'impact IZOD. La transition fragile-ductile a été clairement identifiée à partir des courbes contrainte-déformation avec une valeur maximale d'élongation à la rupture (155%) obtenue pour un mélange contenant 10% en masse d'additif. Les essais d'impact IZOD (éprouvettes entaillées) ont révélé une légère augmentation de la résilience avec une valeur maximale de 3,7 $kJ.m^{-2}$. Cette augmentation modérée par rapport au PLLA seul (2,5 $kJ.m^{-2}$) est en accord avec les valeurs obtenues dans la littérature pour des systèmes similaires tels que des mélanges binaires réalisés avec les PCL, PBS, PBAT ou les PHAs (4-5 $kJ.m^{-2}$). Afin d'augmenter plus significativement la résilience de tels systèmes, un troisième composant agissant en tant que promoteur d'adhésion est généralement additionné au mélange. Cependant, dans ce travail de thèse nous n'avons pas retenu cette solution pour optimiser notre système de renfort. En effet le développement d'un nouveau système plus adapté aux exigences du renfort au choc a été préféré.

Dans une deuxième partie, nous avons centré notre démarche d'investigation sur l'effet de la cristallinité (et donc de la rigidité de l'additif) vis-à-vis de la résilience du matériau formulé par mélange. Pour cela, une gamme de polyesters aliphatiques a été développée par polycondensation du 1,10-decanediol (issu de la plateforme ricin) avec un mélange de deux diacides (acide sébacique et dimère d'acides gras) introduits dans le réacteur en différentes proportions. Ainsi, en faisant varier la proportion des deux diacides, la densité de chaînes pendantes (apportées par le dimère d'acide gras) et donc la cristallinité peut être contrôlée. La gamme de polyesters couvre ainsi des températures de fusion allant de -6°C à 78°C et des enthalpies de fusion allant de 16 $J.g^{-1}$ à 101 $J.g^{-1}$. Il est intéressant de noter que la Tg des matériaux reste relativement constante en fonction de la nature du polyester, permettant d'effectuer la corrélation entre la cristallinité du matériau et la résilience du mélange correspondant. Les mélanges (10 et 20% en masse pour chaque polyester), formulés par extrusion bi-vis ont ensuite été réalisés. Une étude de la morphologie des mélanges a révélé une dispersion relativement fine des particules dans la matrice (diamètre moyen des particules compris entre 0,3 et 1,3µm). De la même façon qu'avec le PEA en tant qu'additif, les polyesters ont une influence sur la cristallisation de la phase PLLA à la fois en cristallisation non-isotherme et isotherme. Ainsi, le temps de demi-cristallisation à 110°C passe de 6,1 minutes pour le PLLA seul à 1,2 minute dans le cas du mélange optimal. Les propriétés mécaniques du PLLA sont sensiblement affectées par l'ajout de polyester. La transition fragile-ductile, accompagnée d'une perte modérée en rigidité, est observable pour tous les mélanges. Concernant les tests d'impact, une augmentation graduelle de la résilience avec une diminution de la cristallinité de l'additif est clairement établie. La dispersion de 10% et 20% en masse du polyester le moins cristallin dans la matrice PLLA permet l'obtention d'un matériau présentant une résilience IZOD (éprouvette entaillée) de 8,6 $kJ.m^{-2}$ et 10,3 $kJ .m^{-2}$ respectivement. Cela représente une augmentation d'un facteur 4,2 par rapport au PLLA seul. De plus ces valeurs de résilience sont comparables à celles généralement obtenues pour des systèmes similaires (additifs de type polyesters amorphes). Il est intéressant de noter que la dispersion de 10% en masse de Biomax® strong 100, un additif éthylène-acrylate commercialisé par Dupont, induit au PLLA une résilience de 12,4 $kJ.m^{-2}$ (IZOD entaillé). Le système de renfort développé dans cette partie amène donc à une résilience proche d'un système commercial. Une étude de la morphologie des éprouvettes fracturées par impact, a montré l'évidence d'un mécanisme typique de renfort au choc. Dans un premier temps, la cavitation (au cœur ou à l'interface) des particules de phase dispersée s'opère donnant lieu ensuite à une déformation plastique de la matrice.

Une fois établi le fait qu'un additif amorphe est plus efficace pour le renfort au choc du PLLA, nous avons ensuite dirigé nos recherches vers l'utilisation du ricinoléate de méthyle en tant que matière première pour le développement d'un nouveau système de renfort au choc du PLLA. Le ricinoléate de méthyle est un ester d'acide gras relativement disponible du fait de son faible coût ainsi que de sa simplicité d'obtention. En effet, une simple étape de transestérification de l'huile de ricin permet d'obtenir ce composé avec un très bon rendement. En outre, le ricinoléate de méthyle possède une grande fonctionnalité (une insaturation, une fonction hydroxyle ainsi qu'une fonction carbonyle) permettant sa directe polycondensation. Le polyester obtenu est complètement amorphe et possède une Tg très basse (de l'ordre de -70°C). Dans cette partie, nous avons donc utilisé le poly(acide ricinoléique) (PRic) pour le renfort au choc du PLA. Cependant, la stratégie visant à la formation de copolymères à blocs a été retenue dans cette partie. Dans ce but, une procédure de synthèse en deux étapes a été adoptée. La polycondensation du ricinoléate de méthyle en présence d'une faible quantité de 1,3-propanediol a dans un premier temps conduit à la formation d'un pré-polymère di-hydroxy téléchélique. Ce pré-polymère a ensuite été utilisé en tant que macroamorceur pour la polymérisation par ouverture de cycle du L-lactide. En faisant varier la proportion en macroamorceur, une large gamme de copolymères a pu être développée (de 35% à 83% en masse de PLLA). L'influence de la composition du copolymère sur la morphologie en masse et sur les propriétés mécaniques a ensuite été étudiée. L'étude morphologique des copolymères à l'état fondu et après recuit a montré une faible ségrégation des deux blocs (PRic et PLLA). En effet, alors qu'à l'état fondu les copolymères à blocs adoptent une morphologie sphérique, cylindrique ou lamellaire typique d'une ségrégation de phase; une fois recuits à 120°C, les copolymères cristallisent sous forme de sphérolites (lamelles cristallines). La force de cristallisation de la phase PLLA l'emporte donc sur la ségrégation des deux blocs. Les essais mécaniques en traction ont révélé une transition fragile-ductile pour tous les copolymères. En fonction de la composition du copolymère, un comportement élastomère ou rigide/ductile a été observé. Cette étude a permis d'entrevoir d'intéressantes perspectives concernant la synthèse de copolymères à blocs bio-sourcés.

Dans la dernière partie de cette thèse, nous nous sommes intéressés à l'utilisation de la polymérisation par métathèse des diènes acycliques (ADMET) pour le développement de nouveaux matériaux potentiels pour le renfort au choc du PLLA. Dans ce but, deux stratégies ont été retenues : la synthèse de copolymères triblocs et le développement d'additifs polyesters de type « LLDPE like ». Dans un premier temps, une plateforme de α,ω-diènes (incluant uréthane, ester, carbonate, éther et amide) a été réalisée en utilisant les dérivés de

l'acide undécénoique comme molécules de base. Ces monomères bis-insaturés ont ensuite été polymérisé par ADMET en masse et en solution dans un solvant « vert ». Cette étude a ainsi permis d'établir les conditions optimales de réaction. De plus, par cette voie, nous avons décrit pour la première fois la synthèse d'un polyuréthane bio-sourcé par ADMET. La formation de copolymères triblocs a ensuite été étudiée selon deux voies. La première approche consiste à utiliser un PLLA terminé par une oléfine terminale en tant qu'agent de transfert. La polymérisation par ADMET des α,ω-diènes ester et carbonate en présence de l'agent de transfert PLLA (présent en différentes proportions) a donc été réalisé en solution. Cependant, les courbes de chromatographie d'exclusion stérique (SEC) obtenues témoignent d'un mauvais contrôle de la structure des polymères formés. Il semble donc que la dynamique de la réaction de métathèse ne permette pas la formation de copolymères à blocs ayant une structure contrôlée.

Une autre stratégie visant à passer par un pré-polymère di-hydroxy téléchélique a été ensuite étudiée. La polymérisation par ADMET des α,ω-diènes uréthane, ester et carbonate a donc été conduite en présence de 5% molaire d'undécénol (agent de transfert). Cependant, malgré l'utilisation d'un inhibiteur d'isomérisation (1,4-benzoquinone), les réactions secondaires d'isomérisation restent trop importantes pour obtenir un bon contrôle des bouts de chaînes. La polymérisation par ouverture de cycle du L-lactide a cependant été réalisée à partir de ces macroamorceurs. Néanmoins, le faible pourcentage de chaînes polymères terminées par des fonctions hydroxyle conduit à une hétérogénéité de compostion (homopolymère, diblocs et triblocs). Cette étude exploratoire concernant la synthèse de copolymères à blocs par ADMET a donc permis d'évaluer les limites de cette technique sur le contrôle macromoléculaire. Les matériaux synthétisés n'ont donc pas été retenus pour une caractérisation complète.

L'état de l'art concernant la synthèse de polyesters issus des acides gras fait ressortir la métathèse comme une méthode adaptée et efficace pour la synthèse de polyesters de type polyéthylène. Cependant, la plupart des exemples de la littérature décrivent le mimétisme du polyéthylène haute densité. Nous nous sommes donc attachés à développer, par ADMET, des polyesters mimant la structure du polyéthylène linéaire basse densité (LLDPE) du fait de l'utilisation extensive de ce dernier pour le renfort au choc du PLLA. Une gamme de copolyesters de type LLDPE a donc été développé par copolymérisation de deux macromonomères α,ω-diène (un linéaire et l'autre ramifié) en différentes proportions. Les copolyesters ont ensuite été hydrogénés afin de s'affranchir de toute dégradation des matériaux par oxydation. Des analyses par DSC ont enfin permis d'établir la relation structure-propriétés des matériaux au vu de la forte influence des chaînes alkyle pendantes sur

le comportement cristallin des polyesters. Malgré la similitude structurale des polyesters synthétisés avec le LLDPE, leurs propriétés thermomécaniques se rapprochent plus de celles du polyéthylène très basse densité (VLDPE). Ces matériaux constituent une alternative prometteuse pour la substitution du LLDPE et du VLDPE dans certaines applications où le caractère hydrolysable du polymère est recherché. Le mélange de ces matériaux avec le PLLA est une perspective encourageante à ce travail de thèse.

Pour conclure, en utilisant des matières premières peu couteuses et accessibles issus de l'oléochimie, la synthèse de polyesters aliphatiques à faible Tg a pu être menée à bien. De plus, dans la mesure du possible, des méthodes de transformation chimique simples et sûres (transestérification, métathèse, addition thiol-ène…) ont été adoptées, afin de garantir une réalité industrielle à ces travaux. Concernant la synthèse des polyesters, la polymérisation en masse a majoritairement été retenue afin d'être en accord avec les principes de la chimie verte qui prônent la limitation de sous-produits et de solvants. La modification des propriétés du PLLA a ensuite été réalisé suivant les méthodes usuelles appliquées en industrie comme l'extrusion ; ceci également afin de garantir des perspectives industrielles aux matériaux développés. En termes de renfort au choc du PLLA, des résultats prometteurs ont été atteints. En effet une augmentation d'un facteur supérieur à 4 a été obtenue concernant la résilience IZOD du mélange optimal. Ce résultat est comparable à certaines valeurs rapportées avec des additifs commerciaux ou des systèmes similaires à celui développé dans notre étude. Ces travaux de thèse ont donc démontré la faisabilité du renfort au choc par des additifs polymères issus de la plateforme oléagineuse. L'optimisation de ces études ainsi que leurs validations à plus grande échelle devrait permettre la mise au point d'additifs compétitifs avec ceux actuellement utilisés industriellement.

LIST OF ABBREVIATIONS

12HD: 12-hydroxydodecanoic acid
12HS: methyl 12-hydroxystearate
ABS: acrylotnitrile-butadiene-styrene copolymer
ADMET: acyclic diene metathesis
AFM: atomic force microscopy
AIBN: azobisisobutyronitrile
BDTBPMB: bis(ditertiarybutylphosphinomethyl)benzene
C20dE: diester obtained by metathesis of methyl 10-undecenoate
CL: ε-caprolactone
CM: cross-metathesis
CO: carbon monoxide
COD: 1,5-cyclooctadiene
$\bar{d}$: mean size diameter
Đ: dispersity
DBTDL: dibutyltin dilaurate
DCC: N,N'-dicyclohexylcarbodiimide
DCM: dichloromethane
DCP: dicumyl peroxide
DFA: dimerized fatty acids
DMA: dynamic mechanical analysis
DMAP: 4-dimethylaminopyridine
DSC: differential scanning calorimetry
DXO: 1,5-dioxepan-2-one
E: Young's modulus
E': storage modulus
E'': loss modulus
Ea: activation energy
EBH: N,N'-ethylenebis (12-hydroxystearamide)
EBSA: N,N'-ethylenebisstearamide
Ecoh: cohesive energy
EVA: ethylene-*co*-vinyl acetate copolymer
e-ROP: enzymatic ring-opening polymerization
F_{di}, F_{pi}, E_{hi}: molar attraction constants
FDA: food and drug administration
FTIR-ATR: Fourrier transformed infra-red-attenuated total reflection
G': storage modulus
G'': loss modulus
GC: gas chromatography
HBP: hyperbranched polymer
HDPE: high-density polyethylene
HDT: heat deflection temperature
IS: impact strength
k: crystallization rate constant
LA: lactide
LAB: lactic acid bacterias
LDI: lysine diisocyanate
LDPE: low-density polyethylene
LLDPE: linear low-density polyethylene
LTI: lysine triisocyanate
MCET: mercaptoethanol
MCL: 6-methyl-ε-caprolactone
MDI: 4,4'-methylenebis(phenylisocyanate)
MeOH: methanol
$\bar{M}_n$: number average molecular weight
MV: β-methyl-δ-valerolactone
$\bar{M}_w$: mass average molecular weight
n: Avrami index
NHCs: N-heterocyclic carbenes
NMP: N-methyl pyrolidone
NMR: nuclear magnetic resonance
PBA: poly(n-butyl acrylate)
PBAT: poly(butylene adipate-*co*-terephtalate)
PBS: poly(butylene succinate)
PBSL: poly(butylene succinate-*co*-lactate)
PCL: poly(ε-caprolactone)
PCOD: poly(1,5-cyclooctadiene)
PDL: pentadecalactone
PDLA: poly(D-lactide)
PDLLA: poly(D,L-lactide)
PE: polyethylene
PEA: poly(ester-amide)
PET: poly(ethylene terephtalate)
PFPE: perfluoropolyether
PHAs: poly(hydroxyalkanoate)s
PHB: poly([R,S]-3-hydroxybutyrate)
PI: polyisoprene
PIB: polyisobutylene
PLA: polylactide or poly(lactic acid)
PLLA: poly(L-lactide)
PM: polymenthide
PMCL: poly(6-methyl-ε-caprolactone)
POM: polarized optical microscopy
PP: polypropylene
PPDL: polypentadecalactone
PRic: poly(ricinoleic acid)
PS: polystyrene
PTMC: poly(trimethylene carbonate)
PU: polyurethane
p-TsOH: p-toluenesulfonic acid
P(ω-OHC14): poly(ω-hydroxytetradecanoate)
R: gas constant
RCM: ring-closing metathesis
ROM: ring-opening metathesis
ROMP: ring-opening metathesis polymerization
ROP: ring-opening polymerization
SA: sebacic acid
SAXS: small-angle X-ray scattering
Sb_2O_3: antimony trioxide
SBS: styrene-butadiene-styrene copolymer
SEC: size exclusion chromatography
SEBS: styrene-ethylene-butadiene-styrene copolymer
SEM: scanning electronic microscopy
SM: self-metathesis
$Sn(Oct)_2$: stannous octoate
T: temperature
$t_{1/2}$: half-time of crystallization
$T_{5\%}$: temperature corresponding to 5wt% loss
tanδ: loss factor

TBD: 1,5,7-Triazabicyclododecene
Tc: crystallization temperature
Tcc: cold-crystallization temperature
Tg: glass transition temperature
TGA: thermogravimetric analysis
THF: tetrahydrofuran
$Ti(iOPr)_4$: titanium isopropoxide
$Ti(OBu)_4$: titanium n-butoxide
Tm: melting temperature
Tmax: temperature corresponding to maximum degradation
TMC: trimethylene carbonate
TPE: thermoplastic elastomer
TPP: triphenyl phosphite
T_α: α-relaxation temperature
T_β: β-relaxation temperature
UndME: methyl 10-undecenoate
V: volume fraction
VL: δ-valerolactone
VLDPE: very low-density polyethylene
WAXD (WAXS): wide-angle X-ray scattering
$ZnAc_2$: Zinc acetate
$ZnEt_2$: Zinc ethane
α_c: relative crystallinity
βBL : [R,S]-β-butyrolactone
δ, δ_d, δ_p, δ_h : solubility parameters
ΔEa: difference of activation energies
ΔHc: crystallization enthalpy
ΔHcc: cold-crystallization enthalpy
ΔHm: melting enthalpy
ΔHm^0: melting enthalpy of the completely crystalline state
$|\eta^*|$: complex viscosity
χc: crystallinity degree
ω-OHC14: ω-hydroxytetradecanoic acid

INTRODUCTION

During the 20th century, a great variety of synthetic polymers became available on the industrial scale. The extensive exploitation of oil and gas as fossil raw materials for the fuel, chemical and polymer industry has led to cost-effectiveness and simplified manufacturing of a wide range of products. Today, synthetic polymers are engineered to satisfy basic human needs for housing, health, food, communication, mobility… Indeed, their combination of high versatility, low cost and easy processing renders high technology and good quality of life affordable. Currently, oil consumption for polymers manufacturing counts for around 7% of the annual oil production.[1] The worldwide annual production of plastics in the time period 2010-2015 is around 300 million tons showing the significant amounts of petroleum needed for their production.

Nevertheless, the continuously growing of oil demand is in opposition with the predicting peak oil that announces dramatic rise of the oil price due to the lowering amount of economically accessible oil.[2-4] Consequently, sustainable solutions to the production of fuels, energy and chemicals need to be adopted in order to satisfy the growing demand. The economics and availability of oil feedstocks is not the only driver to more sustainable alternatives. Global warming as a result of greenhouse gases emissions, accumulation of plastics in landfill sites, acid rain and earth's overpopulation are all drivers contributing to a need for a more sustainable industry.

Biomass offers the only sustainable alternative to fossil feedstocks as a source of carbon for our chemical and material needs. Indeed, biomass offers a regeneration time of the carbon source which is measured in years rather than hundreds of millions of years for fossil resources. An industrial society based on plant-derived feedstocks is thus required. The chemical industry is facing its second paradigm shift since the start of the petrochemistry industry: this time from petrochemistry to bio-based production. The concept of a biorefinery has been imagined and created to allow the production of fuels, energy, chemicals and materials from biomass. In order to be in agreement with a sustainable future, green chemistry principles need to be applied in such biorefineries.[5-7] This implies the application of the principles during all the steps needed to the formation of a product (pre-manufacturing, manufacturing, product delivery, product use, recycling and end of life).

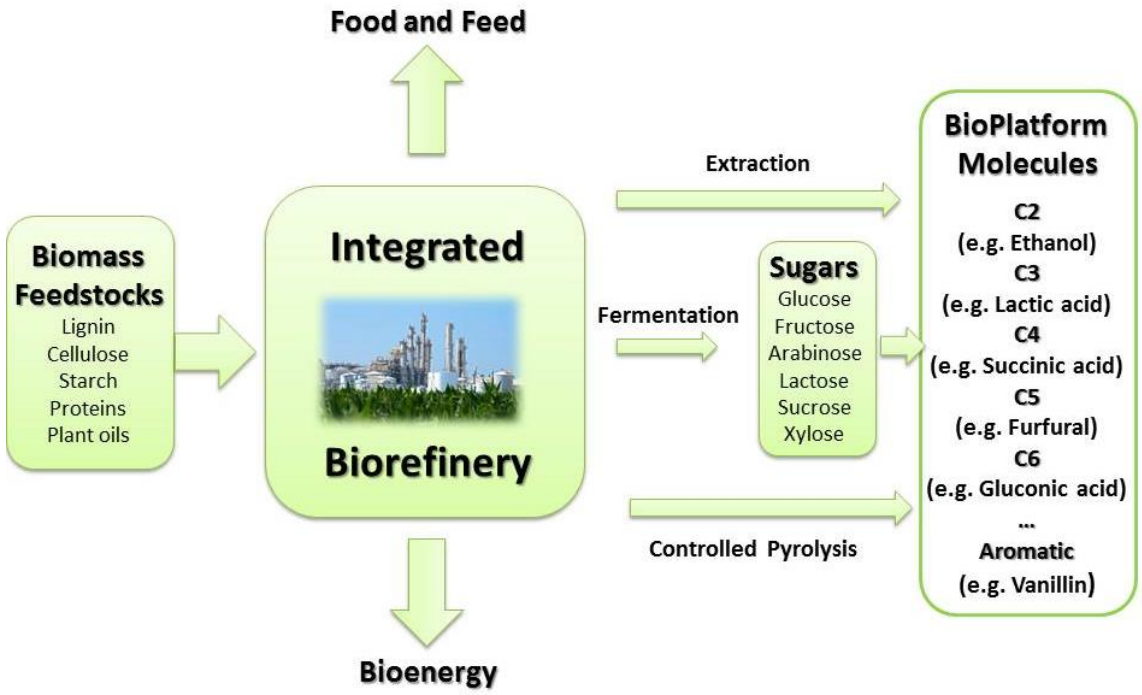

Figure 1.Schematic idealized concept of an integrated biorefinery.

By selecting appropriate biomass feedstock and appropriate transformation process (extraction, fermentation, pyrolysis), a wide range of molecules are accessible (Figure 1). Bioplatform molecules are the beginning of a new and vital challenge for organic chemists. Can we build on these molecules as we have done over the last 70 years with the now well-established petro-platform molecules? We need a substantial growth in research activity on the conversion of these platform molecules to valuable and competitive products.

Regarding bio-based polymers, they are now readily entering the green economy with a global production in 2011 of around 1.1 million tons. Further development of bio-based polymers is expected with an estimated production in 2016 of around 5.8 million tons. There are three principal routes to produce bio-based plastics. The first way is to make use of natural polymers which may be modified or directly used (for instance starch plastics). The second route consists in the production of bio-based monomers by fermentation or conventional chemistry and to polymerize these monomers in a second step. Either mainstream monomers can be used by this way such as bioethylene (obtained from bioethanol), or non-conventional monomers such as lactide. The third approach is to produce bio-based polymers directly in microorganisms or in genetically modified crops (for instance poly(hydroxyalkanoates)). A large range of bio-based plastics are now produced worldwide ranging from polyolefins, polyesters, polyamides, polyurethanes, starch materials… Technical information on the emerging groups of bio-based plastics can be found in the literature.[1, 8-11]

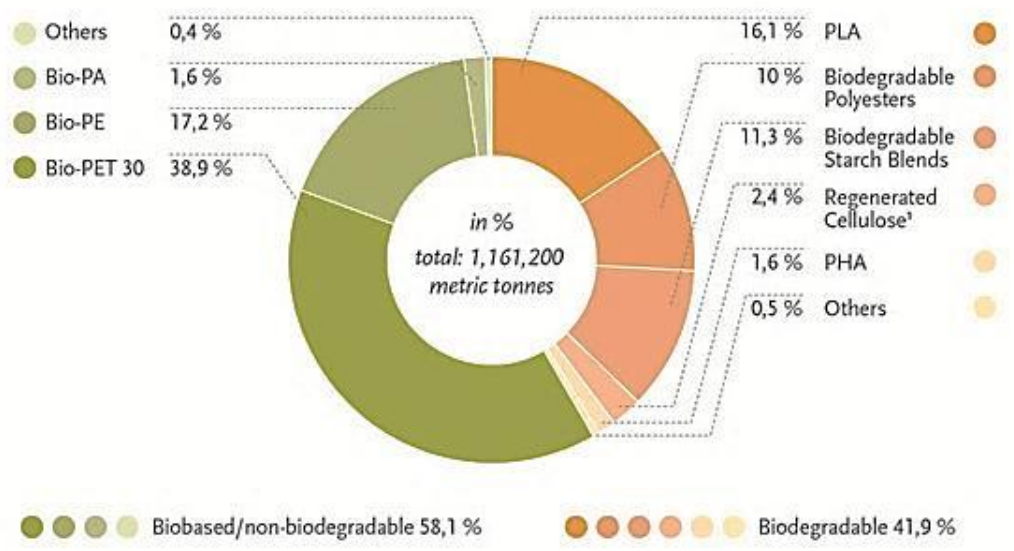

Figure 2.Biobased plastics global production capacity 2011 (by type). Source: European bioplastics.

Poly(lactic acid) or poly(lactide) (PLA) is one of the leading and most mature bio-based plastics with a global capacity of over 180 000 metric tons per year (16% of the bio-based plastics global production capacity in 2011)(Figure 2). Moreover, PLA production capacity is estimated to be around 300 000 metric tons by the year 2016 which correspond to a growth rate of +50%.[12] PLA is a compostable aliphatic polyester which is produced industrially from lactic acid (more precisely lactide), a building block obtained by fermentation of starchy materials. PLA-based materials had their first commercial success as fiber materials for resorbable sutures due to the bioresorbability and the biocompatibility of such materials. Following this commercial success, PLA-based materials were then highly developed for various prosthetic devices in medical applications[13, 14] as well as for drug release systems.[15]

For many years PLA uses were focused on biomedical applications. However PLA is no more restricted to this very sharp area due to recent manufacturing processes that are lowering the production costs of this material. Since the first large-scale PLA production facility became reality in 2002, PLA production cost is continuously decreasing thanks to the huge developments that have been made concerning the biotransformation of biomass into lactic acid at lower price.

The largest producer of PLA is NatureWorks (USA), a company that is highly active in the USA and Thailand, and has a capacity of 140 000 t/year.[16] The other producers have a current capacity of between 1 500 and 10 000 t/year; however, companies such as PURAC, Galactic and Total Petrochemicals announced future significant production of PLA. Currently NatureWorks is using corn as the feedstock due to the availability of this resource in the US coupled with its high starch content. The company intends to build a second plant to increase

the production capacity and within the next 5 to 10 years a third one that will be dedicated to the use of cheap biomass (lignocellulosics from corn stover) as the primary feedstock. The market analysis of PLA shows that, except NatureWorks production, the production capacity worldwide is quite low. Further improvements in production capacity need to be undertaken in order to significantly lower the price of PLA. NatureWorks is currently the only large volume producer of PLA which enables it to supply large volumes of PLA at a price of 1.90€/kg. This price is in agreement with the statements of Inventa Fischer, who have estimated the production costs at 1.30-1.60 €/kg.

The current acceptable price of PLA makes it a serious candidate for a large range of applications thanks to its compostability and its technical substitution potential. Indeed, according to interviewed representatives from the two main producers of PLA, Natureworks and PURAC, PLA components are susceptible to partially replace some petroleum-based thermoplastics such as PET, PS...[8] PLA is becoming an economically viable polymer for packaging applications. PLA is mostly used as a food packaging polymer for short life products such as fruit and vegetable, as containers, drinking cups, salad cups, overwap and lamination films, and blister packages. Commercially available PLA films and packages provide comparable properties to those of PET while better properties compared to PS. While PLA is mostly used in packaging applications for now, in the future new applications opportunities could be in agreement with its price. Especially transportation, electric appliances and electronics should be significant areas of development.[8]

Nevertheless, the inherent brittleness of PLA hinders considerably its use in such applications thus limiting its technical substitution potential. Similarly to polystyrene, PLA was the subject of numerous investigations these past few years, to improve its impact strength. Most of the commercially available impact modifiers are however of petroleum source and non-biodegradable thus impeding the fully compostable characteristic of the resulting PLA material.

This thesis work was financially supported by the French environment and energy management agency (ADEME) and the ITERG technical center. Both of these financial partners are highly involved in promoting the development of biorefineries in France. In order to be fully integrated into the biorefinery approach (in accordance with the green chemistry principles), we will describe in this manuscript several routes that we used for the development of fully bio-based and potentially biodegradable toughened PLA materials. More precisely, the plant oils platform will be employed for the development of low glass transition temperature (Tg) polyesters impact modifiers; thanks to the expertise of our partner

(ITERG) in oleochemistry. The present manuscript is composed of five chapters each of them investigating different aspects of PLA toughening.

In the first chapter we will review both the state-of-the-art in PLA toughening and the synthesis of thermoplastic polyesters from fatty acids. Firstly, the synthesis and properties of PLA materials will be extensively described in order to identify the forces and weaknesses of this polymer family. The state-of-the-art in the rubber-toughening of PLLA will then be done and will allow us to identify the advantages and disadvantages of the most significant impact modifiers developed to date. Low Tg bio-based aliphatic polyesters will be identified as the most sustainable impact modifiers for PLLA. Fatty acids being a suitable resource for the development of aliphatic polyesters, a review of the recent investigations in that field will be presented in order to define the synthetic possibilities for the development of sustainable polyester impact modifiers.

In the second chapter, novel fatty acid-based polyesters and poly(ester-amide)s will be developed. In a first part, the effect of amide functions on the thermal and mechanical properties of the polymer will be evaluated. One selected bio-based diol bearing amide functions will then be reacted with a dimerized fatty acid to obtain a poly(ester-amide) showing a combination of high softness and high thermal endurance. Melt-blending this polymer with PLLA will result in slight improvement of the impact strength.

It will be assumed from chapter 2, that the crystallinity of the impact modifier could be one of the reasons for limited improvement in impact strength of the blend. Thus, in chapter 3 we will aim at investigating the effect of crystallinity of the additive on the impact strength of the resulting PLLA material. A series of bio-based polyesters showing various crystallinity degrees will then be developed and melt-blended with PLLA. Our hypothesis will be verified as seen from the obvious dependence of the blend properties with the crystallinity of the impact modifier.

Based on these results, poly(ricinoleic acid), a low Tg amorphous polyester will then be employed in chapter 4 to toughen PLLA. This study will differ from the previous two chapters as block copolymerization strategy will be retained. An extensive investigation of the properties of these novel block copolymers will highlight their good potential as sustainable tough PLA materials.

Finally, in chapter 5, two strategies will be employed for the potential toughening of PLLA by using Acyclic Diene Metathesis (ADMET) polymerization. In a first study, ABA triblock copolymers formation will be investigated; however, this exploratory work will lead to the

conclusion that such materials are not optimal for the toughening of PLLA due to the lack of control over the polymer architecture by using this approach. In a second part, ADMET will be employed to develop “LLDPE like” polyesters that constitute potential impact modifiers for PLLA.

REFERENCES

1. R. Mülhaupt, *Macromolecular Chemistry and Physics*, 2013, **214**, 159-174.
2. S. Sorrell, J. Speirs, R. Bentley, A. Brandt and R. Miller, *Energy Policy*, 2010, **38**, 5290-5295.
3. S. Sorrell, J. Speirs, R. Bentley, R. Miller and E. Thompson, *Energy*, 2012, **37**, 709-724.
4. R. W. Bentley, *Energy Policy*, 2002, **30**, 189-205.
5. T. A. Paul and C. W. Tracy, in *Green Chemistry*, American Chemical Society, 1996, vol. 626, ch. 1, pp. 1-17.
6. P. T. Anastas and M. M. Kirchhoff, *Accounts of Chemical Research*, 2002, **35**, 686-694.
7. J. H. Clark, F. E. I. Deswarte and T. J. Farmer, *Biofuels, Bioproducts and Biorefining*, 2009, **3**, 72-90.
8. L. Shen, J. Haufe and M. K. Patel, *Pro-Bip Report* 2009.
9. M. Desroches, M. Escouvois, R. Auvergne, S. Caillol and B. Boutevin, *Polymer Reviews*, 2012, **52**, 38-79.
10. I. Bechthold, K. Bretz, S. Kabasci, R. Kopitzky and A. Springer, *Chemical Engineering & Technology*, 2008, **31**, 647-654.
11. B. Laycock, P. Halley, S. Pratt, A. Werker and P. Lant, *Progress in Polymer Science*, 2013, **38**, 536-583.
12. *European Bioplastics Website,* http://en.european-bioplastics.org/.
13. P. B. Maurus and C. C. Kaeding, *Operative Techniques in Sports Medicine*, 2004, **12**, 158-160.
14. A. J. R. Lasprilla, G. A. R. Martinez, B. H. Lunelli, A. L. Jardini and R. M. Filho, *Biotechnology Advances*, 2012, **30**, 321-328.
15. J. M. Anderson and M. S. Shive, *Advanced Drug Delivery Reviews*, 1997, **28**, 5-24.
16. E. T. H. Vink, K. R. Rábago, D. A. Glassner and P. R. Gruber, *Polymer Degradation and Stability*, 2003, **80**, 403-419.

CHAPTER 1:

Bibliographic study: past achievements in the toughening of PLA and evaluation of the potential of fatty acid-based thermoplastics to meet future challenges.

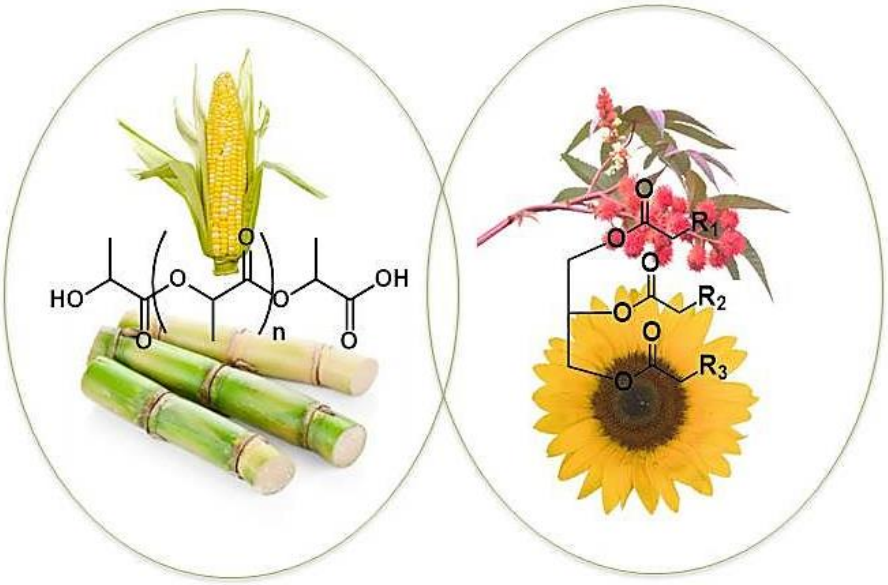

Keywords: lactic acid, lactide, PLA, bio-based, compostable, brittleness, rubber-toughening, high-impact, plant oils, fatty acids, polyesters.

Mots clés: acide lactique, lactide, PLA, bio-sourcé, compostable, fragilité, renfort au choc, huiles végétales, acides gras, polyesters.

PART A. SYNTHESIS AND PROPERTIES OF PLA-BASED MATERIALS

I. POLY(LACTIDE), A BIOBASED AND COMPOSTABLE MATERIAL

I.1. Lactic acid production- towards a biobased precursor to PLA

Nowadays, biobased plastics make up nearly 1.2 million tons of the plastics market (2011).[1] Among them, PLA represents one of the most mature bioplastic as evidenced by its significant production and commercialization. PLA is a linear aliphatic polyester that is derived from lactic acid (2-hydroxypropionic acid), a chiral organic hydroxyacid that exists in two different forms. Indeed, depending on the stereochemistry of the tertiary carbon of lactic acid molecule, the levogyre (L-lactic acid) and the dextrogyre (D-lactic acid) isomers are accessible. Lactic acid can be obtained by chemical synthesis or fermentation. Chemical synthesis of lactic acid is mainly based on the hydrolysis of lactonitrile by strong acids. Other routes are however achievable such as base-catalyzed degradation of sugars, oxidation of propylene glycol, reaction of acetaldehyde, carbon monoxide, and water at elevated temperatures and pressures, hydrolysis of chloropropionic acid and nitric acid oxidation of propylene. Main drawbacks of the chemical routes include the lack of cost effectiveness and the non-stereoselectivity.[2] Indeed lactic acid produced by the petrochemical route exists as a 50/50 optically inactive mixture of L- and D- forms. Due to the above mentioned reasons and environmental concerns, the fermentative pathway to lactic acid has gained widespread interest and is now industrially developed by most of lactic acid producers.[3]

Indeed, the biotechnological production of lactic acid offers various advantages over the chemical pathway like low cost of substrates, low production temperature and low energy consumption. It is also noticeable that, depending on the micro-organism used in the biotransformation, L- or D- isomers are preferentially formed (Figure 1.1).[4] Lactic acid bacterias (LAB) can be classified into two groups: homofermentative and heterofermentative. While the homofermentative LAB convert glucose almost exclusively into lactic acid, the heterofermentative LAB catabolize glucose into ethanol and CO_2 as well as lactic acid. Only the homofermentative LAB are available for the commercial production of lactic acid.[2] The carbon substrates used for microbial production of lactic acid include various sugars, either pure (e.g glucose and sucrose) or impure (e.g starch). Thus, a large variety of raw materials

can be used such as molasses, sugar cane, bagasse and starchy materials from potato, tapioca, wheat, barley, corn etc.[2, 5, 6]

The choice of a specific carbohydrate feedstock depends on different factors such as its price, availability and purity. Food and agro-industrial products or residues generally form the cheaper alternatives to refined sugars for the biotransformation into lactic acid. Thus starchy materials like sugarcane bagasse, cornstarch, corn cob, wheat bran are the most economical substrates for the production of competitive lactic acid.

By using such starchy substrates, several steps are needed to produce lactic acid. In conventional biotechnological processes, a pretreatment step for gelatinization and liquefaction of the biomass is required, which involves the use of high temperatures in the range 90-130°C. Then enzymatic saccharification to glucose is carried out followed by subsequent conversion of glucose into lactic acid by fermentation. However the conversion of starch or cellulose to sugar consumes energy during liquefaction or saccharification and increases the cost of production. In addition, sugar concentration in the hydrolyzate highly affects fermentation as bacterial cells cease to produce lactic acid when the sugar concentration is high.[7]

To overcome these limitations, direct fermentation processes were developed which resulted in cost effective and time saving pathways to the production of lactic acid. The direct conversion of complex starchy or cellulosic substrates to lactic acid includes three different routes. In the first one, the lactic acid producing fungi can directly convert starch to lactic acid with the help of enzymes. In another pathway amylolytic lactic acid bacteria allows direct fermentation of the substrate.[7] Finally the last possibility is to simultaneously treat the carbohydrate substrate with degrading enzymes and lactic acid producing bacteria. These solutions then offer the controlled release of sugar in the optimum growth temperature. Glucose inhibition on the enzyme is therefore minimized.

Due to considerable improvements in production yields (>90% of fermentable sugars), almost all lactic acid produced globally is manufactured by fermentation routes. This is reinforced by lower production cost and market drivers for biorenewable products. Thus current global production is between 300,000-400,000 tons per year with the United States that constitutes the largest regional market for lactic acid, accounting for a significant share of the worldwide market. Western Europe and Asia-Pacific make up the other major lactic acid producers and consumers on a global scale. The major manufacturers of fermentative lactic acid include Natureworks LLC (USA), Purac (Netherlands), Galactic (Belgium), Cargill (USA) and several Chinese companies.

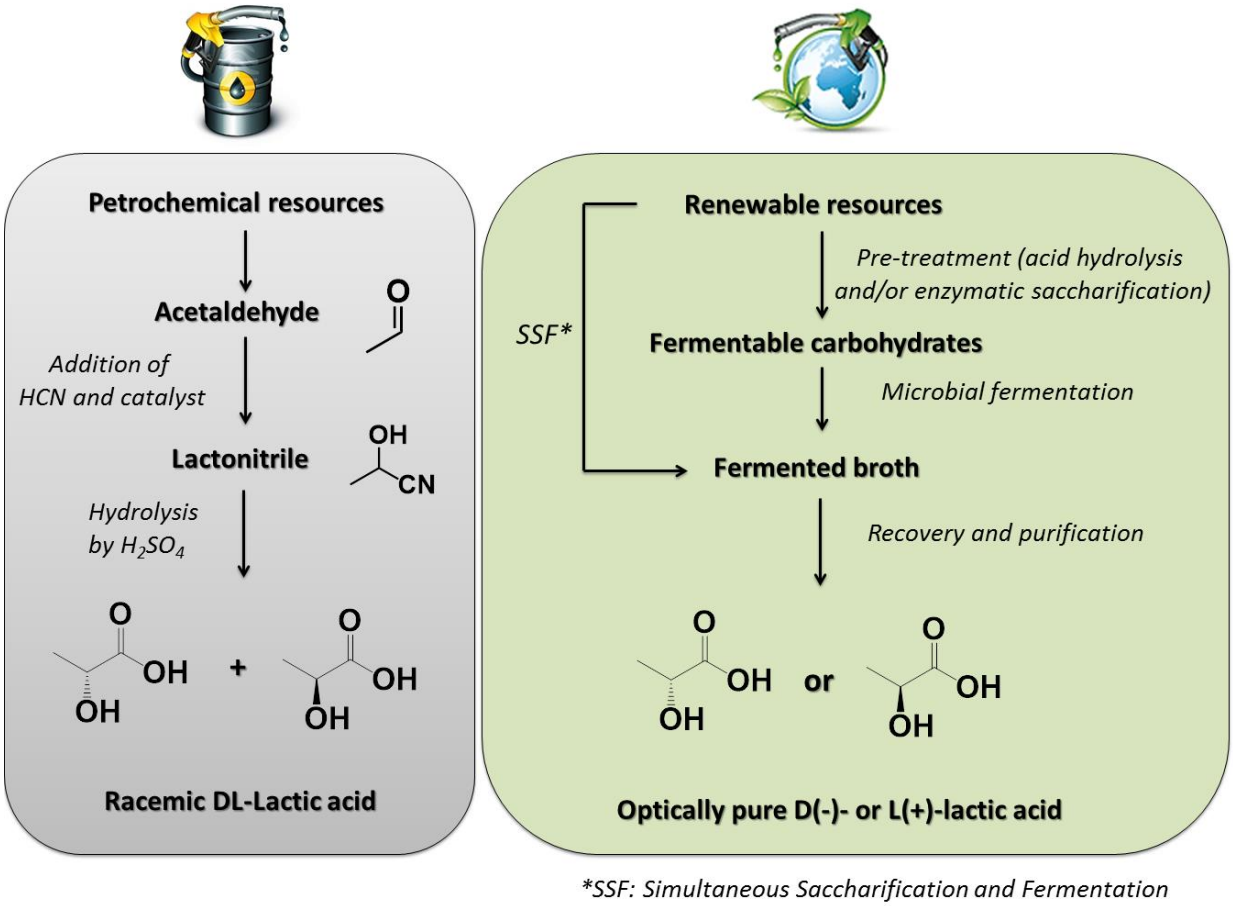

Figure 1.1. Chemical synthesis and microbial fermentation pathways to lactic acid

I.2. PLA production

Two main routes are generally referred to convert lactic acid to PLA. Direct polymerization by polycondensation leads to poly(lactic acid) while the indirect route via lactide (LA), a cyclic dimer of lactic acid, leads to poly(lactide). Both products are referred to as PLA.[8] Owing to the fact that lactic acid bears both a hydroxyl and a carboxylic acid function, polycondensation is inevitably the most direct route to PLA. However, molecular weights obtained by this pathway are not high enough to consider various applications of the resulting polymer. The low reactivity of the secondary hydroxyl function of lactic acid, combined with the need to efficiently removed water to shift the equilibrium toward the formation of the polymer constitute the main drawbacks of simple polycondensation.

I.2.1. PLA synthesis by polycondensation

It is however possible to obtain higher molecular weights using different reaction conditions or via chain extension of the low molecular weight polymers. Indeed, a first strategy involves the polymerization of lactic acid in appropriate solvent that allows azeotropic distillation of

the condensate.[9, 10] Generally reaction time is in the range 30-40h at 130°C making this process unsuitable for low cost PLA production. Moreover high concentration of catalyst is needed to have access to high molecular weight PLA, which facilitates degradation and hydrolysis during processing.

Another approach to synthesize high molecular weight PLA is based on the polycondensation of lactic acid in the presence of difunctional monomers (e.g. diacids or diols) ending up in telechelic prepolymers. These resulting terminal functional groups of the prepolymers can then be reacted by using chain extenders such as diisocyanate,[11] bis(amino-ether).[12] However increase in both cost and complexity of the multistep process, as well as possible unreacted chain-extending agents which alter the final properties are the main drawbacks limiting the industrial use of this method.

An alternative route consists in the melt/solid polycondensation of L-lactic acid (Figure 2.1). In this process, a polycondensate with a low molecular weight of around 20 $kg.mol^{-1}$ is first prepared by ordinary melt polycondensation. Crystallization of the obtained poly(L-lactic acid) (PLLA) is then carried out by heat-treatment at around 105°C followed by heating at temperatures above Tg, yet below Tm of PLLA. Thus polymerization is performed in the amorphous phase, where all the reactive end groups reside, allowing the synthesis of high molecular weight PLLA in the range 100-500 $kg.mol^{-1}$.[13]

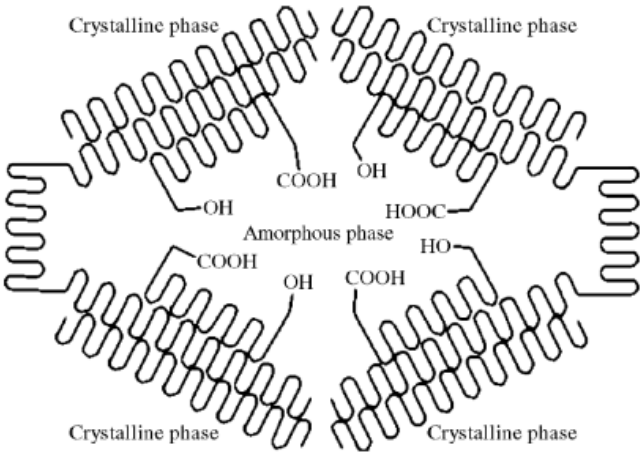

Figure 2.1. Schematic description of the solid-state polycondensation

The advantages of solid-state polymerization include low operating temperatures, which control over side reactions as well as thermal, hydrolytic, oxidative degradations along with reduced coloration and degradation of the polymer. Moreover there is practically no environmental pollution, because no solvent is required.

I.2.2. PLA synthesis by Ring-Opening Polymerization (ROP) of lactide

The most common way to obtain high molecular weight PLA is through ring-opening polymerization (ROP) of lactide (LA). The first step consists in the formation of LA, a cyclic dimer of lactic acid, by oligomerization of L-lactic acid, D-lactic acid or mixtures permitted by removal of the water condensate followed by subsequent catalytic depolymerization through internal "back-bitting" transesterification.

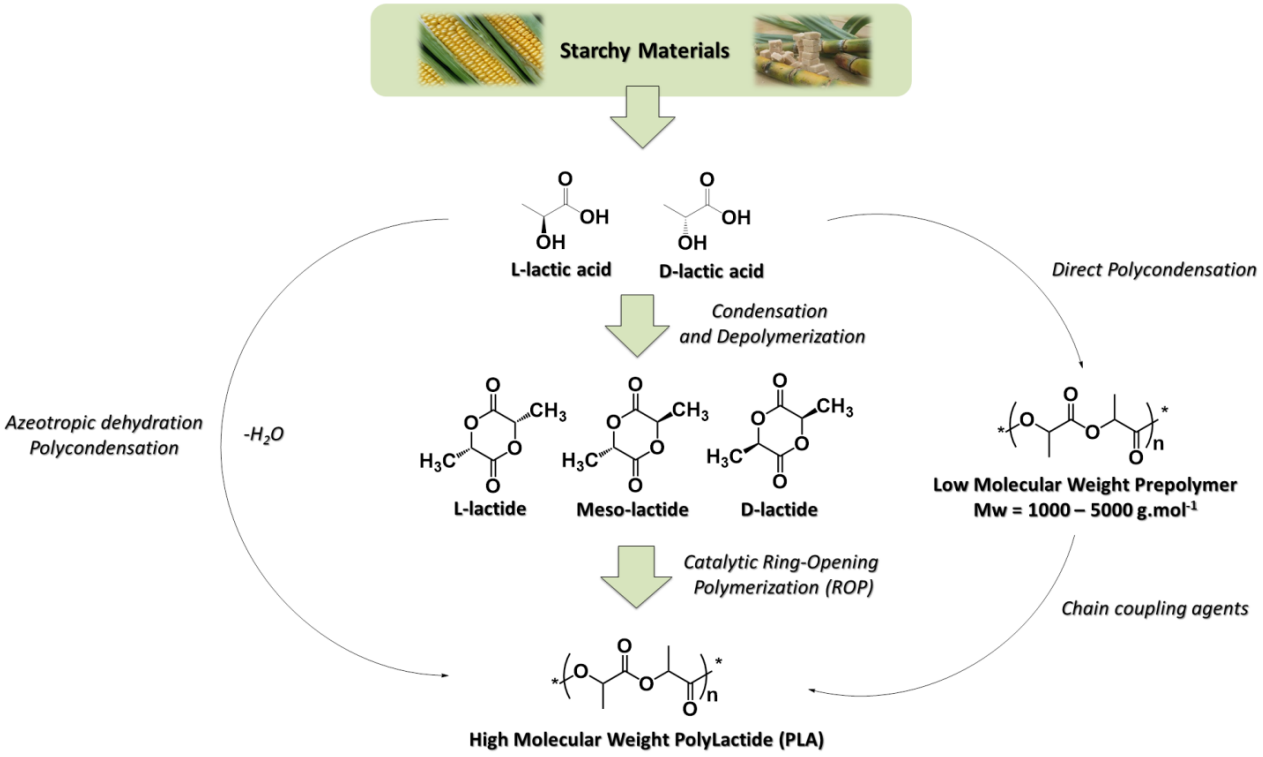

Scheme 1.1. Synthesis methods for high molecular weight PLA

Depending on the feed ratio of L-lactic acid and D-lactic acid, three stereoforms of lactide can be obtained: L-lactide (L-LA), D-lactide (D-LA) and meso-lactide (D,L-LA) (Scheme 1.1). The key point is the separation between each stereoisomer by vacuum distillation in order to control the final PLA structure. In a second step, the purified LA is converted to high-molecular weight poly(lactide) by catalytic ROP.

Polymerization through LA formation is the current method used by most of PLA producers such as Natureworks, Purac…The ROP of lactones is an attractive method to synthesize aliphatic polyesters because it enables living polymerizations to be conducted and therefore provides a route to control the physical and chemical properties of the polymers. The driving force of such a polymerization method is the relief of ring strain. This versatile polymerization method has allowed the preparation of lactic acid based polymers by solution, bulk, melt and suspension polymerizations. The polymerization mechanism involved in ROP

can be anionic, cationic, coordination-insertion or an activated monomer mechanism depending on the initiating system used.[14] A large range of catalytic species have been used to mediate ROP of LA including metal-based complexes, enzymes and small molecule organic catalysts.[15-20] Gupta and Kumar made an effort to review and present a collection of more than 100 catalysts that have been used for the synthesis of PLA by ROP.[21]

A large range of simple metal salts and coordination compounds have been reported as catalysts for the ROP of LA (Scheme 2.1). The catalysts mainly used consist of metal powders, Lewis acids, Lewis bases, organometallic compounds and different salts of metals. Particularly metallic compounds such as alkylmetals and metal halides, oxides and carboxylates are very effective. Metal compounds of tin,[22-25] aluminium,[26] lead,[27] zinc,[28, 29] bismuth,[27] iron,[30] and yttrium[31] constitute relevant examples of catalyst enabling preparation of high molecular weight PLA. Among them, tin(II) octanoate remains the most frequently used. Tin(II) octanoate presents several advantages that made it a suitable catalyst for industrial production of PLA by ROP. First it is soluble in organic solvents and molten LA, it is stable on storage, it allows polymerization up to 180°C, and it has been approved by the food and drug administration (FDA).

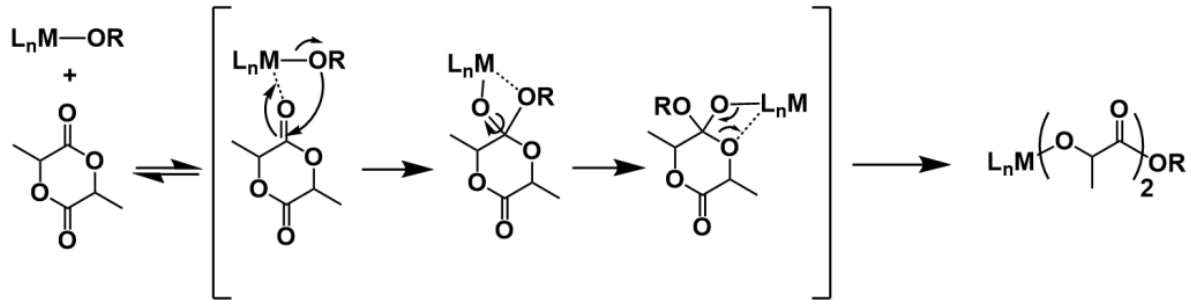

Scheme 2.1. Coordination/insertion polymerization of lactide by metal-based catalysts

The applications of polyesters, and more particularly PLA, in packaging and biomedical applications have motivated efforts to develop metal-free organic catalysts in order to suppress the traces of metal in the final polymeric materials. The development of small molecule organic catalysts for the ROP of LA has resulted in very high levels of polymerization control.[15, 32] Moreover, organic catalysts allow polymerization of LA under milder conditions as evidenced by low temperature and reaction times needed. Organic catalysts are postulated to operate via one of three mechanisms: monomer-activated, pseudo-anionic (chain end activated or general base catalysis) or cooperative dual activation.

In the monomer-activated polymerization method, two types of compounds can promote the ROP of LA. Electrophiles can activate the monomer (more precisely the carbonyl function) by protonation followed by subsequent ring-opening by reaction with a nucleophile, such as

an alcohol. The polymerization is then carried-out by the same mechanism, with the terminal hydroxyl group of the polymer chain that acts as a nucleophile toward the protonated monomer. Nucleophiles can also activate the monomer by direct attack on the monomer to generate a ring-opened alcohol that can propagates by repeated attack on the activated monomer. Nucleophiles such as pyridines, imidazoles, phosphines, and N-heterocyclic carbenes (NHCs) catalyzed ROP of cyclic esters by this mechanism.

The pseudo-anionic mechanism operates by activation of the initiator or the active chain ends (Scheme 3.1). Organic bases such as phosphazenes and nitrogen bases have been postulated to catalyze ROP of cyclic esters by this mechanism. In the case of certain nucleophilic/basic organic catalysts such as NHCs and 4-(dimethylamino)pyridine (DMAP), a mechanistic competition between nucleophilic and pseudo-anionic mechanisms was observed when alcohols initiators were used for the ROP of LA.

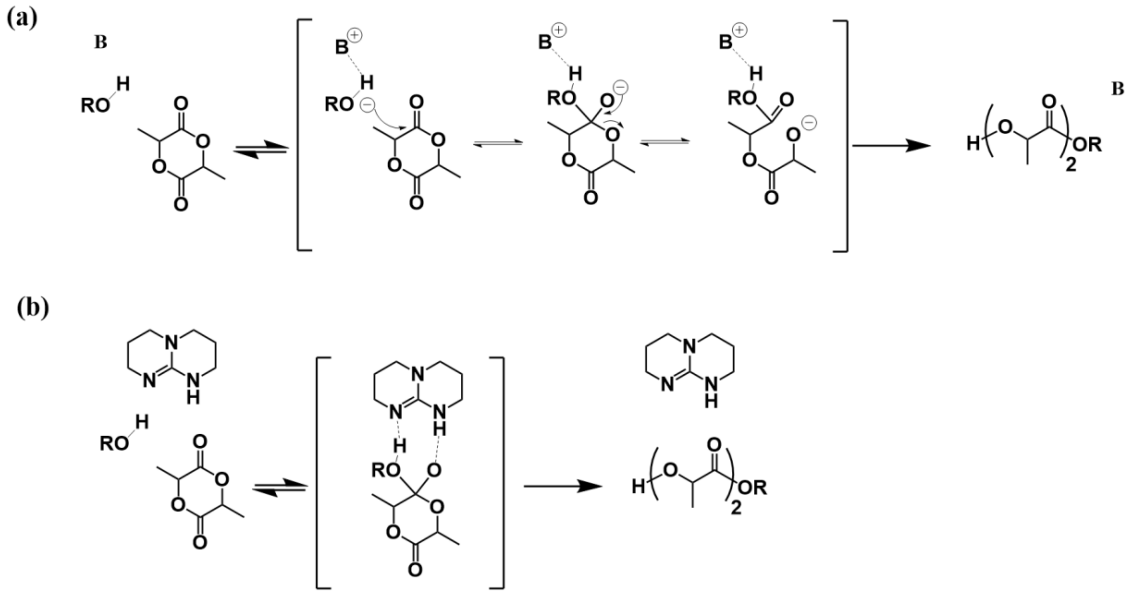

Scheme 3.1. Organo-catalyzed ROP of lactide by (a) pseudo anionic and (b) dual activation mechanisms

The combination of an electrophile to activate the monomer and a general base to activate the initiator/chain end can highly enhance the ROP rate and selectivity. This cooperative dual activation mechanism has been applied with both unimolecular and bimolecular catalysts. Relevant examples of such catalysts include thiourea/amine systems and 1,5,7-Triazabicyclododecene (TBD) (Scheme 3.1). By using the latter at a content of 0.1mol%, the ROP of LA was completed in 1min.

The particularity and potential of PLAs reside in the various stereochemical microstructures enable by the presence of two stereocenters per lactide monomer (Figure 3.1). The ROP of enantiopure L- or D-LA results in the isolation of isotactic PLA in which all stereocenters are

identical. However ROP of either rac-LA (racemic mixture of L- and D-LA) or meso-LA (LA possessing both L- and D-stereocenter) leads to an atactic PLA if the catalyst used lacks stereospecificity. Some recent reviews summarize the different catalytic systems that were used to synthesize stereoregular PLAs.[17, 33] Two types of stereospecific catalysts can be distinguished. First, catalysts that display a *syndio* preference (i.e., a preference to ring-open at the opposite stereocenter as the stereocenter at the end of the propagating polymer chain) will result in the synthesis of heteroatactic PLA in which the polymer displays doubly alternating stereocenters (i.e. -LLDDLLDD-) from *rac*-LA by alternating insertion of monomers of opposite stereochemistry or syndiotactic PLA (alternating L- and D-stereocenters i.e. –LDLDLD-) from *meso*-LA.

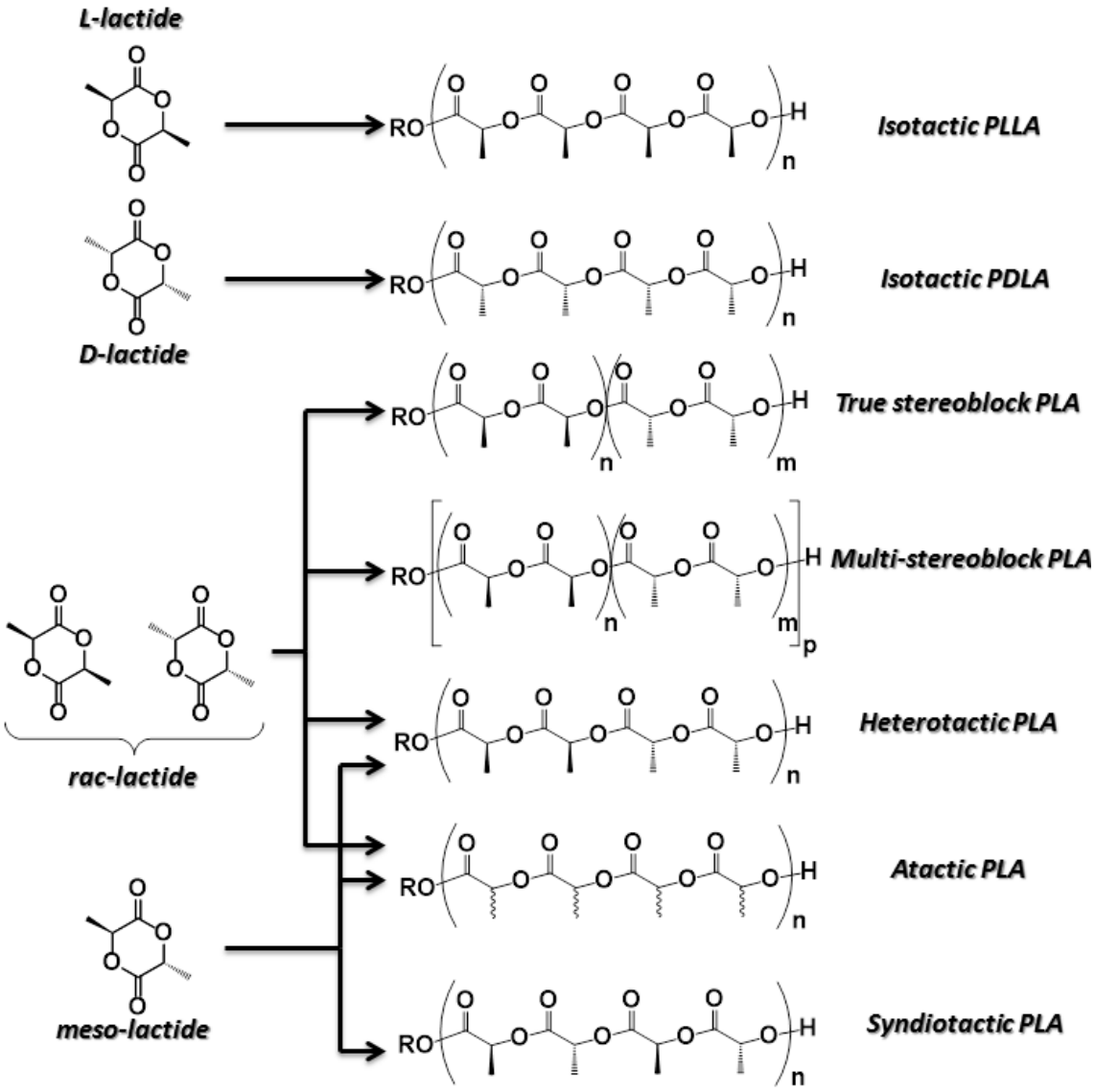

Figure 3.1. Stereochemistry of PLA materials

Second, catalysts that display an *iso* preference (i.e., a preference to ring-open at the same stereocenter as the stereocenter at the end of the propagating polymer chain) will result in the

synthesis of heteroatactic PLA from *meso*-LA but will mediate the synthesis of stereoblock PLAs from *rac*-LA.

In the following, special emphasis was made on isotactic PLLA due its interesting mechanical and thermal properties provided by semi-crystallinity. Isotactic PLLA was preferred over isotactic PDLA due to the higher availability of L-LA from biomass in comparison to D-LA. In order to avoid ambiguity, in this manuscript, PLA was used for the general meaning of polylactides or when the stereochemistry was not mentioned. Otherwise the stereochemistry was defined by the letter (L-, D- or D,L-).

I.3. PLA properties and compostability

I.3.1. Structure, thermal and Physical properties

The properties of high molecular weight PLA are determined by several factors such as the molecular weight which can be controlled by the addition of hydroxyl compounds and the polymer architecture which is mainly linked to the stereochemical composition of the polymer backbone. Due to the three forms of LA monomers, various natures of PLA can be achieved. High purity L- and D-LA form stereoregular isotactic poly(L-lactide) (PLLA) and poly(D-lactide) (PDLA) respectively. Both are semi-crystalline polymers with an equilibrium melting point of 207°C and a glass transition in the range 55-60°C.[34, 35] However typical melting points are in the range 170-180°C due to small and imperfect crystallites, slight racemization and impurities. The meso-LA or a racemic mixture of L- and D-LA, on the other hand form atactic poly(D,L-lactide) (PDLLA) which is completely amorphous and shows a Tg in the range 50-60°C (Table 1.1).

Another family of polylactides includes stereocomplex-type polylactides (sc-PLA) consisting of both enantiomeric PLLA and PDLA. In 1987, Ikada and coworkers discovered that a mixture of enantiomeric PLLA and PDLA forms stereocomplex (or racemic) crystals with a melting temperature at around 240°C.[36] Stereocomplex-type polylactides were first generated from solution and later from melt mixtures.[37] Various factors affect the stereocomplexation such as the molecular weight of PLLA and PDLA, the optical purity of the homopolymers and the process of formation.

Table 1.1. Physical properties of different types of PLA materials.[38]

Physical properties	Stereo-complexed PLA	PLLA	PDLLA	Syndiotactic PLA
Tm (°C)	220-230	170-180	-	151
Tg (°C)	65-72	55-60	50-60	34
ΔHm (100%) (J.g^{-1})	142	93	-	-

For amorphous PLA, the glass transition temperature (T_g) is one of the most important parameters since dramatic changes in polymer chain mobility take place around this temperature. Various physical properties are reached depending on the temperature. Below the β-relaxation temperature, T_β, PLA is completely brittle. Between T_β and T_g the amorphous PLA undergoes physical aging and can show brittle or ductile fracture. Above T_g, amorphous PLA is rubbery and become viscous in the range 110-150°C. Finally, amorphous PLA decomposes between 215 and 285°C.

For semicrystalline PLA, physical properties are also highly dependent on the processing conditions. Indeed the processing conditions will dictate the degree of crystallinity while the stereochemistry will govern the melting point of the polymer. Similarly to amorphous PLA, Tg is an important parameter since it indicates the transition between brittle and ductile fracture. Below Tg, semicrystalline PLA is a brittle material, while above Tg it is a tough material that undergoes a ductile fracture. At the melting point, semicrystalline PLA becomes viscous liquid and degrades above 215°C (Figure 4.1).

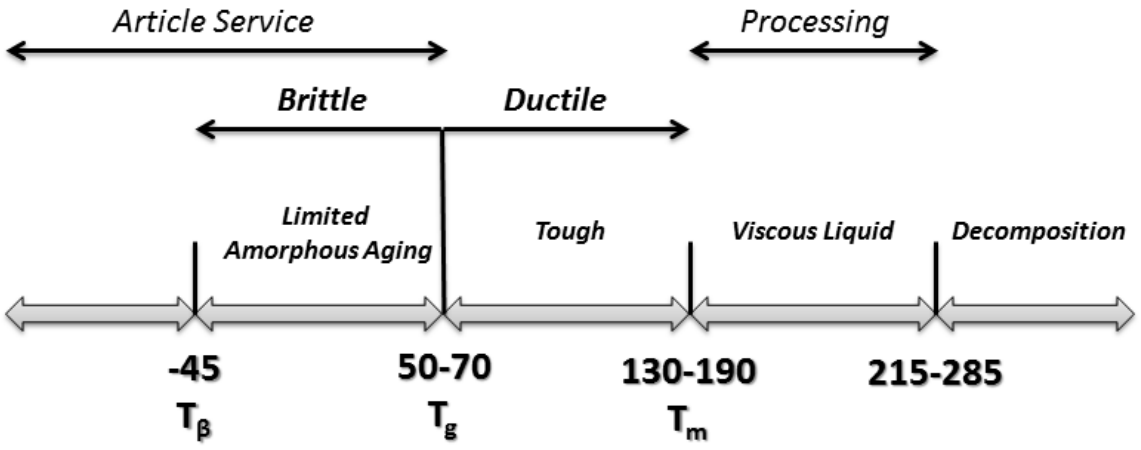

Figure 4.1. Metastable states of high molecular weight semicrystalline PLA

I.3.2. Crystallization behavior and crystallographic properties

Isotactic PLA can crystallize in α-, β-, or γ-forms depending on the processing conditions.[39-44] The most common and stable, which can be developed from the melt or solution under normal conditions, is the α-form with a 10_3 helical chain conformation where two chains are interacting in an orthorhombic (or pseudo-orthorhombic) unit cell. The β- and γ-forms are obtained only under specific conditions, for instance by stretching the α-form at high drawing ratio and high temperature or by epitaxial growth on the hexamethylbenzene substrate. A disordered form, named as α'-form, can also be achieved by crystallization at lower temperature.[45] It was shown that α'-crystals are in fact less perfect crystals of the α-form and

that an α'-to-α transformation generally occurs while heating by a solid-solid transition process which involves the readjustment of the chain conformation into a more stable state.

The crystalline behavior of isotactic PLA has been extensively studied due to the high melting point that confers interesting properties to this material.[9, 34, 35, 46, 47] PLLA was the most investigated semi-crystalline PLA material due to the higher abundance of L-LA monomer compared to D- and meso-LA, thus we will take PLLA as a semi-crystalline PLA material reference. As mentioned above, melting point of PLLA is generally measured in the range 170-180°C depending on the optical purity of the monomer used for the synthesis. The enthalpy of melting (ΔH_m) for a pure crystal (100% crystallinity) was calculated through extrapolation to be 93.7 $J.g^{-1}$ with practical ΔH_m around 40-50 $J.g^{-1}$, yielding polymers with 37-47% crystallinity.[48, 49] Except the stereochemistry, thermal history is the main factor that affects the crystallinity of PLLA. It can be either amorphous or semi-crystalline depending on the cooling rate of the material in the case of non-isothermal crystallization or depending on the time and temperature of annealing in the case of isothermal crystallization. The crystallinity of PLLA is most commonly determined using the differential scanning calorimetry (DSC) technique. By measuring the heat of fusion ΔH_m and heat of cold crystallization $\Delta H_{cc,}$ the crystallinity can be determined based on the following equation:

$$\chi_c = \frac{\Delta H_m - \Delta H_{cc}}{\Delta H_m^0} \times 100$$

Where ΔH_m^0 is the enthalpy of fusion of the completely crystalline state (93.7 $J.g^{-1}$ for PLLA). However this equation only gives an approximate value of the crystallinity as it doesn't take into account the heat capacity of the different crystals.

PLLA is a slow-crystallizing material with fastest rates of crystallization observed in the temperature range of 110-130°C, which yields spherulitic crystalline morphology. However, in industry, it is difficult to make use of the semi-crystalline character of PLLA because the high speed of mass production (e.g. in injection moulding) implies quenching, leading to amorphous structures. One particularity of quenched amorphous PLA is to crystallize upon reheat. This phenomenon is allowed by the enhanced mobility of PLLA chains observed above the Tg. This enhanced mobility allows reorganization and better packing of the chains which lead to crystallization. However, similarly to the crystallization upon cooling, the cold-crystallization upon heating highly depends on the heating rate.

The crystallinity can be either an advantage or a drawback depending on the targeted application. For instance, high crystallinity will not be optimal for packaging solutions due to lack of optical clarity while, in contrast, increased crystallinity will be desirable for injection

moulded articles for which good thermal stability is important (related to the increase of heat distortion temperature (HDT) with crystallinity).

The lack of crystallinity due to fast cooling in industrial PLLA articles can be overcome by several techniques. Post-process heating treatment higher than the Tg and below the Tm can be carried out leading to improved flexural elasticity, Izod impact strength, and heat resistance.[50]

Another strategy to get higher crystallinity is by incorporating nucleating agent in the polymer during extrusion. The surface free energy barrier for nucleation is then lowered by the nucleating agent which plays a role as heterogeneous nuclei and enables crystallization and crystal growth at higher temperature upon cooling. Various nucleating agents including inorganic, organic, and polymeric ones have been reported for PLLA in recent years. Talc represents the most investigated nucleating agent for PLLA. Kolstad showed that the crystallization half-time of PLLA was reduced from 3 minutes at 110°C to approximately 25 seconds when 6wt% talc was added to the PLLA matrix.[51] Other inorganic and carbon-based nucleating agents including clay,[52-54] titanium dioxide ,[55, 56] layered silicate ,[52, 57, 58] saponite,[58] rectorite,[59] fullerene,[60] and carbon nanotubes[61] have also been reported. The enhancement of PLLA crystallization rate was also reported with some organic compounds such as zinc citrate complex,[62] N-aminophthalimide,[63] 1,3,5-benzenetricarboxylamide derivatives,[64, 65] calixarene,[66] myo-inositol,[67] nucleobases,[68] hydrazide compounds,[69-72] and low molecular weight aliphatic amides.[73-76] In the latter category, environmental friendly compounds like N,N'-ethylenebisstearamide (EBSA) and N,N'-ethylenebis (12-hydroxystearamide) (EBH) were showed to act as nucleation agent at the very early stage of PLLA crystallization (Figure 5.1). Thus, PLLA crystallization was highly improved by the addition of these compounds both during non-isothermal crystallization and isothermal crystallization.

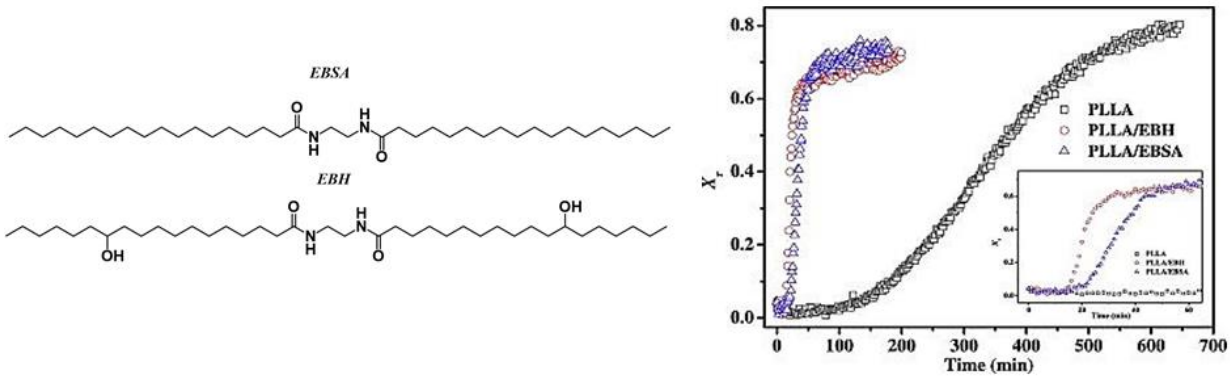

Figure 5.1. Isothermal crystallization curves of neat PLLA and blends of PLLA with low molecular weight aliphatic amides[76]

It was also observed that EBH induced faster crystallization in comparison to EBSA. This phenomenon was justified by the presence of hydroxyl functions in EBH that interact with the carbonyl groups of PLLA.[76]

Some polymers such as PDLA,[77, 78] polyhydroxybutyrate,[79-81] polycaprolactone,[82, 83] polyglycolide,[82] poly(butylene succinate-*co*-L-lactate),[84] starch,[85, 86] cellulose[87] and cyclodextrin[88] have also been described as nucleating agents of PLLA. Crystallization and nucleation of PLLA can be affected by two main phenomena when a polymer is blended with PLLA. In a first case, the added polymer chains will increase the number of crystallite nuclei per unit mass and in a second case, it will increase the growth rate of PLLA (Figure 6.1).[82] In summary, most of polymers are not nucleating agents but nucleating-assisting agents and spherulite growth-accelerating agents. One particular case is the PLLA/PDLA blends. Indeed, PDLA can promote crystallization of PLLA by forming stereocomplex which significantly affects the nucleation efficiency.[78, 89, 90]

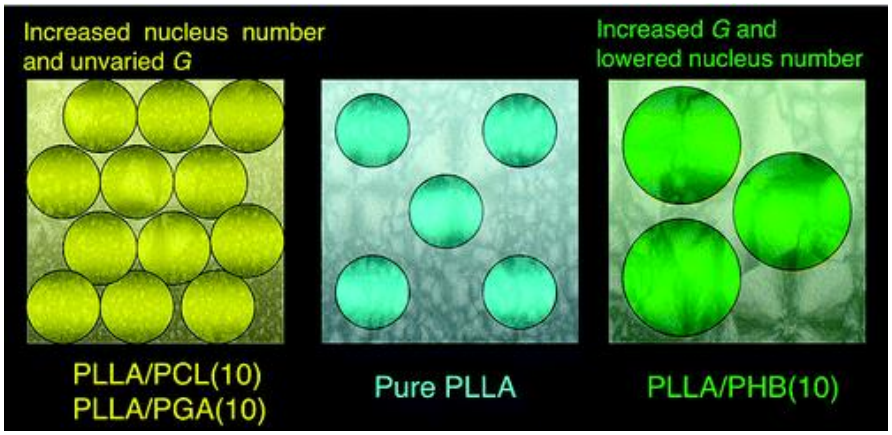

Figure 6.1. PLLA nucleating-assisting ability of some polymers[82]

Strain-induced crystallization also constitutes an effective solution to enhance the PLLA crystallinity. This happened when the polymer is mechanically oriented, which is prevalent during the production of oriented PLLA films, stretch blow molding of bottles, thermoforming of containers, and fiber spinning. The resultant crystallinity generally increases with increasing draw ratio.[91] Other factors such as the mode of stretching (sequential or simultaneous), strain rate, temperature and annealing conditions highly affect the amount of crystallinity.[92]

I.3.3. Physical and Mechanical properties

The specific gravity of amorphous PLLA has been reported as 1.248 $g.cm^{-3}$ and for crystalline PLLA as 1.290 $g.cm^{-3}$ which is lower than that of PET (1.34 $g.cm^{-3}$) but higher than many other conventional thermoplastics which have a specific gravity in the range 0.8 to 1.1 $g.cm^{-3}$

(e.g. PP, PS, LDPE).[93] The optical properties of PLLA are highly dependent to additives and fabrication effects. Indeed, a low degree of crystallinity will induce transparency while highly crystalline PLLA has poor optical properties, even if transparency can be preserved by reducing the crystallites size.

Similarly to the thermal properties, mechanical properties of PLA can be tuned to a large extent depending on the molecular weight, the stereochemical composition and the thermal history of the polymer.[50] Semi-crystalline PLA is generally preferred to the amorphous counterpart when higher mechanical properties are desired. Perego and coll. demonstrated that the modulus of elasticity is almost 20% higher for PLLA than for PDLLA for samples having molecular weights in the range 35 000-55 000 $g.mol^{-1}$.[50] In addition, the same authors showed that the impact strength was also strongly influenced by the crystallinity. Annealing PLLA increases impact strength due to crosslinking effects on the crystalline domains.[9] Furthermore, high molecular weight PLA is generally needed to have access to suitable mechanical properties. Indeed it has been demonstrated that tensile strength and modulus of PLLA increase by a factor of 2 when the weight-average molecular weight is raised from 50 to 100 $kg.mol^{-1}$.[94] Critical molecular weight for entanglement of PLLA melts and entanglement density at 25°C have been reported as 16 $kg.mol^{-1}$ and 0.16 $mmol.cm^{-3}$ respectively.[95]

Isotactic PLA has an approximate tensile modulus of 3 GPa, tensile strength of 50-70 MPa, flexural modulus of 5 GPa, flexural strength of 100 MPa, and an elongation at break of about 4%.[8, 21] As shown in Table 2.1, PLLA presents very similar mechanical properties to standard petroleum based thermoplastics such as PS and PET, especially regarding the values of tensile strength, elastic modulus, flexural strength and flexural modulus. However, similarly to PS, PLLA is a brittle material with regard to its relatively low values of tensile strain at break, tensile toughness and impact strength.

Table 2.1. Mechanical properties of PLLA and some mainstream thermoplastics (PS, PET)

	PLLA	PS	PET
Density ($kg.m^{-3}$)	1.26	1.05	1.40
Tensile strength (Mpa)	59	45	57
Elastic modulus (GPa)	3.8	3.2	2.8-4.1
Elongation at break (%)	4-7	3	300
Notched IZOD IS ($J.m^{-1}$)	26	21	59
Heat deflection (°C)	55	75	67

Heat deflection is also a key parameter which needs to be underlined as one of the main drawbacks of PLLA. Poly(98% L-LA) lost 50% of its elastic modulus and storage modulus at 80°C and 87% of the storage modulus at 100°C. Above the glass transition, non-annealed

PLLA has not sufficient film strength to target a wide range of applications. This lack of film strength at temperature above the Tg can be overcome by increasing the crystallinity of the material. By performing annealing on PLLA sample, heat deflection temperature was increased of 30°C which makes PLLA more suitable for temperature applications.[75]

I.3.4. Rheological properties and Processing

Melt processing of PLLA materials is essential for the conversion into industrial products. Extrusion is the most important technique for continuously melt processing of PLLA. Extrusion is in general linked to a subsequent processing step such as thermoforming, injection molding, fiber drawing, film blowing or extrusion coating. From these, injection molding is the most widely used converting process for PLLA articles.

The different processing technologies for PLLA were reviewed in details by Rubino and coworkers and thus will not be discussed in this manuscript.[10] The success of the conversion process is highly dependent on how the polymer flows. Therefore, melt rheological properties of PLA, which vary with the temperature, the molecular weight and shear rate have to be taken into consideration before processing. The processing of PLLA is a crucial step in the formation of valuable PLLA articles and thus, many attentions have to be taken relative to this process in order to keep the structural, thermal and mechanical properties of the starting polymer. Indeed, PLLA have a narrow processing window due to its tendency to undergo thermal degradation in the molten state. PLLA quickly loses its thermal stability when heated above the melting point with significant molecular weight degradation observed when the material is held 10°C above the melting point for a substantial period of time.[9] The thermal degradation of PLLA has been attributed to many mechanisms such as hydrolysis by trace amounts of water, zipper-like depolymerization, oxidative main-chain scission, intermolecular transesterification to monomer and oligomeric ester, and intramolecular transesterification. During processing, all these degradation mechanisms are influenced by various factors such as the moisture content of the resin, the residual polymerizing catalyst content, the temperature and the residence time of the PLLA melt that need to be optimized to ensure the limitation of the molecular weight drop.[96]

I.3.5. Environmental degradation of PLA

PLLA represents a promising polymer for a wide range of applications due to its good mechanical properties and its biobased character but also due to its compostable behavior. There is a fundamental difference between a biodegradable and a compostable polymer that

need to be mentioned. A biodegradable polymer is a plastic that degrades into carbon dioxide, water and biomass because of the action of naturally occurring microorganisms such as bacteria, fungi, and algae. A compostable polymer also undergoes degradation by biological processes to yield carbon dioxide, water and biomass but it does so in specific conditions to a defined outcome. In general a compostable product breaks down in a specific timeframe in a controlled moist, warm, aerobic environment to produce compost that is non-toxic and can enhance soil and support plant life. All compostable polymers are biodegradable, but not all biodegradable polymers are compostable. PLLA degradation occurs in two stages. First, high molecular weight PLLA is subject to non-enzymatic chain scission of the ester functions by hydrolysis which leads to a reduction of the molecular weight. In a second step, low molecular weight PLLA diffuses out of the bulk polymer and is transformed to lactic acid and low molecular weight oligomers that are naturally metabolized by microorganisms to yield carbon dioxide and water (Figure 7.1).

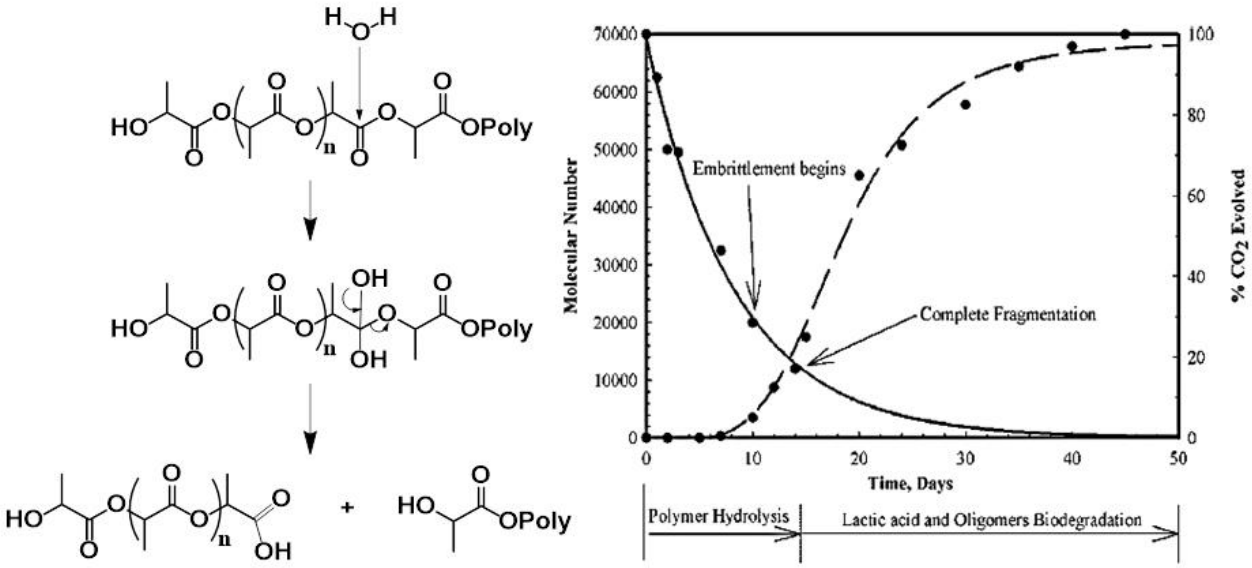

Figure 7.1. Degradation mechanisms of PLA[93]

Various factors have an influence on the biodegradation rate. Indeed exposure conditions can be distinguished from the polymer characteristics. Concerning exposure conditions, moisture, acidity, temperature, aerobic or anaerobic conditions and enzyme specificity are the most influent factors. Other parameters have to be taken into account; i.e. the polymer microstructure that will dictate the chain flexibility and thus the accessibility of the ester functions to water, the crystallinity, the molecular weight, the residual lactic acid concentration and the size and shape of the polymer (surface area). More details about the influence of all these factors on the biodegradation rate can be found elsewhere.[93, 97-102]

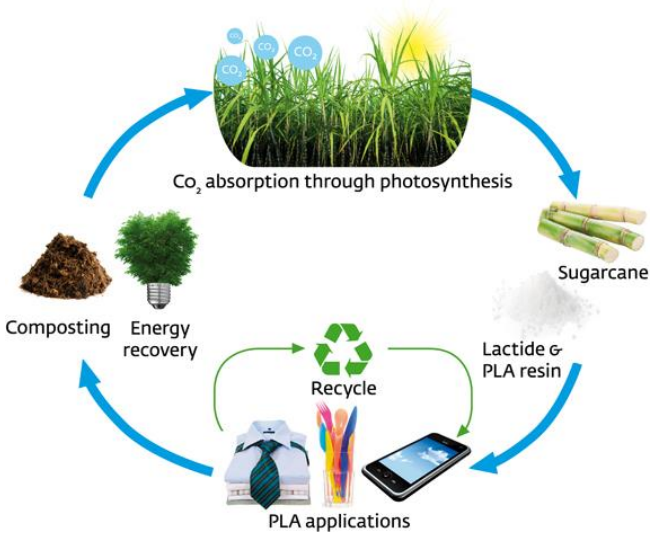

Figure 8.1. PLA life cycle. Source : www.purac.com

Compostability and recyclability of PLLA imply an environmental friendly lifecycle. Indeed, PLLA presents a cradle to cradle lifecycle where products are produced from sustainable and natural resources. In this type of lifecycle, the polymer is used, re-used and recycled as much as possible. At their end-of-life, when the products don't satisfy their functional requirements anymore, these products are transformed back into feedstock for a new product lifecycle (Figure 8.1).

I.4. Summary of PLA development and remaining challenges

PLLA is a very promising and versatile compostable polymer which has an interesting technical substitution potential. The main issue that restricts the development of PLLA in a wide range of applications seems to be its price (1.90€/kg). However this trend is expected to be reversed in the next years as seen from the improvement of biotechnological processes, the increasing oil prices and the implementation of environmental policies from the government. Nevertheless, there are a number of areas for which PLA-based materials drawbacks still need to be overcome to consider efficient and feasible substitution of existing thermoplastics. For instance, in packaging applications where high barrier protection is essential for the conservation of food products, efficient solutions need to be found as barrier properties of PLLA are not in par with those of PET or PE. Examples of current investigations deal with the addition of nanoparticles such as nanoclays.[103, 104] Another drawback that needs to be significantly improved is the enhancement of PLLA crystallization rate. Numerous solutions were already found; however, finding a highly efficient solution fitting with the high speed mass production is still a challenge. We have seen that the compostable character of PLLA represents an important advantage in environmental applications; nevertheless, aging studies

related to the specific conditions of use still need to be conducted in a more precise way in order to anticipate the biodegradation rate. Another area that needs to be studied and improved is the energy and raw materials consumption of PLLA production and its impact on the environment. Related to this, Vink and coworkers published an interesting paper presenting the life cycle assessment (LCA) of NatureWorks PLA.[3] In particular it was mentioned that Cargill Dow's objectives are to decrease the fossil energy use from 54MJ/kg PLA down to about 7MJ/kg PLA and to decrease the greenhouse gases emission from +1.8 down to -1.7 kg CO_2 equivalents/kg PLA. Finally, the inherent brittleness of PLLA is a major bottleneck for its use in applications where toughness and impact resistance are critical.

II. TOUGHENING OF PLA, TOWARD ENLARGED APPLICATIONS

II.1. Principle of toughening of brittle polymers

All the PLA properties that have been mentioned above explain the increasing interest for this versatile material. Despite its numerous advantages, the inherent brittleness of PLA seems to be one of the most limiting factors for its wide applications in many fields. In this section, we will summarize the most prominent works that have been dedicated to the toughening of PLA these last years. A tough material is a material that absorbs a large amount of energy before failure, in contrast to a brittle one that does not. At a given temperature which depends on the structure and morphology of the polymer, the geometry of the specimen, and the nature and speed of the test or other energy input, a polymer material undergoes what is known as a ductile-brittle transition. Below this temperature, the material breaks in a brittle manner; above this temperature, the material breaks in a ductile (high impact energy) fashion (Figure 9.1). Thus the aim of most researches devoted to PLA toughening is to lower the ductile-brittle transition temperature in order to observe a ductile fracture behavior of the material at its service temperature.

The toughness of polymers is generally evaluated by several techniques including tensile elongation tests and impact strength tests. Unlike impact tests, tensile elongation, which generates the well-known stress-strain curve, is a relatively slow-speed test, and is one of the least severe toughness tests. Indeed, a moderate rate of loading is commonly used. Also, the imposed stresses in tensile loading tests are uniaxial, whereas most materials are much more brittle in biaxial and triaxial states of stress than they are in uniaxial loading. Consequently, impact tests are generally carried out to confirm the fracture behavior observed by tensile tests.

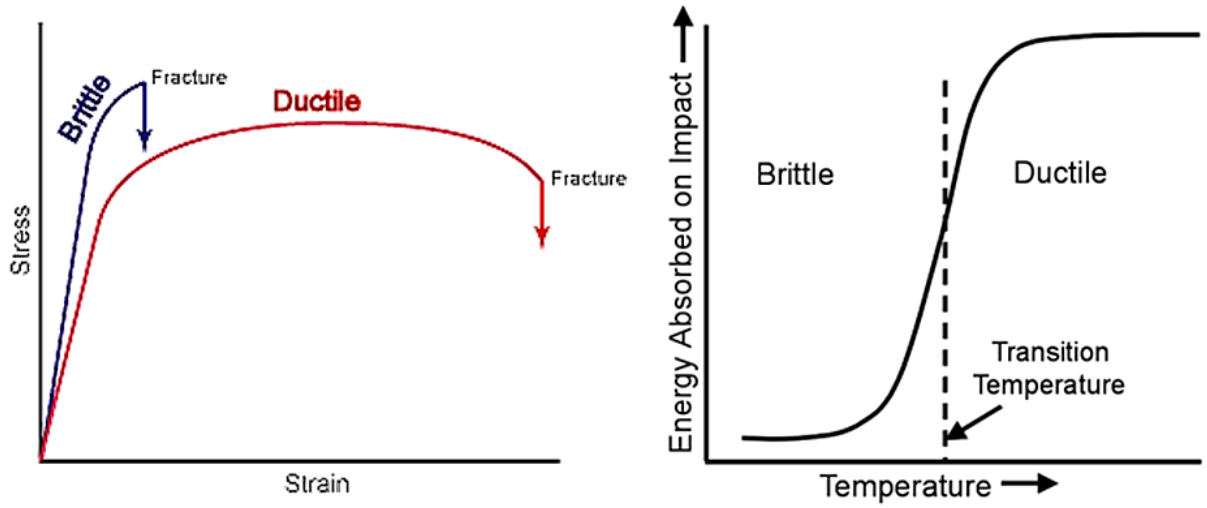

Figure 9.1. Typical stress-strain curves of brittle and ductile materials and evidence of a ductile-brittle transition

Impact strength is not a fundamental material property as it depends upon specimen geometry and the particular test method employed. Impact strength is generally measured by either pendulum tests, falling weight tests or tensile impact tests.

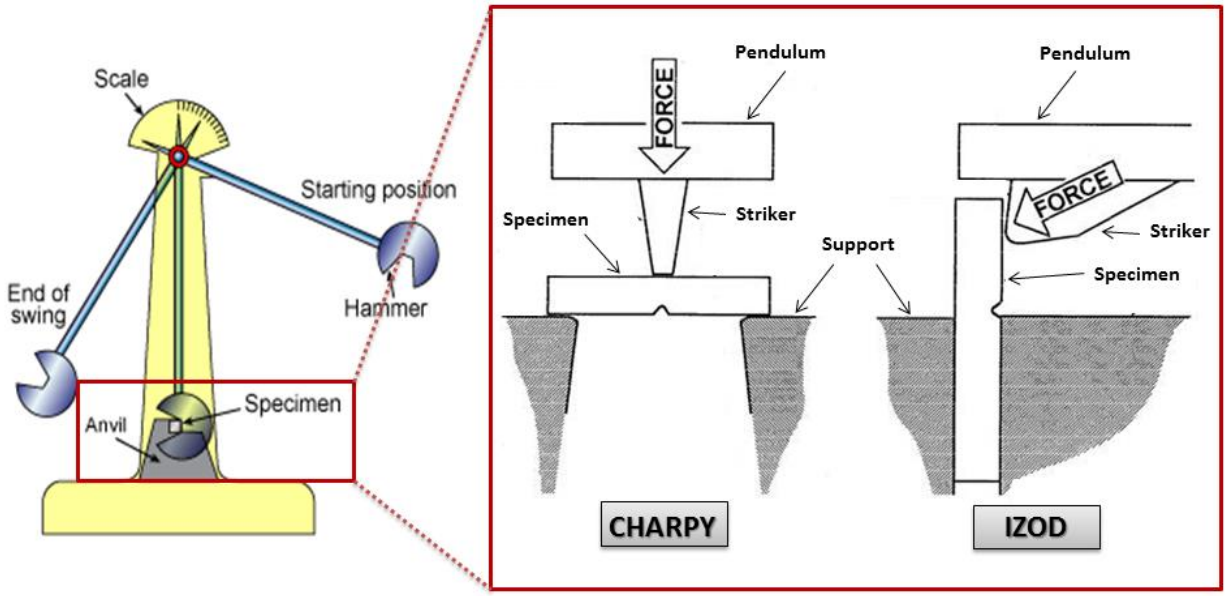

Figure 10.1.Description of Charpy and Izod pendulum impact strength tests.

Pendulum tests are frequently used to determine crack propagation resistance because of the low cost of the instruments, the test simplicity, convenience and acceptance by the polymer industry. Pendulum-type machines are used for notched or unnotched specimens that may be of different sizes and clamped as a cantilever (IZOD) or as an unclamped bar supported at both ends (CHARPY) (Figure 10.1). These tests determine the resistance to breakage by flexural shock, in terms of difference between the potential energy of the striker before and after impact. The impact strength is usually measured in $J.m^{-1}$ (thickness) or $kJ.m^{-2}$ (thickness

+ width). Additional information concerning the impact tests can be found in the ‘methods” part.

It was already mentioned that PLA got close similarities to PS in terms of mechanical properties. PS, being a mainstream thermoplastic widely used in many applications, has been some years ago the subject of extensive investigations related to the limitation of its brittleness. This led to the development of rubber-modified high impact PS and its copolymers such as styrene-butadiene-styrene and acrylonitrile-butadiene-styrene copolymers. The new properties that can be reached by such modifications opened new opportunities in advanced engineering applications. Due to the recent efforts to promote the use of PLA as specialty and commodity plastic, many strategies have been developed to improve the toughness and the impact strength for this polymer. These solutions include plasticization, addition of rigid fillers, copolymerization and blending with flexible polymers or rubbers.

Plasticization was extensively used to improve the processability of PLA but also to enhance its flexibility and ductility. Indeed, in the case of PLA, the ductile-brittle transition is occurring around the glass transition of the polymer (around 50-60°C). Thus the depression in Tg induced by the addition of a plasticizer is thought to lower also the ductile-brittle transition temperature. To evaluate the efficiency of a plasticizer, the depression in Tg and the enhancement in tensile toughness are generally taken into account and are directly linked to the miscibility of the plasticizer with the matrix, its molecular weight and its loading level. Thus various plasticizers of PLA were investigated such as monomeric, oligomeric and polymeric ones. Low molecular weight plasticizers exhibit high plasticizing efficiency, however migration phenomenon responsible for a loss of mechanical properties is generally observed with time. On the contrary, higher molecular weight plasticizers will result in lower efficiency but migration will be limited. Thus a balance between efficiency and migration has to be considered when choosing the plasticizer. Among all the reported plasticizers, polyethylene glycol,[105] lactide[106] and citrate esters are the most used.[107] Plasticizers are effective at increasing the ductility of PLA, however they are more considered as flexibilizing agents than as impact modifiers. Indeed marginal effects of plasticizers on the impact strength of PLA are generally described. Thus, this way of limiting the brittleness of PLA will not be discussed in this manuscript. More information can be found elsewhere in the literature.[32, 107]

Many uncommon techniques were also employed to toughen PLA. For instance rigid fillers such as carbon fibers and calcium carbonate were introduced in PLA matrix, resulting in slight enhancement of the impact strength.[108, 109] Other unusual impact modifiers have been

developed to toughen PLA such as hyperbranched polymers (HBPs)[110-112] and vegetable oils derivatives.[113, 114, 115] Some investigations regarding the formation of semi-interpenetrating networks within a PLA matrix also yielded to enhanced ductility.[116] Improvement in flexibility was also observed by orientation during melt processing or drawing below the glass transition temperature.[117]

Literature regarding the toughening of PLA is abundant and it is a difficult task to make an exhaustive review of the different solutions that were developed these last years concerning this topic. The bibliographic part of this manuscript is designed to provide an overview of rubber-toughening approach (more precisely, the block copolymerization and the melt-blending approaches), as a main strategy adopted in the literature to increase the flexibility as well as the impact strength of PLA. In order to avoid ambiguity, in all this manuscript and more generally in the PLA-toughening domain, the term "rubber" means any low Tg linear thermoplastic.

Almost any engineering plastic can be made tougher without unacceptable loss of stiffness, by the addition of a small amount of rubbery material. Irrespective of the exact toughening mechanism, the rubber should be dispersed as discrete particles on a microscopic scale (nanoscopic scale for block copolymers) and be well bonded to the rigid polymer matrix. The particles can be incorporated via blending a rubber within the polymer matrix, or by copolymerizing a rubber with the matrix polymer, taking advantage of the natural segregation of immiscible polymers. The immiscibility of the rubber with the matrix is one of the main criteria for effective toughening, especially in the case of polymer blends. If phase separation between the rubber particles and the polymer matrix does not occur, the dissolved rubber will act as a plasticizer, thus improving impact resistance in some cases, but most likely lowering the stiffness and thermal resistance to an unacceptable level. On the other hand, rubber should have good interfacial adhesion to the matrix in order to obtain a fine distribution of the rubber particles (usually 0.1-1.0 µm).

The rubber type has a huge influence on the efficiency of the toughening as it will dictate the absorption of energy and the limitation of crack propagation. Thus, it is desirable that the rubber has the lower Tg possible, while still being able to maintain a degree of structural integrity in response to impact loading. In any rubber-toughened system, it exists a temperature below which the toughening becomes ineffective. It generally happens when the viscoelastic response of the rubber becomes too slow to absorb the applied stress. Figure 11.1 shows the importance of the Tg of the rubber. The lower the Tg of the rubber, the lower the ductile-brittle transition temperature of the blend (or the copolymer). Finally the additive

should be thermally stable during processing and subsequent end use to give rise to a stable and efficient polymers alloy.

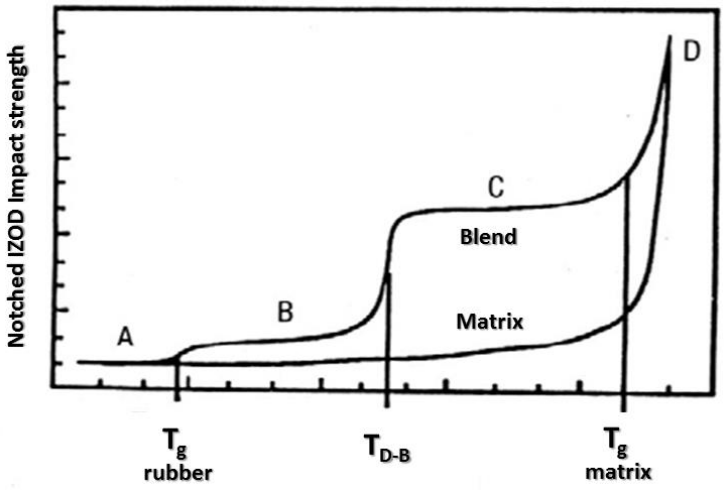

Figure 11.1.Impact strength of rubber-toughening materials as a function of the temperature

In the following, we propose to present the most prominent strategies that were investigated for PLA toughening. The first strategy deals with the copolymerization of PLA with soft and ductile rubbers. This approach is highly efficient in the technical point of view, however the high cost of production of the resulting materials is not in agreement with the industrial expectations regarding the lowering of the price (and thus the production cost) of PLA. The second strategy concerns the toughening of PLA by melt blending with ductile polymers or rubbers.

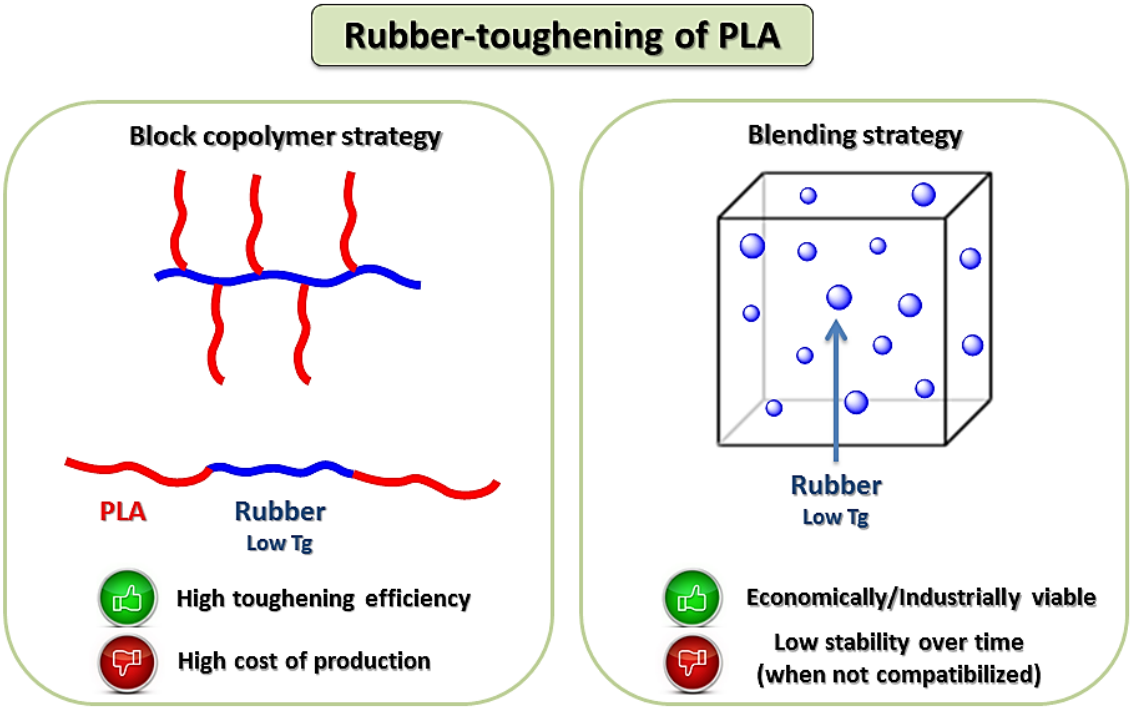

Figure 12.1. Strategies for the rubber-toughening of PLA

Blending is the most industrially used method as seen from the low cost of production and the low processing constraints needed for the elaboration of these toughened polymer alloys (Figure 12.1). Highly efficient solutions were found regarding the toughening of PLA by using non-degradable petroleum-based rubbers, both concerning copolymerization or melt-blending approaches. However due to environmental concerns, the most recent investigations have mainly focused on the use of biodegradable and/or biobased impact modifiers. Thus we decided in this manuscript to highlight these environmentally friendly solutions to PLA brittleness.

II.2. Copolymerization

Copolymerization presents a powerful mean to obtain properties unattainable with homo-PLA. By varying the nature of the comonomers, the composition and the architecture, a large range of properties including tensile and impact performances can be tailored. The synthesis of statistical and block copolymers have been carried out with a range of comonomers either through polycondensation of lactic acid with other condensable monomers or through ring-opening polymerization of LA with cyclic monomers or initiated with various macroinitiators. In this part, special attention is paid onto the direct use of PLA-based copolymers as novel tough materials (not as additives).

II.2.1. Linear random PLA-based copolymers

Lactic acid presents both acid and hydroxyl groups which makes it feasible to copolymerize through polycondensation. Thus, various hydroxyacids were used as comonomers for the design of new random copolymers. L-lactic acid has been polycondensed with D,L-mandelic acid,[118] D,L-α-hydroxybutyric acid,[119] D,L-α-hydroxyisovaleric acid,[119] D,L-α-hydroxycaproic acid[119] and ricinoleic acid.[120] However all these new materials present quite low molecular weights. The needed elimination of the condensated products, which is responsible for the low molecular weights in polycondensation, can be overcome by adopting ring-opening polymerization instead of polycondensation.

Thus various cyclic esters and carbonates were used for the ring-opening copolymerization with lactide. Homopolymers of ε-caprolactone (CL) and trimethylene carbonate (TMC) are two ductile and biodegradable polymers. Indeed the low Tg of PCL and PTMC (-60°C and -20°C respectively) make them good candidates for the toughening of PLA. Random copolymerization is expected to significantly lowered the Tg of PLA and thus to improve the toughness of the resulting material. Hiljanen-Vainio and coll. copolymerized L-LA and D,L-

LA with CL by varying the monomer ratio between LA and CL (from 80/20 to 40/60).[121] Most copolymers exhibited elongation at break above 100%, however a balance with the lowered values of tensile modulus and strength was noticed. Grijpma and coll. copolymerized CL and TMC with LA and observed a significant increase in impact strength and elongation at break values while increasing the amount of CL.[108] Indeed unnotched IZOD impact strengths of the compression molded samples changed from 18 $J.m^{-1}$ for 3% of CL to 219 $J.m^{-1}$ for 10% of CL in the copolymer structure. Similar toughness enhancement by copolymerization with TMC was reported by Ruckenstein and Yuan.[122] Another example of random copolymers synthesized by ROP was described by using β-methyl-δ-valerolactone (MV) as a comonomer of L-LA.[123] Both the Tg and the Tm of the copolymers were decreased with an increase in the MV content. Above 20 mol% of MV, the copolymers became amorphous. The copolymers containing less than 10 mol% MV formed tough and hard films, whereas those with more than 20 mol% formed flexible films. At 8 mol% of MV, the elongation at break reached 680% and tensile strength was 38 MPa.

Thus toughening of PLA by random copolymerization with other cyclic esters or carbonates was proved to be efficient. However the randomness of the copolymers includes a loss of the thermal properties of PLA. To overcome the lowering of the crystallinity by the incorporation of soft segments, block copolymerization is a good approach as it enables a wide range of mechanical properties while maintaining good thermal properties.

II.2.2. Linear and graft PLA-based block copolymers

While statistical copolymerization is limited to monomers that are able to polymerize through a ROP or a polycondensation manifold, block copolymers can be synthesized with a wide range of monomers using various polymerization methods. One can distinguish the PLA-based block copolymers synthesized by sequential ROP when comonomers are cyclic esters or carbonates, and block copolymers synthesized by distinct polymerization methods. In the latter case, most of the time, a macroinitiator is first synthesized by another polymerization method than ROP and then ROP of LA is initiated by the reactive functions of the macroinitiator. By selecting appropriate segments and composition, ABA triblock copolymers and graft block copolymers are able to behave as thermoplastic elastomers (TPEs) or high impact thermoplastics (Figure 13.1). By the same principle, high impact PLA can be obtained by copolymerization with a rubber in minor amount. The soft phase will then absorb the energy during the impact and thus limit crack extension.

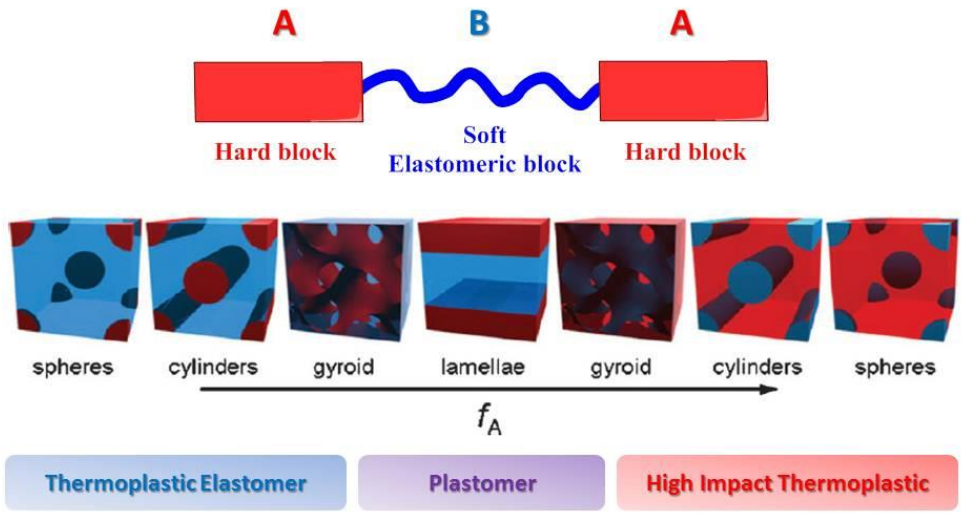

Figure 13.1. Morphologies and mechanical behaviors of block copolymers as a function of the composition

By playing on the chemistry and on the macromolecular architecture, a large range of ABA, graft and multi-block copolymers with PLA as hard segments were reported in the literature. Due to an abundant literature on PLA-based block copolymers, we propose in this part to focus on the works which described the influence of the copolymer composition on the mechanical properties.

ABA block copolymers synthesized by distinct polymerization methods.

In a first example, Hillmyer and coll. described the synthesis, by anionic polymerization, of α,ω-hydroxyl poly(isoprene) (PI).[124] The α,ω-hydroxyl PI was then used as macroinitiator for the ROP of LA resulting in PLA-*b*-PI-*b*-PLA triblock copolymers with different compositions depending on the ratio LA/HO-PI-OH. All the triblock copolymers displayed evidence of microphase separation as seen from the spherical, hexagonal and lamellar PLA phases revealed by SAXS analysis. The cylindrical phase-forming copolymer presented the highest value of strain at break (650%) but for all copolymers, Young's modulus and ultimate strength values were quite low in comparison to neat PLA due to the high content of soft phase in these materials.[125]

Perfluoropolyether (PFPE) and PLLA block copolymers have also been evaluated. PLLA-*b*-PFPE-*b*-PLLA triblock copolymers were prepared by ROP of L-LA initiated by a commercially available α,ω-hydroxyl PFPE.[126] A dramatic increase in elongation at break was observed (>300% vs 10-15% for neat PLLA) with a PFPE content as low as 5wt%. This improvement of the ultimate strain value was linked to a slight decrease of the tensile strength and modulus of the copolymers.

In order to enlarge the scope of soft polymers used for the toughening of PLA by copolymerization, Pitet and Hillmyer have described the synthesis of ABA triblock copolymers with PLA as end blocks and poly(1,5-cyclooctadiene) (PCOD), synthesized by the ring-opening polymerization (ROMP) of 1,5-cyclooctadiene, as mid-block (Scheme 4.1).[127] A hydroxyl terminated telechelic PCOD was used as a macroinitiator for the ROP of LA. By varying the chemical composition of the copolymers ($0.24<f_{PLA}<0.89$), a wide range of ordered-state morphologies and thermo-mechanical properties were obtained.

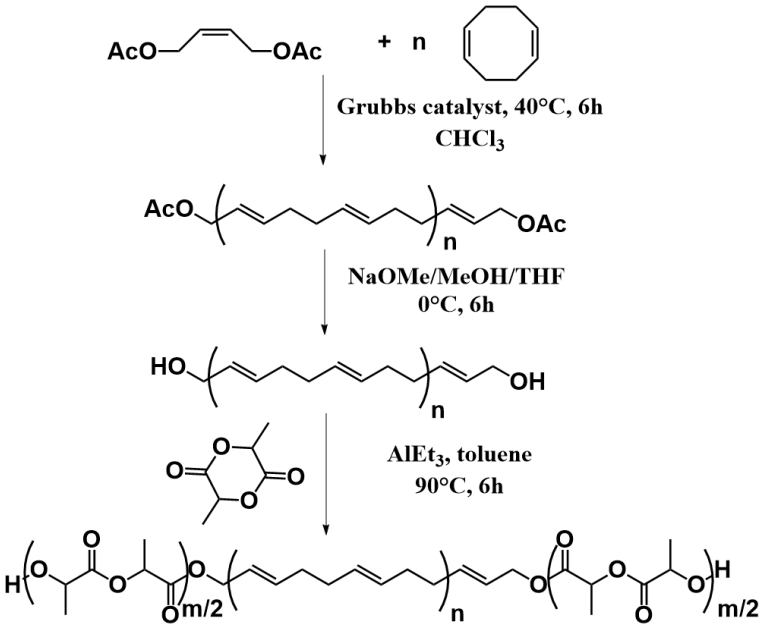

Scheme 4.1. Successive Ring Opening Metathesis Polymerization of cyclooctadiene and ROP of lactide to the synthesis of triblock copolymers[127]

Stiff and ductile materials were realized as evidenced by the good mechanical properties obtained, in particular for low content of PCOD. Most notably, the sample with a PLA volume fraction of 0.89 showed a modulus of 1.3 GPa, an average elongation of 42%, a yield strength of 38 MPa, and tensile strength of 33 MPa.

Toughening modification of PLA has been also attempted by graft copolymerization using PCOD as a rubber part.[128] Similar approach than the previous study has been employed, namely the ROMP of 1,5-cyclooctadiene (COD). Branching points were introduced by using 5-norbornene-2-methanol as a hydroxyl-bearing comonomer. The statistically distributed pendant primary hydroxyl groups were then used to initiate the ROP of LA. In this study, the aim was to get a large amount of PLA in the copolymer (95wt% of PLA) in order to keep the interesting mechanical properties of PLA. Tensile experiments pointed out an improved ductility (1700 % increase in the elongation at break relative to PLA) for the block copolymer with slight lowering of the stiffness compared to neat PLA (Young's modulus value of 1.86 GPa vs 2.03GPa for neat PLA).

Triblock copolymers of various compositions were synthesized by ROP of L-LA initiated with hydroxyallyl telechelic polyisobutylene (PIB).[129] Two macroinitiators were used with molecular weights of 3400 g.mol^{-1} and 6700 g.mol^{-1} respectively. Chain-extension of the triblock copolymers was then carried-out with 4,4'-methylenebis(phenylisocyanate) (MDI) yielding multi-block copolymers with molecular weights up to 71 kg.mol^{-1}. The block copolymers showed two distinct glass transition temperatures indicating microphase separation. Tensile properties of these multi-block copolymers were highly dependent on the amount of PLA segment in the copolymer structure. Tensile strengths were in the range 8-24 MPa with elongations at break in the range 2.5-400%.

ABA block copolymers formation by sequential ROP.

Preparation of block copolymers by ROP from sequential addition of lactone or cyclic carbonate compounds and LA is a much more practical technique than all the studies described above. Indeed, the living character of most of catalyzed ROP enables the easy control of the macromolecular architecture by choosing the appropriate initiator and monomers. Several cyclic monomers were copolymerized with LA such as glycolide, β-butyrolactone (βBL), ε-caprolactone (CL), 1,5-dioxepan-2-one (DXO) and trimethyl carbonate (TMC). In most of the studies, the synthetic strategy was based on the ROP or random ring-opening copolymerization of cyclic esters or carbonates initiated by a diol. Thus soft α,ω-hydroxyl telechelic prepolymers are formed. Addition of LA monomer is then performed yielding in a α,ω-hydroxyl telechelic triblock copolymer (Scheme 5.1). The resulting material can then be used as it is or can be chain-extended by using diisocyanates to obtain multiblock copolymers.

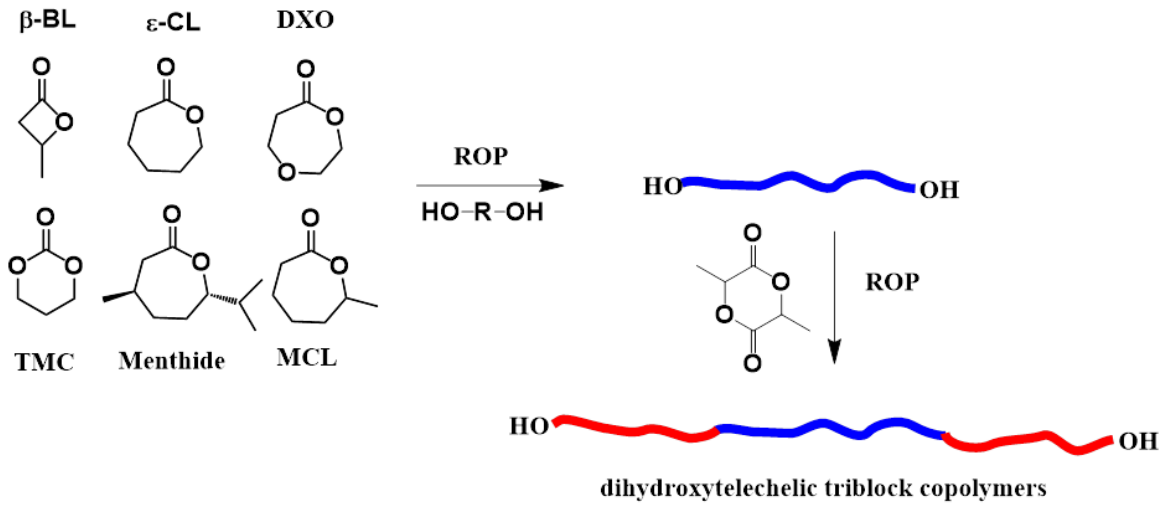

Scheme 5.1. Main cyclic monomers and schematic pathway to the synthesis of triblock copolymers by sequential ROP

In a first example, Grijpma and coll. reported the use of various rubbers as mid-block in the preparation of ABA triblock copolymers where A is a 85/15 L/D lactide block.[130] Rubbers were prepared from TMC and 50/50 (mole ratio) mixtures of TMC and CL by ROP using 1,6-hexanediol as an initiator. These soft polymers are of high interest for PLA toughening due to the hydrolysable behavior of both PTMC and PCL. Thus the resulting block copolymers should be compostable. Moreover, investigations undertook to promote the use of PTMC as a biobased material, have led to the efficient conversion of glycerine, a by-product of biodiesel production into TMC via 1,3-propanediol.[131] In the case of block copolymers with PTMC as a rubber part, the amount of rubber block in the copolymer composition was varying from 8 to 21 wt%. A significant improvement in the strain at break and the impact strength values was noticed while increasing the amount of rubber. Strain at break changed from 7.5% for neat PLA to 280% for the sample with a PTMC weight fraction of 21%. However tensile strength decreased from 62 MPa to 36 MPa. Similar trend was observed for the block copolymers with P(TMC/CL) as a rubber part.

Subsequently, Feijen and coll. investigated the effect of the stereochemistry of the PLA blocks (in PLA-*b*-PTMC-*b*-PLA triblock copolymers) on the mechanical properties of these materials.[132] In this study, thermoplastic elastomer behavior was targeted as seen from the low content of PLA in the copolymers structure (from 9.6 to 42.3 mol% of LA content). Better mechanical properties were obtained when L-LA or D-LA were used instead of D,L-LA due to the crystallization of the end-blocks that induced higher Young's modulus and higher tensile strength. Further improvement in the mechanical and thermal performances was achieved by stereocomplexation when equimolar blends of PLLA-*b*-PTMC-*b*-PLLA and PDLA-*b*-PTMC-*b*-PDLA were realized.

More recently, Guillaume and coll. reported the sequential copolymerization of TMC and L-LA using several catalytic systems.[133] Various macromolecular architectures were studied such as diblock PLLA-*b*-PTMC, triblock PLLA-*b*-PTMC-*b*-PLLA and 3-arm star PTMC-*b*-PLLA depending on the functionality of the initiator used. Significant improvement of PLA brittleness was achieved as seen from the elongation at break value that reached 328% for a PTMC segment of 10 $kg.mol^{-1}$ and a PLLA segment of 23 $kg.mol^{-1}$.

Triblock copolymers with PLLA as end-blocks and a rubber prepared from TMC and 1,5-dioxepan-2-one (DXO) as mid-block was also prepared for biomedical applications.[134] In this study, the influence of the chemical composition of the rubber part was correlated to the toughness of the copolymer. Thus the properties of the PLLA-*b*-P(TMC/DXO)-*b*-PLLA copolymers with various amounts of TMC and DXO were compared with those of PLLA-*b*-

PTMC-*b*-PLLA and PLLA-*b*-PDXO-*b*-PLLA copolymers.[135] It was observed that the copolymer with a rubber block made from equimolar amounts of TMC and DXO showed the better mechanical properties with values of Young's modulus and strain at break of 66 MPa and 1089 % respectively.

Poly(ε-caprolactone) (PCL) is a common aliphatic polyester, mainly used in biomedical applications due to its biocompatibility and to its degradability in hydrolytical conditions. However, very few studies report the interesting mechanical properties that these materials exhibit. In a first study, Ha Kim and coll. reported the synthesis and characterization of PLLA-PCL multi-block copolymers.[136] The corresponding random and ABA triblock copolymers were synthesized in order to compare the properties with the multi-block copolymers. It was shown that the random copolymer was completely amorphous, the multi-block copolymers exhibited only one melting peak corresponding to the PLLA phase, while the triblock copolymer exhibited two melting peaks corresponding to PLLA and PCL phase. The triblock copolymer had the best mechanical properties showing the effect of the macromolecular architecture on the overall properties.

Thermoplastic elastomers based on PLLA-PCL multi-block copolymers were also designed by Hotovely Salomon and Cohn.[137] In this study, the authors carried out the chain extension of ABA triblock copolymers composed of PCL mid-block and PLLA hard end-blocks, by using hexamethylene diisocyanate. In the ABA triblock copolymers, the PCL flexible segment was maintained at 2000 $g.mol^{-1}$ while each PLLA blocks covered the 550-6000 $g.mol^{-1}$ molecular weight range. After chain-extension, the multi-block copolymers were obtained with molecular weights between 89 and 124 $kg.mol^{-1}$. These thermoplastic elastomers exhibited high strength (ultimate tensile strength around 32 MPa), high flexibility (Young's modulus as low as 30 MPa) and remarkable elongation (elongation at break above 600%).

Triblock copolymers were also synthesized by ROP of L-LA initiated by a CL based hydroxyl terminated rubber.[138] The latter was prepared by random ring-opening copolymerization of L-LA and CL leading to a completely amorphous rubber. Good flexibility of the copolymers was noticed with elongation at break values above 200%.

The synthesis of amorphous ABA triblock copolymers was also conducted from a poly(6-methyl-ε-caprolactone) (PMCL) rubber mid-block.[139] The polymerization of MCL by ROP initiated by a 4-benzenedimethanol/$Sn(Oct)_2$ system yielded a low Tg (-45°C) amorphous hydroxyl-terminated PMC that was subsequently used as macroinitiator for the ROP of LA. Two triblock copolymers with PLA content of 20 and 34wt% respectively were selected for

tensile test investigations. Young's modulus values were 1.87 MPa and 31 MPa, and elongation at break values were 1880 % and 1360 % respectively.

Hillmyer, Tolman and coll. have investigated the conversion of (-)-menthone into (-)-menthide by a Baeyer-Villiger procedure in order to synthesize a new polyester rubber.[140] Indeed, (-)-menthide, a seven-membered lactone was readily polymerized by ROP yielding an amorphous low Tg (-22°C) aliphatic polyester. By using a central diethylene glycol initiating unit with $ZnEt_2$, a dihydroxyl terminated poly(menthide) (PM) was obtained which was used to initiate the chain growth of *rac*-LA (Scheme 6.1). The low amounts of PLA blocks in these PLA-*b*-PM-*b*-PLA copolymers yielded materials with good flexibility (960% at break) but poor stiffness (Young's modulus of 1.4 MPa).

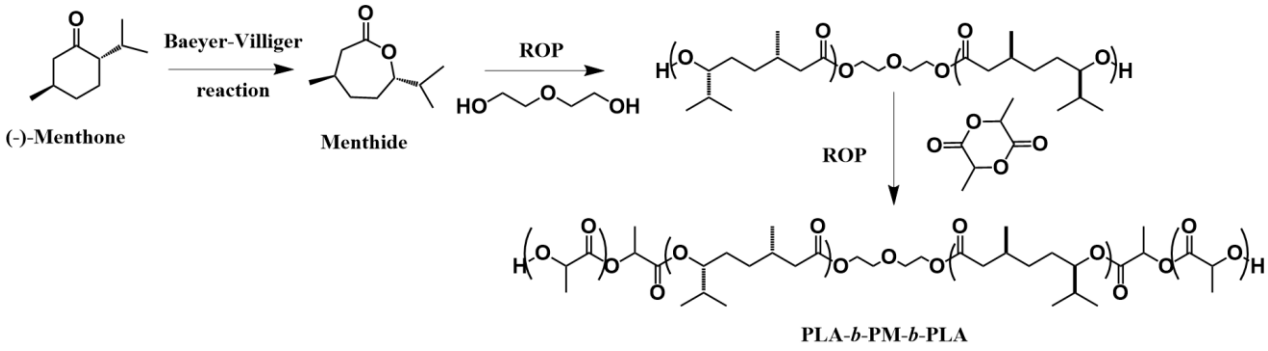

Scheme 6.1. Synthesis of PLA-b-PM-b-PLA copolymers by successive ROP of menthide and lactide[141]

The same authors evaluated the influence of the PLA blocks stereochemistry on the mechanical properties of these triblock copolymers.[142] Interestingly, the copolymers with enantiopure PLLA blocks showed a three-fold increase in tensile strength and a two-fold increase of the Young's modulus compared to the amorphous atactic PLA-containing copolymers. Further improvement of the mechanical properties was performed by blending PLLA-*b*-PM-*b*-PLLA with equal amounts of PDLA-*b*-PM-*b*-PDLA resulting in stereocomplex formation. By this way, Young's modulus value was about 30 MPa, tensile strengths of around 20 MPa and ultimate elongations of around 1000 %.

Sequential ROP was also used for the preparation of triblock copolymers with a poly([R,S]-3-hydroxybutyrate) (PHB) mid-block.[143] ROP of [R,S]-β-butyrolactone (βBL) was first carried out in the presence of 1,4-butanediol with distannoxane as a catalyst. The resulting low Tg (between -6°C to 5°C) hydroxyl-terminated PHB was then used to initiate the ROP of L-LA. The obtained triblock copolymers had a Young's modulus which increased with increase in PLLA content (from 30 to 160 MPa for 44 to 69 % PLLA respectively) in line with a decrease in elongation at break from 200 to 86%. In another approach, Mehrkhodavandi and coll. synthesized PLLA-*b*-PHB-*b*-PLLA and PLLA-*b*-PHB-*b*-PDLA triblock copolymers by a

convenient and simple consecutive addition of monomers.[144] In all cases, copolymers with high molecular weights (above 100 kg.mol^{-1}) were obtained. In this study, low PHB contents (from 4 % to 30 %) were targeted in order to obtain stiff and tough materials. Similarly to the previous study, tensile experiments showed an increase of the flexibility (elongation at break up to 21%) with increase in PHB content. Relatively high values of tensile strength and elastic modulus were maintained due to a low incorporation of soft block in the copolymer structure.

Summary of block copolymerization solutions.

From all the reported investigations regarding linear ABA, graft or multi-block copolymers (Figure 14.1), we can ensure that this approach to the toughening of PLA is efficient and versatile. In all cases, improvement in flexibility was noticed (nevertheless, very few data can be found on the impact strength of these systems). However most of the described examples targeted thermoplastic elastomer applications. Thus, high contents of rubber were needed which implied a lowering of the stiffness.

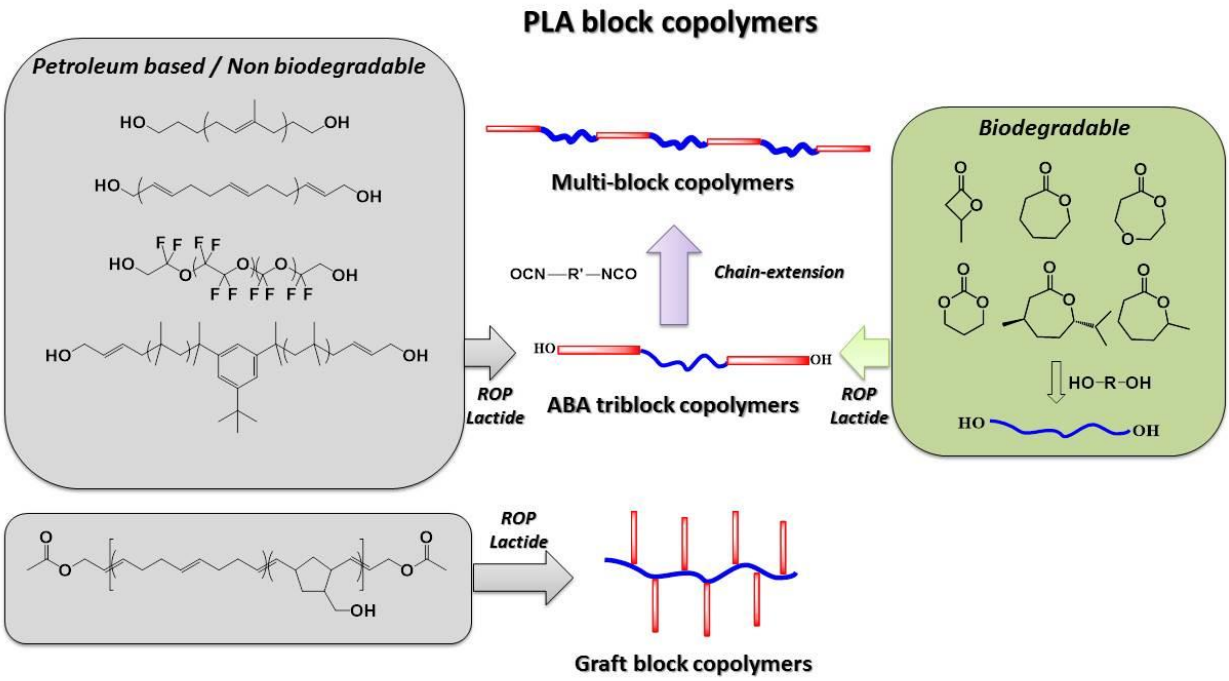

Figure 14.1.Synthetic strategies to PLA block copolymers.

Development of similar systems with a higher content of PLA could bring much more interesting properties for the targeted applications of PLA. The major drawback of the copolymerization approach to toughen PLA is the high cost of production of such materials. The use of these block copolymers as additives in blends with PLLA could be a solution to

lower the price, however it would result in nano-sized soft domains while micro-sized domains (0.1-1µm) are required for efficient toughening. Therefore, PLA-based block copolymers would be more adapted to high value and specialty applications. More economical solutions need to be found in order to target commodity applications.

II.3. Melt blending with other polymers

Polymer blends have provided an efficient way to fill new requirements for material properties. Indeed melt blending allows access, in an economic and convenient way, to properties unattainable with the homopolymers. Based on these concepts, various types of rubber were melt-blended with PLLA in an effort of increasing the impact strength of the resulting material. In the next part, biodegradable were distinguished from non-biodegradable rubbers in order to identify the most suitable additives. A special emphasis has been made on biodegradable additives as the rubber melt-blended with PLLA should ideally be biodegradable to maintain the compostability of PLLA.

II.3.1. Non-biodegradable polymeric impact modifiers

Having recourse to non-biodegradable petroleum-based polymers for the toughening of PLLA by melt blending constitutes an economic and viable mean to overcome the brittleness of PLLA. Indeed, the chemistry and the mechanical properties of readily available petroleum-based thermoplastics such as olefinic, acrylic and styrenic based polymers are well-known which provide the insurance to get the expected modifications of PLLA. Nevertheless, due to the abundant literature and the publication of exhaustive reviews focusing on the toughening of PLLA, we decided to only give an overview of the most significant works that used non-biodegradable and petroleum-based polymeric impact modifiers.

Polyethylene (PE) is currently the most produced polymer in the world which makes it an economic solution for a wide range of applications. Moreover PE is a highly versatile material with properties that can be tuned by playing on its density. In particular, low density PE (LDPE) is a highly ductile material with high impact strength (700 $J.m^{-1}$). Thus PE based polymers have been extensively used for the toughening of PLLA by melt blending.[145-152] Various grades of PE have been used such as high density PE (HDPE) and linear low density PEs (LLDPE) which include ethylene-octene copolymers. Various solutions were found to improve the miscibility between the two phases such as the addition of diblock copolymers (Figure 15.1) or the use of ethylene-*co*-vinyl acetate (EVA) copolymers that showed improved interfacial adhesion with PLLA as compared to PE. The reactive extrusion of PLLA

with PE based materials bearing reactive functions such as glycidyl methacrylate units was also reported (Figure 16.1). In all compatibilization approaches, significant increase of the impact strength was noticed.

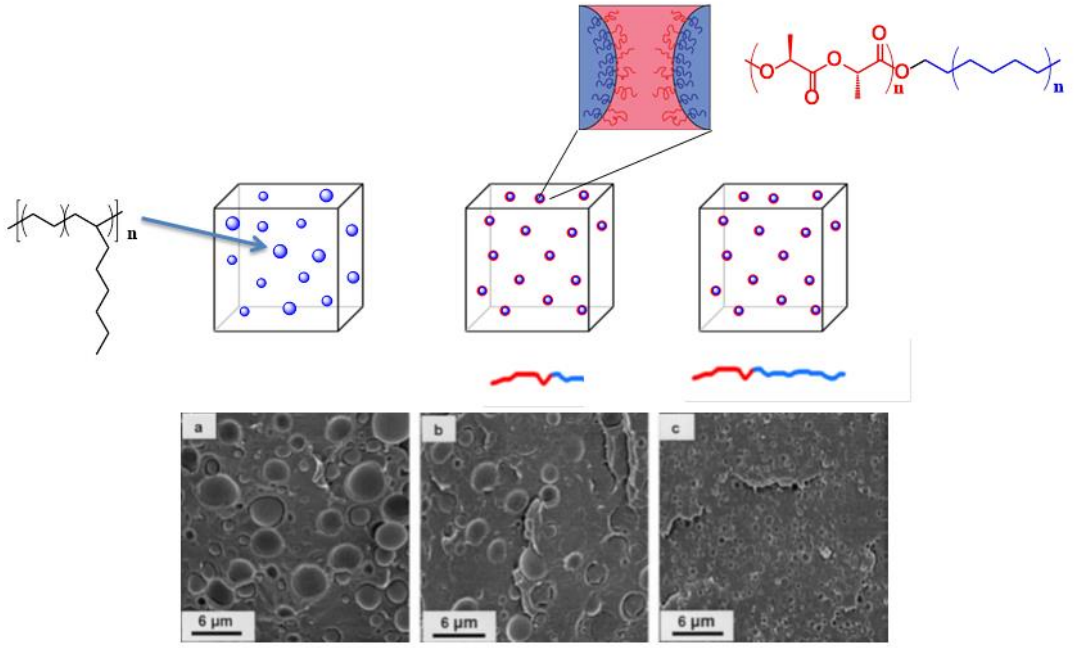

Figure 15.1. Influence of PLA-b-PE copolymers on the microstructure of binary PLLA/PE blends[146]

It is noteworthy that some of these systems are commercially available. For instance Biomax® Strong 100 and 120 are two commercial modifiers for PLLA from DuPont Company that are said to be ethylene-acrylate copolymers. To evaluate the efficiency of such industrial impact modifiers, Murariu and coll. studied toughening effects of Biomax Strong 100 on PLLA and measured a notched Izod impact strength of 12.4 $kJ.m^{-2}$ for 10 wt% of additive in the blend as compared to 2.6 $kJ.m^{-2}$ for neat PLLA.[153]

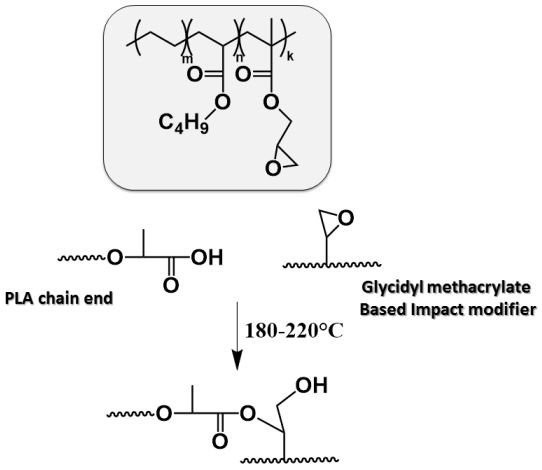

Figure 16.1. Use of glycidyl methacrylate based rubbers for the reactive compatibilization of binary blends

Acrylic polymers were also used as impact modifiers for PLLA.[154, 155] From them, poly(n-butyl acrylate) (PBA)-based materials were the most investigated. In order to improve the miscibility between PLLA and PBA, He and coll. used PBA-*g*-PLLA and PBA-*g*-PDLA copolymers as impact modifiers in blends with PLLA.[156] Interestingly PBA-*g*-PDLA led to a much tougher material due to stereocomplexation of the grafted copolymer with the PLLA matrix. Examples of commercially available acrylic impact modifiers include the ParaloidTM BPM-500, an acrylic-based impact modifier introduced by Rohm & Hass Co., and two grades of core-shell particles launched by Arkema, Biostrength™ 130 and 200 that are suggested to be added at 2-6 wt% in PLLA.

Biostrength™ 280, another impact modifier commercialized by Arkema, is a methyl methacrylate-butadiene-styrene-type core-shell used for opaque applications. Numerous studies have been carried out regarding the use of styrenic impact modifiers such as hydrogenated styrene-*b*-butadiene-*b*-styrene block copolymers (SBS), styrene-*b*-ethylene/butylene-*b*-styrene block copolymers (SEBS) and acrylonitrile-*b*-butadiene-*b*-styrene copolymers (ABS). Improvement of the miscibility between the two phases while in blends with PLLA has been carried out by using glycidyl methacrylate compatibilizers, peroxides or maleic anhydride grafted SEBS.

This overview of non-biodegradable impact modifiers for PLLA, highlights the efficiency of rubber toughening by mainstream petroleum-based elastomers. Furthermore, the well-known chemistry of olefinic, acrylic and styrenic polymers allows the easy introduction of reactive functions towards PLLA chemical structure in order to improve the interfacial adhesion in blends. Several series of commercial impact modifiers for PLLA have been launched, mainly based on non-biodegradable linear elastomers of low Tg or cross-linked core-shell polymers. The latter category generally consists of a low Tg rubbery core encapsulated by a glassy shell that has good interfacial adhesion with the PLLA matrix. However such polymeric additives do not constitute long-term and suitable solutions as they modify the compostable feature of the final PLLA material thus suppressing one of the main advantages of PLLA.

For this reason, industrials and academics are currently undertaking a lot of efforts to promote the development of a second generation of impact modifiers for PLLA that consists of biodegradable and ideally biobased low Tg polymers.

II.3.2. Biodegradable polymeric impact modifiers

Polycaprolactone based polyesters

The excellent flexibility and ductility of polycaprolactone (PCL) have been widely used for the toughening of PLLA by melt blending. However, the immiscibility between PCL and PLLA resulted in marginal improvement in toughness when simple physical bending was carried out.[157, 158] A better adhesion can be obtained by using compatibilizers that will ensure a stable structure with a uniform distribution of rubber particles.

In a first example, Wang and coll. used triphenyl phosphite (TPP) as a small molecule reactive additive during melt-blending of PCL with PLLA.[159] The measurement of the Torque during melt blending showed an increase in this value when TPP (2 phr) was added to a blend comprising 80 wt% of PLLA and 20 wt% of PCL. This clearly demonstrated that coupling and grafting reactions were occurring during the process. Improvement in toughness was observed for the reactive blend as seen from the value of elongation at break that goes from 3% for the pure PLLA to 28% for the uncompatibilized blend to over 120% for the reactively compatibilized blend. This can be logically attributed to the *in-situ* formation of block copolymers which move to the interface between PLLA and PCL and which act as adhesion promoters.

Reactive compatibilization of PLLA/PCL blends was also carried out using dicumyl peroxide (DCP) during blending leading to improved mechanical properties.[160, 161] Indeed, in the case of a PLLA/PCL (70/30, w/w) blend, addition of 0.1-0.2 phr of DCP resulted in a dramatic increase in the elongation at break. While the uncompatibilized blend broke at 15% elongation, the compatibilized blend had an elongation at break value of around 130%. Further addition of DCP beyond the optimum amount had an opposite effect on elongation. The impact strength of the blend was also significantly increased by the addition of DCP (2.5 times higher than without DCP) while no difference was observed for DCP addition into neat PLLA. Atomic Force Microscopy (AFM) observations were realized in order to have more information about the morphology of the blends. A decrease in the diameter of the dispersed PCL domains with increasing DCP content was noticed. This confirms the grafting and cross-linking reactions which are occurring between the PLLA and the PCL chains thus improving the interfacial adhesion. The grafting can be explained by the formation of free radicals induced by DCP which then recombine with other radicals resulting in chains coupling (Figure 17.1).

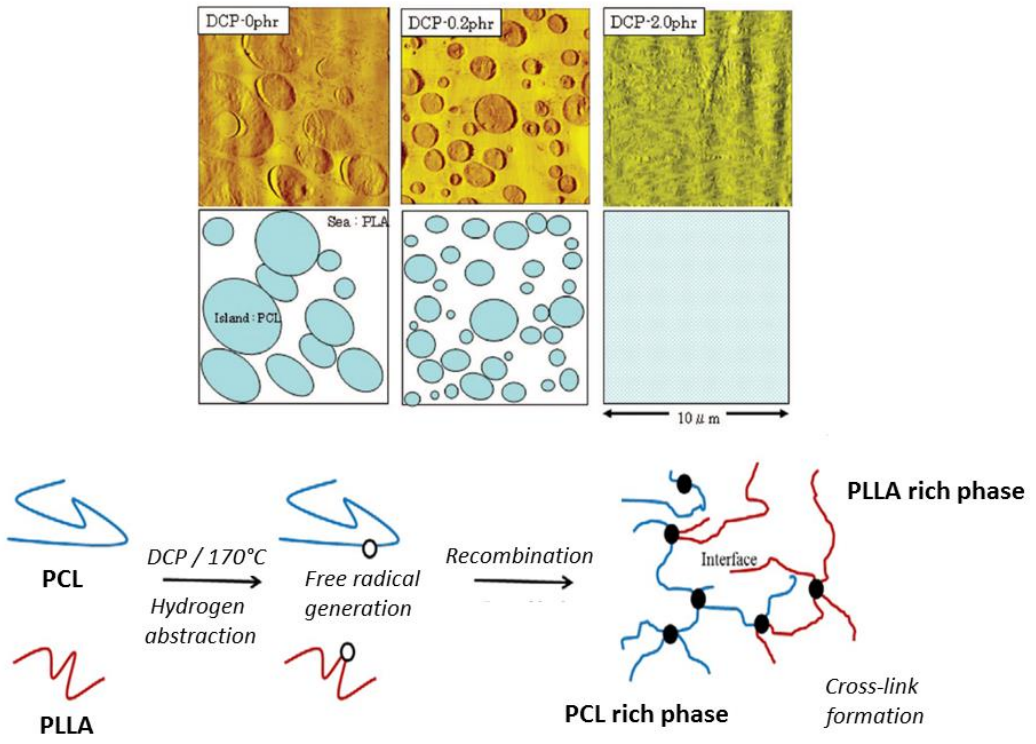

Figure 17.1. AFM images of PLLA/PCL (70/30, w/w) blends with various contents of DCP and schematic representation of radical coupling reactions[160]

Reactive compatibilization of PLLA/PCL blends was also achieved by using lysine triisocyanate (LTI) as a reactive agent (Figure 18.1).[162, 163] In this study, the enhanced interfacial adhesion was allowed by the reaction between the isocyanate functions and the chain end functional groups (hydroxyl and carboxylic acid functions) of both PCL and PLLA. It is noteworthy, that the addition of LTI resulted in a drastic decrease in the mean size of PCL domains suggesting better compatibility between the two phases. This was accompanied by an improvement of the impact strength with the amount of LTI as a consequence of multiple grafting reactions.

Based on these considerations, Harada and coll. compared LTI with other reactive agents such as lysine diisocyanate (LDI), other triisocyanate compounds (Duranate TPA 100 and 24A-100) and a triepoxy molecule (Epiclon 725) in PLLA/PCL (80/20, w/w) blends.[164] All additives showed good efficiency in the compatibilization process except Epiclon 725. This suggests better reactivity of the addition of isocyanates with hydroxyl or carboxylic acid groups than the ring-opening of the epoxide functions by the chain end functions. Among the four isocyanates used, LTI showed the most promising results as the sample did not broke during unnotched charpy impact test. With 0.5 phr of LTI, the notched Charpy impact strength and elongation at break reached 17.3 $kJ.m^{-2}$ and 268 % respectively while maintain good tensile strength (47.3 MPa).

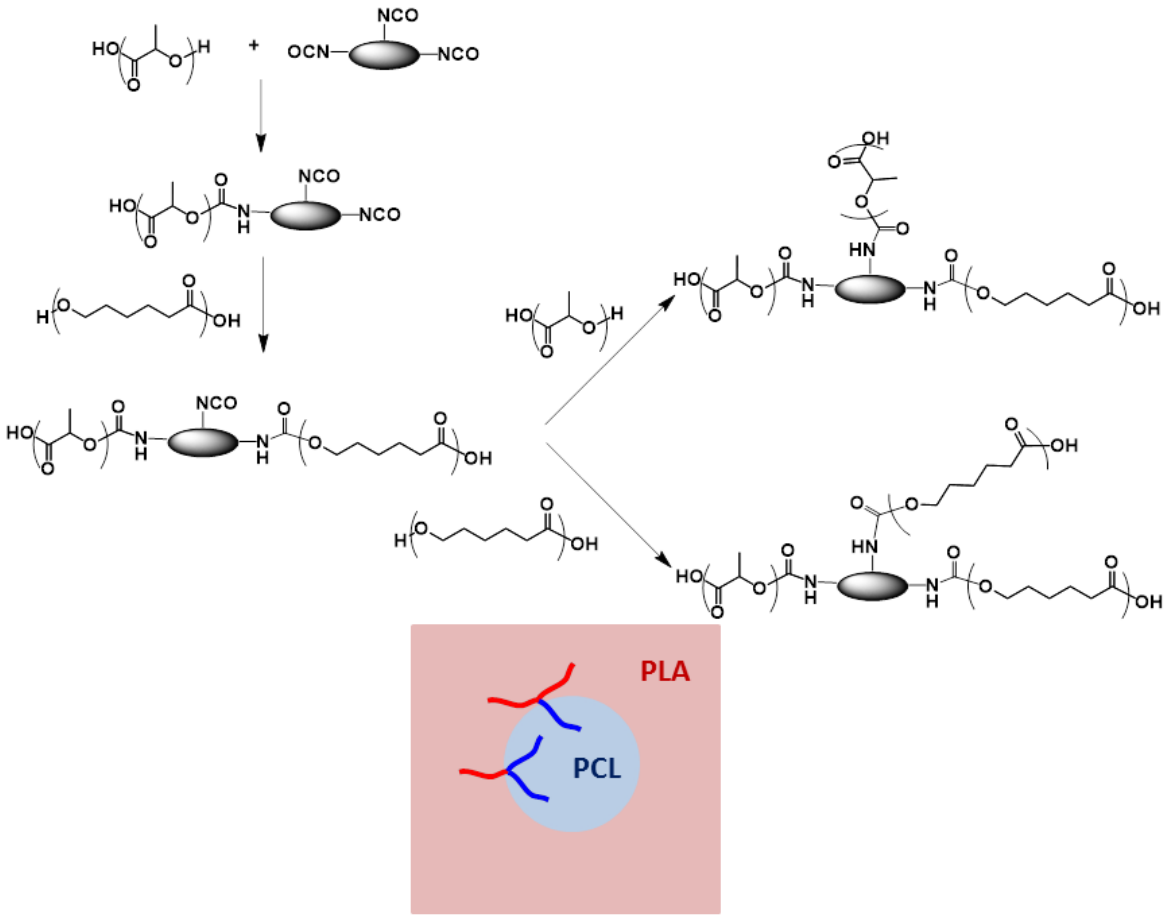

Figure 18.1. Compatibilization reactions with isocyanate compounds

Odent and coll. synthesized PCL based rubbers by copolymerizing CL with δ-valerolactone (VL) in order to lower the crystallinity of the resulting polymer.[165] Indeed, one criterion of toughening efficiency is the amorphous or slightly crystalline behavior of the impact modifier. By varying the composition of the copolymer, a wide range of thermo-mechanical properties were obtained. The molecular weight was also varied in order to evaluate its influence on the impact strength of the resulting blends. It was claimed that the use of copolymers of higher molar mass with a molar composition of 45/55 mol% (CL/VL) gave significant improvement in the impact strength (7.1 $kJ.m^{-2}$ compared to 2.5 $kJ.m^{-2}$ for neat PLLA).

In order to impart partial miscibility to PLLA/PCL blends and thus to stabilize the blends, Odent and coll. used random copolyesters of CL and D,L-LA as rubber additives instead of PCL.[166] By varying the chemical composition of the copolyester, various morphologies and mean sizes of dispersed phase domains were obtained. The correlation between the morphology and the impact strength of the blends was realized and showed the best results in terms of impact strength (11.4 $kJ.m^{-2}$ for 10 wt% of additive compared to 2.7 $kJ.m^{-2}$ for neat PLLA) for the P(CL-*co*-LA) copolyester with a molar composition of 72/28 mol%.

Interestingly, this rubber additive formed nano-sized elongated structures in the PLA matrix which are thought to be responsible for new impact performances.

Always with the aim to improve the toughness of PLLA/PCL blends, Bai and coll. recently described the effect of the crystallinity of the PLLA matrix on the impact strength of the blends. Starting from different blend compositions, the authors incorporated various amounts of a nucleating agent in order to induce crystallization of PLLA (matrix crystallinity in the range 10-50%). The results showed that there is a linear relationship between PLLA matrix crystallinity and impact toughness (Figure 19.1). Previously, chemical pathways to improve the toughness of PLLA/PCL blends were described. This study shows that also physical means can be used to induce better efficiency in terms of impact strength.

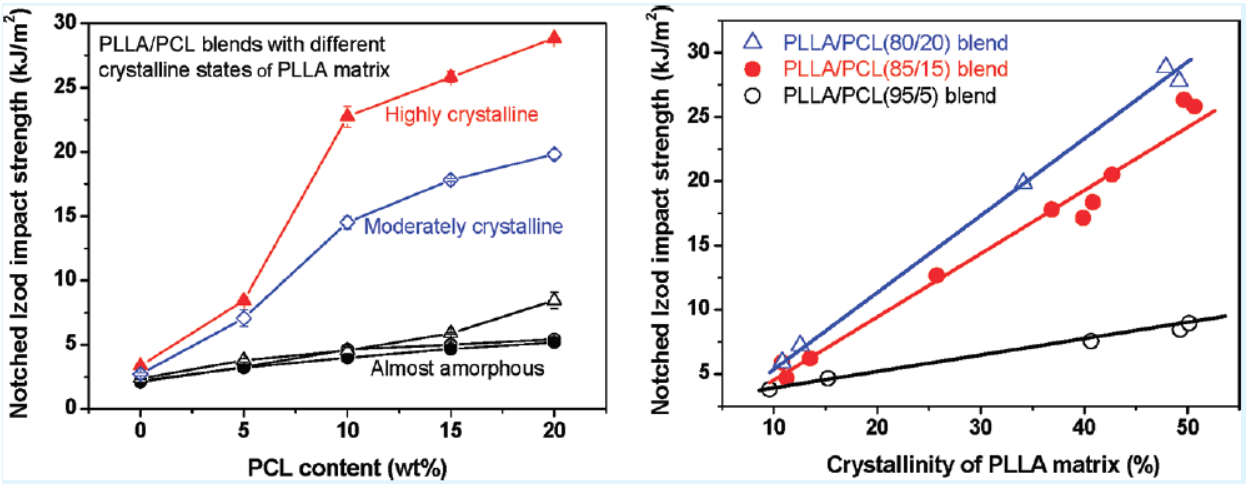

Figure 19.1. Effect of the crystallinity of the PLLA matrix on the impact strength of PLLA/PCL binary blends[167]

Poly(butylene succinate) (PBS) and their copolyesters

Poly(butylene succinate) (PBS) is a biodegradable aliphatic polyester that is produced by polycondensation of succinic acid with 1,4-butanediol, two monomers which can be derived from renewable resources.[168] Thus, PLLA/PBS blends could retain the biodegradable and renewable characteristics. PBS is a crystalline thermoplastic with a melting point of around 110-120°C and a low glass transition temperature of around -20°C. PBS and copolymers such as poly(butylene succinate-*co*-adipate) (PBSA) and poly(butylene succinate-*co*-lactate) (PBSL) are highly flexible and exhibit similar mechanical properties to polyethylene.

In a first study, Benson and coll. described physical blends of PLLA with Bionolle which is a commercial poly(ethylene/butylene succinate) copolyester.[169] However, the important immiscibility of the two polymers resulted in poor enhancement of the mechanical properties. However one beneficial effect that was observed during this study was an enhancement of the crystallization rate of PLLA with this additive.

Miyoshi and coll. investigated two different blend systems for the toughening of PLLA.[84] In a first case, PBS was melt blended with PLLA in various amounts and in a second case similar study was realized by replacing PBS by PBSL copolyester. The commercial PBSL contained the lactate unit of ca. 3mol%. Despite the presence of lactate units that should enhance the compatibility with PLLA, the two systems presented similar morphologies based on finely dispersed immiscible blends. Stress-strain curves of both systems showed a ductile-brittle transition with improved elongation at break values. As a whole, PLLA/PBSL blends showed higher elongation at break and lower tensile strength and modulus than PLLA/PBS blends. It was also mentioned that PBSL addition enhanced both the isothermal and non-isothermal PLLA crystallization from the melted state. On the other hand, PBS showed moderately effect on the crystallization behavior of PLLA.

As reactive compatibilizers were successfully used to enhance interfacial adhesion between PLLA and PCL, and as PCL and PBS based polyesters bear similar chain end functional groups, they were also employed for the reactive melt processing of PLLA/PBS and PLLA/PBSL blends. Similarly to the studies dealing with PLLA/PCL blends, isocyanates (LTI and LDI) were introduced in PLLA/PBS[170] and PLLA/PBSL[171] blends as well as DCP in PLLA/PBS blends.[172] This resulted in all cases in a plastic deformation and a significant improvement of the impact strength and the elongation at break compared to the corresponding uncompatibilized blends.

Poly(butylene adipate-*co*-terephtalate) (PBAT)

PBAT is an aliphatic-aromatic copolyester which is fully biodegradable and which is commercialized under the tradename Ecoflex (BASF Co.). PBAT is a highly flexible and ductile thermoplastic showing elongation superior to 700%. It is thus a good candidate for the toughening of PLLA. The first study that described PLLA/PBAT blends was conducted by Zhang and coll. in 2006.[173] The authors blended PBAT with PLLA in different amounts by twin-screw extrusion. The immiscible blends showed improved elongation at break (even with as low as 5 wt% of PBAT, elongation at break value was superior to 200%) as seen from the brittle to ductile transition by adding PBAT. The elongation at break value was also increased with the PBAT amount without severe loss in tensile strength and modulus. Regarding the impact strength, the blends showed a moderate improvement with a value going from 2.6 $kJ.m^{-2}$ for neat PLLA to 4.4 $kJ.m^{-2}$ for the PLLA/PBAT (80/20, w/w) blend.

To further improve the impact strength of PLLA/PBAT blends, Wang and coll. added a random terpolymer of ethylene, acrylic ester and glycidyl methacrylate to the blend in order to favor grafting and/or crosslinking reactions.[174] Indeed, the carboxylic acid and hydroxyl

terminal groups of PLLA were reactive in the processing conditions towards the ring-opening of the epoxide groups of the terpolymer. These grafting reactions resulted in a drastic increase in the impact strength and the elongation at break with amounts of terpolymer as low as 2 wt%. For the PLLA/PBAT (70/30, w/w) blend with 1-3 wt% of terpolymer, the notched impact strength reached 30-40 $kJ.m^{-2}$, two times that of the corresponding uncompatibilized blend.

More recently, Chen and coll. used 2,2'-(1,3-phenylene)bis-2-oxazolin and phthalic anhydride as compatibilizers during melt blending of PLLA with PBAT.[175] Using this approach, PBAT particles became smaller and better dispersed in the PLLA matrix which indicated better interfacial adhesion. Thus elongation at break values were significantly enhanced even with compatibilizer amounts as low as 1 wt%.

Polyhydroxyalkanoates (PHAs)

PHAs are biodegradable aliphatic polyesters known to be produced by many microorganisms. These polymers possess a wide range of thermo-mechanical properties ranging from stiff thermoplastics to elastomers. The mechanical properties of PHAs are largely in correlation with their chemical structure. The general chemical structure of PHAs is presented in Figure 20.1. PHAs are divided into three classes: short-chain-length PHAs with carbon atom number of monomers ranging from C3 to C5, medium-chain-length PHAs with carbon atoms number ranging from C6 to C14, and long-chain-length PHAs with carbon atoms number of more than C14. Due to their elastomeric behavior, medium-chain-length PHAs are more prone to be used as toughening modifiers of PLLA.

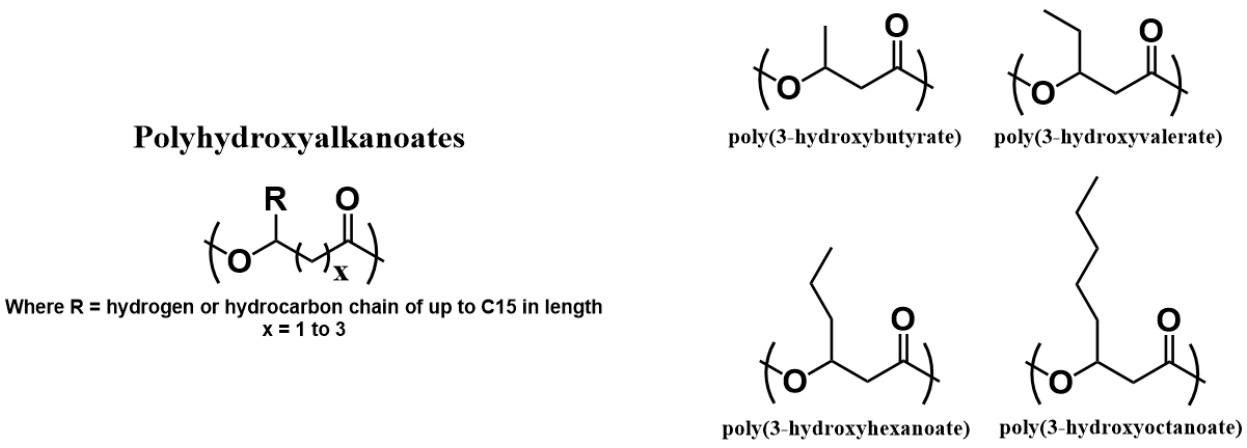

Figure 20.1. Chemical structures of polyhydroxyalkanoates

Marcott and coll. used a commercially available PHA, which tradename is NodaxH6, for the toughening of PLLA.[176] The PHA used was a poly(3-hydroxybutyrate-*co*-3-hydroxyhexanoate) containing 5 mol% of 3-hydroxyhexanoate unit.[177] Neat NodaxH6 is a

crystalline material; however when it was used with less than 20wt% of the total composition of the blend, its crystallization was largely restricted leading to an almost amorphous dispersed rubbery phase. Tensile toughness of the PLLA/NodaxH6 (90/10, w/w) blend was significantly higher than the one of neat PLLA (10 times higher) as evidenced by the elongation at break value of more than 100%. Moreover the blends with a PHA content less than 20 wt% were transparent which can be underlined for packaging applications perspectives.

In order to induce grafting reactions with PLLA chain ends, Yamane and coll. functionalized a PHA containing a major amount of 3-hydroxyoctanoate with some epoxy groups (Figure 21.1).[178] Melt-blending of this PHA with PLLA in various amounts, as well as melt-blending of the unfunctionalized PHA with PLLA were then realized. The morphologies of the blends observed by TEM showed smaller PHA particles in the case of the epoxy-functionalized PHA due to *in-situ* reactive compatibilization. Impact strength was also improved in comparison to the uncompatibilized blends (total absorbed energy of 0.14 J and 0.17 J respectively for blends with 20 wt% of dispersed phase).

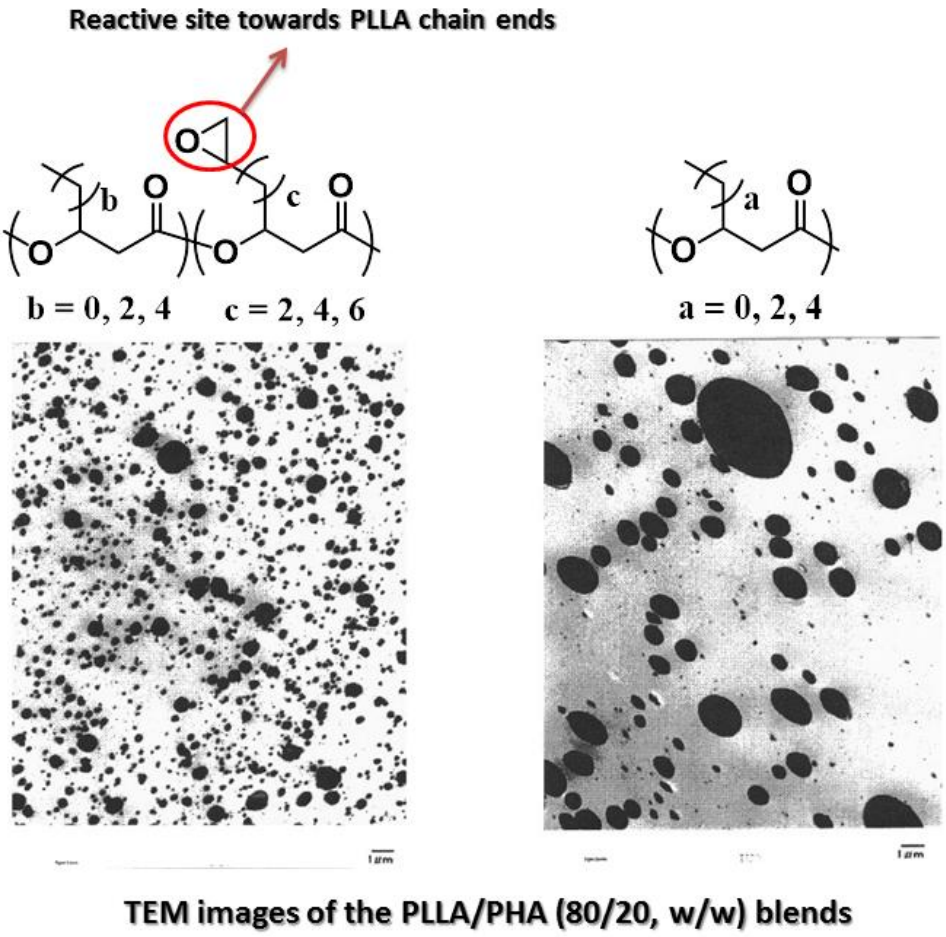

Figure 21.1. Reactive compatibilization of PLLA/PHA blends by using oxirane functions in the additive's backbone

Hillmyer and Schreck also used a NodaxH6 containing 7 mol% of 3-hydroxyhexanoate unit to toughen PLLA.[179] Notched Izod impact strength was significantly improved by addition of NodaxH6 with a value going from 22 $J.m^{-1}$ for neat PLLA to 44 $J.m^{-1}$ for the PLLA/NodaxH6 (85/15, w/w) blend. To lower the mean size of the dispersed particles, the authors synthesized oligoNodax-*b*-PLLA diblock copolymers that were added to the binary blends. Even if mean particles size was lowered by the addition of the block copolymer, impact strength was not improved. This was explained by some degradation of the NodaxH6 polymer during processing that resulted in limited entanglement of the polymer chains at the particle/matrix interface.

Other biodegradable elastomers

Linear polyurethane elastomers are generally composed of soft polyether or polyester segments and hard segments. These elastomers generally exhibit a unique combination of toughness, durability and flexibility that make them useful for improving the toughness of PLLA. Li and Shimizu used a commercial biodegradable poly(ether)urethane elastomer in physical blends with PLLA.[180] The authors observed a partial miscibility between the two components that is thought to arise from molecular interactions between PLLA and the soft segment polyether of the PU elastomer. This partial miscibility was responsible for a fine dispersion (sub-micrometer scale domains) of the PU elastomer in PLLA matrix. Improvement of the mechanical properties was observed by addition of the PU elastomer. Compared to neat PLLA, the PLLA/PU (80/20, w/w) blend had a lower static modulus (1,5 GPa vs 3,5 GPa), higher elongation at break (250% vs 4%) and higher unnotched impact strength (138 $J.m^{-2}$ vs 64 $J.m^{-2}$).

A commercial polyamide elastomer (PEBAX 2533) based on polyamide-12 (22 wt%) and poly(tetramethyleneoxide) (78 wt%) was also used in blends with PLLA. Similarly to the previous work concerning PLLA/PU blends, PLLA and PEBAX showed partial miscibility explained by the combination of good interactions between PLLA and the soft polyether segments and hydrogen bonding between amide functions and ester functions of PLLA. By addition of PEBAX, the ductile-brittle transition occurred with an elongation at break value of 161% for an amount of PEBAX as low as 5 wt%. Moreover little change in tensile modulus was noticed compared to neat PLLA (1.5 vs 1.8 GPa). Surprisingly, these blends showed a shape memory behavior even after high deformation.[181]

The growing diversity in terms of building blocks obtained from renewable resources have pushed Coates and coll. to design a new polyester elastomer synthesized from the biobased itaconic acid, succinic acid, 1,3-propanediol, 1,4-butanediol and sebacic acid.[69] The resulting

bioelastomer showed a weight-average molecular weight of ~181,000 g.mol^{-1}, a dispersity index of 3.7 and a Tg of -56°C. This bioelastomer was then melt-blended with PLLA in different amounts which yielded a ductile-brittle transition as seen from stress-strain curves.[182] Maximum elongation at break value was obtained for the blend containing 11.5 vol% of bioelastomer (179% vs 7% for neat PLLA). An increase in the impact strength was also noticed with increasing the amount of bioelastomer in the blend. Value up to 13.4 kJ.m^{-2} (2.4 kJ.m^{-2} for neat PLLA) was obtained for the blend containing 22.6 vol% of bioelastomer.

II.3.3. Summary of melt-blending solutions.

From all the reported investigations regarding the rubber-toughening of PLLA by melt-blending, it is noteworthy that highly efficient solutions were developed. Both non biodegradable and degradable rubbers were used to toughen PLLA resulting in improved toughness (Figure 22.1). However, the incompatibility of most rubbers with PLLA caused important phase segregation of the matrix and the additive yielding high heterogeneity of the mean size of the particles and thus limited improvement in the impact toughness of the final material. To solve this issue, a third component was often added to the binary blends in order to improve the interfacial adhesion between the two phases. Another solution involved the incorporation of reactive sites in the backbone of the additive to induce grafting and cross-linking reactions between the dispersed phase and the matrix.

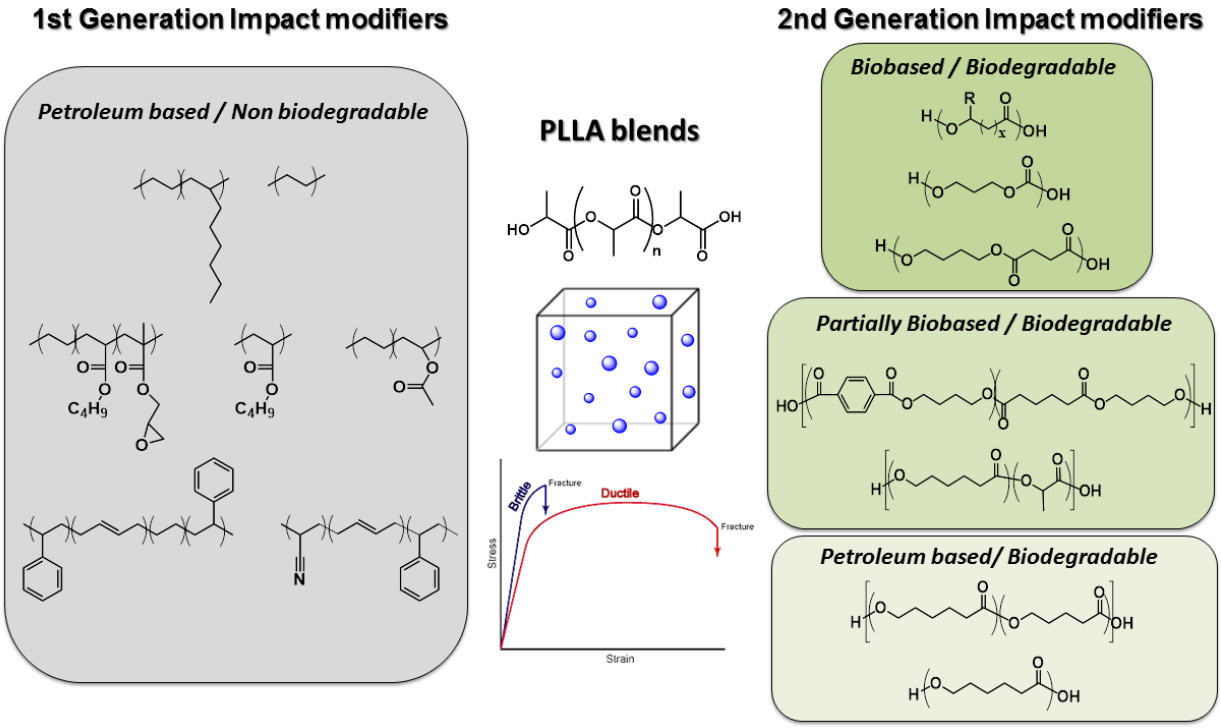

Figure 22.1. Summary of 1st and 2nd generation impact modifiers melt-blended with PLLA

II.4. Summary and perspectives

The extensive literature regarding the toughening of PLA by biodegradable modifiers shows the great challenges of keeping the compostable characteristic of PLA based materials (Figure 14.1 and Figure 22.1). We have also seen that some biobased modifiers were employed to yield better eco-friendly solutions. Only limited examples of such polymers can undergo hydrolytic or biodegradation. Generally an aliphatic nature of the polymer backbone is needed coupled with a hydrolytically cleavable organic function such as acetal, anhydride, carbonate or ester. In the above mentioned examples of biodegradable impact modifiers for PLA, mainly aliphatic polyesters were reported.

Indeed, ester linkage is known to be hydrolysable and degradable thus polyesters are prone toward degradability. Due to their lower impact on environment, aliphatic polyesters are no more restricted to biomedical applications, but are subjected to great potential in packaging applications, elastomers, etc. Moreover, hydroxylic and carboxylic derivatives, needed for the synthesis of polyesters, are easily obtained from biomass which enables an easy chemical or biochemical synthesis of strategic building blocks. Indeed poly(hydroxyalkanoate)s (PHAs), poly(trimethylene carbonate) (PTMC), poly(butylene succinate) (PBS), poly(butylene adipate-*co*-terephtalate) (PBAT) are all examples of biodegradable and biobased (or partially biobased) polyesters that were employed for the toughening of PLA. These polymers are usually obtained from carbohydrates fermentation except for PTMC which is obtained from glycerol, a byproduct of biodiesel production.

Sustainability in polymer science involves the utilization of building blocks coming from multiple renewable resources in order to preserve the carbon feedstock and the diversity of biomass. Thus, in the case of the modification of PLA mechanical properties that generally involves additive amounts up to 20%, it is of high interest to develop impact modifiers that are originated from other renewable resources than carbohydrates (or lignocellulosic materials).

Plant oils and more particularly fatty acids represent promising feedstock for aliphatic polyester production as the substrate already provides aliphatic acidic or ester functions. In the following, we summarize recent developments in the synthesis of aliphatic polyesters starting from fatty acid derivatives. A critical discussion will then permit to envisage the potential of such polyesters for the toughening of PLA.

PART B. POLYESTERS FROM FATTY ACIDS AS PROMISING CANDIDATES FOR THE TOUGHENING OF PLA

I. PLANT OILS, A SUITABLE AND SUSTAINABLE RESOURCE FOR POLYMER CHEMISTRY

Vegetable oils, which are annually renewable, are the most important sustainable raw materials for the chemical industry. Indeed, vegetable oils are already heavily used as raw materials in industry for surfactants, as cosmetic products, lubricants, in paint formulations, as flooring materials and for coating and resin applications. The annual global production of the major vegetable oils in 2011/2012 amounted 156 million tons.[183] About 20% is devoted to industrial applications mainly as sources of energy, compared with around 75% and 5% for respectively food and feed utilizations.[184] Vegetable oils are composed of different triglycerides which are the esterification products between glycerol and three various fatty acids (fatty acids account for around 95% of the total weight of triglycerides) (Figure 23.1). The composition of fatty acids in the triglyceride depends on the plant, the crop, the season and the growing conditions. The most important parameters affecting the physical and chemical properties of plant oils are the stereochemistry of the double bonds (cis or trans) of the fatty acid chains, their degree of unsaturation as well as the length of the fatty acid chain. Iodine value (amount of iodine in g that can react with double bonds present in 100 g of sample under specific conditions) is generally used to measure the degree of unsaturation and allows to divide plant oils in three categories: drying (iodine value>170; e.g. linseed oil), semi-drying (100<iodine value<170; e.g. sunflower oil) and non-drying (iodine value<100; e.g. palm kernel oil) oils. Fatty acids are classified by their number of carbon atoms in the chain as well as their number of unsaturation. For instance, oleic acid which bears 18 carbon atoms and one unsaturation is classified as a 18:1 compound. Table 3.1 summarizes the chemical composition of some industrially important plant oils with the chemical structure of the main unsaturated fatty acids.

From plant oils can be distinguished saturated from unsaturated ones. In this manuscript we propose to focus on the unsaturated ones as the presence of double bonds implies plurifunctionnality which is one requirement for polymer synthesis. Three approaches can be followed to synthesize polymers from unsaturated plant oils (Figure 24.1).[185]

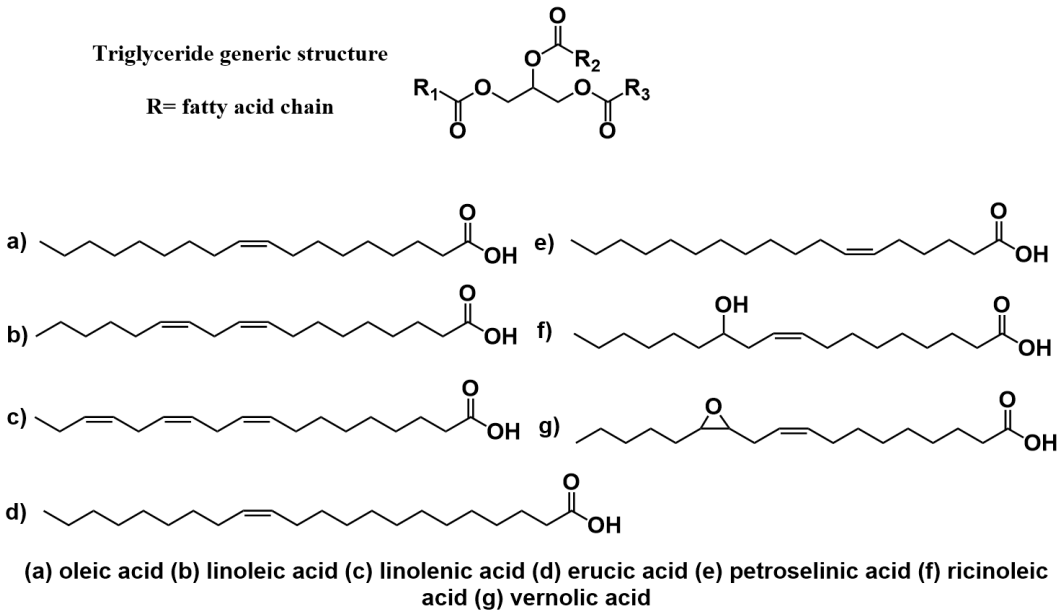

Figure 23.1. Chemical structure of triglyceride and main industrial fatty acids

Table 3.1. Fatty acid composition of the main industrial plant oils

	16:0	16:1	18:0	18:1	18:1 OH	18:2	18:3	20:0	20:1	22:1
Canola	4.1	0.3	1.8	60.9	0.0	21.0	8.8	0.7	1.0	0.0
Corn	10.9	0.2	2.0	25.4	0.0	59.6	1.2	0.4	0.0	0.0
Linseed	5.5	0.0	3.5	19.1	0.0	15.3	56.6	0.0	0.0	0.0
Olive	13.7	1.2	2.5	71.1	0.0	10.0	0.6	0.9	0.0	0.0
Palm	44.4	0.2	4.1	39.3	0.0	10.0	0.4	0.3	0.0	0.0
Soybean	11.0	0.1	4.0	23.4	0.0	53.2	7.8	0.3	0.0	0.0
Sunflower	6.1	0.0	3.9	42.6	0.0	46.4	1.0	0.0	0.0	0.0
Sunflower high oleic	6.4	0.1	3.1	82.6	0.0	2.3	3.7	0.2	0.4	0.0
Rapseed high erucic	3.0	0.0	1.0	16.0	0.0	14.0	10.0	0.0	6.0	50.0
Castor	0.5-1	0.0	0.5-1	2-6	85-95	1-5	0.5-1	0.0	0.0	0.0

In the first approach, naturally occurring functions such as double bonds or hydroxyl groups react to yield networks in most of the cases. In a second strategy, the chemical modification of the double bonds is carried out to introduce functional groups which are easier to polymerize (hydroxyl, epoxide, acrylate groups…). In both of these approaches, polymer networks are generally formed. Moreover it does not allow good control of the macromolecular characteristics due to the distribution of double bonds per triglycerides that induce heterogeneity of the monomers. Nevertheless, a remarkable large series of papers and reviews investigated the functionalization of triglycerides to get interesting monomers for polymer networks as it constitutes an economical and practical way to biobased materials.[186-188] From these commodity vegetable oils, fatty acids (for instance oleic acid from sunflower, erucic acid from rapeseed and ricinoleic acid from castor oil) are available in such purity that they can be used as polymer precursors by chemical conversions. Examples of commercially

available fatty acid derivatives include azelaic acid, sebacic acid, 10-undecenoic acid, brassylic acid… The nine carbon dicarboxylic acid, azelaic acid can be obtained by ozonolysis of oleic acid. Alkali pyrolysis of ricinoleic acid produces the ten carbon dicarboxylic acid, sebacic acid and pyrolysis of ricinoleic acid gives undecenoic acid. Oxidation of erucic acid yields the thirteen carbon dicarboxylic acid, brassylic acid. Chemical transformation of fatty acids is the most suitable mean to obtain bifunctional compounds, with a highly controlled chemical structure, that acts as precursors for linear polymers synthesis. From this approach a large range of linear polymers including polyurethanes, polyethers, polyesters, polyamides, polyacetals… were developed.

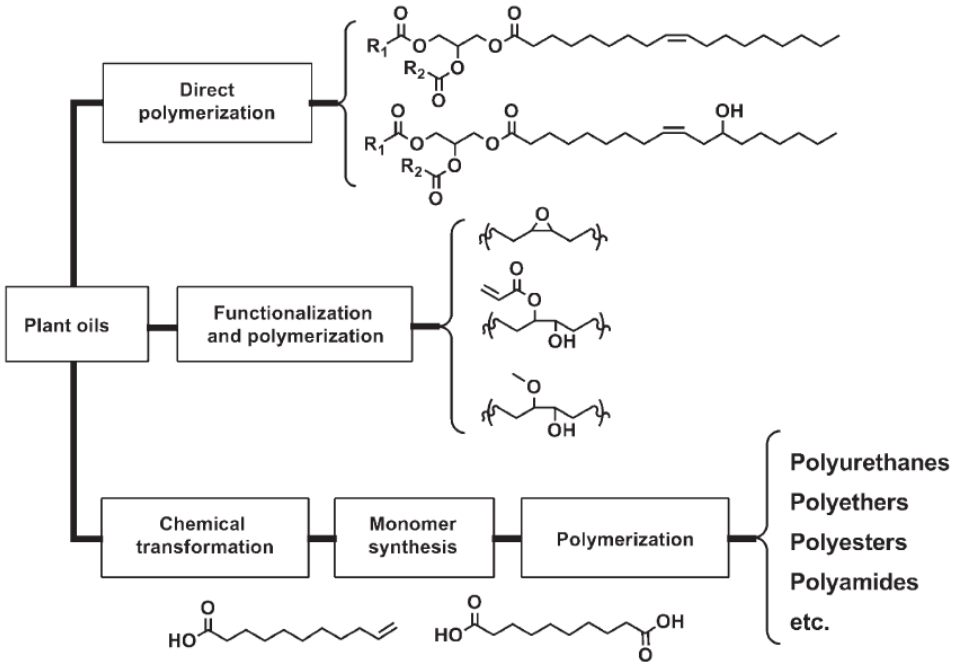

Figure 24.1. Three pathways to polymers from plant oils[185]

In this section, we summarize recent developments in the synthesis of aliphatic polyesters starting from fatty acid derivatives; the aim being to establish the structure-properties relationship in order to select the best profile for a fatty acid-based impact modifier for PLA.

II. SEMI-CRYSTALLINE ALIPHATIC POLYESTERS: TOWARD POLYETHYLENE MIMICS

In the first part of this chapter, it was shown that most of the impact modifiers currently used for the toughening of PLLA are low Tg and semi-crystalline polymers. Among them, polyethylene-based materials constitute undoubtedly the most widely used additives due to their tunable properties and low price. However, polyethylene does not constitute a sustainable solution when applied to the toughening of PLLA as it is not biobased and it

suffers from a lack of biodegradability thus impeding the efficient compostability of the resulting PLLA materials.

It is of high interest to find "greener" alternatives to polyolefins (polyethylene, polypropylene) in order to lower the carbon footprint of this huge class of materials and to provide them with biodegradability. Recent efforts to find new pathways to biopolyolefins production have led to the development of biopolyethylene (bioPE) from ethanol.[189] Nevertheless, while the bio sourcing issue was resolved from this approach, the resulting material still lacks the biodegradability characteristic.

Another approach is to design new class of bio-based building blocks that can lead to polymers with similar properties to polyethylene while presenting original features such as biodegradability and polarity. Ester linkage can solve these issues. Thus it is of great interest to develop polyester that could mimic polyethylene or other polyolefins.

Polyethylene mimics can be expected by a significant increase of the number of methylene units between two ester functions while keeping a purely linear structure in order to dilute the ester functions and thus to tend to the polyethylene crystal structure. To that aim, fatty acids from plant oils represent the perfect feedstock as fatty acids already contain long alkyl chain linear segments. A number of investigations have been done to introduce bifunctionality to these fatty acids as the latter usually contains one carboxylic acid function and one double bond that need to be activated for step growth polymerization.

II.1. Thiol-ene click reaction

One type of double bond modification is based on the thiol-ene click reaction that can bring either an alcohol or a carboxylic function to a fatty acid backbone. In a first example, Meier's group described an efficient route to the development of a set of renewable monomers for polyester synthesis. [190] Starting from castor oil derivatives, i.e. methyl 10-undecenoate and 10-undecenol, they synthesized various monomers ranging from hydroxyl methyl ester, diol and methyl diesters by using several thiols such as mercaptoethanol, butanedithiol, methylthioglycolate and thioglycerol in solvent-free conditions (Scheme 7.1). The obtained monomers were then polymerized, using TBD as a transesterification catalyst, leading to purely linear aliphatic polyesters bearing thio-ether linkages. The thermal properties of the resulting polymers revealed melting points ranging from 50°C to 71°C and thermal stabilities up to 300°C. The structure-property revealed higher crystallinity and higher melting points for longer chain length between ester linkages.

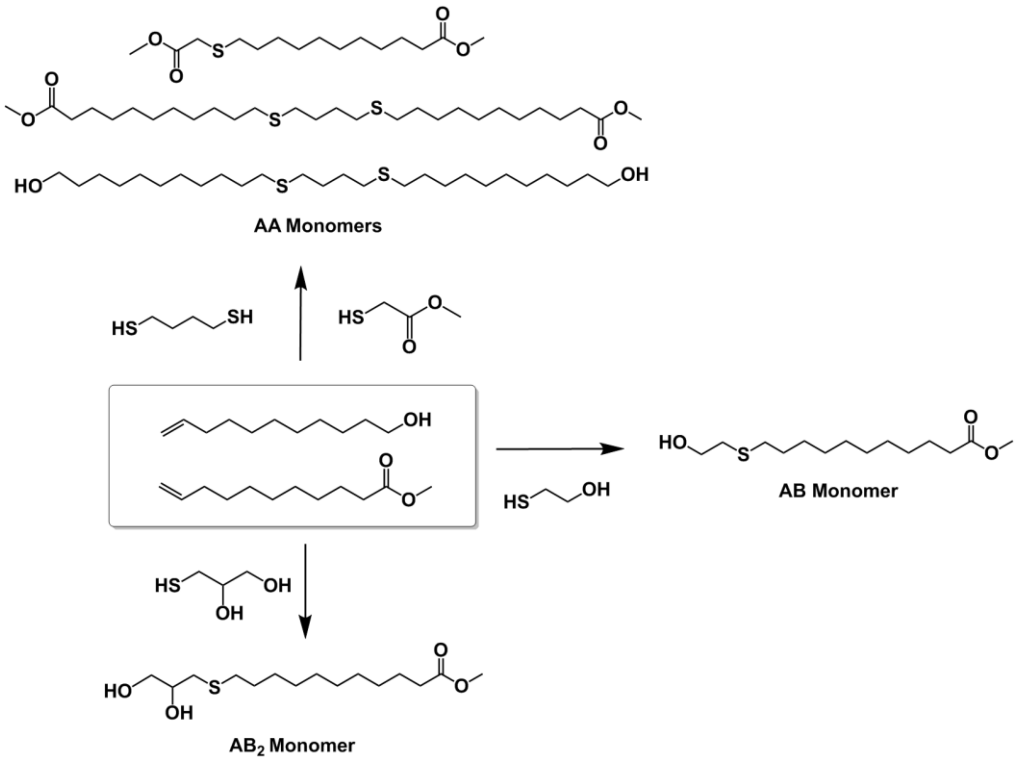

Scheme 7.1.Synthesis of condensable monomers by thiol-ene click reaction.[190]

The same group used a bis-unsaturated diester, obtained by transesterification of methyl 10-undecenoate with bio-based 1,3-propanediol, as starting material for polyester synthesis by thiol-ene addition with bis(2-mercaptoethyl) ether or ADMET polymerization using Zhan metathesis catalyst.[191] Higher molecular weights were obtained for polyesters obtained from thiol-ene polyaddition. Nevertheless, the melting points of the so-formed materials, 44-45°C were similar regardless of the polymerization techniques. It should be noted that degradation of such polyesters towards enzymatic or acidic conditions was demonstrated in order to target biomedical applications.

II.2. Metathesis and ADMET

Functional monomers from unsaturated fatty acids can be obtained from metathesis reaction. Due to the presence of double bonds in the chemical structure of fatty acids, olefin metathesis with oleochemicals has been extensively investigated since the development of function tolerant catalysts. [192-194]

To illustrate these recent pathways to functional monomers, Warwel and coll. used ω-unsaturated fatty acids in self-metathesis reactions to obtain diesters that were polycondensated with diols.[195] First the ω-unsaturated fatty acids were obtained by ethenolysis using various oils. These unsaturated compounds were then dimerized using homogeneous ruthenium or tungsten alkylidene complexes leading to C26, C20 and C18

symmetrical unsaturated diesters. These long uncommon unsaturated diesters were then polymerized with ethylene glycol, 1,4-butanediol or 1,4-bis(hydroxymethyl)cyclohexane by using $Ca(ac)_2/Sb_2O_3$ or $Ti(OBu)_4$ as catalytic systems. High molecular weights in the range 21-109 $kg.mol^{-1}$ were obtained. These polyesters showed melting points ranging from 53°C to 92°C depending on the monomers used. The authors also investigated a different pathway to obtain the same polymer using ADMET polymerization of bis-unsaturated diester (Scheme 8.1). Similar melting points but lower molar masses were observed.

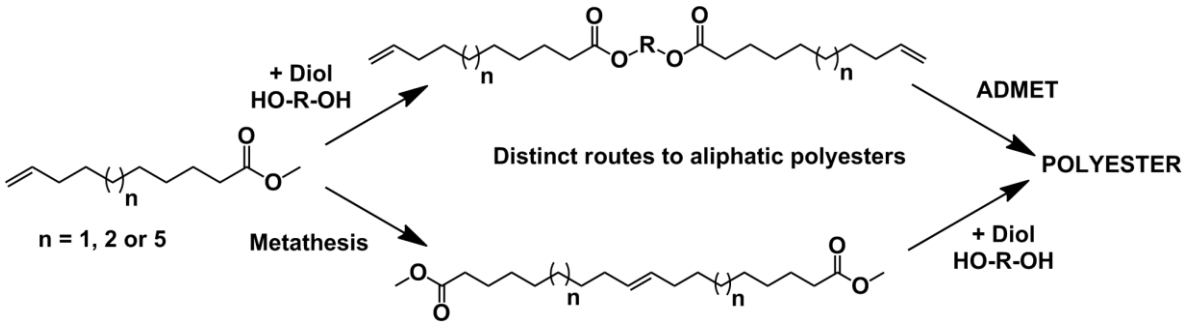

Scheme 8.1.Distinct pathways to unsaturated polyesters starting from ω-unsaturated fatty acid derivatives.[195]

Several studies based on this concept were done these past years to always get higher number of methylene units between the ester functions and purely saturated aliphatic features. For instance Meier and Rybak reported the synthesis of a α,ω-diene by using the transesterification of 10-undecenoic acid with the corresponding alcohol (10-undecenol). [196] ADMET of this 100% sustainable monomer resulted in an unsaturated polyester bearing 20 carbons between the ester functions. The possibility to control the polyester molecular weights was demonstrated using monofunctional chain stopper such as methyl 10-undecenoate. Based on the same principle, ABA triblock copolymers were prepared by adding an oligo (ethylene glycol) methyl ether acrylate as end-capping agent.

To further control the molecular architecture, the same group took advantage of the high selectivity of the cross-metathesis reaction between acrylates and terminal alkenes.[197,198] Using 10-undecenyl acrylate, an head-to-tail polymer was obtained by ADMET polymerization. Moreover, by adding a polymeric chain containing a terminal acrylate function as end-capper, such as acrylate-ended poly(ε-caprolactone), the formation of a diblock copolymer was observed (Scheme 9.1). In the same way, the addition of a multi-functional acrylate core resulted in the synthesis of a star polymer.

Such metathesis reactions, especially with 2nd generation catalyst,[199] exhibit side reactions as isomerization of the unsaturation. This creates flaw in the polyester structure decreasing its

thermo-mechanical properties. Different parameters, such as the temperature or the catalyst nature, can suppress or limit double bond isomerization.[200-202]

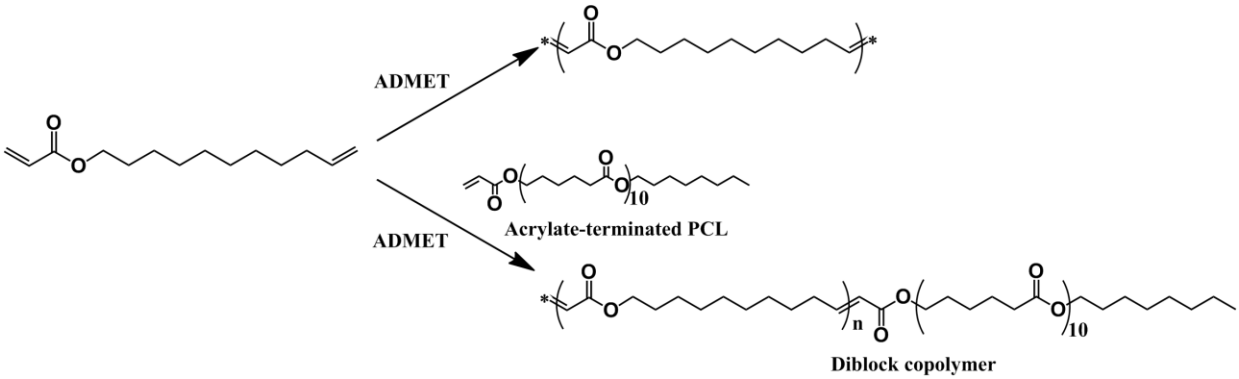

Scheme 9.1.Head-to-tail ADMET polymerization of 10-undecenyl acrylate.[198]

Fokou and Meier evaluated the influence of the reaction temperature and of the catalyst nature on the degree of isomerization during ADMET reaction of a 100% renewable bis-unsaturated diester formed by transesterification of methyl 10-undecenoate with isosorbide.[203] To that aim, the synthesized polyesters were degraded and analyzed by GC-MS to determine the degree of isomerization (Scheme 10.1). With Grubbs 2nd generation catalyst, high degrees of isomerization were observed: from 48% at 60°C to 69% at 80°C. For Grubbs 1st generation, isomerization remains extremely low even at 80°C (4%). As expected, the thermo-mechanical properties of the resulting polyesters were highly dependent on the degree of isomerization. Indeed the melting temperature decreased with the isomerization degree from 56°C to 17°C at 3% and 76% of isomerization, respectively.

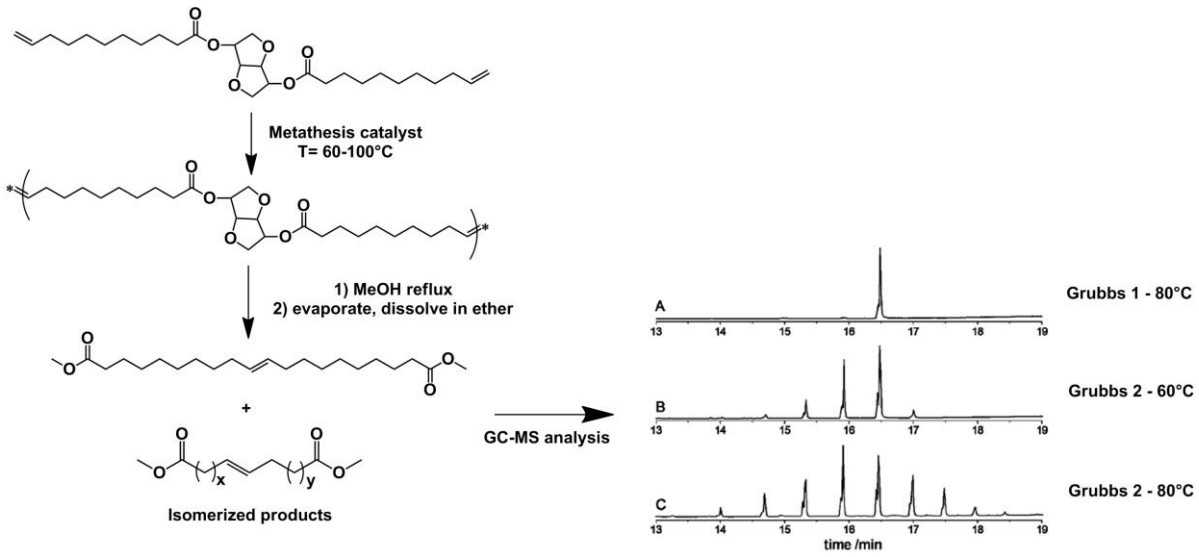

Scheme 10.1.Investigation of isomerization reactions dependence to temperature and nature of catalyst during ADMET of a 100% biobased monomer.[203]

The limitation of isomerization, when 2nd generation catalysts are used, can be performed by adding 1,4-benzoquinone, known to be a very efficient additive to prevent isomerization. The isomerization decreased from 91% at 80°C using Hoveyda-Grubbs 2nd generation to 18% when 2 mol% benzoquinone was added.[204,205] This study shows that a good control of the polymer microstructure is possible even with 2nd generation metathesis catalysts.

All the described examples of aliphatic polyesters obtained by metathesis showed promising thermo-mechanical properties; however melting points are too low to expect similar thermal properties to polyethylene. This is partially due to the remaining internal double bonds in the final polymer structure that limit the crystallization. To solve this limitation, Mecking and coll. used metathesis reaction to synthesize unsaturated α,ω-dicarboxylic acid by coupling two undecenoic acid fragments.[206] This compound was hydrogenated to yield purely saturated long chain C20 diacid. The reduction of this diacid using $LiAlH_4$ afforded the corresponding C20 diol. Polycondensation of these two monomers catalyzed by titanium alkoxides in bulk yielded a polyester 20,20 with a molecular weight of 10 $kg.mol^{-1}$ and a melting point of 108°C (Scheme 11.1). Similar thermal properties (Tm=103°C) were observed for the hydrogenated polymer resulting from the ADMET polymerization of undecenyl undeceneoate. The large difference in terms of thermo-mechanical properties (+40°C in melting points) of the saturated and unsaturated polyesters highlights the importance of a purely saturated nature of the polyester to reach acceptable crystallinity.

By following the same strategy, erucic acid [(Z)-Docos-13-enoic acid], a monounsaturated fatty acid readily available from rapeseed or cramble oils, was converted into 1,26-diacid and diol.[207] These two monomers were polycondensated yielding a polyester 26,26 with a molecular weight of 14 $kg.mol^{-1}$ (Scheme 11.1). This polyester showed a melting transition at 104°C with a temperature corresponding to 5 wt % degradation equal to 386°C. The crystal structure corresponds to the one of polyethylene since similar wide-angle X-ray diffraction spectra were observed.

Very recently, Mecking and coll. extended the library of long-chain aliphatic polyesters obtained from plant oils by describing new polyesters 38,23 and 44,23 by ADMET.[208] After hydrogenation of these polyesters, measured melting points were 109°C and 111°C showing no increase compare to PE 26,26. This feature underlines that a much higher dilution of the ester functions in the polymer backbone is necessary to expect reaching, as an asymptote, the polyethylene thermo-mechanical properties.[209, 210]

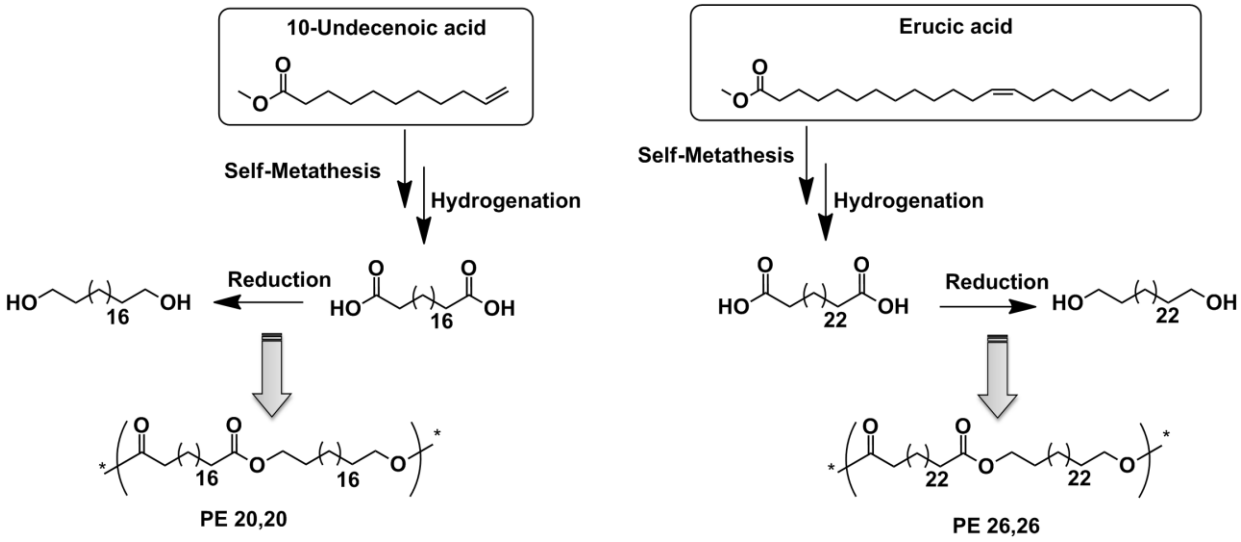

Scheme 11.1.Long chain aliphatic polyesters prepared by polycondensation of monomers obtained from 10-undecenoic acid and erucic acid.[206, 207]

All the above studies using metathesis of fatty acid derivatives were performed on relatively pure compounds thus increasing the number of steps necessary to obtain polyesters from the crude plant oil. Recently, Meier and coll. demonstrated that a mixture of fatty acid methyl esters with a high ratio of polyunsaturated ones can constitute a very efficient material to obtain α,ω-difunctional monomers by self-metathesis.[211] Indeed, the volatile products such as 1,4-cyclohexadiene, hex-3-ene, non-3-ene, dodec-3-ene and dodec-6-ene can be easily removed from the equilibrium reaction mixture thus shifting the equilibrium toward the desired α,ω-diester. From this approach, the authors isolated a mixture of C18 and C21 α,ω-diesters (the C18 being predominant) that were subsequently hydrogenated and reduced to form the saturated mixture of diols. Both diesters and diols were then polycondensated, to produce an aliphatic long-chain polyester with a melting point of 95°C.

This section clearly demonstrates that metathesis reaction represents a powerful tool for the design of polyethylene like materials. Moreover the easy hydrogenation of the resulting monomers or polymers allows the synthesis of highly crystalline materials.

II.3. Carbonylation / Isomerizing alkoxycarbonylation

Another route to get semi-crystalline linear polyesters from fatty acids is based on alkoxycarbonylation methodology. Quinzler and Mecking used $[Co_2(CO)_8]$/pyridine catalytic systems for the copolymerization of undec-1-en-10-ol with carbon monoxide (CO).[212] Molecular weights up to 23 kg.mol^{-1} were achieved at high temperature (160°C) and high pressure of CO (>100 bar). ^{1}H and ^{13}C NMR studies revealed the presence of some alkyl

branches as a result of 2,1-insertion of terminal double bonds or reaction of internal double bonds caused by isomerization thus leading to complex melt behavior around 65°C.

The same group reported the efficient carbonylation of methyl oleate and methyl erucate by exposure to carbon monoxide in methanol or ethanol respectively in the presence of catalytic amounts of $Pd(OAc)_2$, 1,2-bis[(di-tert-butylphosphino)methyl]benzene and methanesulfonic acid[213] or bis(trifluoromethanesulfonato){1,2-bis(di-tert-butylphosphinomethyl)benzene} palladium(II)[214, 215] which exhibit enhance activity and selectivity toward linear ester. By this way, C19 and C23 diesters were obtained when using methyl oleate and methyl erucate, respectively. The reduction of these diesters afforded the corresponding C19 and C23 diols that were subsequently polycondensated with their respective diacids. The resulting polyester 19,19 showed a Tm at 103°C while polyester 23,23 melts at 99°C. Wide-angle X-ray scattering revealed a degree of crystallinity of 70% for polyester 19,19 and 75% for polyester 23,23, values close to the one of polyethylene's. Polyamides were also synthesized starting from the C19 and C23 diesters.

To further target industrial applications of this synthetic method to α,ω-diesters, Cole-Hamilton and coll. reported an elegant route concerning the methoxycarbonylation of various commercial plant oils such as olive, rapeseed or sunflower oils.[216] To that aim, a palladium-based catalyst modified by the ligand bis(ditertiarybutylphosphinomethyl)benzene (BDTBPMB) was used and afforded the diesters in good yield ranging from 3.4g to 6.9g of diester directly from 10mL of oil (Scheme 12.1).

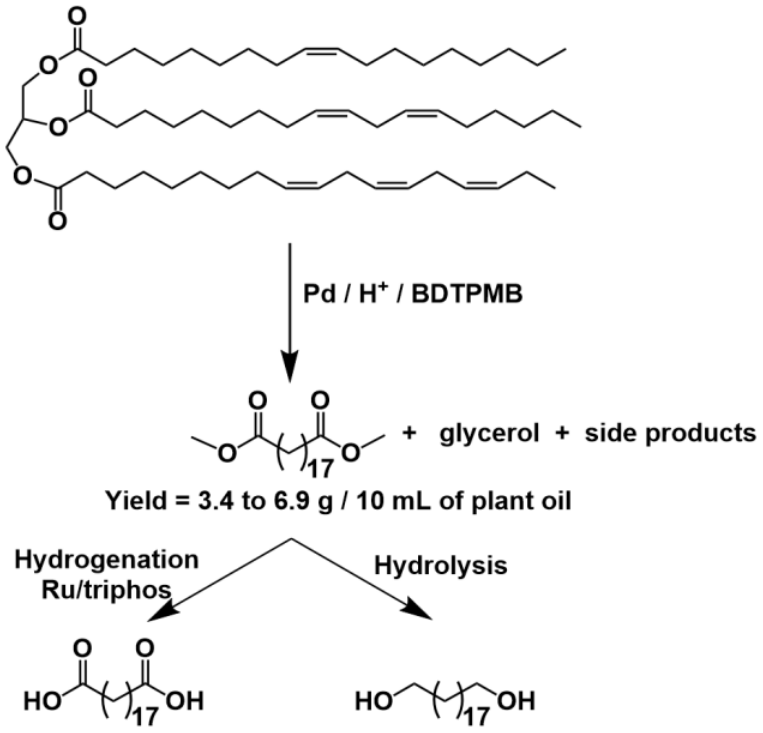

Scheme 12.1.Synthesis of α,ω-diester and diol by methoxycarbonylation of commercial plant oils.[216]

II.4. Other methodologies

Using a totally different approach, Petrovic and coll. synthesized an oil-based polyester using 9-hydroxynonanoic acid methyl ester as an AB monomer. [217] To obtain this hydroxyl fatty acid methyl ester, ozonolysis of castor oil was first carried out followed by reduction and subsequent methanolysis of the triglyceride polyol. The resulting methyl 9-hydroxynonanoate was then polymerized using Ti(IV) isopropoxide as transesterification catalyst (Scheme 13.1). High molecular weight polyester of 62 kg.mol^{-1} was obtained. This polyester was revealed to be close to poly(ε-caprolactone) with a higher melting point (70°C), higher Tg and better thermal stability. Tensile properties of this polyester were typical for a highly crystalline material with a ductile behavior.

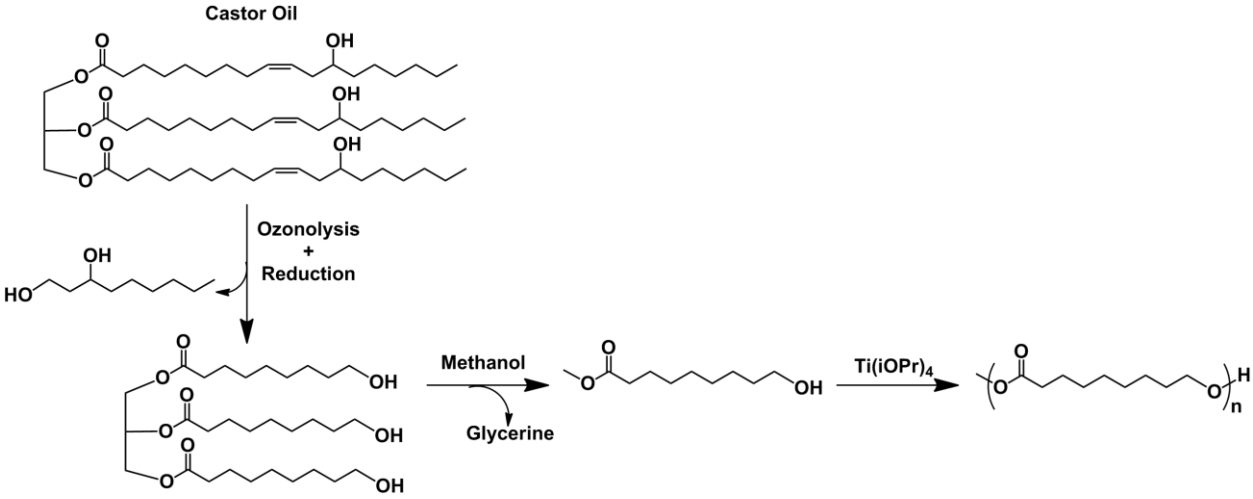

Scheme 13.1.Preparation of poly(9-hydroxynonanoic acid) from castor oil.[217]

Narine and coll. used the same hydroxyl fatty acid but ring opening polymerization method was retained after 9-hydroxynonanoic acid was converted to the dilactone with the help of two different catalysts (lanthanum chloride and aluminium isopropoxide).[218] The dilactone (1,11-dioxacycloicosane-2,12-dione), obtained in high yield (98%) and high purity (98%), was then subjected to ring-opening polymerization. Molecular weights in the range 5-7 kg.mol^{-1} were obtained with dispersities of 1.4 and 1.5 depending on the catalyst used. The thermo-mechanical properties of these poly(nonanolactone)s were investigated by means of DSC analyses and revealed melting point of 69°C similar to the poly(9-hydroxynonanoic acid).

In order to increase the ratio between the number of methylene units over the ester functions, Matsumura and coll. used 12-hydroxydodecanoic acid as starting material.[219] This linear C12 ω-hydroxyacid can be obtained from vernonia oil by oxidative cleavage. This monomer was

subjected to polycondensation and the obtained polyester ($\bar{M}_w$=105 kg.mol^{-1}, Đ=2.9) revealed a melting point of 88°C.

Another promising monomer that can be obtained from fatty acid is ω-pentadecalactone (PDL). However the low ring strain of this lactone makes its ring opening polymerization difficult using traditional chemical methods. Contrarily, lipases have been reported to be highly active initiators for ROP of large ring size lactones.[220] Indeed, the rate determining step which is the formation of the lipase-lactone complex in enzymatic ROP (e-ROP), is promoted by the hydrophobicity of the lactone monomer.[221] Thus larger lactone rings induce higher e-ROP rates. Therefore, polypentadecalactone (PPDL) synthesis by e-ROP was reported to be highly efficient using Novozym 435 and produced high molecular weights ($\bar{M}_n$ up to 480 kg.mol^{-1}).[222-224] Copolymerizations of ω-pentadecalactone with other lactone monomers such as *p*-dioxanone and ε-caprolactone were also reported as well as block copolymerization by using hydroxyl-terminated polybutadiene as macroinitiator for the eROP of PDL.[225-228] Physical characterizations of PPDL revealed a Tg of -27°C and a melting point of 97°C. High values of crystallinity were observed in the range 54-64%. The mechanical behavior, evaluated by tensile tests, revealed comparable features than low-density polyethylene indicating the great potential of this biodegradable polyester in a wide range of applications (Scheme 14.1).[229]

In order to highlight the similarities between PPDL and polyethylene, Gross and coll. investigated the effects of the molecular weight of PPDL on its mechanical and thermal properties.[224] A series of PPDL of $\bar{M}_w$ ranging from 25 to 480 kg.mol^{-1} were prepared by lipase catalysis. Tensile tests revealed a brittle-to-ductile transition for samples with $\bar{M}_w$ values between 45 and 81 kg.mol^{-1} while samples with $\bar{M}_w$ over 189 kg.mol^{-1} showed a tough behavior with elongation at break around 600%. This strain hardening can be explained by enhanced entanglement strength in the amorphous regions. Young's Modulus and stress at yield decreased with the molecular weight and presented similar trends as crystallinity. Thus, in comparison with high density polyethylene (HDPE), PPDL presented similar feature in terms of Young's Modulus and stress at yield with molecular weight but differing trends with respect to elongation at break. These differences can be explained by the presence of C-O bonds in ester linkages of PPDL.

Some attempts of metal-catalyzed ROP of PDL were carried out with initiators such as Y(OiPr)$_3$ and Ln(BH4)3(THF)$_3$, however lower molecular weight (30-40 kg.mol^{-1}) PPDL were obtained.[230, 231] Recently, Duchateau and coll. described the synthesis of high molecular weight ($\bar{M}_n$>155 kg.mol^{-1}) PPDL by using an aluminium-salen complex as the initiator.[232, 233]

Thus, this study revealed the feasibility of ROP of PDL by using cheap and robust metal-based catalysts.

More recently the same group published a complementary route to PDL ROP by using TBD as an organocatalyst in combination with an alcohol initiator.[234] Various other N-heterocyclic organic molecules such as guanidines, amidines and N-heterocyclic carbenes (NHCs) were investigated as catalysts for PDL ROP, however the combination of TBD with an alcohol initiator was the only efficient system.

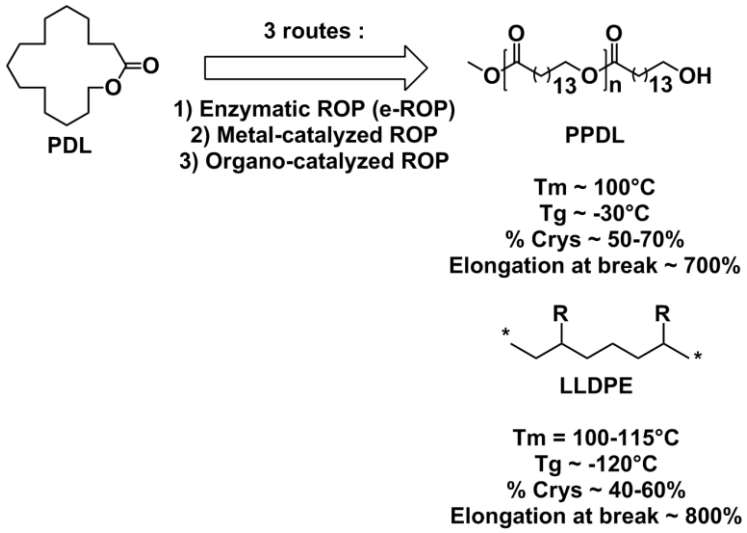

Scheme 14.1.Various catalytic routes to PPDL.[222-224, 229, 232-234]

A linear long aliphatic polyester bearing 14 methylene units between two ester functions was also synthesized by Gross and coll. To that aim, they first described the biosynthesis of ω-hydroxytetradecanoic acid (ω-OHC14) and other long chain hydroxyacids from fatty acids (C12 and C16) by using engineered *C.tropicalis*.[235] The resulting ω-OHC14 methyl ester was then polymerized by AB-type self-condensation using $Ti(OiPr)_4$ as a catalyst.[236] By varying the polymerization conditions such as the catalyst concentration or the reaction time, a series of poly(ω-hydroxytetradecanoate)s (P(ω-OHC14)) were prepared with various molecular weights (from 53 kg.mol^{-1} to 140 kg.mol^{-1}). Thermal analysis showed a melting point of around 94°C which is in accordance with PPDL result (polyester with one additional methylene unit between two ester functions). As PPDL, P(ω-OHC14) showed a dependence of its mechanical properties with respect to molecular weight. A brittle-to-ductile transition was observed with $\bar{M}_w$ values between 78 kg.mol^{-1} and 140 kg.mol^{-1} while the sample with $\bar{M}_w$ of 53 kg.mol^{-1} exhibited a brittle behavior due to a lack of entanglement network strength in amorphous regions. The tough behavior of high $\bar{M}_w$ P(ω-OHC14) is underlined as seen from high values of elongation at break (around 700%) coupled with a high tensile strength (around 50MPa). These values are comparable to the ones of HDPE. Copolymerization of ω-

OHC14 with 1,4-butanediol and dimethyl terephthalate was carried out, by the same group, in order to target similar properties than the commercial product Ecoflex®. By varying the ratio between the comonomers, a large range of thermo-mechanical properties was obtained. Particularly, the copolymer comprising 60mol% of biobased ω-OHC14 repeating units showed similar tensile properties than Ecoflex.[237]

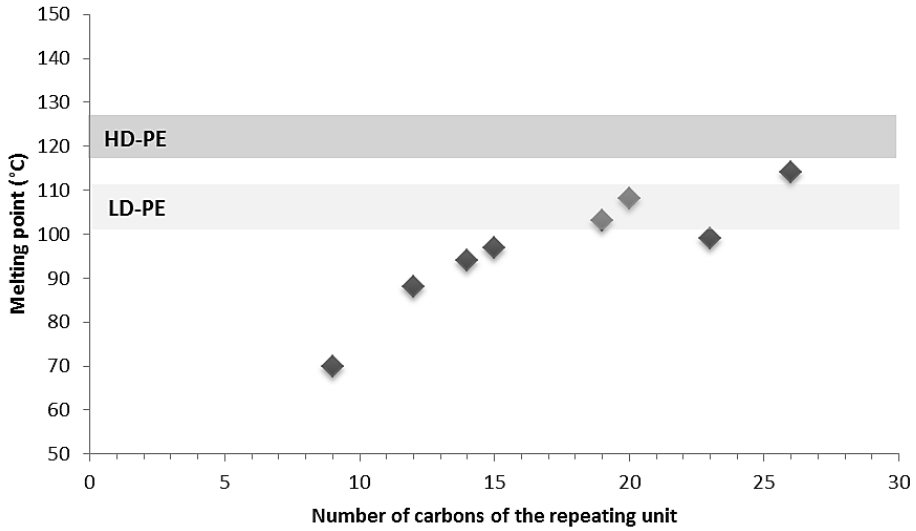

Figure 25.1.Melting point of various polyethylene « like » aliphatic polyesters synthesized from fatty acids.

To conclude, many routes have been investigated to mimic polyethylene starting from plant oils feedstock. Indeed, fatty acids already contain long chain linear segments that make them suitable for the design of long methylene chain building blocks. Thiol-ene reaction was proposed as a powerful tool to induce bifunctionality to fatty acid derivatives. However, the presence of sulfur atoms in the resulting polymer backbone leads to more flexible materials and thus to lower melting points. Metathesis was revealed to be highly efficient for the design of polyethylene mimics. This reaction can be applied to many substrates and can be used for the design of step-growth polymerization building blocks or directly as a polymerization method (ADMET). By that way, several long methylene chain polyesters were synthesized. It is however necessary to perform a hydrogenation step of the building blocks or the unsaturated polymer in order to reach maximum crystallinity. To date, one drawback of this pathway is the high price of the metathesis catalysts. Other strategies were reported such as the carbonylation polymerization or the isomerizing alkoxycarbonylation of fatty acids. This last strategy was highly efficient due to complete feedstock molecule utilization. Various other chemical synthesis or biosynthesis of monomers were reported and allowed the polymerization of C9 to C15 ω-hydroxyacids (or lactones). To conclude, thermo-mechanical properties of linear polyethylene were approached with long chain fatty acid-based polyesters

(Figure 25.1). However, further dilution of the ester functions in the polymer backbone remains necessary to completely mimic polyethylene and to get similar crystalline lamellar thickness. Concerning low-density polyethylene, similar thermal and mechanical properties were obtained by using fatty acids as feedstock with the additional particularity of being hydrolytically degradable. This statement shows the great potential of plant oils as a reliable feedstock for polymer industry even if biodegradability or biocompostability studies still need to be investigated.

In view of the extensive use of polyethylene-based materials for the toughening of PLLA, all these "polyethylene like" polyesters are of great interest in that field. Indeed, similar properties than HDPE or LDPE were achieved with the additional presence ester linkages as hydrolysable sites. Moreover, the ester linkages and the hydroxyl or carboxylic acid chain ends could be of great interest to perform *in-situ* compatibilization during melt-blending with PLLA by using epoxide or isocyanate third components.

III. SOFT AND ELASTOMERIC POLYESTERS

The inherent internal position of the fatty acid double bonds can be of great interest when soft materials are targeted. Indeed, after reaction of the internal function, an alkyl dangling chain remains in the structure of the so-formed molecule. In the particular case of polymers, the alkyl dangling chains will serve as internal plasticizers leading to low Tg materials which are either amorphous or in the melted state at room temperature. When copolymerized with linear monomers or cross-linked, thermoplastic elastomers or thermosetting elastomers with interesting properties are achievable. Regarding the wide use of thermoplastic elastomers such as styrenics or acrylics for the rubber-toughening of PLLA (See Part A), it is thus of high interest to develop such a type of materials with an additional bio-based character. Moreover, in the case of polyesters, hydrolytic degradability given by the ester functions could be exploited for environmental concerns.

Among the triglyceride oils, castor oil has attracted much attention as it contains approximately 85-90% of ricinoleic acid, a naturally hydroxylated fatty acid which can be readily polymerized.[193, 238] In this line, Hayes and coll. used the bifunctionality of ricinoleic acid to synthesize low molecular weight star-shaped poly(ricinoleic acid)(PRic).[239] Lipase-catalysed transesterification of ricinoleic acid with a polyol such as trimethylolpropane, pentaerythritol or dimer diol was used in this study. The resulting polymers showed melting points below -7°C and high viscosity index suggesting their potential use as lubricants. The same fatty acid was used for the synthesis of a cross-linked elastomer.[240] Authors first

synthesized high molecular weight PRic by lipase-catalyzed polycondensation (Scheme 15.1). The effect of several reaction parameters on the molecular weigth of the polymer was investigated and revealed that high lipase loadings (up to 50wt%) together with the use of molecular sieves were requested to yield significant molecular weights. A PRic with a $\bar{M}_w$ of 98 kg.mol^{-1} showed a fully amorphous feature with a low Tg of -75°C. This value is close to the one of natural rubber and of synthetic polyisoprene (Tg in the range of -62 to -67°C) suggesting the potential use of PRic as an elastomer after crosslinking. The cured PRic with dicumyl peroxide showed a Tg of -65°C.

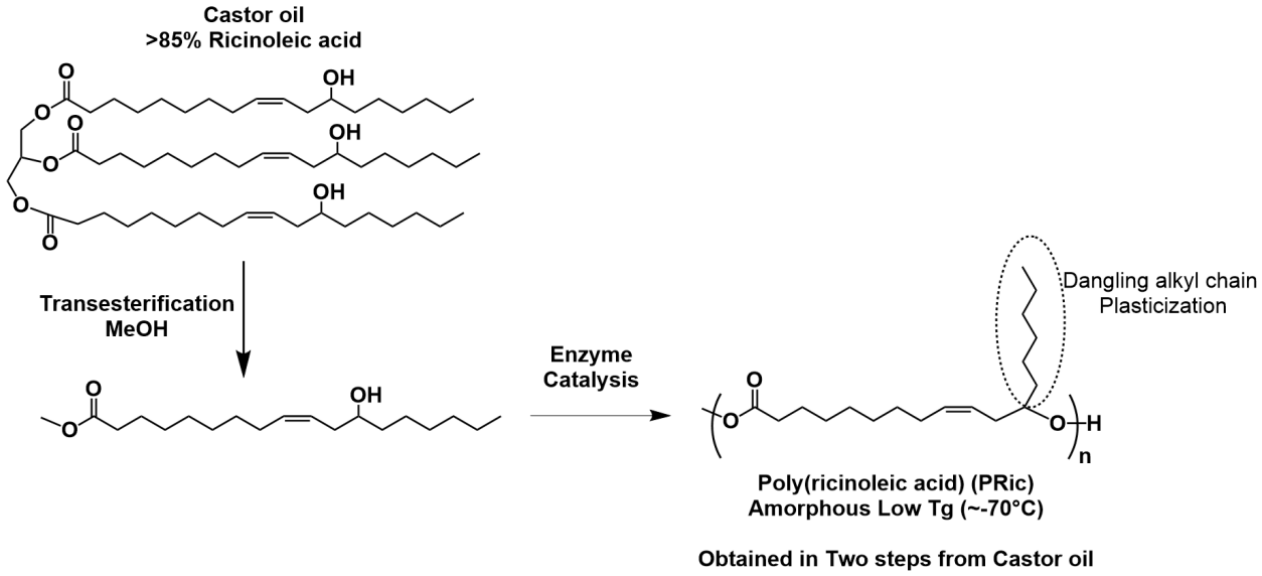

Scheme 15.1.Two-steps synthesis of amorphous Poly(ricinoleic acid) (PRic) from castor oil.[240]

The same authors carried out the vulcanization of PRic of different molecular weights with sulfur curatives in the presence of carbon black as filler.[241] The thermosetting elastomers obtained formed a rubber-like sheet with a smooth and non-sticky surface. Mechanical properties of the elastomers were highly dependent on the molecular weight of the PRic ($\bar{M}_w$ of 52 and 108 kg.mol^{-1} were used in the study) as well as on the amount of the sulfur curatives introduced in the formulation. Optimal formulation revealed a tensile strength at break of 6.9MPa with a corresponding elongation of 350%. Thus high molecular weight PRic may become a promising bio-based thermosetting elastomer that could substitute some of petroleum based synthetic rubbers.

The copolymerization of ricinoleic acid with lactic acid was also reported.[120] In a first method, ricinoleic acid and L-lactic acid were directly copolymerized by thermal polycondensation leading to random copolyesters of low molecular weights between 2 and 8 kg.mol^{-1}. The random copolymers exhibited melting points below 100°C; over 20% of ricinoleic acid unit, the copolymers were viscous liquid at room temperature. A second

method was based on the transesterification of high molecular weight PLA with ricinoleic acid and post-polyesterification. In comparison to the previous methodology, this second route leads to semi-crystalline multiblock copolyesters of molecular weights ranging from 6 to 14 kg.mol^{-1}.

Following a similar methodology, the same group investigated the synthesis of poly(ester-anhydride)s prepared by the melt polycondensation of diacid oligomers of poly(sebacic acid) transesterified with ricinoleic acid.[242] Molecular weights in the range 2-60 kg.mol^{-1} and melting temperatures of 24°C-77°C were reported depending on the amount of ricinoleic acid that reacted. Stability to sterilization by γ-irradiation was confirmed allowing the use of these copolymers for biomedical applications.[243-245]

In another study, the same authors reported the stereocomplexation of poly(L-lactic acid-ricinoleic acid)s multiblock copolyesters with PDLA.[246] The copolyesters were synthesized by polycondensation of ricinoleic acid with PLLA oligomers of various molecular weights. Stereocomplexation by solvent mixing was observed only for copolyesters with PLLA blocks of more than 10 repeating units as seen from the characteristic melting point of the stereocomplex. Ricinoleic lactone formation was also investigated by using intramolecular esterification of ricinoleic acid with DCC, DMAP and hydrochloric acid.[247] This procedure resulted in a mixture of lactones containing up to 6 ricinoleic units. Ring-opening polymerization of the isolated C12 and C24 or the C12-C72 mixture of lactones was carried out using two different initiators ($Y(O^iPr)_3$ and $Sn(octoate)_2$). All were inactive except the tin catalyst for the ROP of C24 lactone that gave low molecular weight PRic ($\bar{M}_n$=4.4 kg.mol^{-1}). Copolymerization of the lactone mixture with lactide by ROP using $Sn(Oct)_2$ as a catalyst yielded copolyesters of $\bar{M}_n$ in the range 5-16 kg.mol^{-1} (Scheme 16.1). The limitation of the molecular weight was explained by the low reactivity of the ricinoleic acid lactone due to low ring strain and steric hindrance of the lactone ester function.

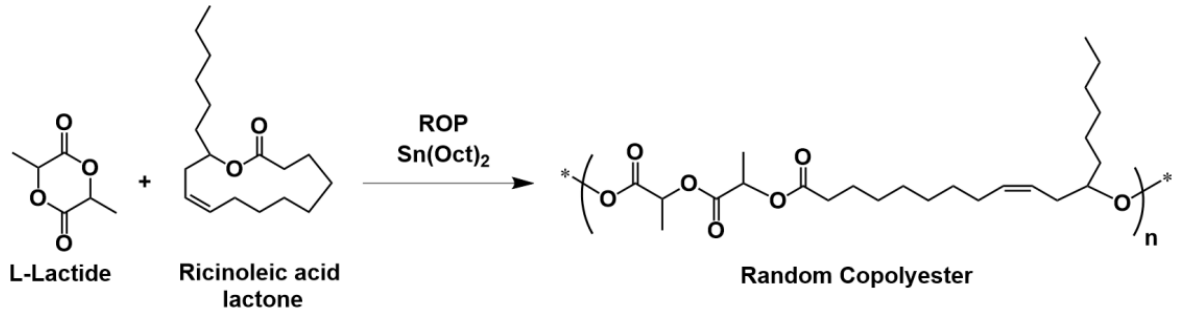

Scheme 16.1.Copolymerization of L-lactide with ricinoleic acid lactone.[247]

Since the remaining double bond of ricinoleic acid repeating unit can be subjected to oxidation and to a loss of thermal stability, Matsumura and coll. used hydrogenated methyl

ricinoleate (methyl 12-hydroxystearate) (12HS) as an AB-type monomer for polyester synthesis.[219]

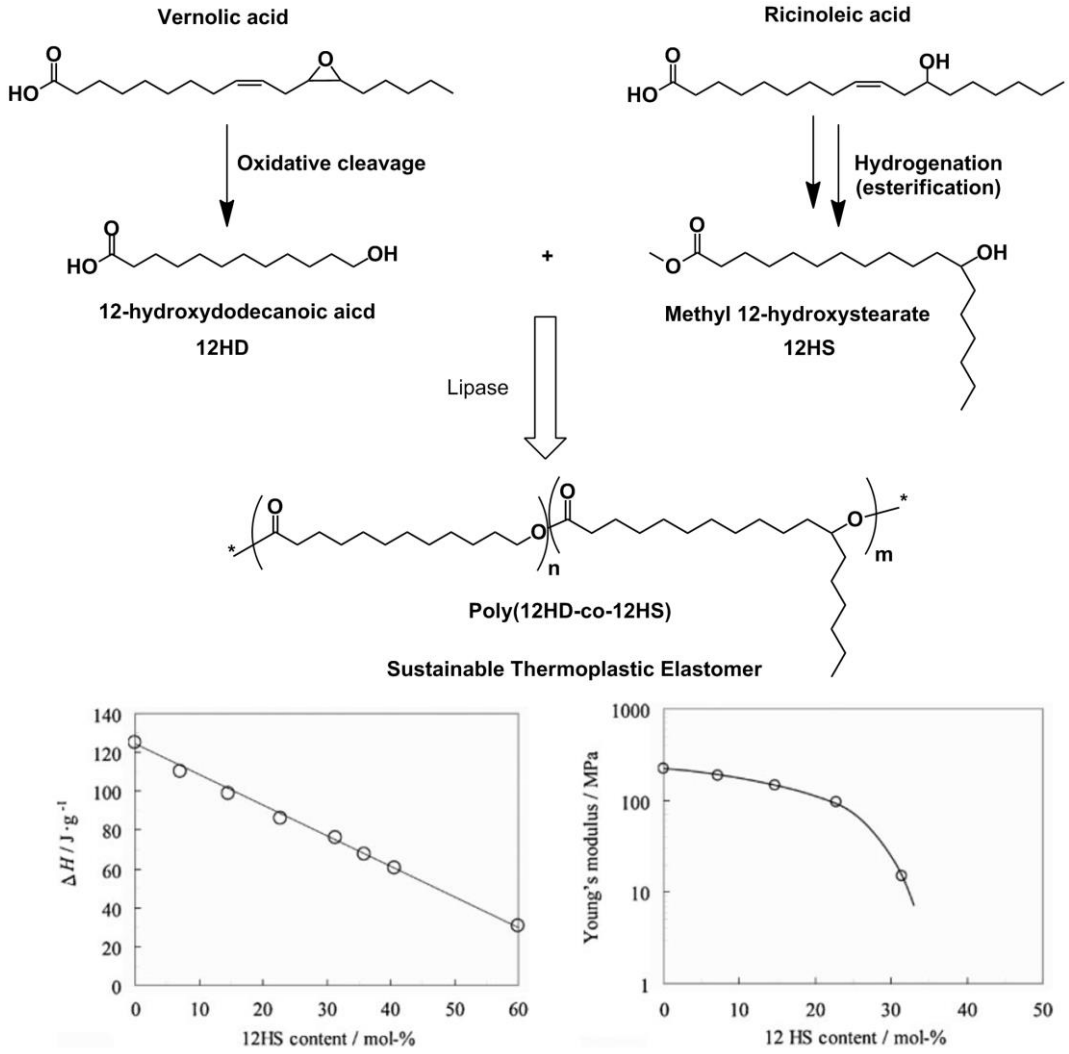

Scheme 17.1.AB type self-condensation route to biobased and biodegradable thermoplastic elastomers. Both melting enthalpy and Young's modulus decrease with an increase of 12HS content.[219]

The authors have synthesized copolyesters by using 12-hydroxydodecanoic acid (12HD), which is obtained from vernolic acid, as a comonomer. By varying the amount between the two AB monomers, a series of high molecular weight copolyesters ($\bar{M}_w$ around 100 kg.mol^{-1}) were synthesized by polycondensation in the presence of lipase (Scheme 17.1). The thermo-mechanical properties of the copolyesters were varying with the amount of 12HS in the copolymer. Indeed, while poly(12HD) showed a melting temperature of 88°C, the copolyesters melting point (as well as the corresponding enthalpy) was highly decreasing with an increase of 12HS units (Tm around 20°C for 60 mol% 12HS). Similar trend was observed for the Young's modulus. Moreover these copolyesters were proved to be biodegradable allowing their use as green and sustainable soft materials. In terms of physico-chemical and

mechanical properties, these bio-based thermoplastic elastomers present close similarities with the petroleum-based ethylene-octene and ethylene-hexene copolymers.

Copolymerization of methyl 12-hydroxystearate with pentadecalactone (PDL) was also reported with the same goal to develop bio-based thermoplastic elastomers.[248] Copolymers of various compositions were prepared by lipase-catalyzed copolymerization. By this way, a wide range of thermo-mechanical properties was obtained with respect to the amount of hard (PDL units) and soft (12HS units) segments in the copolymer structure. Indeed, while neat PPDL shows a Young's modulus of 367MPa and an elongation at break of 500%, copolymer with 60wt% hydroxystearate presents a Young's modulus of 3MPa and breaks at 2400% elongation. Biodegradation investigations were carried out on these copolymers and showed an improvement of the biodegradability with the 12HS content in the copolymer.

Recently, Meier and Kolb proposed an interesting route to soft materials by using saturated fatty acid methyl esters as substrates.[249] The strategy employed in this study was the conversion of various saturated fatty acids to their malonate derivatives bearing an aliphatic chain of 6 to 16 methylene units depending on the saturated fatty-acid used. These malonate derivatives were then polymerized with 1,6-hexanediol using different catalysts (TBD, p-TsOH, $Ti(OiPr)_4$) yielding polyesters with aliphatic dangling chains differing in length (Scheme 18.1).

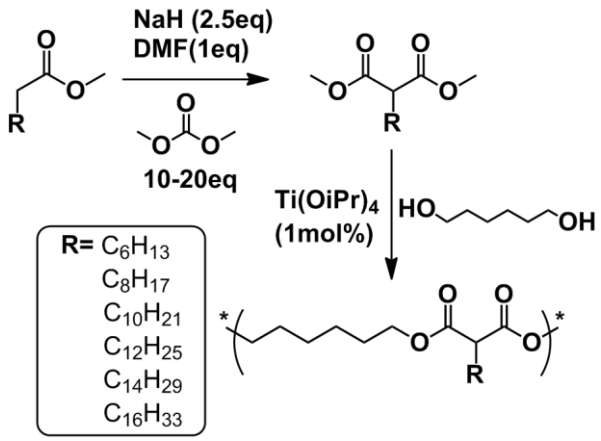

Scheme 18.1.Malonate synthesis from saturated fatty acids followed by subsequent polycondensation with 1,6-hexanediol.[249]

Thermo-mechanical analysis of the resulting polyesters showed different behaviors depending on the length of the side chain. The polyesters with dangling chain composed of 6 to 8 methylene units were fully amorphous with Tg below -65°C. The polyesters synthesized from malonates with longer side chains were semi-crystalline with very low melting point. The latter increased with the length of the side chain to reach 27°C for the longer side chain

polyesters studied. The non-polar interactions of the long alkyl dangling chains were found responsible for the crystallinity of these polyesters.

Regarding the reported studies concerning the synthesis of soft polyesters, it is obvious that the choice and the modification of the substrate play a crucial role in defining the properties of the resulting materials. Indeed, a large palette of polyesters with a broad range of thermo-mechanical properties is accessible depending on the nature (linear or branched) and the ratio of comonomer incorporated. These soft polyesters could be applied as lubricants, cosmetics, pharmaceutics, specialty polymers (cross-linked elastomers or thermoplastic elastomers) but also as additives or precursors of new tough PLLA materials.

IV. FUNCTIONAL POLYESTERS

As demonstrated in the previous parts, many examples of aliphatic polyesters obtained from fatty acids have been reported. Most of them are potentially biodegradable suggesting their potential use for environmental applications. However these materials are free of functional groups for further modification.[250, 251] In the first part of this chapter, it was shown that when melt-blending strategy was retained to toughen PLLA, a third component or reactive sites were generally needed to improve the interfacial adhesion between the PLLA matrix and the additive. Thus, in view of the use of fatty acid-based polyesters as additives, it could be of great interest to incorporate functional groups into the structure of the additive in order to induce branching, grafting or cross-linking during the blending process.

The functionalization of polyesters has been extensively studied. [251, 252] Poly(hydroxyester)s and poly(epoxyester)s represent the most studied functionalized polyesters. Indeed hydroxyl and epoxide functions are very versatile due to a large number of functionalization possibilities in mild conditions. Furthermore, these organic functions are well adapted to the compatibilization of blends composed of PLLA and polyester additives. For instance, epoxide functions could readily react with the carboxylic acid chain ends of PLLA leading to grafting between the matrix and the dispersed phase. Some relevant examples of functionalized polyesters that have been synthesized from fatty acids feedstock are described in the following part.

IV.1. Polyesters with functional groups in the side-chains

A first study involves the use of ADMET and thiol-ene methodologies to synthesize functionalized polyesters from hydroxyl-bearing unsaturated compounds.[253] First, methyl erucate and methyl oleate were epoxidized and subsequently reacted with allyl alcohol in

acidic conditions yielding the corresponding α,ω-dienes. These monomers were then polymerized by ADMET or thiol-ene addition with 1,4-butanedithiol to give poly(hydroxyester)s with molecular weights in the range 3-18 kg.mol^{-1} depending on the monomer and polymerization method used (Scheme 19.1). Thermo-mechanical analysis of these polyesters has revealed low Tg of around -60°C and a melting transition at -18°C in the case of the polyhydroxyester synthesized from the erucic acid-based α,ω-diene by thiol-ene polymerization.

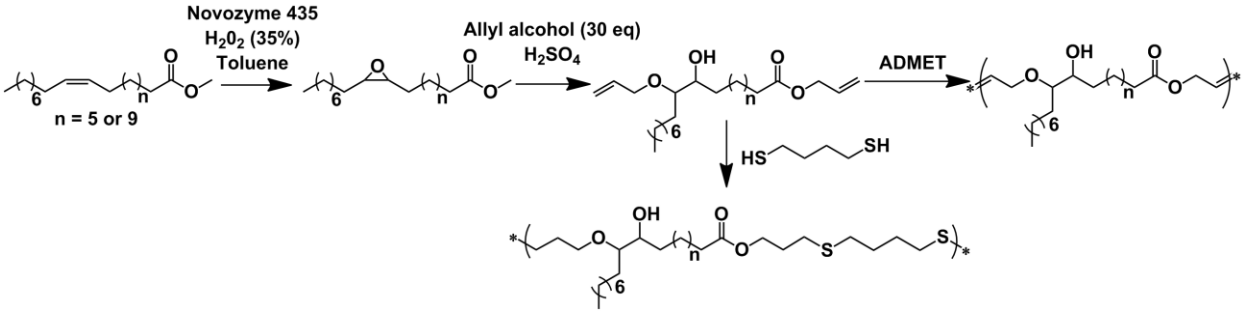

Scheme 19.1.ADMET and thiol-ene approaches to poly(hydroxyester).[253]

In a similar work, another hydroxyl-bearing α,ω-diene was synthesized by reaction of two equivalents of 10-undecenoic acid with one equivalent of 1,3-dichloro-2-propanol yielding through ADMET a semi-crystalline polyester of 5 kg.mol^{-1} molecular weight with a Tg of -25°C and a melting point of 41°C.[254] Copolymerizations of this hydroxyl-bearing monomer with a phosphorous-bearing α,ω-diene synthesized from 10-undecenoic acid were carried out to target flame-retardant applications of the resulting materials.[255] Thermal properties of the copolymers were varying with the amount of phosphorous-bearing monomer introduced in the copolymer structure. Tg increased from -25°C to 6°C when 75mol% of phosphorous-bearing monomer was reacted. Post-functionalization of the hydroxyl functions was then carried out by acrylation. The acrylated polyesters were then cross-linked using dicumyl peroxide. The resulting thermosets showed Tg in the range 35°C to 52°C, good thermal stabilities, and good flame retardancy.

The synthesis of poly(hydroxyester)s by reaction of a diacid with a triol is possible but is generally limited by the numerous branching reactions that occur prior to cross-linking of the system. Thus, it is necessary to control the stoichiometry as well as the reaction conditions in order to avoid undesirable side reactions. Gross and coll. demonstrated that immobilized *Candida Antarctica* Lipase B efficiently catalyzed the polycondensation of a diacid with a triol with very low degrees of branching and no cross-linking, which enables the synthesis of linear poly(hydroxyester)s.[256] For that purpose, the authors used an oleic diacid (1,18-cis-9-

octanedecenedioic acid) synthesized using *Candida tropicalis* ATCC20962. This diacid was then reacted with glycerol yielding polyol polyesters by enzyme catalysis.

Also by using Lipase as a catalyst, Kobayashi and coll. synthesized epoxide-bearing polyesters using two functionalization routes.[257] The first one was the synthesis of aliphatic polyesters containing an unsaturated group in the side chain by reaction of divinyl sebacate, glycerol and unsaturated fatty acids[258] followed by the epoxidation of unsaturated fatty acid side chains using hydrogen peroxide and *Candida Antarctica* lipase. In the second route, fatty acids were epoxidized and polymerized with divinyl sebacate and glycerol to give the epoxy-bearing polyesters. In all cases, high epoxidized ratios were achieved. The resulting functionalized polyesters were then thermally cured to yield biodegradable films.

Pre-functionalization pathway to functional polyester was also reported by using an epoxy-bearing diacid.[259] This diacid was synthesized by a two-step procedure from oleic acid. Epoxidation of the internal double bond was first carried out using hydrogen peroxide and Novozym 435. The resulting epoxy fatty acid was then converted to the epoxy-bearing α,ω-dicarboxylic acid by using *Candida tropicalis* ATCC20962. The lipase catalyzed copolymerization of this diacid with various diols yielded the corresponding copolyesters with molecular weight values in the range 25-57 kg.mol^{-1} (Scheme 20.1).

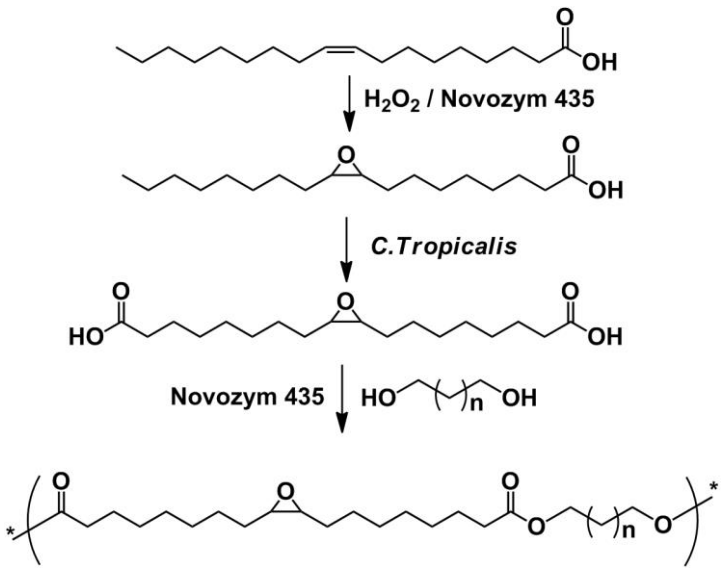

Scheme 20.1.Lipase catalyzed polymerization of an epoxide-bearing diacid with various diols.[259]

Thiol-ene chemistry was also used for grafting functional groups onto polyesters bearing terminal double bonds that are more reactive. In order to synthesize a monomer with a terminal double bond, malonization of methyl 10-undecenoate was carried out.[260] The resulting malonate was then subjected to polycondensation with 1,6-hexanediol to afford unsaturated aliphatic polyester. Thiol derivatives were reacted with the polyester in quantitative yields. In a second approach, the authors investigated cross-metathesis as a

functionalization tool and observed very good conversions of the unsaturated polyesters into their functionalized counterparts.

IV.2. Generation of functional groups during the polymerization

An elegant and simple route to polyhydroxyester was proposed by Dettloff and coll. regarding the use of 10,11-epoxyundecanoic acid as a monomer.[261] This epoxy fatty acid was polymerized via nucleophilic ring-opening of the epoxide group with the carboxylic acid moiety (Scheme 21.1). Initiation of the polymerization was carried out using quaternary ammonium or phosphonium salts. The polyester was fully characterized and exhibited similar thermomechanical properties to LLDPE as seen from the values of yield stress, elongation and Young's modulus. In addition, this polyester showed interesting adhesion and barrier properties to oxygen.

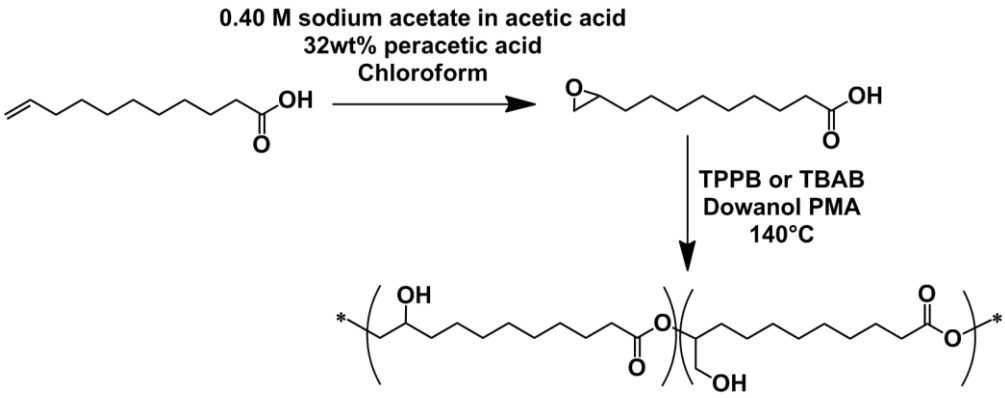

Scheme 21.1.Synthesis of poly(hydroxyester) by nucleophilic ring-opening polymerization.[261]

Similarly, Wang and coll. used epoxidized oleic acid for the preparation of poly(hydroxyester)s by simple heating of the monomer.[262] Characterization of the obtained polymers showed mainly the presence of ester linkages that confirm the ring-opening of the epoxide by the carboxylic acid function of the monomer. Only a small amount of ether linkages, resulting from the nucleophilic ring-opening of the epoxide by alcohol moieties, was observed. These functionalized polyesters were subsequently cross-linked using various diisocyanates.

The same strategy was adapted to diglycidyl sebacate, a bisepoxy derived from sebacic acid.[263] This bisepoxy compound was reacted by nucleophilic ring–opening polymerization with sebacic acid to yield a polyester bearing free hydroxyl groups. Structural characterization of the so-formed polyester revealed a very low degree of branching of around 10%. This value is much lower than the one observed for the corresponding polyester synthesized by polycondensation of sebacic acid with glycerol. Free hydroxyl functions of this polyester were

then functionalized by esterification in mild conditions with Boc-protected glycine. Functionalization by reaction with maleic anhydride was also investigated. In both cases, high degrees of functionalization were reached (80 to 90%).

IV.3. Functional groups at the chain ends

Another functionalization approach is to introduce a specific functionality at the chain ends of the polyester for macromolecular engineering purposes. In a first example, e-ROP of pentadecalactone (PDL) was performed by using Novozyme 435 in the presence of glycidol and a divinyl ester of adipic acid.[264] By this way, bisepoxy functional PPDL was synthesized. By playing on the stoichiometry of the building blocks, polyesters of various molecular weights were achieved (from 1.4 to 2.7 $kg.mol^{-1}$). Curing of these macromonomers by photopolymerization with a cycloaliphatic bisepoxide resulted in polyester networks. In the same line, PPDL was reacted with equimolar amounts of functional initiator and terminator yielding α,ω-PPDL with thiol-thiol, acrylate-acrylate or thiol-acrylate end groups.[265]

Functionalization at the chain ends generally leads to mono- or bi-functional chains regarding the linear structure of most of the polyesters. When a higher functionalization degree is needed, the use of hyperbranched structures may reveal appropriate. Meier and coll. reported the thiol-ene addition between methyl 10-undecenoate and 1-thioglycerol as an efficient route for the synthesis of an AB_2 monomer (Scheme 22.1).[190] Polycondensation with or without a core-molecule (glycerol) was then carried out using TBD as a catalyst. The degree of branching, calculated using a reported equation[266], was in the range 0.40-0.47 which is in agreement with the values generally reported for similar systems. Interestingly, such hyperbranched (HB) polyesters exhibited a semi-crystalline character with a melting point at 50°C. The unusual long aliphatic chain between two branching point allowed the crystallization of this polyester while amorphous polymers are generally obtained in HB structures. The same polyester was investigated after the polycondensation of this AB_2 monomer was carried out by using various catalysts such as titanium butoxide ($Ti(OBu)_4$), antimony trioxide (Sb_2O_3) and zinc acetate ($Zn(Ac)_2$).[267] Polyesters with high molecular weight were obtained when these catalysts were used instead of TBD.

Hydroformylation/hydrogenation is a well-known procedure in oleochemistry to introduce hydroxyl functions in the structure of plant oils and fatty acids, which can be used to produce HB polymers. Applied to methyl soyate, which consists of a mixture of saturated and unsaturated fatty acid methyl esters, hydroformylation followed by hydrogenation yield to a mixture of fatty acid methyl esters bearing zero, one, two and three hydroxyl groups.[268]

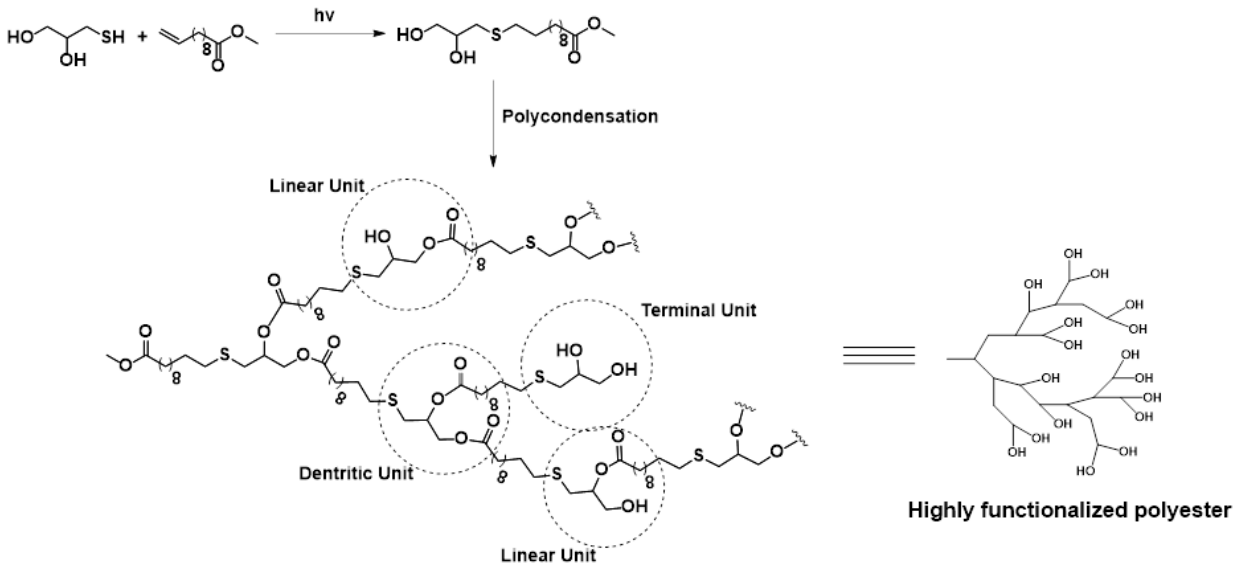

Scheme 22.1. Hyperbranched polyester synthesized from an AB_2 monomer obtained from methyl 10-undecenoate.[190, 267]

As the bis-hydroxyl compound is the major compound, it is then possible to synthesize HB polyesters by simple polycondensation. Molecular weights up to 42 kg.mol^{-1} were obtained. By this way, very high values of weight average functionality can be obtained despite the presence of non-functional compounds.

We can conclude from this section that a large variety of functionalized polyesters are accessible from plant oils thanks to the various routes investigated to modify fatty acids. Similarly to glycidyl methacrylate-based impact modifiers that have been used for the toughening of PLLA, the described functionalized polyesters offer various possibilities for the compatibilization of binary blends between PLA and polyester rubbers.

V. SUMMARY

This state-of-the-art concerning fatty acid-based polyesters showed the great versatility of this feedstock for the synthesis of well-defined polymers. Indeed, in a first part we demonstrated the possible mimicry of existing petroleum-based polymers such as polyethylene by using the plant oils platform. Very similar properties than polyethylene were achieved by decreasing the ester function density in the polyester backbone. In view of the extensive use of polyethylene-based materials for the toughening of PLLA, fatty acids thus offer appropriate perspectives in that field. Another class of materials widely used as impact modifiers for PLLA is the thermoplastic elastomers family (such as SBS, SEBS, ABS…). The bibliographic study also revealed the feasibility of such materials by using fatty acids as feedstock. By combining branched and linear aliphatic segments, thermoplastic elastomers can be easily synthesized.

The wide range of mechanical properties achievable by this approach thus indicates their good potential as impact modifiers for PLLA. Finally, in a last part, we reported several examples of functionalized aliphatic polyesters. It was shown that functional groups such as double bonds, hydroxyl and epoxide groups can be easily incorporated into a polyester backbone. This is of great interest in the context of PLLA toughening as functional polymers are often added to binary blends in order to improve interfacial adhesion between the PLLA matrix and the dispersed phase. To conclude, plant oils platform represents a suitable feedstock for the development of novel impact modifiers matching with PLLA toughening requirements. The lack of reported examples in that field prompted us to investigate the development of new fatty acid-based impact modifiers for PLLA.

REFERENCES

1. *European Bioplastics Website,* http://en.european-bioplastics.org/.
2. K. Hofvendahl and B. Hahn–Hägerdal, *Enzyme and Microbial Technology*, 2000, **26**, 87-107.
3. E. T. H. Vink, K. R. Rábago, D. A. Glassner and P. R. Gruber, *Polymer Degradation and Stability*, 2003, **80**, 403-419.
4. K. Madhavan Nampoothiri, N. R. Nair and R. P. John, *Bioresource Technology*, 2010, **101**, 8493-8501.
5. R. John, K. M. Nampoothiri and A. Pandey, *Applied Microbiology and Biotechnology*, 2007, **74**, 524-534.
6. R. Datta and M. Henry, *Journal of Chemical Technology & Biotechnology*, 2006, **81**, 1119-1129.
7. G. Reddy, M. Altaf, B. J. Naveena, M. Venkateshwar and E. V. Kumar, *Biotechnology Advances*, 2008, **26**, 22-34.
8. A. Södergård and M. Stolt, *Progress in Polymer Science*, 2002, **27**, 1123-1163.
9. D. Garlotta, *Journal of Polymers and the Environment*, 2001, **9**, 63-84.
10. L. T. Lim, R. Auras and M. Rubino, *Progress in Polymer Science*, 2008, **33**, 820-852.
11. K. Hiltunen, J. V. Seppälä and M. Härkönen, *Journal of Applied Polymer Science*, 1997, **63**, 1091-1100.
12. J. Tuominen and J. V. Seppälä, *Macromolecules*, 2000, **33**, 3530-3535.
13. S. I. Moon, C. W. Lee, I. Taniguchi, M. Miyamoto and Y. Kimura, *Polymer*, 2001, **42**, 5059-5062.
14. S. Penczek, A. Duda, R. Szymanski and T. Biela, *Macromolecular Symposia*, 2000, **153**, 1-15.
15. A. P. Dove, *ACS Macro Letters*, 2012, **1**, 1409-1412.
16. A.-C. Albertsson and R. K. Srivastava, *Advanced Drug Delivery Reviews*, 2008, **60**, 1077-1093.
17. C. M. Thomas, *Chemical Society Reviews*, 2010, **39**, 165-173.
18. O. Dechy-Cabaret, B. Martin-Vaca and D. Bourissou, *Chemical Reviews*, 2004, **104**, 6147-6176.
19. C. Jérôme and P. Lecomte, *Advanced Drug Delivery Reviews*, 2008, **60**, 1056-1076.
20. N. E. Kamber, W. Jeong, R. M. Waymouth, R. C. Pratt, B. G. G. Lohmeijer and J. L. Hedrick, *Chemical Reviews*, 2007, **107**, 5813-5840.
21. A. P. Gupta and V. Kumar, *European Polymer Journal*, 2007, **43**, 4053-4074.
22. A. J. Nijenhuis, D. W. Grijpma and A. J. Pennings, *Macromolecules*, 1992, **25**, 6419-6424.
23. H. R. Kricheldorf, I. Kreiser-Saunders and C. Boettcher, *Polymer*, 1995, **36**, 1253-1259.
24. A. Kowalski, A. Duda and S. Penczek, *Macromolecules*, 2000, **33**, 7359-7370.
25. J. Dahlmann and G. Rafler, *Acta Polymerica*, 1993, **44**, 103-107.
26. P. Dubois, C. Jacobs, R. Jerome and P. Teyssie, *Macromolecules*, 1991, **24**, 2266-2270.
27. H. Kricheldorf and A. Serra, *Polymer Bulletin*, 1985, **14**, 497-502.
28. F. Chabot, M. Vert, S. Chapelle and P. Granger, *Polymer*, 1983, **24**, 53-59.
29. M. Bero, J. Kasperczyk and Z. J. Jedlinski, *Die Makromolekulare Chemie*, 1990, **191**, 2287-2296.
30. M. Stolt and A. Södergård, *Macromolecules*, 1999, **32**, 6412-6417.
31. B. M. Chamberlain, B. A. Jazdzewski, M. Pink, M. A. Hillmyer and W. B. Tolman, *Macromolecules*, 2000, **33**, 3970-3977.
32. R. M. Rasal, A. V. Janorkar and D. E. Hirt, *Progress in Polymer Science*, 2010, **35**, 338-356.
33. M. J. Stanford and A. P. Dove, *Chemical Society Reviews*, 2010, **39**, 486-494.
34. R. Vasanthakumari and A. J. Pennings, *Polymer*, 1983, **24**, 175-178.
35. B. Kalb and A. J. Pennings, *Polymer*, 1980, **21**, 607-612.
36. Y. Ikada, K. Jamshidi, H. Tsuji and S. H. Hyon, *Macromolecules*, 1987, **20**, 904-906.
37. H. Tsuji and Y. Ikada, *Macromolecules*, 1993, **26**, 6918-6926.
38. H. Tsuji, *Macromolecular Bioscience*, 2005, **5**, 569-597.
39. W. Hoogsteen, A. R. Postema, A. J. Pennings, G. Ten Brinke and P. Zugenmaier, *Macromolecules*, 1990, **23**, 634-642.

40. J. Kobayashi, T. Asahi, M. Ichiki, A. Oikawa, H. Suzuki, T. Watanabe, E. Fukada and Y. Shikinami, *Journal of Applied Physics*, 1995, **77**, 2957-2973.
41. B. Eling, S. Gogolewski and A. J. Pennings, *Polymer*, 1982, **23**, 1587-1593.
42. J. Puiggali, Y. Ikada, H. Tsuji, L. Cartier, T. Okihara and B. Lotz, *Polymer*, 2000, **41**, 8921-8930.
43. L. Cartier, T. Okihara, Y. Ikada, H. Tsuji, J. Puiggali and B. Lotz, *Polymer*, 2000, **41**, 8909-8919.
44. P. Pan and Y. Inoue, *Progress in Polymer Science*, 2009, **34**, 605-640.
45. J. Zhang, Y. Duan, H. Sato, H. Tsuji, I. Noda, S. Yan and Y. Ozaki, *Macromolecules*, 2005, **38**, 8012-8021.
46. J. R. Sarasua, A. L. Arraiza, P. Balerdi and I. Maiza, *Polymer Engineering & Science*, 2005, **45**, 745-753.
47. K. Kishore, R. Vasanthakumari and A. J. Pennings, *Journal of Polymer Science: Polymer Physics Edition*, 1984, **22**, 537-542.
48. H. Tsuji and Y. Ikada, *Polymer*, 1995, **36**, 2709-2716.
49. H. Tsuji and Y. Ikada, *Polymer*, 1996, **37**, 595-602.
50. G. Perego, G. D. Cella and C. Bastioli, *Journal of Applied Polymer Science*, 1996, **59**, 37-43.
51. J. J. Kolstad, *Journal of Applied Polymer Science*, 1996, **62**, 1079-1091.
52. G. Z. Papageorgiou, D. S. Achilias, S. Nanaki, T. Beslikas and D. Bikiaris, *Thermochimica Acta*, 2010, **511**, 129-139.
53. J.-J. Hwang, S.-M. Huang, H.-J. Liu, H.-C. Chu, L.-H. Lin and C.-S. Chung, *Journal of Applied Polymer Science*, 2012, **124**, 2216-2226.
54. V. Krikorian and D. J. Pochan, *Macromolecules*, 2004, **37**, 6480-6491.
55. Y. Li, C. Chen, J. Li and X. S. Sun, *Journal of Applied Polymer Science*, 2012, **124**, 2968-2977.
56. R. Liao, B. Yang, W. Yu and C. Zhou, *Journal of Applied Polymer Science*, 2007, **104**, 310-317.
57. J. Y. Nam, S. Sinha Ray and M. Okamoto, *Macromolecules*, 2003, **36**, 7126-7131.
58. S. Sinha Ray, K. Yamada, M. Okamoto, Y. Fujimoto, A. Ogami and K. Ueda, *Polymer*, 2003, **44**, 6633-6646.
59. B. Li, F.-X. Dong, X.-L. Wang, J. Yang, D.-Y. Wang and Y.-Z. Wang, *European Polymer Journal*, 2009, **45**, 2996-3003.
60. H. Tsuji, H. Takai, N. Fukuda and H. Takikawa, *Macromolecular Materials and Engineering*, 2006, **291**, 325-335.
61. M. J. Sobkowicz, R. Sosa and J. R. Dorgan, *Journal of Applied Polymer Science*, 2011, **121**, 2029-2038.
62. P. Song, G. Chen, Z. Wei, Y. Chang, W. Zhang and J. Liang, *Polymer*, 2012, **53**, 4300-4309.
63. J. Li, D. Chen, B. Gui, M. Gu and J. Ren, *Polymer Bulletin*, 2011, **67**, 775-791.
64. H. Nakajima, M. Takahashi and Y. Kimura, *Macromolecular Materials and Engineering*, 2010, **295**, 460-468.
65. H. Bai, W. Zhang, H. Deng, Q. Zhang and Q. Fu, *Macromolecules*, 2011, **44**, 1233-1237.
66. L. Wen, Z. Xin and D. Hu, *Journal of Polymer Science Part B: Polymer Physics*, 2010, **48**, 1235-1243.
67. Y. Tachibana, T. Maeda, O. Ito, Y. Maeda and M. Kunioka, *Polymer Degradation and Stability*, 2010, **95**, 1321-1329.
68. P. Pan, J. Yang, G. Shan, Y. Bao, Z. Weng and Y. Inoue, *Macromolecular Materials and Engineering*, 2012, **297**, 670-679.
69. T. Wei, L. Lei, H. Kang, B. Qiao, Z. Wang, L. Zhang, P. Coates, K.-C. Hua and J. Kulig, *Advanced Engineering Materials*, 2012, **14**, 112-118.
70. N. Kawamoto, A. Sakai, T. Horikoshi, T. Urushihara and E. Tobita, *Journal of Applied Polymer Science*, 2007, **103**, 198-203.
71. N. Kawamoto, A. Sakai, T. Horikoshi, T. Urushihara and E. Tobita, *Journal of Applied Polymer Science*, 2007, **103**, 244-250.
72. Y. Cai, S. Yan, J. Yin, Y. Fan and X. Chen, *Journal of Applied Polymer Science*, 2011, **121**, 1408-1416.
73. P. Song, Z. Wei, J. Liang, G. Chen and W. Zhang, *Polymer Engineering & Science*, 2012, **52**, 1058-1068.

74. J. Y. Nam, M. Okamoto, H. Okamoto, M. Nakano, A. Usuki and M. Matsuda, *Polymer*, 2006, **47**, 1340-1347.
75. A. M. Harris and E. C. Lee, *Journal of Applied Polymer Science*, 2008, **107**, 2246-2255.
76. Q. Xing, X. Zhang, X. Dong, G. Liu and D. Wang, *Polymer*, 2012, **53**, 2306-2314.
77. K. S. Anderson and M. A. Hillmyer, *Polymer*, 2006, **47**, 2030-2035.
78. J. Narita, M. Katagiri and H. Tsuji, *Macromolecular Materials and Engineering*, 2011, **296**, 887-893.
79. T. Furukawa, H. Sato, R. Murakami, J. Zhang, Y.-X. Duan, I. Noda, S. Ochiai and Y. Ozaki, *Macromolecules*, 2005, **38**, 6445-6454.
80. Y. Hu, H. Sato, J. Zhang, I. Noda and Y. Ozaki, *Polymer*, 2008, **49**, 4204-4210.
81. M. Zhang and N. L. Thomas, *Advances in Polymer Technology*, 2011, **30**, 67-79.
82. H. Tsuji, M. Sawada and L. Bouapao, *ACS Applied Materials & Interfaces*, 2009, **1**, 1719-1730.
83. J.-T. Yeh, C.-J. Wu, C.-H. Tsou, W.-L. Chai, J.-D. Chow, C.-Y. Huang, K.-N. Chen and C.-S. Wu, *Polymer-Plastics Technology and Engineering*, 2009, **48**, 571-578.
84. M. Shibata, Y. Inoue and M. Miyoshi, *Polymer*, 2006, **47**, 3557-3564.
85. J. Cai, M. Liu, L. Wang, K. Yao, S. Li and H. Xiong, *Carbohydrate Polymers*, 2011, **86**, 941-947.
86. T. Ke and X. Sun, *Journal of Applied Polymer Science*, 2003, **89**, 1203-1210.
87. A. Pei, Q. Zhou and L. A. Berglund, *Composites Science and Technology*, 2010, **70**, 815-821.
88. R. Zhang, Y. Wang, K. Wang, G. Zheng, Q. Li and C. Shen, *Polymer Bulletin*, 2013, **70**, 195-206.
89. H. Tsuji, H. Takai and S. K. Saha, *Polymer*, 2006, **47**, 3826-3837.
90. S. C. Schmidt and M. A. Hillmyer, *Journal of Polymer Science Part B: Polymer Physics*, 2001, **39**, 300-313.
91. R. E. Drumright, P. R. Gruber and D. E. Henton, *Advanced Materials*, 2000, **12**, 1841-1846.
92. J. K. Lee, K. H. Lee and B. S. Jin, *European Polymer Journal*, 2001, **37**, 907-914.
93. R. Auras, B. Harte and S. Selke, *Macromolecular Bioscience*, 2004, **4**, 835-864.
94. I. Engelberg and J. Kohn, *Biomaterials*, 1991, **12**, 292-304.
95. J. J. Cooper-White and M. E. Mackay, *Journal of Polymer Science Part B: Polymer Physics*, 1999, **37**, 1803-1814.
96. V. Taubner and R. Shishoo, *Journal of Applied Polymer Science*, 2001, **79**, 2128-2135.
97. R. Cairncross, J. Becker, S. Ramaswamy and R. O'Connor, *Appl Biochem Biotechnol*, 2006, **131**, 774-785.
98. G. Kale, R. Auras, S. P. Singh and R. Narayan, *Polymer Testing*, 2007, **26**, 1049-1061.
99. G. Kale, T. Kijchavengkul, R. Auras, M. Rubino, S. E. Selke and S. P. Singh, *Macromolecular Bioscience*, 2007, **7**, 255-277.
100. K. I. Park and M. Xanthos, *Polymer Degradation and Stability*, 2009, **94**, 834-844.
101. A. A. Shah, F. Hasan, A. Hameed and S. Ahmed, *Biotechnology Advances*, 2008, **26**, 246-265.
102. Y. Tokiwa and A. Jarerat, *Biotechnology Letters*, 2004, **26**, 771-777.
103. J.-W. Rhim, H.-M. Park and C.-S. Ha, *Progress in Polymer Science*.
104. P. Bordes, E. Pollet and L. Avérous, *Progress in Polymer Science*, 2009, **34**, 125-155.
105. O. Martin and L. Avérous, *Polymer*, 2001, **42**, 6209-6219.
106. N. López-Rodríguez and J. R. Sarasua, *Polymer Engineering & Science*, 2013, **53**, 2073-2080.
107. H. Liu and J. Zhang, *Journal of Polymer Science Part B: Polymer Physics*, 2011, **49**, 1051-1083.
108. D. W. Grijpma, A. J. Nijenhuis, P. G. T. Wijk and A. J. Pennings, *Polymer Bulletin*, 1992, **29**, 571-578.
109. *NatureWorks. Technology Focus Report, http://www.natureworksllc.com/*.
110. J.-F. Zhang and X. Sun, *Polymer International*, 2004, **53**, 716-722.
111. R. Bhardwaj and A. K. Mohanty, *Biomacromolecules*, 2007, **8**, 2476-2484.
112. Y. Lin, K.-Y. Zhang, Z.-M. Dong, L.-S. Dong and Y.-S. Li, *Macromolecules*, 2007, **40**, 6257-6267.
113. M. L. Robertson, K. Chang, W. M. Gramlich and M. A. Hillmyer, *Macromolecules*, 2010, **43**, 1807-1814.
114. W. M. Gramlich, M. L. Robertson and M. A. Hillmyer, *Macromolecules*, 2010, **43**, 2313-2321.
115. M. L. Robertson, J. M. Paxton and M. A. Hillmyer, *ACS Applied Materials & Interfaces*, 2011, **3**, 3402-3410.
116. Y. Yuan and E. Ruckenstein, *Polymer Bulletin*, 1998, **40**, 485-490.

117. K. S. Anderson, K. M. Schreck and M. A. Hillmyer, *Polymer Reviews*, 2008, **48**, 85-108.
118. H. Fukuzaki, Y. Aiba, M. Yoshida, M. Asano and M. Kumakura, *Die Makromolekulare Chemie*, 1989, **190**, 2407-2415.
119. H. Fukuzaki, Y. Aiba, M. Yoshida, M. Asano and M. Kumakura, *Die Makromolekulare Chemie*, 1989, **190**, 2571-2577.
120. R. Slivniak and A. J. Domb, *Macromolecules*, 2005, **38**, 5545-5553.
121. M. Hiljanen-Vainio, T. Karjalainen and J. Seppälä, *Journal of Applied Polymer Science*, 1996, **59**, 1281-1288.
122. E. Ruckenstein and Y. Yuan, *Journal of Applied Polymer Science*, 1998, **69**, 1429-1434.
123. A. Nakayama, N. Kawasaki, I. Arvanitoyannis, J. Iyoda and N. Yamamoto, *Polymer*, 1995, **36**, 1295-1301.
124. E. M. Frick and M. A. Hillmyer, *Macromolecular Rapid Communications*, 2000, **21**, 1317-1322.
125. E. M. Frick, A. S. Zalusky and M. A. Hillmyer, *Biomacromolecules*, 2003, **4**, 216-223.
126. D. Haynes, A. K. Naskar, A. Singh, C.-C. Yang, K. J. Burg, M. Drews, G. Harrison and D. W. Smith, *Macromolecules*, 2007, **40**, 9354-9360.
127. L. M. Pitet and M. A. Hillmyer, *Macromolecules*, 2009, **42**, 3674-3680.
128. G. Theryo, F. Jing, L. M. Pitet and M. A. Hillmyer, *Macromolecules*, 2010, **43**, 7394-7397.
129. U. Ojha, P. Kulkarni, J. Singh and R. Faust, *Journal of Polymer Science Part A: Polymer Chemistry*, 2009, **47**, 3490-3505.
130. D. W. Grijpma, R. D. A. Van Hofslot, H. Supèr, A. J. Nijenhuis and A. J. Pennings, *Polymer Engineering & Science*, 1994, **34**, 1674-1684.
131. A. Behr, J. Eilting, K. Irawadi, J. Leschinski and F. Lindner, *Green Chemistry*, 2008, **10**, 13-30.
132. Z. Zhang, D. W. Grijpma and J. Feijen, *Macromolecular Chemistry and Physics*, 2004, **205**, 867-875.
133. W. Guerin, M. Helou, J.-F. Carpentier, M. Slawinski, J.-M. Brusson and S. M. Guillaume, *Polymer Chemistry*, 2013, **4**, 1095-1106.
134. N. Andronova and A.-C. Albertsson, *Biomacromolecules*, 2006, **7**, 1489-1495.
135. M. Ryner and A.-C. Albertsson, *Biomacromolecules*, 2002, **3**, 601-608.
136. O. Jeon, S.-H. Lee, S. H. Kim, Y. M. Lee and Y. H. Kim, *Macromolecules*, 2003, **36**, 5585-5592.
137. D. Cohn and A. Hotovely Salomon, *Biomaterials*, 2005, **26**, 2297-2305.
138. J. F. Kong, V. Lipik, M. J. M. Abadie, G. R. Deen and S. S. Venkatraman, *Polymer International*, 2012, **61**, 43-50.
139. M. T. Martello and M. A. Hillmyer, *Macromolecules*, 2011, **44**, 8537-8545.
140. D. Zhang, M. A. Hillmyer and W. B. Tolman, *Biomacromolecules*, 2005, **6**, 2091-2095.
141. C. L. Wanamaker, L. E. O'Leary, N. A. Lynd, M. A. Hillmyer and W. B. Tolman, *Biomacromolecules*, 2007, **8**, 3634-3640.
142. C. L. Wanamaker, M. J. Bluemle, L. M. Pitet, L. E. O'Leary, W. B. Tolman and M. A. Hillmyer, *Biomacromolecules*, 2009, **10**, 2904-2911.
143. S. Hiki, M. Miyamoto and Y. Kimura, *Polymer*, 2000, **41**, 7369-7379.
144. D. C. Aluthge, C. Xu, N. Othman, N. Noroozi, S. G. Hatzikiriakos and P. Mehrkhodavandi, *Macromolecules*, 2013, **46**, 3965-3974.
145. K. S. Anderson and M. A. Hillmyer, *Polymer*, 2004, **45**, 8809-8823.
146. K. S. Anderson, S. H. Lim and M. A. Hillmyer, *Journal of Applied Polymer Science*, 2003, **89**, 3757-3768.
147. Y. Feng, Y. Hu, J. Yin, G. Zhao and W. Jiang, *Polymer Engineering & Science*, 2013, **53**, 389-396.
148. Z. Su, Q. Li, Y. Liu, G.-H. Hu and C. Wu, *European Polymer Journal*, 2009, **45**, 2428-2433.
149. P. Ma, D. G. Hristova-Bogaerds, J. G. P. Goossens, A. B. Spoelstra, Y. Zhang and P. J. Lemstra, *European Polymer Journal*, 2012, **48**, 146-154.
150. X. Zhang, Y. Li, L. Han, C. Han, K. Xu, C. Zhou, M. Zhang and L. Dong, *Polymer Engineering & Science*, 2013, DOI: 10.1002/pen.23507.
151. H. Liu, W. Song, F. Chen, L. Guo and J. Zhang, *Macromolecules*, 2011, **44**, 1513-1522.
152. H. Liu, F. Chen, B. Liu, G. Estep and J. Zhang, *Macromolecules*, 2010, **43**, 6058-6066.

153. M. Murariu, A. D. S. Ferreira, E. Duquesne, L. Bonnaud and P. Dubois, *Macromolecular Symposia*, 2008, **272**, 1-12.
154. B. Meng, J. Deng, Q. Liu, Z. Wu and W. Yang, *European Polymer Journal*, 2012, **48**, 127-135.
155. N. Petchwattana, S. Covavisaruch and N. Euapanthasate, *Materials Science and Engineering: A*, 2012, **532**, 64-70.
156. S. Ye, T. Ting Lin, W. Weei Tjiu, P. Kwan Wong and C. He, *Journal of Applied Polymer Science*, 2013, **128**, 2541-2547.
157. N. López-Rodríguez, A. López-Arraiza, E. Meaurio and J. R. Sarasua, *Polymer Engineering & Science*, 2006, **46**, 1299-1308.
158. V. Vilay, M. Mariatti, Z. Ahmad, K. Pasomsouk and M. Todo, *Journal of Applied Polymer Science*, 2009, **114**, 1784-1792.
159. L. Wang, W. Ma, R. A. Gross and S. P. McCarthy, *Polymer Degradation and Stability*, 1998, **59**, 161-168.
160. T. Semba, K. Kitagawa, U. S. Ishiaku and H. Hamada, *Journal of Applied Polymer Science*, 2006, **101**, 1816-1825.
161. T. Semba, K. Kitagawa, U. S. Ishiaku, M. Kotaki and H. Hamada, *Journal of Applied Polymer Science*, 2007, **103**, 1066-1074.
162. T. Takayama and M. Todo, *Journal of Materials Science*, 2006, **41**, 4989-4992.
163. T. Takayama, M. Todo, H. Tsuji and K. Arakawa, *Journal of Materials Science*, 2006, **41**, 6501-6504.
164. M. Harada, K. Iida, K. Okamoto, H. Hayashi and K. Hirano, *Polymer Engineering & Science*, 2008, **48**, 1359-1368.
165. J. Odent, J.-M. Raquez, E. Duquesne and P. Dubois, *European Polymer Journal*, 2012, **48**, 331-340.
166. J. Odent, P. Leclère, J.-M. Raquez and P. Dubois, *European Polymer Journal*, 2013, **49**, 914-922.
167. H. Bai, H. Xiu, J. Gao, H. Deng, Q. Zhang, M. Yang and Q. Fu, *ACS Applied Materials & Interfaces*, 2012, **4**, 897-905.
168. I. Bechthold, K. Bretz, S. Kabasci, R. Kopitzky and A. Springer, *Chemical Engineering & Technology*, 2008, **31**, 647-654.
169. X. Liu, M. Dever, N. Fair and R. S. Benson, *Journal of environmental polymer degradation*, 1997, **5**, 225-235.
170. M. Harada, T. Ohya, K. Iida, H. Hayashi, K. Hirano and H. Fukuda, *Journal of Applied Polymer Science*, 2007, **106**, 1813-1820.
171. V. Vannaladsaysy, M. Todo, T. Takayama, M. Jaafar, Z. Ahmad and K. Pasomsouk, *Journal of Materials Science*, 2009, **44**, 3006-3009.
172. R. Wang, S. Wang, Y. Zhang, C. Wan and P. Ma, *Polymer Engineering & Science*, 2009, **49**, 26-33.
173. L. Jiang, M. P. Wolcott and J. Zhang, *Biomacromolecules*, 2005, **7**, 199-207.
174. N. Zhang, Q. Wang, J. Ren and L. Wang, *Journal of Materials Science*, 2009, **44**, 250-256.
175. W. Dong, B. Zou, P. Ma, W. Liu, X. Zhou, D. Shi, Z. Ni and M. Chen, *Polymer International*, 2013, DOI: 10.1002/pi.4568.
176. I. Noda, M. M. Satkowski, A. E. Dowrey and C. Marcott, *Macromolecular Bioscience*, 2004, **4**, 269-275.
177. I. Noda, P. R. Green, M. M. Satkowski and L. A. Schechtman, *Biomacromolecules*, 2005, **6**, 580-586.
178. Y. Takagi, R. Yasuda, M. Yamaoka and T. Yamane, *Journal of Applied Polymer Science*, 2004, **93**, 2363-2369.
179. K. M. Schreck and M. A. Hillmyer, *Journal of Biotechnology*, 2007, **132**, 287-295.
180. Y. Li and H. Shimizu, *Macromolecular Bioscience*, 2007, **7**, 921-928.
181. W. Zhang, L. Chen and Y. Zhang, *Polymer*, 2009, **50**, 1311-1315.
182. H. Kang, B. Qiao, R. Wang, Z. Wang, L. Zhang, J. Ma and P. Coates, *Polymer*, 2013, **54**, 2450-2458.

183. PlasticsEurope, *Plastics – the Facts 2012 An analysis of European plastics production, demand and recovery for 2011*, 2012.
184. A. Gandini, *Green Chemistry*, 2011, **13**, 1061-1083.
185. G. Lligadas, J. C. Ronda, M. Galià and V. Cádiz, *Biomacromolecules*, 2010, **11**, 2825-2835.
186. Z. S. Petrović, *Polymer Reviews*, 2008, **48**, 109-155.
187. M. A. R. Meier, J. O. Metzger and U. S. Schubert, *Chemical Society Reviews*, 2007, **36**, 1788-1802.
188. L. Montero de Espinosa and M. A. R. Meier, *European Polymer Journal*, 2011, **47**, 837-852.
189. P. Wells and C. Zapata, *Journal of Industrial Ecology*, 2012, **16**, 665-668.
190. O. Türünç and M. A. R. Meier, *Macromolecular Rapid Communications*, 2010, **31**, 1822-1826.
191. O. Turunc and M. A. R. Meier, *Green Chemistry*, 2011, **13**, 314-320.
192. M. A. R. Meier, *Macromolecular Chemistry and Physics*, 2009, **210**, 1073-1079.
193. H. Mutlu and M. A. R. Meier, *European Journal of Lipid Science and Technology*, 2010, **112**, 10-30.
194. S. Chikkali and S. Mecking, *Angewandte Chemie International Edition*, 2012, **51**, 5802–5808.
195. S. Warwel, J. Tillack, C. Demes and M. Kunz, *Macromolecular Chemistry and Physics*, 2001, **202**, 1114-1121.
196. A. Rybak and M. A. R. Meier, *ChemSusChem*, 2008, **1**, 542-547.
197. S. Demel, C. Slugovc, F. Stelzer, K. Fodor-Csorba and G. Galli, *Macromolecular Rapid Communications*, 2003, **24**, 636-641.
198. L. Montero de Espinosa and M. A. R. Meier, *Chemical Communications*, 2011, **47**, 1908-1910.
199. B. Schmidt, *European Journal of Organic Chemistry*, 2004, **2004**, 1865-1880.
200. S. E. Lehman Jr, J. E. Schwendeman, P. M. O'Donnell and K. B. Wagener, *Inorganica Chimica Acta*, 2003, **345**, 190-198.
201. F. C. Courchay, J. C. Sworen and K. B. Wagener, *Macromolecules*, 2003, **36**, 8231-8239.
202. M. Arisawa, Y. Terada, K. Takahashi, M. Nakagawa and A. Nishida, *The Chemical Record*, 2007, **7**, 238-253.
203. P. A. Fokou and M. A. R. Meier, *Journal of the American Chemical Society*, 2009, **131**, 1664-1665.
204. S. H. Hong, D. P. Sanders, C. W. Lee and R. H. Grubbs, *Journal of the American Chemical Society*, 2005, **127**, 17160-17161.
205. P. A. Fokou and M. A. R. Meier, *Macromolecular Rapid Communications*, 2010, **31**, 368-373.
206. J. Trzaskowski, D. Quinzler, C. Bährle and S. Mecking, *Macromolecular Rapid Communications*, 2011, **32**, 1352-1356.
207. C. Vilela, A. J. D. Silvestre and M. A. R. Meier, *Macromolecular Chemistry and Physics*, 2012, **213**, 2220-2227.
208. F. Stempfle, P. Ortmann and S. Mecking, *Macromolecular Rapid Communications*, 2013, **34**, 47-50.
209. P. Ortmann and S. Mecking, *Macromolecules*, 2013, **46**, 7213-7218.
210. M. P. F. Pepels, M. R. Hansen, H. Goossens and R. Duchateau, *Macromolecules*, 2013, **46**, 7668-7677.
211. H. Mutlu, Hofsa, R. E. Montenegro and M. A. R. Meier, *RSC Advances*, 2013, **3**, 4927-4934.
212. D. Quinzler and S. Mecking, *Chemical Communications*, 2009, **0**, 5400-5402.
213. D. Quinzler and S. Mecking, *Angewandte Chemie International Edition*, 2010, **49**, 4306-4308.
214. F. Stempfle, D. Quinzler, I. Heckler and S. Mecking, *Macromolecules*, 2011, **44**, 4159-4166.
215. P. Roesle, C. J. Dürr, H. M. Möller, L. Cavallo, L. Caporaso and S. Mecking, *Journal of the American Chemical Society*, 2012, **134**, 17696-17703.
216. M. R. L. Furst, R. L. Goff, D. Quinzler, S. Mecking, C. H. Botting and D. J. Cole-Hamilton, *Green Chemistry*, 2012, **14**, 472-477.
217. Z. S. Petrović, J. Milić, Y. Xu and I. Cvetković, *Macromolecules*, 2010, **43**, 4120-4125.
218. G. Liu, X. Kong, H. Wan and S. Narine, *Biomacromolecules*, 2008, **9**, 949-953.
219. H. Ebata, K. Toshima and S. Matsumura, *Macromolecular Bioscience*, 2008, **8**, 38-45.
220. S. Kobayashi, *Macromolecular Rapid Communications*, 2009, **30**, 237-266.

221. A. Duda, A. Kowalski, S. Penczek, H. Uyama and S. Kobayashi, *Macromolecules*, 2002, **35**, 4266-4270.
222. M. de Geus, I. van der Meulen, B. Goderis, K. van Hecke, M. Dorschu, H. van der Werff, C. E. Koning and A. Heise, *Polymer Chemistry*, 2010, **1**, 525-533.
223. K. S. Bisht, L. A. Henderson, R. A. Gross, D. L. Kaplan and G. Swift, *Macromolecules*, 1997, **30**, 2705-2711.
224. J. Cai, C. Liu, M. Cai, J. Zhu, F. Zuo, B. S. Hsiao and R. A. Gross, *Polymer*, 2010, **51**, 1088-1099.
225. A. Kumar, B. Kalra, A. Dekhterman and R. A. Gross, *Macromolecules*, 2000, **33**, 6303-6309.
226. G. Ceccorulli, M. Scandola, A. Kumar, B. Kalra and R. A. Gross, *Biomacromolecules*, 2005, **6**, 902-907.
227. Z. Jiang, H. Azim, R. A. Gross, M. L. Focarete and M. Scandola, *Biomacromolecules*, 2007, **8**, 2262-2269.
228. A. Kumar, R. A. Gross, Y. Wang and M. A. Hillmyer, *Macromolecules*, 2002, **35**, 7606-7611.
229. M. Letizia Focarete, M. Scandola, A. Kumar and R. A. Gross, *Journal of Polymer Science Part B: Polymer Physics*, 2001, **39**, 1721-1729.
230. Y. Nakayama, N. Watanabe, K. Kusaba, K. Sasaki, Z. Cai, T. Shiono and C. Tsutsumi, *Journal of Applied Polymer Science*, 2011, **121**, 2098-2103.
231. Z. Zhong, P. J. Dijkstra and J. Feijen, *Macromolecular Chemistry and Physics*, 2000, **201**, 1329-1333.
232. I. van der Meulen, E. Gubbels, S. Huijser, R. l. Sablong, C. E. Koning, A. Heise and R. Duchateau, *Macromolecules*, 2011, **44**, 4301-4305.
233. M. P. F. Pepels, M. Bouyahyi, A. Heise and R. Duchateau, *Macromolecules*, 2013, **46**, 4324-4334.
234. M. Bouyahyi, M. P. F. Pepels, A. Heise and R. Duchateau, *Macromolecules*, 2012, **45**, 3356-3366.
235. W. Lu, J. E. Ness, W. Xie, X. Zhang, J. Minshull and R. A. Gross, *Journal of the American Chemical Society*, 2010, **132**, 15451-15455.
236. C. Liu, F. Liu, J. Cai, W. Xie, T. E. Long, S. R. Turner, A. Lyons and R. A. Gross, *Biomacromolecules*, 2011, **12**, 3291-3298.
237. A. Celli, P. Marchese, S. Sullalti, J. Cai and R. A. Gross, *Polymer*, 2013, **54**, 3774-3783.
238. D. S. Ogunniyi, *Bioresource Technology*, 2006, **97**, 1086-1091.
239. A. R. Kelly and D. G. Hayes, *Journal of Applied Polymer Science*, 2006, **101**, 1646-1656.
240. H. Ebata, K. Toshima and S. Matsumura, *Macromolecular Bioscience*, 2007, **7**, 798-803.
241. H. Ebata, M. Yasuda, K. Toshima and S. Matsumura, *Journal of Oleo Science*, 2008, **57**, 315-320.
242. M. Y. Krasko, A. Shikanov, A. Ezra and A. J. Domb, *Journal of Polymer Science Part A: Polymer Chemistry*, 2003, **41**, 1059-1069.
243. A. Shikanov, A. Ezra and A. J. Domb, *Journal of Controlled Release*, 2005, **105**, 52-67.
244. A. Shikanov and A. J. Domb, *Biomacromolecules*, 2005, **7**, 288-296.
245. A. Shikanov, B. Vaisman, M. Y. Krasko, A. Nyska and A. J. Domb, *Journal of Biomedical Materials Research Part A*, 2004, **69A**, 47-54.
246. R. Slivniak, R. Langer and A. J. Domb, *Macromolecules*, 2005, **38**, 5634-5639.
247. R. Slivniak and A. J. Domb, *Biomacromolecules*, 2005, **6**, 1679-1688.
248. T. Kobayashi and S. Matsumura, *Polymer Degradation and Stability*, 2011, **96**, 2071-2079.
249. N. Kolb and M. A. R. Meier, *Green Chemistry*, 2012, **14**, 2429-2435.
250. P. Lecomte, R. Riva, S. Schmeits, J. Rieger, K. Van Butsele, C. Jérôme and R. Jérôme, *Macromolecular Symposia*, 2006, **240**, 157-165.
251. C. K. Williams, *Chemical Society Reviews*, 2007, **36**, 1573-1580.
252. I. Taniguchi, W. A. Kuhlman, A. M. Mayes and L. G. Griffith, *Polymer International*, 2006, **55**, 1385-1397.
253. O. Kreye, T. Tóth and M. A. R. Meier, *European Polymer Journal*, 2011, **47**, 1804-1816.
254. L. M. de Espinosa, M. A. R. Meier, J. C. Ronda, M. Galià and V. Cádiz, *Journal of Polymer Science Part A: Polymer Chemistry*, 2010, **48**, 1649-1660.

255. L. M. De Espinosa, J. C. Ronda, M. Galià, V. Cádiz and M. A. R. Meier, *Journal of Polymer Science Part A: Polymer Chemistry*, 2009, **47**, 5760-5771.
256. Y. Yang, W. Lu, J. Cai, Y. Hou, S. Ouyang, W. Xie and R. A. Gross, *Macromolecules*, 2011, **44**, 1977-1985.
257. H. Uyama, M. Kuwabara, T. Tsujimoto and S. Kobayashi, *Biomacromolecules*, 2003, **4**, 211-215.
258. T. Tsujimoto, H. Uyama and S. Kobayashi, *Biomacromolecules*, 2000, **2**, 29-31.
259. Y. Yang, W. Lu, X. Zhang, W. Xie, M. Cai and R. A. Gross, *Biomacromolecules*, 2009, **11**, 259-268.
260. N. Kolb and M. A. R. Meier, *European Polymer Journal*, 2013, **49**, 843-852.
261. J. E. White, J. D. Earls, J. W. Sherman, L. C. López and M. L. Dettloff, *Polymer*, 2007, **48**, 3990-3998.
262. S. Miao, S. Zhang, Z. Su and P. Wang, *Journal of Polymer Science Part A: Polymer Chemistry*, 2008, **46**, 4243-4248.
263. Z. You, H. Cao, J. Gao, P. H. Shin, B. W. Day and Y. Wang, *Biomaterials*, 2010, **31**, 3129-3138.
264. M. Eriksson, L. Fogelström, K. Hult, E. Malmström, M. Johansson, S. Trey and M. Martinelle, *Biomacromolecules*, 2009, **10**, 3108-3113.
265. M. Takwa, K. Hult and M. Martinelle, *Macromolecules*, 2008, **41**, 5230-5236.
266. C. J. Hawker, R. Lee and J. M. J. Frechet, *Journal of the American Chemical Society*, 1991, **113**, 4583-4588.
267. Y. Bao, J. He and Y. Li, *Polymer International*, 2013, **62**, 1457-1464.
268. Z. S. Petrović, I. Cvetković, J. Milić, D. Hong and I. Javni, *Journal of Applied Polymer Science*, 2012, **125**, 2920-2928.

CHAPTER 2:

Synthesis of novel fatty acid-based polyesters and poly(ester-amide)s, their characterization and use as impact modifier for poly(L-lactide).

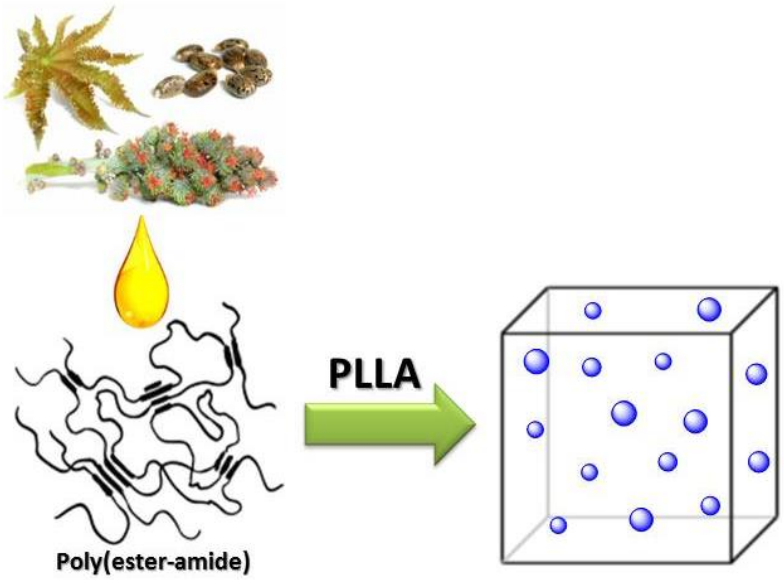

Keywords: fatty acids, castor oil, 10-undecenoic acid, dimerized fatty acids, polycondensation, impact modifier, rubber-toughening, melt-blending, PLLA, poly(ester-amide).

Mots clés: acides gras, huile de ricin, acide 10-undécénoique, dimère d'acides gras, polycondensation, modificateur d'impact, renfort au choc, mélange de polymères, PLLA, poly(ester-amide).

PART A. SYNTHESIS OF ORIGINAL DIOLS FROM METHYL 10-UNDECENOATE AND STRUCTURE-PROPERTIES INVESTIGATION OF THE POLYESTERS AND POLY(ESTER-AMIDE)S SO-FORMED

I. INTRODUCTION

As seen previously, vegetable oils represent a promising class of raw materials for polymer industry owing to their abundant availability, sustainability and biodegradability. The presence of ester functions and double bonds in their backbones enables the design of tailored functional building blocks, in particular diols and diacids, for the synthesis of novel polyesters. Owing to their long alkyl aliphatic segments, the obtained polyesters are generally flexible materials that can be easily processed.

However, such long alkyl chain polyesters lack the thermal performance (high Tm) and the mechanical strength necessary for broader applications and need to be modified, for instance by introducing aromatic segments in their backbone or by further increasing the number of carbons between two ester functions to get relatively high melting points.[1-3] The incorporation of amide segments is another alternative to yield materials with higher thermal behaviour. Aliphatic polyamides are generally not biodegradable but have good solvent and heat stability and display better mechanical and thermal endurance than polyesters due to strong hydrogen bonding. Therefore, the introduction of amide linkages randomly distributed in a polyester skeleton can be a good way to give access to materials with improved thermal endurance. Only few studies were found in the literature that focus on the design of fatty acid based poly(ester-amide)s.[4, 5] In this part, we aimed at developing new polyester and poly(ester-amide) precursors in order to investigate their influence on the properties of the polymers so-formed.

II. SYNTHESIS OF POLYESTER PRECURSORS FROM RENEWABLE RESOURCES

II.1. Synthetic strategy

In order to obtain tunable polyesters based on fatty acid methyl esters, a series of well-defined diols were synthesized starting from methyl 10-undecenoate (UndME). UndME, obtained by steam cracking of methyl ricinoleate (up to 90% in ricin oil) at high temperature (>400 °C)

was chosen to obtain well-defined linear diols.[6] The commercial availability of this compound presented another key factor in the choice of this starting material as it is used industrially by Arkema in large scale for the synthesis of sustainable polyamide-11 (*Rilsan*®).

In order to tune the end-properties of the polymers, the diols were composed of linear or cyclic central blocks with one or two ester linkages (UndPdE-diol, UndIdE-diol and UndPmE-diol), one or two amide linkages (UndBdA-diol and UndPmA-diol) or both ester and amide linkages (UndPEA-diol), as reported in Figure 1.2. The diols were synthesized by a two-step procedure. First a transesterification/amidation or a transamide-esterification was carried out with renewable diols (1,3-propanediol or isosorbide), aminoalcohol (1,3-aminopropanol) or diamine (1,4-diaminobutane) to obtain bis-unsaturated diesters, monoester, esteramide or diamide respectively with different central blocks. [7-11] In a second step, the radical addition of 2-mercaptoethanol MCET (photo- or thermal- initiation) was carried out on the terminal double bonds leading to dihydroxytelechelic compounds. The chemical structure of the synthesized diols and intermediates was assessed by ^{1}H and ^{13}C-NMR and FTIR-ATR spectroscopy. The purity of the final diols and their melting points were determined by GC and Kofler bench, respectively. These diols were also of interest as potential precursors for the synthesis of polyurethanes.[12] Once synthesized, the last step consisted in the polycondensation with a diacid methyl ester to obtain aliphatic polyesters and poly(ester-amide)s. The structure-properties relationship of the so-formed polymers was then investigated.

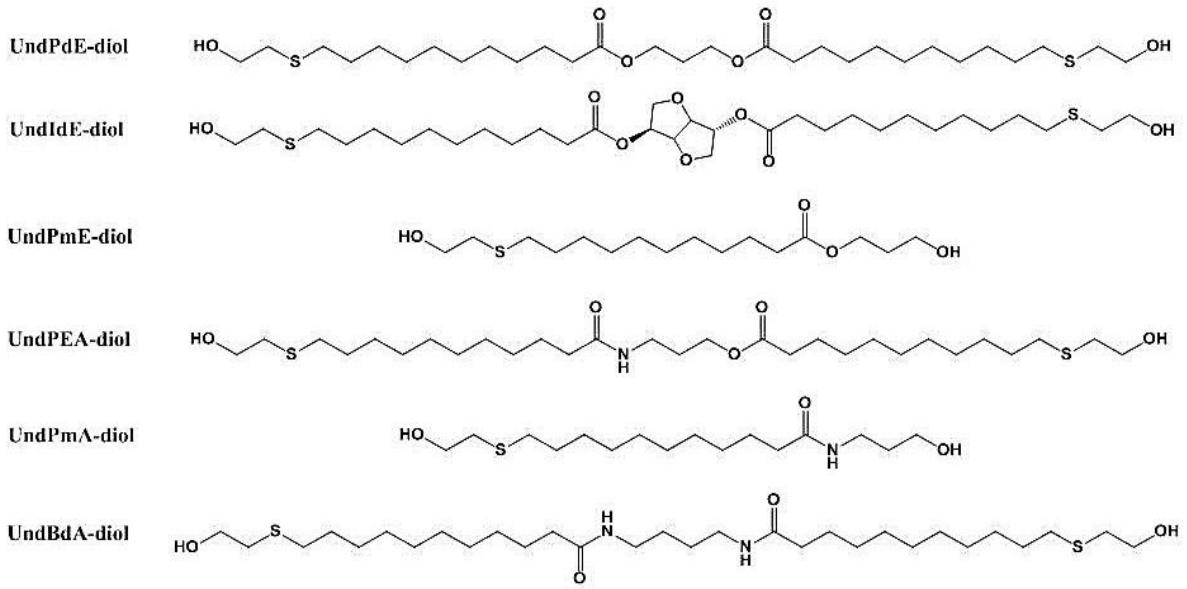

Figure 1.2. Chemical structures of the six diol precursors. Abbreviations used are as follows: [Und= from methyl undecenoate]; [P=propyl, I=from isosorbide, B=butyl] ; [d=di-, m=mono-] ; [E=ester, A=amide, EA=EsterAmide].

II.2. Synthesis of alkene-terminated esters

Scheme 1.2 illustrates the synthesis of UndPdE-diol as a linear diol for the preparation of polyester starting from UndME. The synthesis involved a transesterification step with 5 mol% of 1,5,7-triazabicyclo[4.4.0]dec-5-ene (TBD) as an organo-catalyst followed by the thiol-ene reaction.

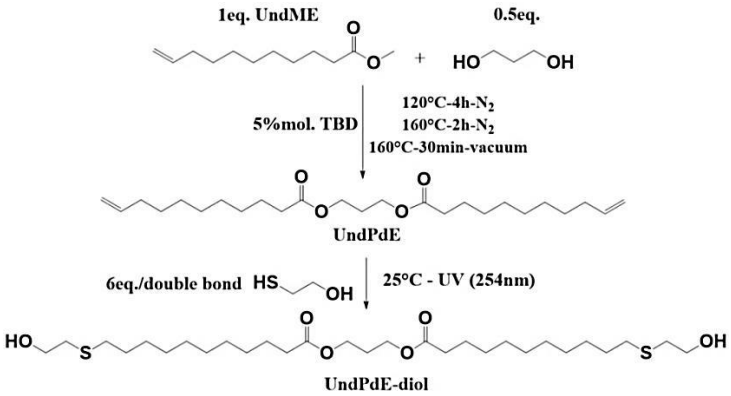

Scheme 1.2. Synthetic pathway to diols containing ester linkages: UndPdE-diol (Undecenoate Propyl diEster-diol) synthesized from methyl undecenoate and 1,3-propanediol.

In the line with the environmentally friendly and high efficiency process, the use of an organic catalyst and click chemistry reaction were preferred over the classical methods. The transesterification reactions were performed in two stages, at 120°C- 160°C under nitrogen atmosphere and then at 160 °C under vacuum.

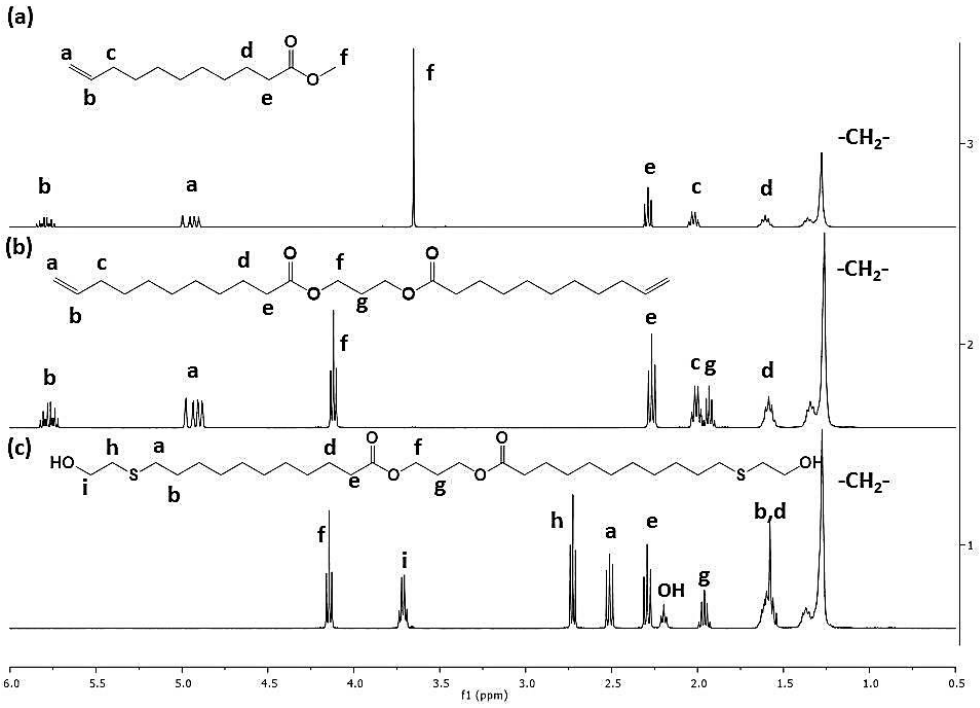

Figure 2.2. Stacked ^{1}H-NMR spectra of (a) UndME (methyl undecenoate) (b) UndPdE and (c) UndPdE – diol in $CDCl_3$.

The progress of the transesterification reactions was monitored by ^{1}H-NMR spectroscopy. The ester linkage methyl protons in methyl undecenoate (See Figure 2.2.a, H_f protons at 3.6 ppm) disappeared as a function of time. After transesterification, a triplet corresponding to the methylene protons nearby the ester oxygen appeared at 4.1 ppm (for the diester UndPdE and the ester-amide UndPEA) and at 4.2 ppm (for the monoester UndPmE).

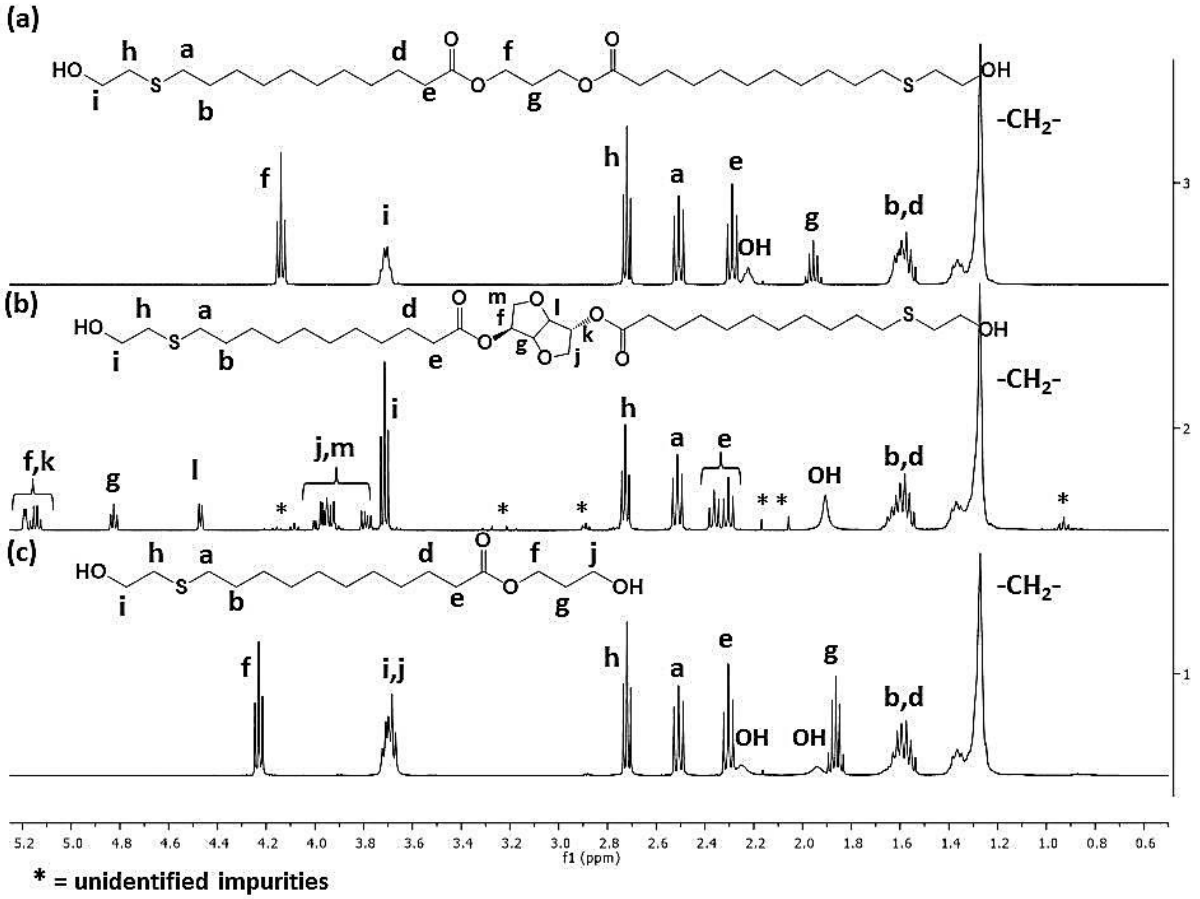

Figure 3.2. Stacked ^{1}H-NMR spectra of (a) UndPdE-diol, (b) UndIdE-diol and (c) UndPmE-diol (all in $CDCl_3$). Abbreviations used are as follows: [Und=from methyl undecenoate]; [P=propyl, I=from isosorbide] ; [d=di-, m=mono-] and [E=ester].

For isosorbide containing diol (UndIdE), the appearance of two signals at 5.2 ppm and 5.1 ppm (See Figure 3.2.b, H_f and H_k protons) confirmed the diester formation between methyl undecenoate and isosorbide and not the monoester one (5.2 ppm and 4.3 ppm). The percentages of undesirable products and remaining methyl undecenoate were determined through SEC. For UndPdE, only 0.7% of methyl undecenoate was left. However, undesirable products were remaining in UndIdE (34% of monoester) and UndPmE (30% of diester). To isolate selectively either the diester or the monoester, purifications by column chromatography were carried out on UndIdE and UndPmE (See experimental part). After purification, the proton ratios were in agreement with the resonance intensity ratios for UndPdE (See Figure 2.2).

II.3. Synthesis of alkene-terminated amides

As an illustration, Scheme 2.2 shows the synthesis of the diamide diol UndBdA-diol. The amidation reactions of UndBdA and UndPEA were performed at 120 °C followed by 160°C under nitrogen atmosphere using TBD with quantitative conversion.[13] For the diamide UndBdA synthesis, potentially bio-based 1,4-butanediamine was used instead of 1,3-propanediamine.

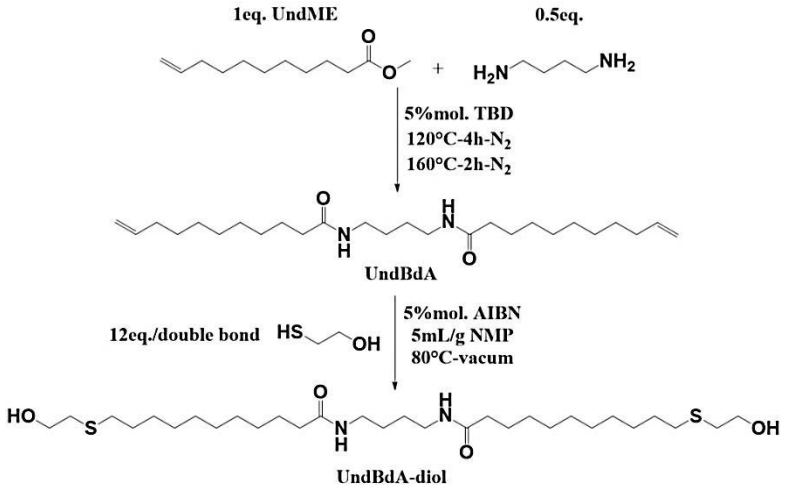

Scheme 2.2. Synthetic pathway to Undecenoic Butyl diAmide-diol (UndBdA-diol) from methyl undecenoate and 1,4-diaminobutane.

In the particular case of UndPmA, no catalyst was used to avoid the formation of ester function and the amidation step was performed at 150 °C - 160 °C.[14] In all cases, the amidation reactions were monitored by means of FTIR-ATR, ^{1}H-NMR spectroscopy and SEC (when the samples were soluble). FTIR-ATR spectra of UndPdE-diol, UndPEA-diol, UndBdA-diol and UndPmA-diol are presented in Figure 4.2. The FTIR-ATR of UndPEA, UndBdA and UndPmA showed two absorption bands at 1632 cm^{-1} and 1540 cm^{-1} characteristic of amide carbonyl stretching vibration (O=C-NH) and deformation vibration (C-N-H) respectively. Ester carbonyl stretching (O=C-O) at 1720 cm^{-1} decreased for UndPEA, UndBdA and UndPmA during the reaction. Besides, the FTIR-ATR spectra showed signal between 3000 cm^{-1} and 3500 cm^{-1}, corresponding to O-H. Diols with amide linkages display also a band at 3290 cm^{-1} specific of N-H stretching vibrations.

The disappearance of ester methyl group protons of UndME was also monitored by means of ^{1}H-NMR. A multiplet corresponding to the H_f protons in the formed amide linkages appeared at respectively 3.0 ppm (for UndBdA), 3.2 ppm (for UndPEA) and 3.4 ppm (for UndPmA) (See Figure 5.2). The ^{1}H-NMR revealed the formation of 11% monoamide for UndPEA and 7% ester-amide during UndPmA synthesis. Due to the presence of these side products,

purifications by column chromatography were performed. In the case of UndBdA which was insoluble in any solvent at room temperature, a filtration method was employed.

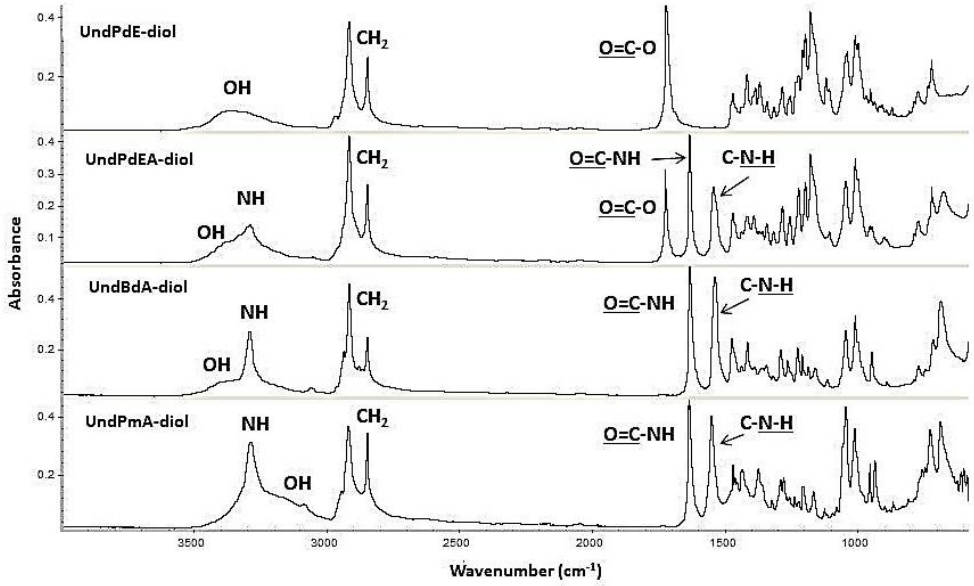

Figure 4.2. Stacked FTIR-ATR spectra of UndPdE-diol, UndPEA-diol, UndBdA-diol and UndPmA-diol. Abbreviations used are as follows: [Und=from methyl undecenoate]; [P=propyl, B=butyl] ; [d=di-, m=mono-] and [E=ester, A=amide, EA=ester-amide].

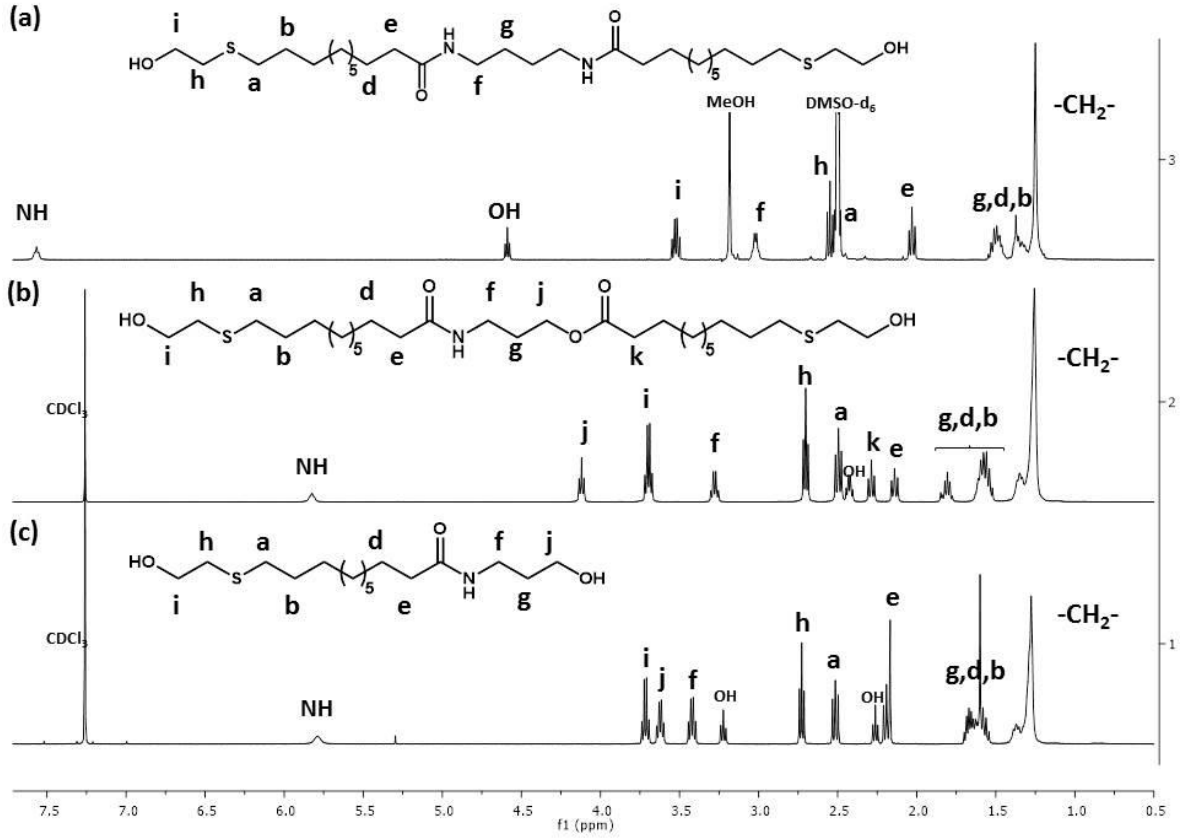

Figure 5.2. Stacked ^{1}H-NMR spectra of (a) UndBdA-diol (in DMSO-d6), (b) UndPEA-diol and (c) UndPmA-diol (latter two in $CDCl_3$). Abbreviations used are: [Und=from methyl undecenoate]; [P=propyl, B=butyl] ; [d=di-, m=mono-] and [A=amide, EA=ester-amide].

II.4. Hydroxyl functionalization by thiol-ene reaction

Thiol-ene reactions were then carried out using an excess of mercaptoethanol (MCET), in different experimental conditions (solvent and initiator were not necessarily used, see experimental part). The reaction progress was followed by the disappearance of double bond protons by ^{1}H-NMR spectroscopy (See Figure 2.2.b/c for UndPdE-diol, H_a and H_b protons at 5.73 ppm and 4.88 ppm). Full conversion was attained in all cases. In the ^{1}H-NMR spectra of ester (See Figure 3.2) and amide containing diols (See Figure 5.2), protons H_a, H_b, H_h and H_i confirm the addition of MCET onto the double bonds. SEC analyses indicated no coupling reaction such as disulfides formation, during the thiol-ene addition.

Amide containing diols showed higher melting points than diols with ester linkages. Asymmetric diols (UndPmE-diol and UndPmA-diol) and diol containing isosorbide as central block (UndIdE-diol) exhibited lower melting points.

All diols were of polymerization grade with purities measured by GC ranging from 92 to 99% (Table 1.2). The structure of these six diols is presented in Figure 1.2.

Table 1.2. Yields, purities and melting points of the synthesized diols.

Synthesized diol	Yield (Step 1 / 2)	%purity GC	T_m (°C)
Esters			
UndPdE-diol	73 / 82	92.3	70
UndIdE-diol	50 / 74	93.0	64
UndPmE-diol	55 / 76	97.1	57
Amides			
UndPEA-diol	58 / 70	94.5	92
UndBdA-diol	83 / 92	nd	145
UndPmA-diol	45 / 72	99.9	86

II.5. Synthesis of the diester

In order to achieve fully bio-based material, the diester (C20dE) was also synthesized from UndME by metathesis reaction using Grubb's 2nd generation catalyst as reported in the literature. [15] C20dE was obtained with a conversion of 96% (by ^{1}H-NMR) according to the disappearance of the characteristic peaks of the terminal double bond protons at 4.88 ppm and 5.73 ppm and the appearance of one multiplet at 5.35 ppm, due to the symmetrical character of the central double bond (Figure 6.2). It is noteworthy that isomerization side reactions were avoided (absence of peaks at 0.8-0.9 ppm) due to the quite low reaction temperature (45°C). C20dE was then purified by column chromatography in order to obtain a monomer with a purity of 98% according to GC analysis.

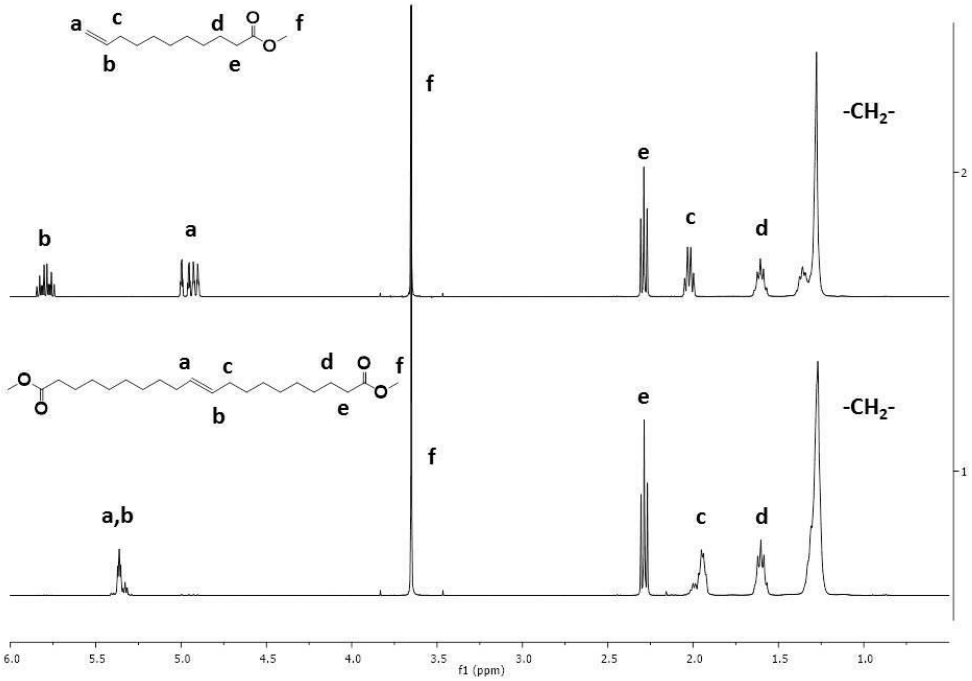

Figure 6.2. Stacked ^{1}H-NMR spectra of UndME and C20dE in $CDCl_3$.

III. POLYESTERS AND POLY(ESTER-AMIDE)S SYNTHESIS

The well-defined diols were reacted with C20dE in the presence of 1,5,7-triazabicyclo[4.4.0]dec-5-ene (TBD) as an organocatalyst to prepare, in bulk, polyesters and poly(ester-amide)s (Scheme 3.2). TBD was employed as a catalyst due to its high efficiency for transesterification and amidation reactions through a dual activation mechanism. [13, 16]

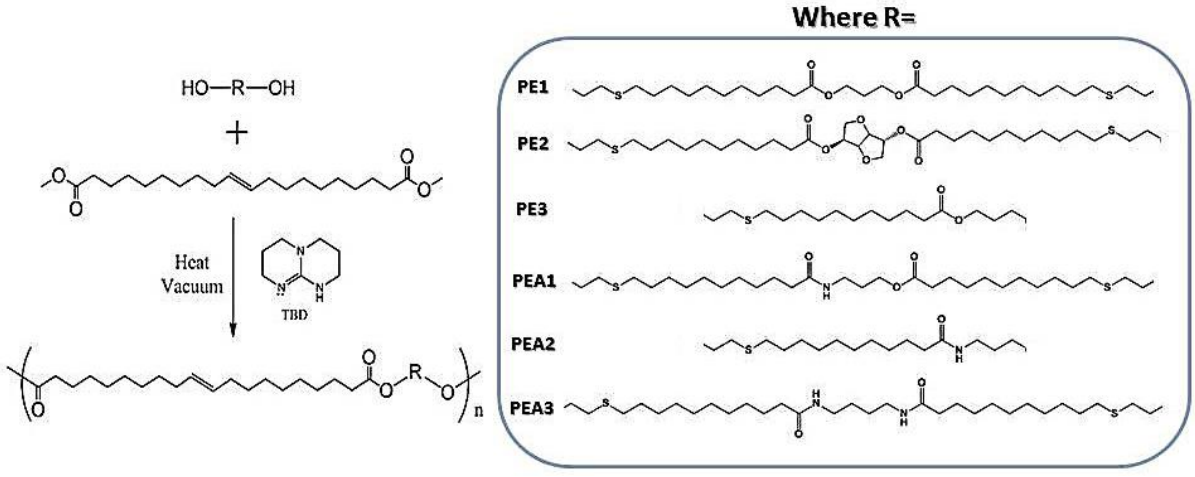

Scheme 3.2. Reaction pathway to polyesters and poly(ester-amide)s.

Because the molecular weights of both diol and C20dE monomers were relatively high preventing the volatility under reduced pressure at high temperature, bulk polymerization was

adapted as a preferred process. All polymerizations were carried out at 140°C (except for PEA3 where the reaction temperature was set at 180°C) by using a TBD amount of 20 mol%.

Table 2.2. Molecular weights and dispersities of polyesters and poly(ester-amide)s.

Polymer	Diol	ester:amide ratio	$\bar{M}_n$ (g.mol^{-1})	$\bar{M}_w$ (g.mol^{-1})	$Đ$
PE 1	UndPdE	1:0	18 400	35 000	1.9
PE 2	UndIdE	1:0	8 900	13 300	1.5
PE 3	UndPmE	1:0	6 100	7 900	1.3
PEA 1	UndPEA	3:1	17 500	33 100	1.9
PEA 2	UndPmA	2:1	10 902	19 500	1.8
PEA 3	UndBdA	1:1	19 300	29 000	1.5

SEC in THF-PS calibration. For PEA3, trifluoroacetic anhydride was used to dissolve the polymer using standard method

Few polymerizations were also attempted at lower temperature (100 and 120°C) by using lower catalyst amount (4 to 10 mol%), however, a temperature of 140°C and an amount of 20 mol% of catalyst per ester function were found necessary to give significant molecular weights. In the case of polymerizations starting from UndBdA-diol, the higher reaction temperature (180°C) was used due to the high melting point of the monomer (150°C). In general, TBD tends to sublime at such temperature reducing the catalytic activity; however, we were enabled to obtain reasonably good molecular weights for this poly(ester-amide) (PEA3). Dynamic vacuum was applied during the polymerization reaction in order to remove methanol and then to push the equilibrium toward the polymer formation. After reaction, the polyesters were dissolved in DCM (NMP in the case of PEA3), precipitated in methanol and dried under vacuum. The polyesters were obtained as white fibrous materials. Table 2.2 presents the molecular weights as well as the dispersities of the polyesters and poly(ester-amide)s. The molecular weights of polyesters and polyester-amides were found in the range 6 000 to 20 000 g.mol^{-1} with dispersities in the range 1.3 to 1.9. However, the values provided by SEC should not be taken as absolute values as the SEC calibration was carried out using polystyrene standards. It is also important to note that for PEA3, SEC analysis was made on the trifluoroacetic anhydride derivatized sample in order to help solubilization in THF. It is reported that the trifluoroacetic anhydride derivatized polymer usually tends to degrade resulting in chain scissions. It is also to notify that reaction conditions were not the same for PEA3 in comparison to other polymers impeding the comparison in terms of molecular weight.

The progress of the polymerization was measured by ^{1}H-NMR spectroscopy by following the integration decrease of methyl protons peak (3.6 ppm) with time and the downfield shift of

the hydrogen peak of methylene groups, adjacent to the hydroxyl function of the diol precursor (3.72 ppm), after the formation of ester linkage (Figure 7.2).

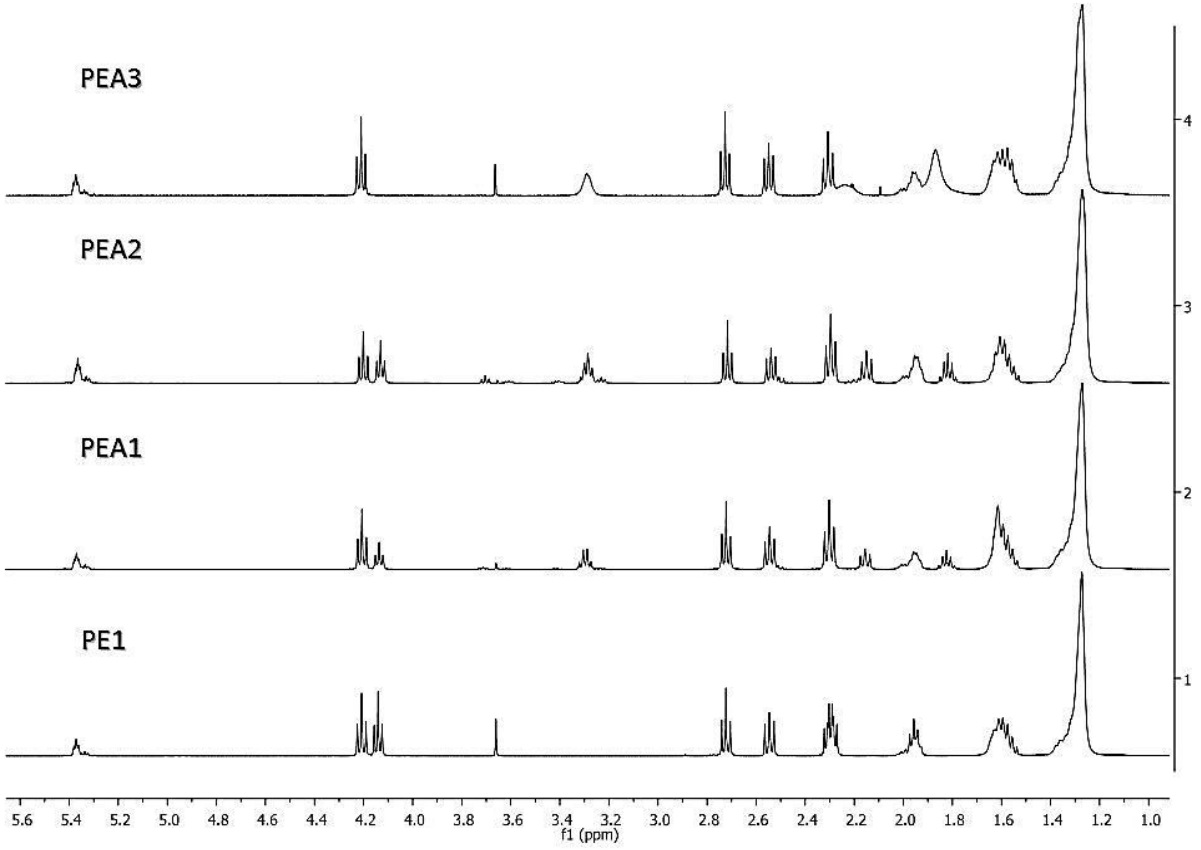

Figure 7.2. ^{1}H-NMR spectra of PE1 and poly(ester-amide)s in $CDCl_3$.

We also calculated the ratio between ester and amide functions for each polymer with ^{1}H-NMR spectroscopy. Protons of the methylene group adjacent to the nitrogen atom of the amide function, display a triplet between 3.20 and 3.35 ppm while protons of methylene group adjacent to oxygen atom of ester function display characteristic peaks between 4.10 and 4.25 ppm. The ratio of the 4.10-4.25 to 3.20-3.35 ppm peak integrals was 1 for PEA3, 1.7 for PEA2 and 2.8 for PEA1, values in accordance with the feed ratio when taking into account the measure error of NMR analysis.

The chemical structures were also confirmed by FTIR-ATR analyses (Figure 8.2). In all FTIR spectra, typical ester carbonyl stretching vibration was found at around 1734 cm^{-1}. In FTIR spectra of poly(ester-amide)s, the N-H amide stretching vibrations was found at 3299 cm^{-1} confirming the presence of amide sequences in the polymer chains. Moreover, the increase in the peak area was observed with the decrease of the ester to amide ratio of the precursor confirming the anticipated chemical structure. Other characteristic bands can be found at 1633 cm^{-1} (amide carbonyl stretching vibrations) and 1540 cm^{-1} (C-N-H deformation vibrations).

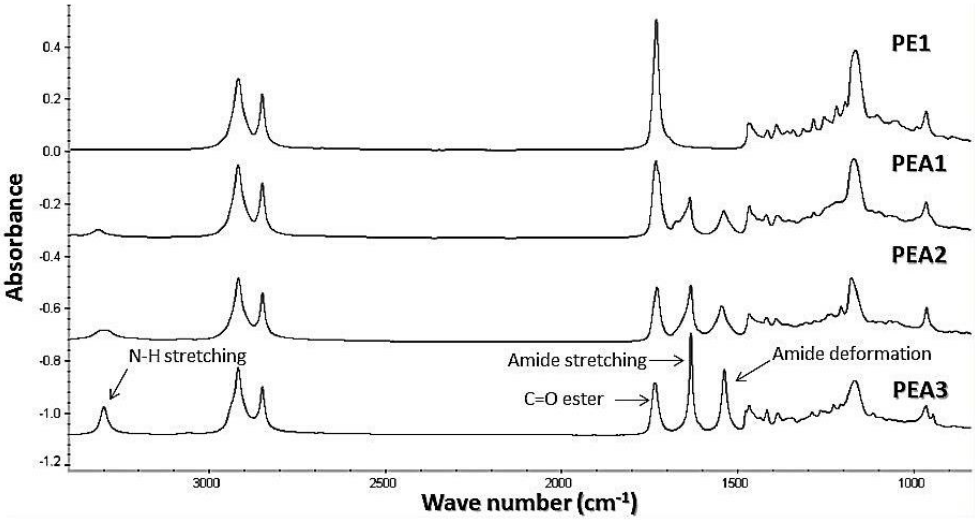

Figure 8.2. FTIR-ATR spectra of PE1 and poly(ester-amide)s.

IV. PROPERTIES OF THE POLYMERS

IV.1. Thermal stability

The thermal stability of the polyesters and poly(ester-amide)s under non-oxidative conditions was investigated by thermal gravimetric analysis. The thermal decomposition data obtained are given in Table 3.2 and illustrated in Figure 9.2.

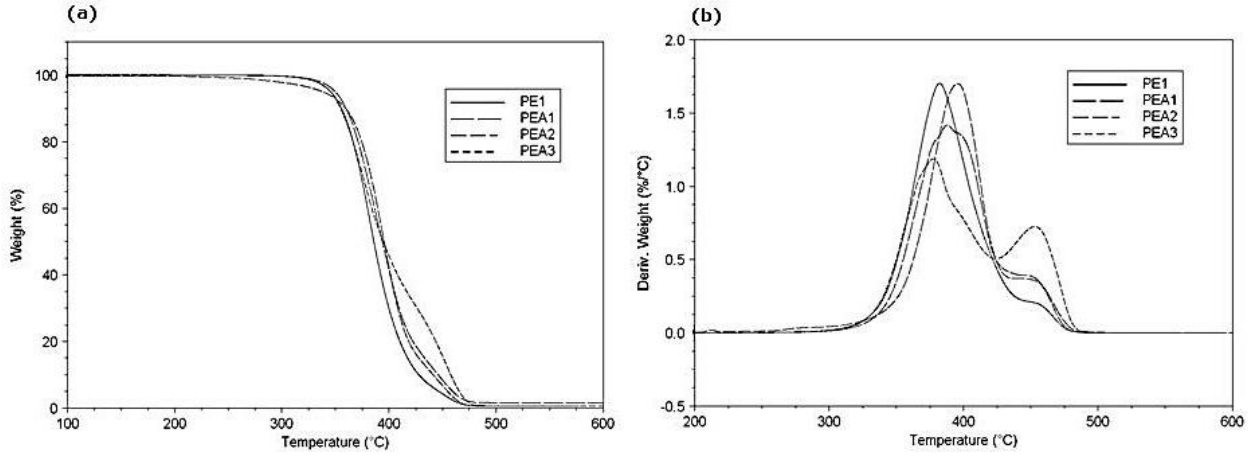

Figure 9.2. (a) TGA curves and (b) TGA derivatives curves of PE1 and poly(ester-amide)s at a heating rate of 10°C.min^{-1}.

One important observation is that all polymers were having a large difference between their decomposition temperatures and melting transitions easing the compression molding thereof. In almost all polymer systems, no significant weight loss was observed below 325°C which is comparable with the thermal stabilities of petroleum based aliphatic polyesters and poly(ester-amide)s.[17] Another point identified from Figure 9.2.b was the two-state thermal decomposition. A first weight loss is observed near 320°C followed by another significant weight loss at around 425°C. This behaviour is generally mentioned for poly(ester-amide)s

thermal decompositions[4, 18-20] and can be attributed to an earlier decomposition of ester linkages over the amide ones. We can conclude that for all polyesters or poly(ester-amide)s, similar thermal stabilities were observed. No particular influence of insertion of amide functions was observed on the thermal stability except to that two-stage decomposition process.

Table 3.2. Thermogravimetric data of polyesters and PEAs.

Polymer	ester:amide ratio	$T_{5\%}$ (°C)[a]	Tmax (°C)[b]	Weight residue (%)
PE 1	1:0	346	474	0.8
PE 2	1:0	338	482	1.2
PE 3	1:0	327	479	0.9
PEA 1	3:1	350	485	1.6
PEA 2	2:1	338	475	0.8
PEA 3	1:1	345	484	0.6

(a) Temperature for 5% weight degradation (b) Temperature for total degradation

Concerning polyesters, we also investigated the influence of the central block type on the thermal decomposition. Isosorbide is known to induce less thermal stability due to its heterocyclic nature, however no significant thermal stability differences were noticed between isosorbide and 1,3-propanediol based polyesters. However, an earlier decomposition was observed when UndPmE-diol (PE3) was used instead of UndPdE-diol (PE1) due to a higher ester function density (Table 3.2). Moreover, all polymers present negligible weight residues (less than 2%). As a conclusion, all the bio-based polyesters and poly(ester-amide)s present good thermal stabilities in accordance with petroleum based aliphatic polyesters.

IV.2. Thermo-mechanical properties

The thermo-mechanical properties of the polyesters and poly(ester-amide)s were determined by DSC. The crystallization, melting temperatures and corresponding enthalpies of the polymers were recorded from first cooling and second heating scan at a rate of 10°C.min^{-1}. The DSC traces varied with the monomers used (Figure 10.2). However, all samples were found to be semi-crystalline as one or more endotherms corresponding to melting transitions were observed. Mostly fatty acid based polymers are amorphous in nature due to the presence of pendant alkyl chains. For instance, the self-polymerization of methyl ricinoleate leads to an amorphous polyester with very low Tg (around -70°C). [21] Here the linear nature of the designed monomers based on UndME provided chain packing leading to a better organization of the polyester chains, permitting the crystallization. Table 4.2 displays thermal characteristics of the polymers such as melting points, crystallisation temperatures and the corresponding enthalpies.

Table 4.2. Melting values obtained from 2nd DSC heating scan and 1st cooling scan at a rate of 10°C.min^{-1}. Enthalpy (J.g^{-1}) is the area under the peak.

	ester:amide ratio	Tm1(°C)	ΔHm1 (J.g^{-1})	Tm2(°C)	ΔHm2 (J.g^{-1})	Tc1(°C)	ΔHc1 (J.g^{-1})	Tc2(°C)	ΔHc2 (J.g^{-1})
PE 1	1:0	36.1	79.9	-	-	21.9	77.7	-	-
PE 2	1:0	29.9	31.4	37.2	2.4	13.5	11.9	17.8	37.3
PE 3	1:0	16.9	18.8	22.7	40.7	-15.2	5.6	13.2	53.3
PEA 1	3:1	47.7	41.5	-	-	23.2	42.8	-	-
PEA 2	2:1	50.2	2.6	76.1	37.7	29.7	43.5	-	-
PEA 3	1:1	121.1	64.3	126.5	7.1	104.6	21.9	112.5	71.5

As melting enthalpies were relatively high, it was difficult to distinguish any variation of the heat flow for the glass transition phenomenon. Thus Tg values were determined by dynamical mechanical analyses. First, the influence of the central block on melting points and melting enthalpies of the polyesters synthesized from diols UndPdE and UndIdE (PE1 and PE2) was studied. Despite the fact that PE1 and PE2 melting points are relatively close, the corresponding melting enthalpies are quite different indicating that degrees of crystallinity strongly depend on the central block nature. Indeed, this feature can be explained by the conformational differences between the two building blocks. The high flexibility of the polyester chain and low free space induced by 1,3-propanediol, resulted in high packing of the chains permitting high crystallinity. Reversibly, isosorbide, composed of two cis-fused tetrahydrofuran rings, nearly planar V-shaped with a bond angle of 120° between rings, induces a higher free volume resulting in a decrease in the crystallinity. These hypotheses are confirmed by measuring the melting enthalpies. In the case of PE1, the melting enthalpy is 79.9 J.g^{-1} in comparison to 33.8 J.g^{-1} for PE2. It is also of interest to note that PE1 presents a single melting point while PE2 exhibits two melting points suggesting less perfect crystals and metastable forms. The thermal behaviour difference between PE1 and PE3 was also investigated in order to determine the influence of the diol symmetry as well as the ester function density. As observed from the 2nd heating scan (Figure 10.2), melting temperatures are very close. The presence of two or more melting points in the case of PE3 suggests that the lack of symmetry in UndPmE-diol gave rise to multiple crystalline phases more or less thermodynamically stable.

In order to study the effect of amide functions on the thermal properties, DSC analyses on poly(ester-amide)s were carried out. As expected, an obvious increase in the melting points is noticed with an increase in amide to ester ratio. It can be logically attributed to hydrogen bonding due to amide linkages leading to strong interactions between the polymer chains and thus more stable crystalline phases. Melting point values are given in Table 4.2.

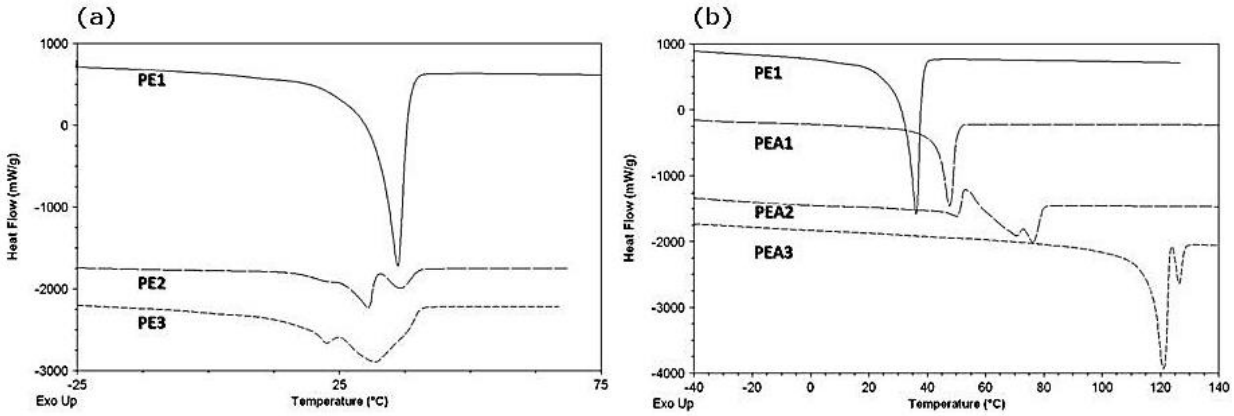

Figure 10.2. (a) DSC curves of polyesters-2nd heat scan 10°C.min^{-1} (b) DSC curves of PE1 and poly(ester-amide)s-2nd heat scan 10°C.min^{-1}.

A large range of polyester thermal features were obtained as melting points were varying from 30°C for PE1 to 125°C for PEA3. Total melting enthalpies were also varying with the structure of the diol. Indeed, high enthalpy values were obtained for PE1 and PEA3 suggesting that symmetry and regularity of the chemical structures play an important role in the crystallinity. Total melting enthalpies were quite similar for PE1 (79.9 J.g^{-1}) and PEA3 (71.4 J.g^{-1}) and were higher than for PEA1 (41.5 J.g^{-1}) and PEA2 (40.32 J.g^{-1}). Complex melting pattern was observed for PEA2. This feature can be explained by the unsymmetrical nature of the diol affecting the mobility of the chains and thereby impeding the formation of stable crystals. It has to be emphasized that many semi-crystalline polymers, including polyesters and poly(ester-amide)s show multiple melting peaks on heating, which in general is ascribed to the existence of polymorphism or to melting-recrystallization processes occurring during the DSC scan. In the case of PEA2, modulated DSC at a heating rate of 3°C.min^{-1} revealed three melting points (Figure 11.2). An exotherm was also observed during the first melt transition. This behavior is typical from the melting of a metastable crystalline form, which crystallizes immediately into a more stable one.

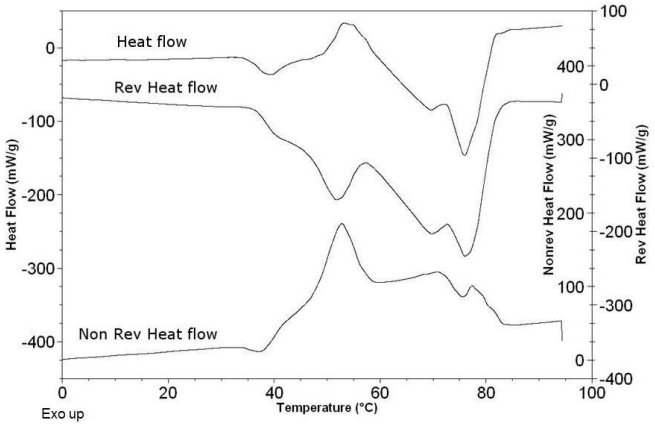

Figure 11.2. Modulated DSC curves of PEA2- 3°C.min^{-1}.

A multiple melting behavior was also noticed for PEA3 despite the symmetry of the diol. Modulated DSC (Figure 12.2) was performed using a heating rate of 3°C.min^{-1}. As can be seen from the DSC trace, reversible heat flow signal shows two endothermic peaks with maxima at 122°C and 127°C related to two melting transitions. The non-reversible heat flow signal presents a major exothermic transition at 124°C related to a crystallization phenomenon. This behavior is in agreement with the first melt of a metastable phase that immediately re-crystallizes into a more stable crystalline form.

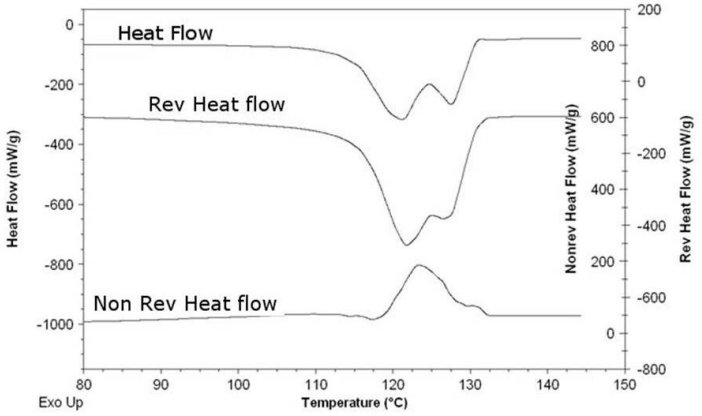

Figure 12.2. Modulated DSC curves of PEA3 – 3°C.min^{-1}.

Gan and coll. investigated multiple melting behavior of poly(butylene succinate-co-ethylene succinate) copolyesters and have concluded about correspondence of multiple melting peaks to different thickness of the crystals so formed and not to polymorphism.[22] Based on PEA3 DSC trace, this sample was annealed at 112°C or 124°C to see if one of the two crystalline phases could be accentuated. The temperature of 124°C was chosen because it corresponds to the maximum of the exothermic peak. As observed on Figure 13.2, the second endotherm is accentuated by annealing the sample at 124°C showing that the first meta-stable crystalline form was melted and recrystallized in the second more stable form.

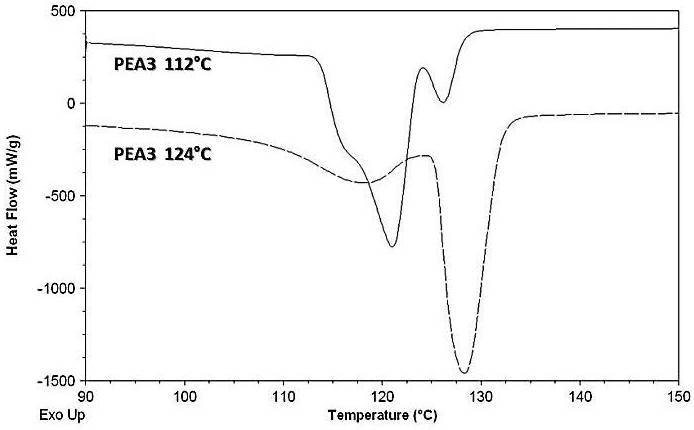

Figure 13.2. DSC curves of PEA3 sample annealed from the melt at 112 or 124°C for 30 minutes- 10°C.min^{-1}.

IV.3. Crystallographic properties

Due to the semi-crystalline behavior of all polyesters and poly(ester-amide)s synthesized in this work, wide angle X-ray diffraction (WAXD) analyses were performed in order to determine typical crystalline forms. Due to similarities with polyamide structure, we aimed at identifying characteristic crystalline phases of PA-6. PA-6 can exist in two stable crystal structures, either the α crystal with hydrogen bonds between antiparallel chains or the γ crystal with hydrogen bonds between parallel chains. PA-6 can also exist in a series of metastable crystal structures which vary continuously in size, perfection and structural parameters from a pseudohexagonal structure to either of the two stable forms (α-form or γ-form).[23, 24]

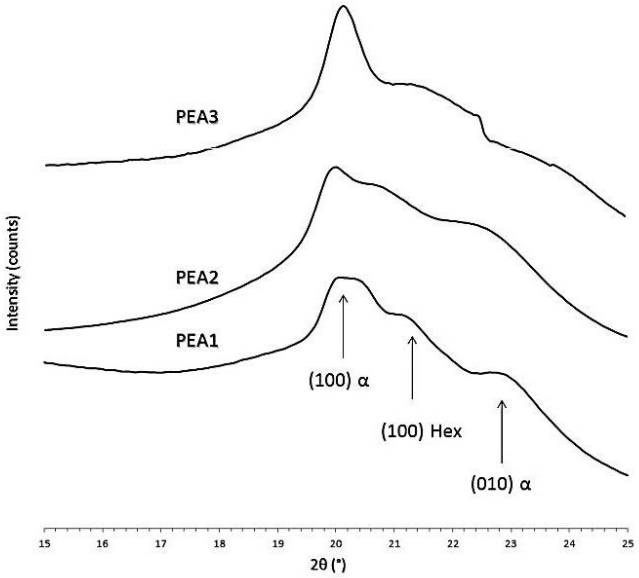

Figure 14.2. WAXD spectra of poly(ester-amide)s at room temperature after cooling from the melt at 10°C.min^{-1}.

Regarding WAXD patterns of PEAs (Figure 14.2), typical reflections of a α-type crystalline phase similar to the α-phase of PA-6 are noticed. Indeed, 20.2° and 22.6° lines (4.5Å and 4.0Å) correspond to spacings from the (100) and (010) reflections of the α-form at room temperature. These reflections are characteristic of the distance between two amide-amide intermolecular H-bonded chains (~4.8Å) and the distance between two Van der Waals packed sheets (~3.7Å).[25] The distances between two amide-amide intermolecular bonds are lower for PEAs than for PA-6 probably due to the non-fully polyamide structure of the synthesized polymers. The broader reflection around 20.2° in the case of PEA1 may indicate significant disorder involved by the high amount of ester functions that decrease the hydrogen-bond density. However no clear demonstration for this phenomenon was found. No γ-form was

noticed; however typical reflection of a pseudohexagonal structure was underlined regarding the appearance of a peak at 21.2° (4.3Å). This crystalline form was revealed to be less stable than the α-phase. Indeed by performing WAXD analyses on PEA3 sample at different temperatures (30°C, 121°C, 124°C and 128°C), a decrease in the peak intensity of hexagonal form was noticed by increasing the temperature (Figure 15.2). This is in accordance with the observations made from DSC measurements that demonstrate a melting of a first phase (hexagonal one) followed by crystallization into a second phase (α-form) and finally the melting of the most stable crystalline form.

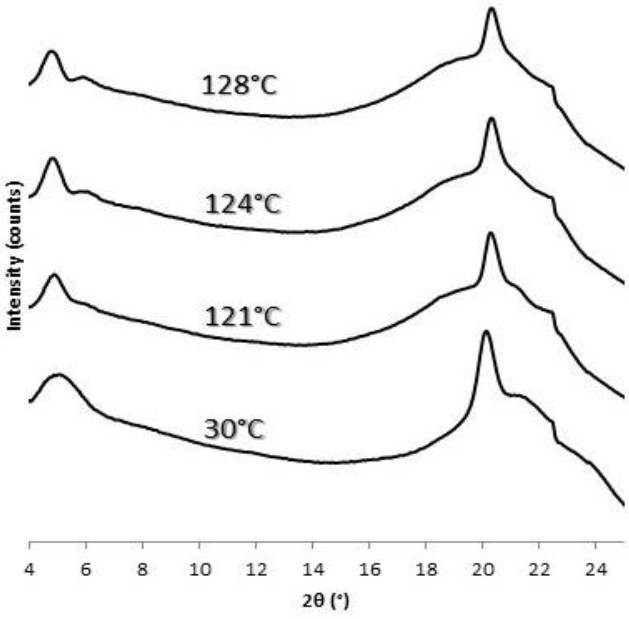

Figure 15.2. WAXD spectra of PEA3 at different temperatures.

IV.4. Dynamical mechanical analysis

Dynamical mechanical analysis was performed on each sample in order to evaluate the viscoelasticity of the polymers. These experiments were done in the compression mode due to the low melting point values for the polyesters, which induce a soft character to the materials hence limiting their processing into tensile bars. In Figure 16.2 is represented the compression storage modulus of PE1, PE2 and the poly(ester-amide)s as a function of the temperature. When comparing PEAs at room temperature (20°C), a decrease in the compression storage modulus can be identified as the ester to amide ratio goes from 1:1 to 2:1 and to 3:1. This trend was expected as the storage modulus generally increases with the hydrogen bonds density. The difference of storage modulus before and after the glass transition is more important for PEA1 and PEA2 than for PEA3 revealing a stronger crystallinity for PEA3. A drastic decrease in storage modulus during glass transition means that the polymer sample is

highly affected by the glass transition due to the low amount of chains packed into crystalline structures. These packed chains are then not capable to maintain a sufficient elastic modulus. The elasticity of the polymers was also evaluated by analysing tanδ values, ratio of loss modulus (E") to storage modulus (E').

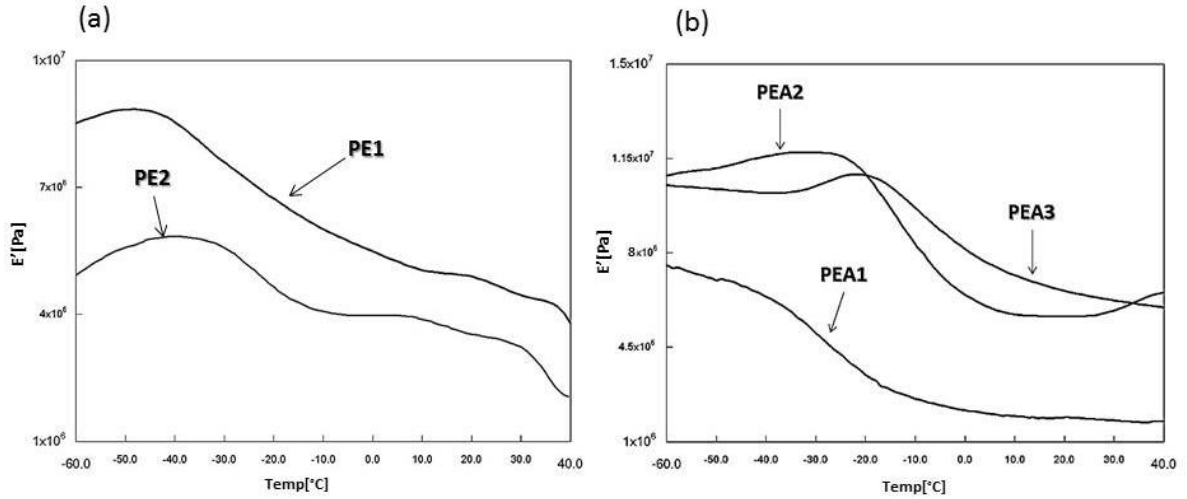

Figure 16.2. Storage modulus as a function of temperature for(a) PE1, PE2 and (b) poly(ester-amide)s.

As can be observed from Figure 17.2, tanδ in the temperature range -60 to 20°C is lower for PE1 than for PE2 indicating that for PE1 more of the energy needed to deform the sample is elastically recovered than being dissipated. Polyester from 1,3-propanediol (PE1) has then the highest rubbery elasticity. It is also noticeable that maximum intensity of tanδ is lower for PE1 than for PE2, indicating a higher crystallinity for PE1. This observation confirms DSC results. By changing the central block nature, our hypothesis was that isosorbide should induce higher rigidity due to its ring structure, hence increasing Tg value. In fact, the maximum of tanδ for PE2 shifts to higher temperature compare to PE1 revealing a higher glass transition (Table 5.2).

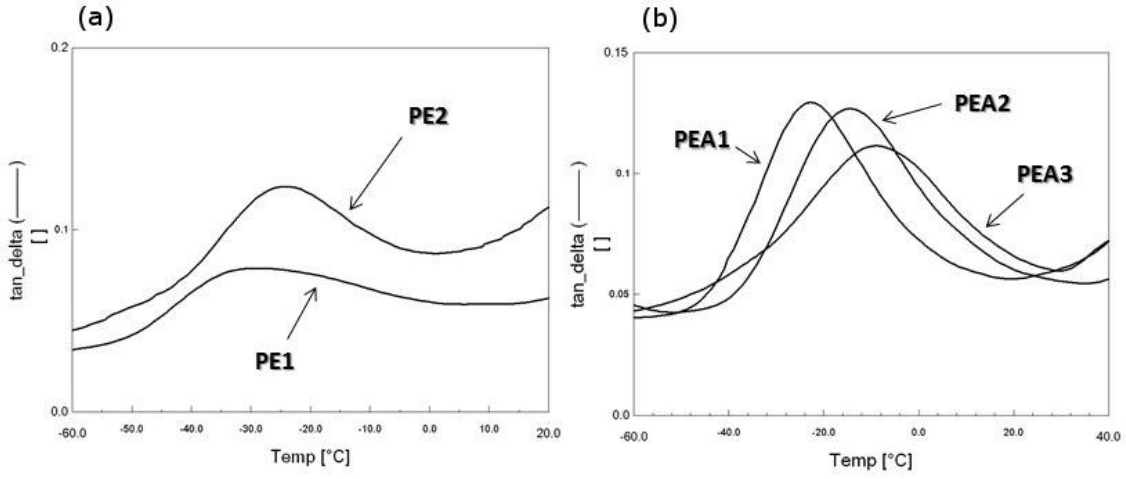

Figure 17.2. Tan δ as a function of temperature for (a) PE1, PE2 and (b) poly(ester-amide)s.

Tanδ of PEAs was also recorded as a function of the temperature. As can be seen, tanδ maximum shifts to higher temperature as amide to ester ratio increases, suggesting that incorporation of amide function in the polymer backbone leads to an increase in Tg value. Maximum intensity of tanδ is lower for PEA3 than for PEA1 and PEA2 suggesting a stronger crystallinity for PEA3 as well as a higher rubbery elasticity.

Table 5.2. Dynamical mechanical properties in compression mode – Tg corresponds to temperature for Tanδ max.

	ester:amide ratio	Tg(°C)	E' (20°C) (Mpa)	Tanδ max
PE 1	1:0	-31	4.97	0.079
PE 2	1:0	-24	3.51	0.123
PEA 1	3:1	-22	1.92	0.129
PEA 2	2:1	-14	5.65	0.127
PEA 3	1:1	-8	6.56	0.111

IV.5. Tensile properties

Tensile analyses were also performed using a strain rate of 3 $mm.min^{-1}$ in order to investigate the mechanical properties of the so-formed polyesters and poly(ester-amide)s. For each sample, tensile stress versus strain curves were plotted permitting to measure ultimate tensile strength, maximum strain and Young's modulus (Table 6.2).

Table 6.2. Tensile properties of PE1 and poly(ester-amide)s.

	Young's Modulus (MPa)	Ultimate Strength (MPa)	Strain at break (%)
PE1	93.0 ± 10.4	2.9 ± 0.8	4.1 ± 1.3
PEA1	82.7 ± 15.2	5.4 ± 1.2	11.1 ± 2.4
PEA2	131.5 ± 17.5	3.5 ± 0.3	3.4 ± 0.7
PEA3	363.0 ± 89.1	10.0 ± 3.5	3.3 ± 0.7

The stress-strain curves of the poly(ester-amide)s (Figure 18.2) show low strain at break which can be correlated to the relatively low molecular weights obtained for these materials. Indeed, it is known that for some materials, molecular weight can have a real impact on strain at break.[26] Thus all materials synthesized exhibit a brittle character, which can be overcome by enhancing molecular weights. It would not be expedient to directly compare ultimate strengths and strains at break of the materials as mechanical properties could be improved, however a significant enhancement in ultimate strength can be noted as it doubles when the ester to amide ratio goes from 3:1 to 1:1. The dramatic effect of hydrogen bonding on tensile properties is also underlined by the difference of ultimate strength between PE1 and PEA3.

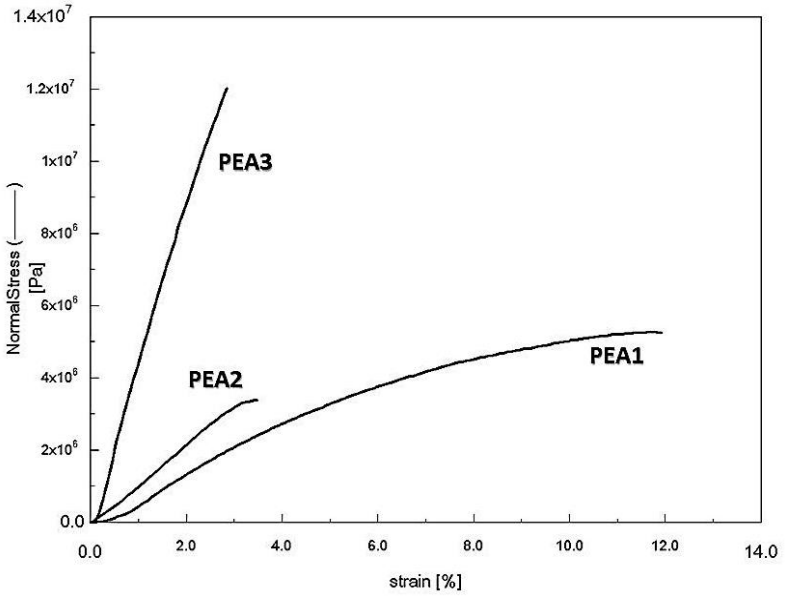

Figure 18.2. Stress-strain curves of poly(ester-amide)s- 3mm.min^{-1}.

Indeed, when two ester linkages are substituted by two amide ones in the repeating unit, the ultimate strength increases from 2.9 MPa to 10.0 MPa, with quite similar elongations at break. Young's Modulus provides also useful information concerning polyesters and poly(ester-amide)s mechanical behaviours. The Young's modulus increases dramatically with hydrogen bond density, with values ranging from 82.7 MPa for PEA1 to 363.0 MPa when one more hydrogen bonding site is incorporated into the diol precursor structure (PEA3). However, PE1 and PEA1 present similar Young's modulus values despite the incorporation of one more hydrogen bonding site in PEA1 compared to PE1. This suggests that not only the amide function density plays a significant role on the enhancing of Young's modulus but also the symmetry of the repetitive unit.

V. CONCLUSION

In summary, new bio-based polyesters and poly(ester-amide)s were obtained by polycondensation of a series of diols with a C20 dimethyl ester (C20dE), all issued from vegetable-oil based methyl 10-undecenoate, in the presence of TBD as a catalyst. The number average molecular weight of the polymers so-formed was in the range 6 000 to 19 000 g.mol^{-1} and the thermo-mechanical properties were highly dependent on the diol chemical structure. The thermal degradation of the derived polyesters and poly(esteramide)s revealed to be in the range 330 to 350°C for temperature corresponding to 5wt% weight loss. Thermal properties were proved to be in accordance with our expectations. Incorporation of rigid segments such as isosorbide or more cohesive functions resulted in a T_g increase of the polymers. Melting points were higher for higher amide to ester ratio, while no sensitive improvement was

noticed by incorporation of isosorbide unit in the polymer structure. Melting enthalpies were highly dependent on the chemical structure of the diol showing that asymmetry and larger free volume resulted in a drastic decrease in the crystallinity. Crystalline structures of PEAs were investigated by WAXD, which revealed similar crystalline forms to PA-6. Two phases were observed, a metastable pseudohexagonal form and a more stable α-form. Finally mechanical properties were studied by tensile tests. An increase in Young's modulus was noticed with an increase in hydrogen bond density revealing a higher stiffness of the poly(ester-amide)s compared to polyesters. The first part of this chapter clearly demonstrated that both the heat stability (governed by the melting point of the polymer) and the stiffness (Young's modulus) of polyesters can be significantly improved by the incorporation of amide functions in the backbone of the polyester.

However, in the case of the rubber-toughening of PLLA, the additive must not be too stiff to efficiently absorb impact energy during stress. Thus, in the next part of this chapter, we propose to keep the diamide diol (UndBdA-diol) as precursor for rubber synthesis while replacing the C20dE monomer by a dimerized fatty acid (DFA) presenting alkyl dangling chains. Indeed, the latter will lower the stiffness of the so-formed polymer while keeping the good thermal stability provided by the two amide functions of the repeating unit.

VI. EXPERIMENTAL

1. Undecenoate diester diols (UndPdE-diol and UndIdE-diol)

Transesterification step. UndME, diol and TBD (1: 0.5: 0.05) were stirred under nitrogen flow at 120 °C (4 h), at 160 °C (2 h) then under vacuum at 160 °C (30 min). The reaction mixture was dissolved in ethyl acetate and washed with water (3 times). The organic layer was dried over anhydrous sodium sulfate, filtered and the solvent was evaporated under reduced pressure.

UndPdE: UndME (20 g, 101 mmol), 1,3-propanediol (3.8 g, 50 mmol) and TBD (702 mg, 5 mmol). UndPdE was obtained as a yellow viscous liquid. Yield = 73%.

UndIdE: UndME (20 g, 101 mmol), isosorbide (7.4 g, 50 mmol) and TBD (702 mg, 5 mmol). UndIdE was purified by column chromatography (eluent: cyclohexane / ethyl acetate (70/30)) and obtained as a yellow viscous liquid. Yield = 50%.

Thiol-ene reaction. Undecenoate diesters and MCET (3 eq. / double bond) were stirred at room temperature under UV irradiation (254 nm). After the disappearance of double bond protons (monitored by ^{1}H-NMR spectroscopy), the reaction mixture was taken into dichloromethane (DCM) and thoroughly washed with water (4 times). The DCM solution was

dried over anhydrous sodium sulfate, filtered and solvent was removed on rotary evaporator to obtain UndPdE-diol and UndIdE-diol as white powders.

UndPdE-diol: UndPdE (17 g, 39 mmol) and MCET (18 g, 232 mmol). The purity of UndPdE-diol (92.3%) was determined by GC. Yield = 82%.

UndIdE-diol: UndIdE (13.5 g, 28 mmol) and MCET (13 g, 169 mmol). The purity of UndIdE-diol (94.9%) was determined by GC. Yield = 74%.

2. Undecenoate propyl monoester diol (UndPmE-diol)

Transesterification step. UndME (10 g, 50 mmol) with 1,3-propanediol (384 g, 5 mol) and TBD (351 mg, 2.5 mmol) (1: 100: 0.05) were stirred under nitrogen flow at 120 °C for 1 h. The reaction mixture was then dissolved in ethyl acetate (200 mL) and washed with water (3 x 50 mL). The organic layer was dried over anhydrous sodium sulfate, filtered and solvent was removed on rotary evaporator. A column chromatography (eluent: heptane / ethyl acetate (70/30 then 50/50)) was performed to purify UndPmE compound obtained as a yellow liquid. Yield = 55%.

Thiol-ene reaction. The experimental procedure carried out was similar to the preparation of undecenoate diester diols. UndPmE (5.4 g, 12 mmol) and MCET (6 eq. / double bond - 5.8 g, 74 mmol). UndPmE-diol was obtained as a white powder, and the purity of UndPmE-diol (97.1%) was determined by GC. Yield = 76%.

3. Undecenoic propyl esteramide diol (UndPEA-diol)

Amidation-transesterification step. UndME (30 g, 151 mmol), 1,3-aminopropanol (5.7 g, 76 mmol) and TBD (1 g, 7.6 mmol) (1: 0.5: 0.05) were stirred under nitrogen flow at 120 °C (4 h) then at 160 °C (2 h). The reaction mixture was dissolved in ethyl acetate (200 mL) and washed with water (3 x 50 mL). The organic layer was dried over anhydrous sodium sulfate, filtered and solvent was removed on rotary evaporator. UndPEA compound was purified by column chromatography (eluent: DCM / MeOH (95/5)) and obtained as a white powder. Yield = 58%.

Thiol-ene reaction. The experimental procedure for the synthesis of UndPEA-diol was similar to the preparation of UndPdE-diol, except that DCM (5 mL / g) was used as a solvent. UndPEA (14 g, 34 mmol) and MCET (18 eq. / double bond - 97 g, 1.2 mol). UndPEA-diol was obtained as pink / off white powder and the purity of UndPEA-diol (94.5%) was determined by GC. Yield = 70%.

4. Undecenoic butyl diamide diol (UndBdA-diol)

Amidation step. UndME (20 g, 101 mmol), 1,4-diaminobutane (4.4 g, 50 mmol) and TBD (702 mg, 5 mmol) (1: 0.5: 0.05) were stirred under nitrogen flow at 120 °C (4 h) then at 160 °C (2 h). The reaction flask was cooled down at 90 °C and NMP (60 mL) was added to obtain a homogeneous phase. The required UndBdA was slowly precipitated while reaching room temperature. The precipitated solid was filtered and washed with methanol to obtain UndBdA as a white powder. Yield = 83%.

Thiol-ene reaction. UndBdA (16 g, 38 mmol), MCET (12 eq. / double bond – 71 g, 913 mmol) and AIBN (5% molar / UndBdA – 312 mg, 1.9 mmol) were stirred in NMP (5 mL / g), under static vacuum into a bath preheated at 80 °C. After two hours, the reaction mixture was cooled to room temperature. The UndBdA–diol got precipitated and was filtered. The white solid obtained was washed thouroughly with water and dried. Yield = 92%.

5. Undecenoic propyl monoamide diol (UndPmA-diol)

Amidation step. UndME (20 g, 101 mmol) and 1,3 aminopropanol (15 g, 202 mol) (1: 2) were stirred under nitrogen flow at 150 °C (2 h) then at 160 °C (2 h). After completion of the reaction, the reaction mixture was dissolved in THF (70 mL) and reprecipitated in water. The solid obtained was filtered and washed with water. UndPmA compound was purified by column chromatography (eluent: cyclohexane / ethyl acetate (70/30 then 30/70)) and obtained as a yellow / brown product. The purity of the compound (99.9%) was determined by GC-FID. Yield = 53%.

Thiol-ene reaction. The experimental procedure for the synthesis of UndPmA-diol was similar to the preparation of UndPEA-diol. UndPmA (5 g, 12 mmol) and MCET (6 eq. / double bond – 5.7 g, 73 mmol). UndPmA-diol was obtained as a white powder with a purity of 99.9% as determined by GC. Yield = 72%.

6. *Synthesis of dimethyl 1,20-eicos-10-enedioate (C20dE)*

Into a 100 mL round-bottom flask equipped with a mineral oil bubbler and a nitrogen inlet, 20 g (101mmol) of UndME was charged with 85 mg (0.101mmol) of 2nd generation Grubbs catalyst. The contents were vigorously stirred at 45°C for 3 days under nitrogen flow. After 3 days the reaction mixture was cooled to room temperature and 2mL of ethylvinyl ether was added to deactivate the Grubbs catalyst. Dynamic vaccum was then applied in order to remove remaining excess of ethylvinyl ether. The product was then purified with column chromatography using a mixture of cyclohexane and ethyl acetate as eluent (95/5: v/v). C20dE was obtained as a white solid with 98% purity (determined by GC). Yield = 69%.

7. General procedure for polyesters and poly(ester-amide)s synthesis

In a general polymerization procedure using UndPdE, UndIdE, UndPmE, UndPEA and UndPmA diols, 1 equivalent of diol with 1 equivalent of C20dE was stirred under dynamic vaccum in the presence of 10 mol% of TBD relative to ester functions at 140°C for 24 hours. Polymer was then dissolved in dichloromethane, precipitated in methanol and dried under reduced pressure. When UndBdA-diol was used, the procedure was the same except that reaction was performed at 160°C for 2 hours then at 180°C for 22 hours.

PART B. USE OF A NOVEL POLY(ESTER-AMIDE) RUBBER TO TOUGHEN POLY(L-LACTIDE) BY MELT-BLENDING

I. INTRODUCTION

The development of bio-based rubbers remains an important challenge. Thermoplastic elastomers represent promising and versatile materials as they exhibit properties of cross-linked elastomers while keeping their processing ability due to their linear structure. These types of material are composed of soft segments that will provide high flexibility and low modulus and hard segments that will act as physical cross-linking points thus providing enough mechanical strength. In the previous part, we have seen that amide functions, when incorporated in a polyester backbone, can provide semi-crystallinity and high melting point to the resulting materials.

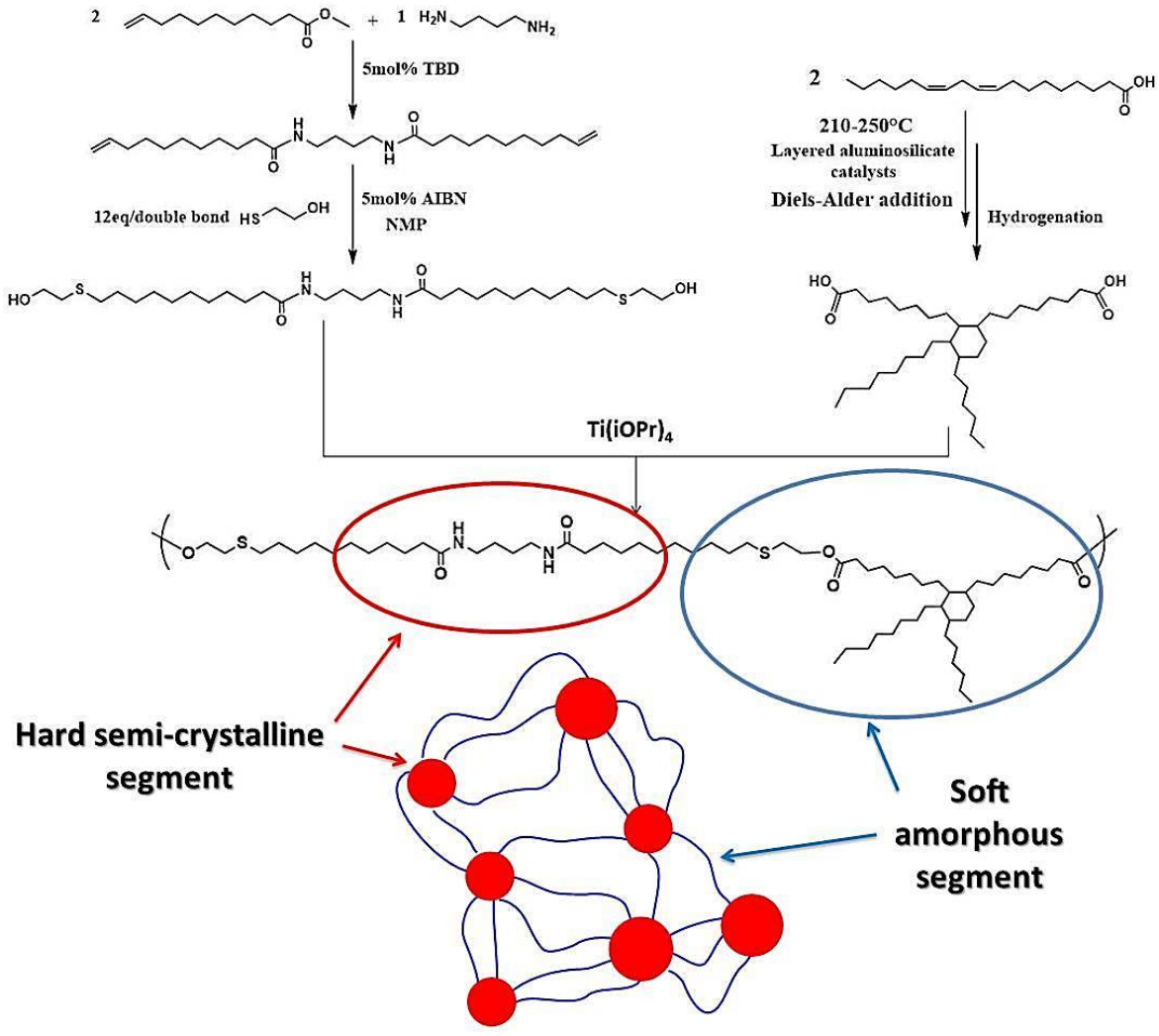

Scheme 4.2. Synthetic strategy to novel poly(ester-amide) thermoplastic elastomer.

Thus undecenoate butylene diamide diol (UndBdA-diol) was used to design a new thermoplastic elastomer. Instead of C20dE, dimerized fatty acids (DFA) was selected as soft segment due to the dangling alkyl chains present in its structure which act as internal plasticizers thus limiting the crystallinity of the final material (Scheme 4.2). DFA is industrially used in applications where softness is a main criterion. Thus it is thought that reacting DFA with UndBdA-diol by polycondensation could lead to thermoplastic elastomer behavior.

In this part of the chapter we were interested in evaluating the potential of the PEA resulting from the polycondensation of DFA and UndBdA-diol as an impact modifier of PLLA. Consequently, the so-formed PEA was first analysed to see if it meets the requirements for PLLA toughening. PEA was then melt-blended, in different amounts, with PLLA resulting in binary blends which were extensively investigated to evaluate the toughening efficiency of such a system.

II. SYNTHESIS AND PROPERTIES OF THE POLY(ESTER-AMIDE) RUBBER

The PEA was synthesized by polycondensation of undecenoate butylene diamide diol (UndBdA-diol) with a hydrogenated dimer fatty acid (DFA). The structure of the polymer was confirmed by ^{1}H-NMR spectroscopy as evidenced by ester linkages formation (peaks at 4.22 ppm and 2.28 ppm) and expected peaks integration (Figure 19.2).

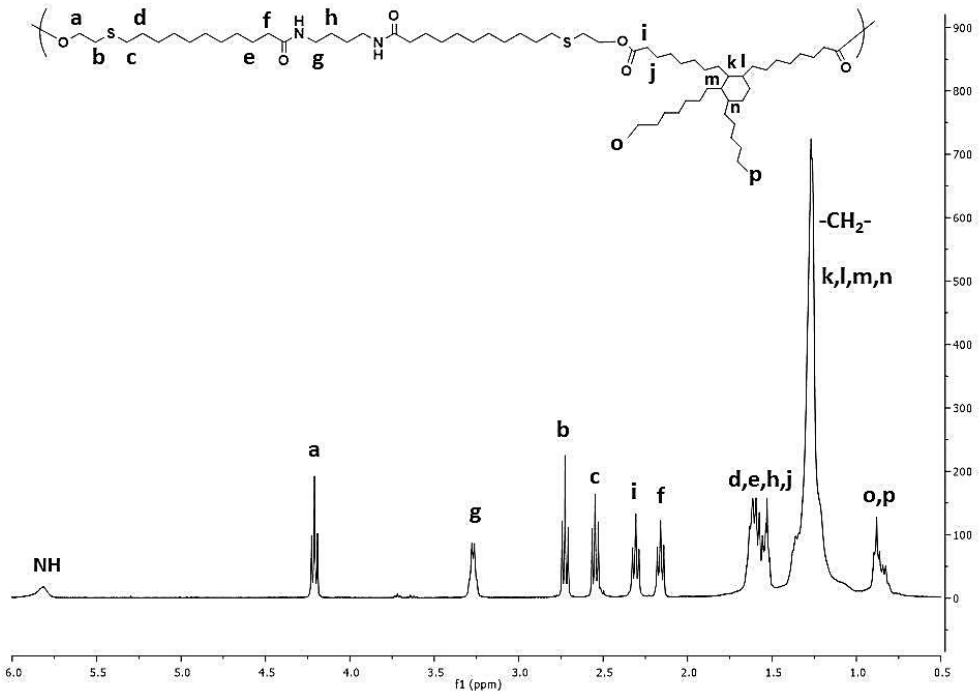

Figure 19.2. ^{1}H-NMR spectra of PEA in $CDCl_3$.

Before melt-blending the so-formed PEA with PLLA, some requirements have to be fulfilled in order to obtain an efficient toughening of PLLA. First, the molecular weight of the rubber must not be too low in order to maintain a degree of structural integrity in response to impact loading. Moreover, by lowering the molecular weight below a certain value, compatibility of the two polymers could happen which would result in no improvement of the impact strength of PLLA. A sufficient structural integrity and incompatibility between the two phases was expected with a PEA showing a $\bar{M}_w$ of 27 000 g.mol^{-1} with a dispersity of 1.6. Thus it is thought that sufficient structural integrity and sufficient incompatibility between the two phases should be obtained.

Then, the glass transition temperature of the rubber must be at least 20°C lower than the test/use temperature to efficiently absorb the applied stress during the impact. Thermo-mechanical analysis of the PEA by DSC showed a Tg well below room temperature (Tg ~ -28°C) which is in accordance with the requirements for rubber toughening of PLA (Figure 20.2 and Table 7.2).

Table 7.2.Physical properties of PEA and PLLA.

material	$\bar{M}_w$ (kg.mol^{-1})[a]	$Đ$[a]	Tg (°C)[b]	Tm (°C)[b]	E (MPa)[c]
PLLA	181	1.5	61	175	1 510 ± 304
PEA	27	1.6	-28	109	191 ± 1

(a) SEC in THF, PS calibration, (b) DSC 10°C.min^{-1}, (c) Tensile tests, v = 10 mm.min^{-1}.

Interestingly, the PEA showed a semi-crystalline behaviour with a melting point at 109°C and a melting enthalpy of 42 J.g^{-1} despite the presence of long alkyl dangling chains that act as internal plasticizers. The highly cohesive amide segments are thought to be responsible for the crystallinity of the material.

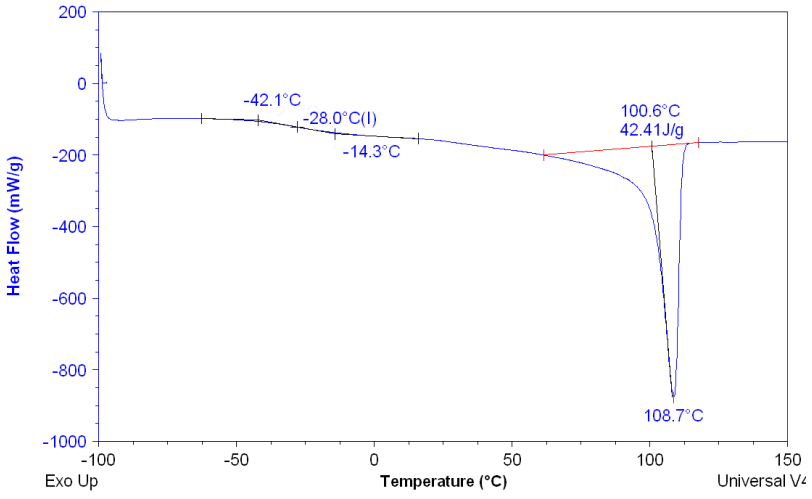

Figure 20.2. DSC trace of PEA. Second heating curve (10°C.min^{-1}).

Tensile tests, performed on PEA showed a Young's modulus value of 191 MPa at room temperature which is much lower than the one of PLLA (1.5 GPa). The low elastic modulus is also in accordance with the requirements for effective toughening of PLLA (Figure 21.2).

Another requirement to the use of PEA for the modification of PLLA mechanical properties by melt-blending is the thermal stability. Indeed the rubber must be thermally stable to PLLA processing temperatures which are in general around 190-200°C. Thus TGA experiments were carried out with PEA and PLLA. The first weight loss (temperature corresponding to 5% weight loss) is observed near 350°C and 335°C for PEA and PLLA respectively. The higher thermal stability of PEA confirmed the applicability of PEA as an additive of PLLA.

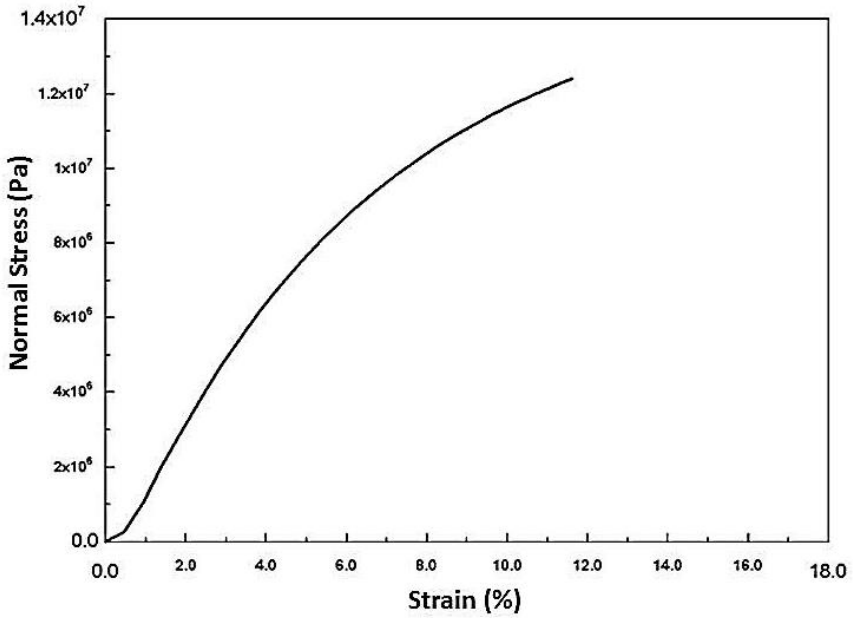

Figure 21.2. stress-strain curve of PEA – v= 10 mm.min^{-1}.

Finally both polymers need to be immiscible to observe phase segregation at the micro-scale and thus efficient rubber toughening. Solubility parameter (δ) is usually used to roughly estimate compatibility of polymers with solvents, small molecules or other polymers. The solubility parameter is a measure of the cohesive strength between molecules and it can be calculated for any molecule from its constituent functional groups:

$$\delta = \left(\frac{E_{coh}}{V}\right)^{1/2} \quad \textbf{(eq 1.2)}$$

Where E_{coh} is the molar attraction constant for a particular functional group with volume V. Solubility parameters of PLLA and PEA were calculated from Hoy method. The obtained values are 11.11 and 10.06 $(cal.cm^{-3})^{0.5}$ for PLLA and PEA respectively. The difference between the two solubility parameters (difference higher than 0.5) suggests that the system

should be immiscible which is in accordance with the requirements needed for effective toughening of PLLA by PEA.[27]

All these preliminary characterizations on PEA prompted us to investigate its melt-blending with PLLA in view of the good potential of PEA as an impact modifier of PLLA.

III. PROCESSABILITY AND MORPHOLOGY OF THE BLENDS

The PEA rubber was added in various amounts into a commercially available PLLA (Table 7.2) using a twin-screw micro-compounder in order to reach final contents of 5, 10, 15 and 20 wt% rubber. Based on the conditions generally reported in the literature for such systems, following conditions have been selected : melt-compounding for 5 min at 190°C and 50 rpm followed by injection molding at 200°C in a mold kept at 50°C. Such processing conditions can afford a good compromise between good dispersion (related to shear) and limited material thermal degradation.

III.1. Processability

The thermal stability of the PLLA/PEA blends under non-oxidative conditions was investigated by thermal gravimetric analysis in order to evaluate the processability of the materials. Thermal decomposition parameters are given in Table 8.2 and illustrated in Figure 22.2. As expected a two-step thermal decomposition is observed for the blends. A first weight loss occurring near 300°C is assigned to the degradation of the matrix PLLA and a second weight loss observed around 350-400°C is characteristic from PEA thermal degradation. Regarding the TGA curves and the corresponding derivatives (Figure 22.2), a slight decrease in initial degradation temperature of PLLA phase must be underlined. Indeed the temperature corresponding to 5% of weight loss shifted from 335°C for neat PLLA to 308°C when only 5wt% of PEA was dispersed in the matrix. However, further increase in the PEA weight composition did not changed notably the thermal degradation. For all samples, the temperature corresponding to the final degradation was above 490°C and negligible weight residues were measured (less than 3.2%). To summarize, good thermal stability of the blends was noticed despite the slight decrease in initial degradation temperature of PLLA with the addition of PEA. Thus the good thermal stability indicates the possible melt-process of such materials in terms of thermal stability.

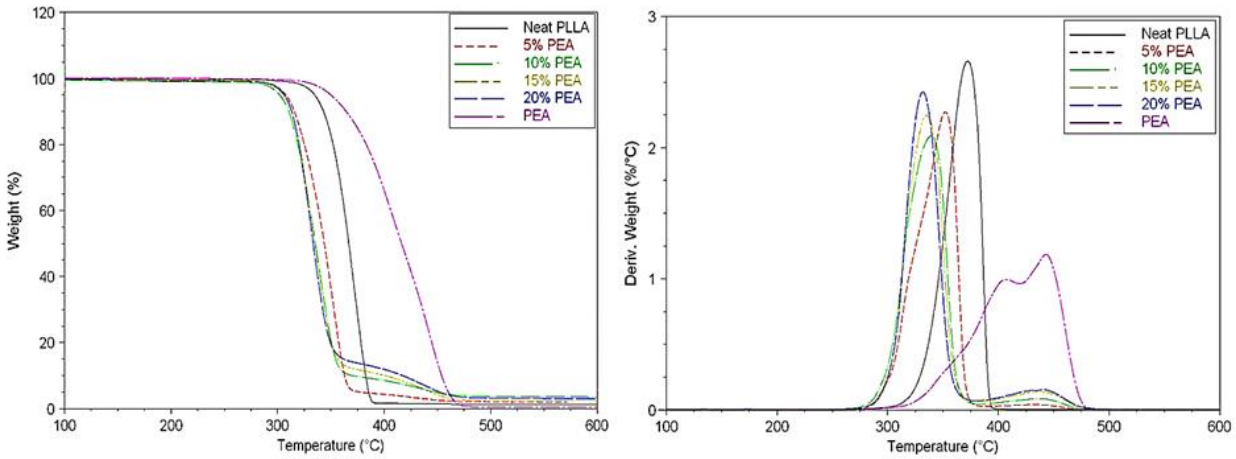

Figure 22.2. TGA curves (left) and TGA derivative curves (right) of the two homopolymers and the blends recorded from 20 to 700°C at 10°C.min^{-1} under a nitrogen atmosphere.

Table 8.2. Thermal properties, weight compositions of the blends and mean diameter size of the PEA particles.

wt% PEA $_{theo}$	wt% PEA $_{TGA}$	$T_{5\%}$ (°C)[a]	$\bar{d}$ (µm)[b]
0	-	335	-
5	5.4	308	1.2 ± 0.3
10	11.4	303	1.6 ± 0.4
15	14.1	306	1.8 ± 0.6
20	16.5	306	3.1 ± 1.4
100	-	350	-

(a) TGA, 20 to 700°C, 10°C.min^{-1} (b) calculated from SEM images using Image J

Dynamic melt rheological properties of neat PLLA and PLLA/PEA blends were measured at 190°C (temperature used during melt-blending) in order to better identify the interaction between both phases and to better evaluate the melt processability of the blends. Polymeric complex viscosity (η*) is relating to the storage modulus (G') and loss modulus (G") which represent the elastic and viscous components of the polymeric modulus respectively. Figure 23.2 shows the rheological curves of neat PLLA and those of the PLLA/PEA blends comprising different amounts of PEA.

In Figure 23.2.a is displayed the storage modulus versus the angular frequency. It is noteworthy that G' of the blends increases with PEA content at low frequencies (below 5 rad.s^{-1}), which means that the elasticity of the blend melt increases with PEA. The enhancement of blend elasticity over neat PLLA can be attributed to the relaxation of the dispersed phase under slight shear deformation. The higher elasticity of the blends with high contents of PEA is logically explained by a longer relaxation process of the dispersed phase due to an increase in the diameter of the dispersed phase as will be discussed in the

morphology part (See Figure 24.2 and Table 8.2). At higher frequencies (above 5 rad.s^{-1}), the slight decrease in G' with an increase in PEA content (reversed trend) can be attributed to a plasticizing effect of the dispersed particles that become highly deformed. The loss modulus (G") (Figure 23.2.b) remains mostly unaffected by the dispersion of PEA in the PLLA matrix. The complex viscosities, η*, of neat PLLA and PLLA/PEA blends as a function of the angular frequency, ω, are shown in Figure 23.2.c. From these curves, it appears that neat PLLA and the blends exhibit a typical Newtonian behavior in the low-frequency region and shear thinning for higher frequencies which is characteristic for linear polymers. While neat PLLA shows shear thinning tendency at about 10 rad.s^{-1}, the blends present this tendency at lower frequencies meaning that the Newtonian region for the blends is narrower. The dynamic complex viscosities of blends are lower than that of neat PLLA which shows an improved processability of PLLA.

In Figure 23.2.d is displayed the plot showing the relationship between the storage modulus (G′) and the loss modulus (G″) (Han plot).[28] The Han plot gives information on the viscoelastic properties of the blends. Indeed, the straight line, G′=G″, divides the coordinate into two parts. Above the straight line, the major property of materials presents elasticity; on the contrary it shows viscosity. Neat PLLA and PLLA/PEA blends are all located below the straight line showing that these materials were more viscous than elastic component at the melting state. It is noticeable that the curves shifted to the straight line, indicating that the elastic component of blends increases with increasing PEA content. This enhancement of the blend elasticity may arise from molecular interactions between the amide functions of the PEA and the ester functions of the PLLA matrix.

The procesability investigation of the blends showed good thermal stability over the processing temperature range of PLLA. Thus, further investigations have been done to evaluate the general properties of the novel PLLA materials.

III.2. Morphology

Since the mechanical properties of polymer blends highly depend on the immiscibility of the different phases, it is important to know the microstructure of the blend. Rheological measurements were previously used to evaluate the processabilty of the blends. The Han plot (Figure 23.2.d) can also give information on the miscibility of two polymeric phases while in blends.[28] Indeed, it is clearly observed an upturning of the curves for the blends at low modulus while the curve of neat PLLA remains almost linear. This observation indicates that PLLA/PEA blends are immiscible at all concentrations of the dispersed phase.[27, 29, 30]

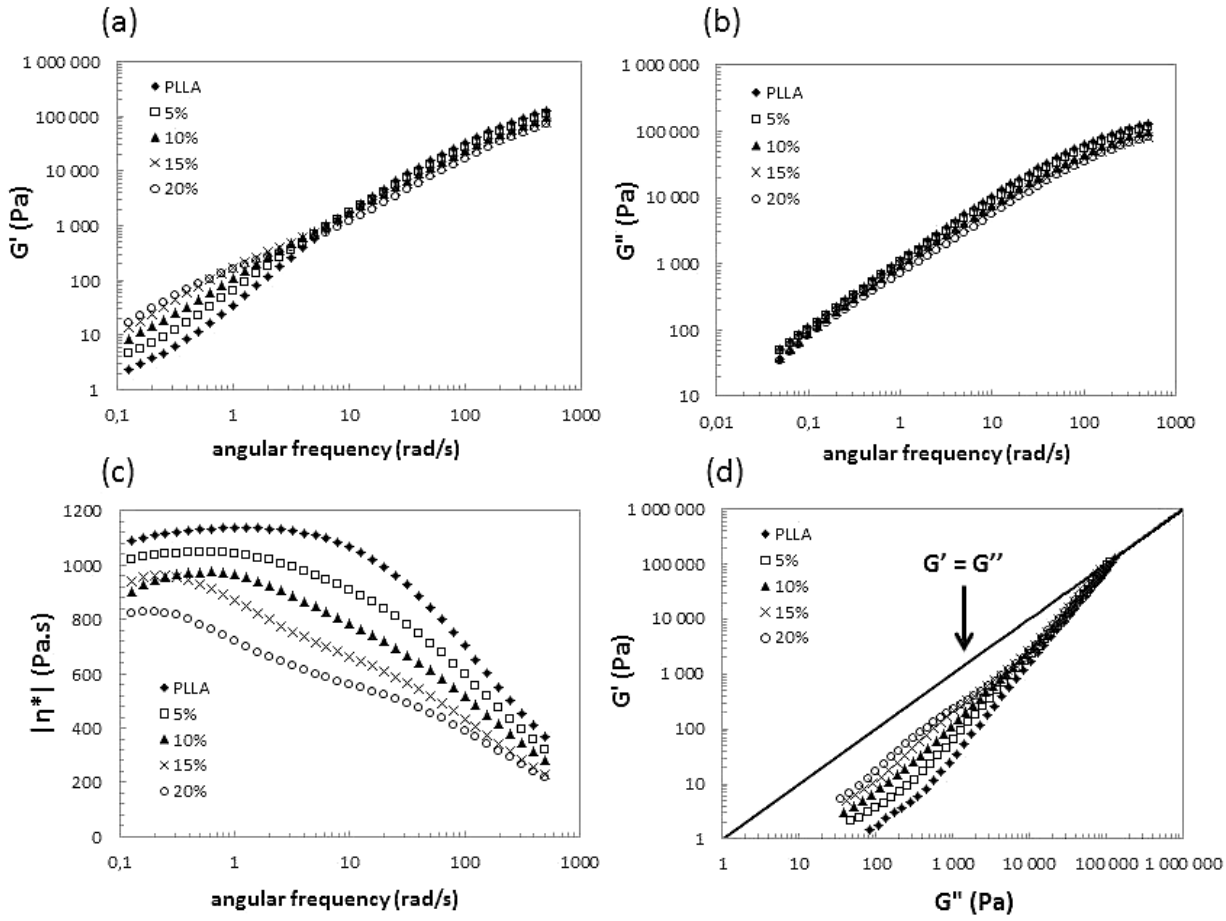

Figure 23.2.(a) Storage modulus, (b) loss modulus, (c) complex viscosity of neat PLLA and the blends as a function of angular frequency. (d) Han plot showing the storage modulus versus the loss modulus. All measurements were performed at 190°C using a strain deformation of 5%.

Scanning electron microscopy (SEM) was then employed to study more in details the morphologies of the blends. Figure 24.2 shows cryo-fractured surfaces of the different blend compositions observed by SEM. For all samples, the morphologies were characterized by spheres and holes of PEA phase dispersed into the PLLA matrix. The obvious interface between the two phases suggested incompatibility. The size of the PEA phase domains, calculated from the images of the cryo-fractured surfaces, increased with its content from 1.2 µm to 3.1 µm (Table 8.2). The particles were well-dispersed into the PLLA matrix for the blend containing up to 10wt% of PEA, while high heterogeneity of the particle size was observed for the blends containing 15 and 20 wt% of PEA. This high increase in particle diameter coupled with the increase in standard deviation can be explained by the important incompatibility between the two phases. It has been shown that blend morphology does not change significantly over time during the melt blending process. Indeed the invariant morphology is due to a rapid establishment of equilibrium between drop breakup and coalescence of the dispersed phase. For uncompatibilized blends, an increase in final particle size with the dispersed phase concentration can be due to an enhanced coalescence process.[31]

The observation of such a trend confirms the incompatibility of PEA and PLLA. One solution to lower the dispersed phase particle size would be to add compatibilizers to limit coalescence similarly to the addition of surfactants in water/oil emulsions.

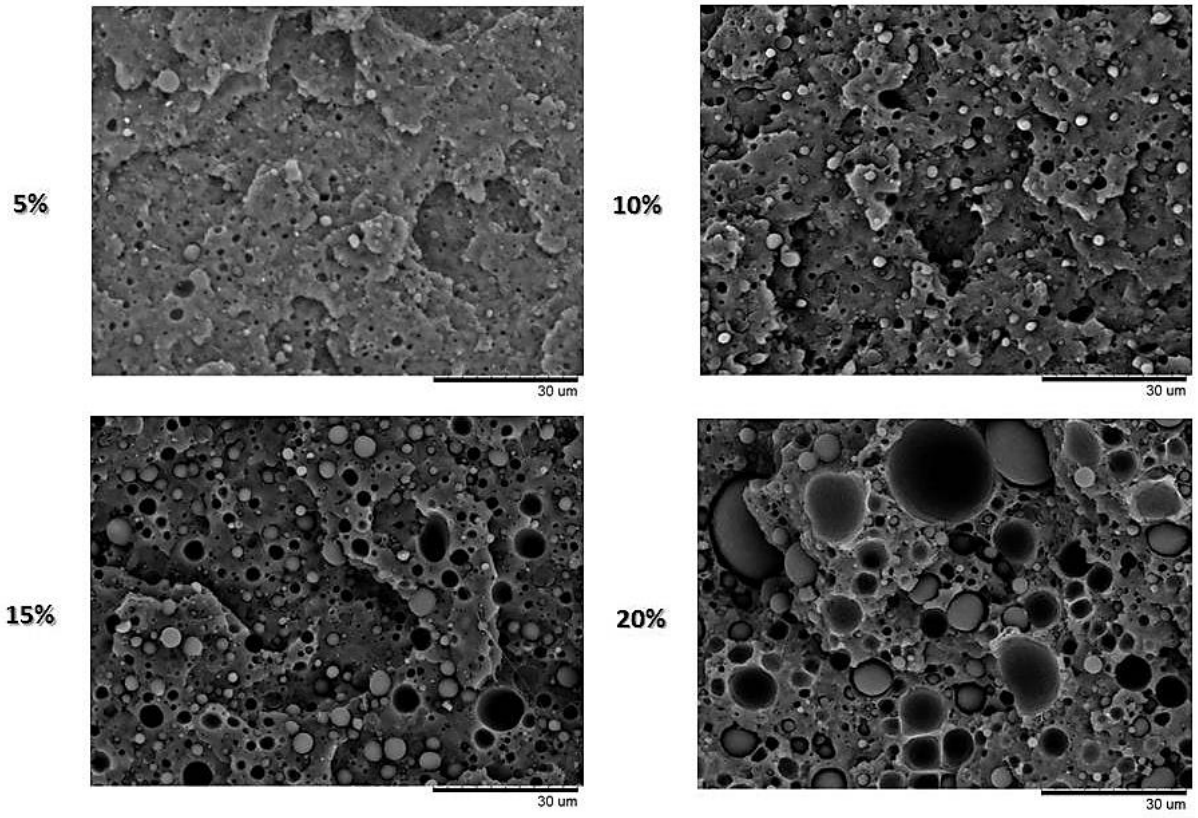

Figure 24.2. Cryo-fractured surfaces of the blends observed by SEM at room temperature.

IV. CRYSTALLIZATION BEHAVIOR OF THE BLENDS

One of the reasons of the great enthusiasm regarding the use of PLLA as a commodity and specialty material resides in its crystalline ability. Indeed isotactic PLA (PLLA) has been extensively studied due to the high melting point that confers interesting properties to this material. In industrial practice, it is therefore difficult to make use of the semi-crystalline character of PLLA because the high speed of mass production (e.g. in injection moulding) implies quenching, leading to amorphous structures. Some polymers have been described as nucleating-assisting agents and spherulite growth-accelerating agents (See Chapter 1). Due to the specific chemical structure of PEA (amide segments that can interact with the matrix and DFA that can plasticize PLLA at the interface), we were interested to evaluate the crystallization behavior of the blends.

IV.1. Non-Isothermal crystallization behavior

DSC cooling curves from the melt and subsequent heating curves of PLLA and PLLA/PEA blends are shown in Figure 25.2 and Figure 26.2. From the cooling curves collected at a cooling rate of 5°C.min^{-1}, it is noteworthy that neat PLLA displayed a very small exothermic peak compared to the blends. This indicates an enhanced crystalline ability during cooling of PLLA when PEA is dispersed in the matrix. A second smaller exothermic peak is noticed around 93°C which corresponds to the crystallization of the dispersed PEA phase. By subsequent heating of the samples, cold crystallization of neat PLLA is observed at 107°C. This phenomenon is often observed in the case of PLLA. It is explained by the enhanced mobility given to the polymeric chains after the Tg that allows better packing of the chains and thus crystallization. Interestingly, no visible cold crystallization was observed for the blends except for the PLLA/PEA (95/5: w/w) blend that showed a small exotherm at 98°C. This value is slightly lower than the cold crystallization of neat PLLA (111°C) indicating an enhanced crystalline ability. The absence of cold crystallization for the blends with higher contents of PEA may suggest important crystallization of the PLLA phase during cooling. However, a small endothermic peak assigned to the melting transition of the PEA phase at around 106°C is situated in the temperature window of cold-crystallization of PLLA phase. Thus, the superimposition of these two physical transitions doesn't allow the exact determination of both the cold-crystallization enthalpy and the crystallinity of the PLLA phase. Melting of PLLA phase occurred in all cases (neat PLLA and blends) at 177°C indicating that the dispersion of PEA into the matrix had no influence on the melting transition of PLLA.

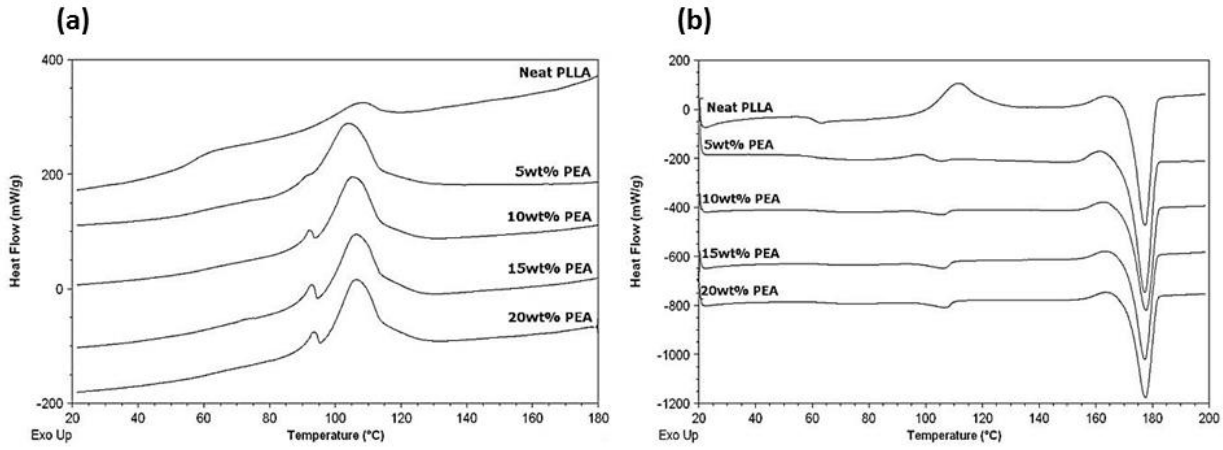

Figure 25.2. (a) Cooling curves and (b) heating curves of neat PLLA and the blends – 5°C.min^{-1} from 0°C to 200°C

By measuring the heat of fusion ΔH_m and the heat of cold crystallization ΔH_{cc}, an estimation of the crystallinity of the PLLA phase in the blends can be determined using the equation 2.2:

$$\chi_c = \frac{\Delta H_m - \Delta H_{cc}}{\Delta H_m^0} \times \frac{100}{\omega} \quad (eq\ 2.2)$$

Where ΔH_m^0 is the enthalpy of fusion of the completely crystalline state (93 $J.g^{-1}$ for PLLA) and ω the weight fraction of PLLA in the blend. Values of enthalpies and temperatures of fusion and cold crystallization as well as the values of estimated crystallinity degrees of the PLLA phase are displayed in Table 9.2. Two cooling and heating rates were employed during DSC analyses (5°C.min^{-1} and 10°C.min^{-1}). It is noticeable that cooling and heating rates have a strong influence on the crystallization kinetic. Indeed, while at 5°C.min^{-1} no or almost no cold crystallization was noticed for the PLLA/PEA blends, at 10°C.min^{-1} an important cold crystallization exothermic peak was observed for all the samples (Figure 26.2).

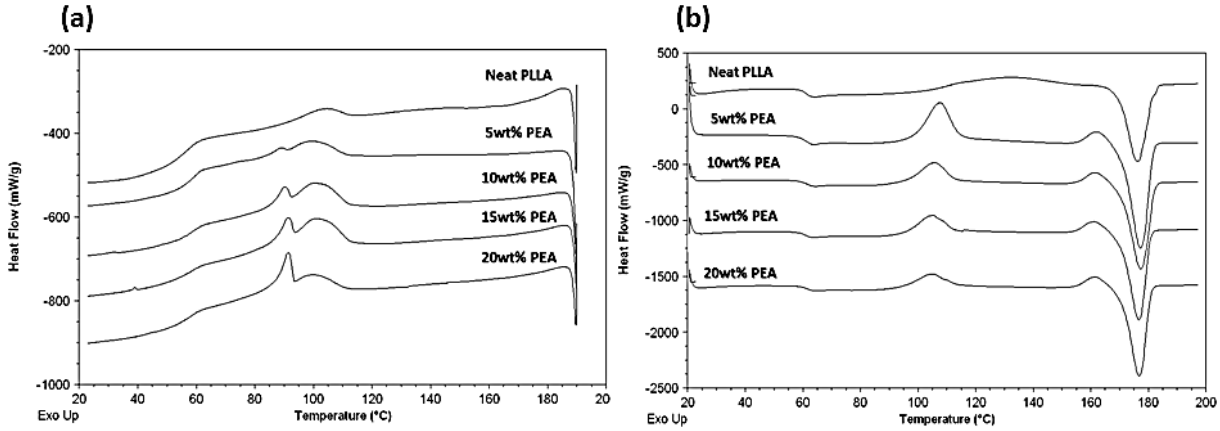

Figure 26.2. (a) cooling curves and (b) heating curves of neat PLLA and the blends – 10°C.min^{-1}.

This suggests that PLLA phase did not have enough time to complete crystallization at the higher heating rate leading to a drop of PLLA crystallinity. For instance the crystallinity of PLLA phase in the PLLA/PEA (90/10: w/w) blend goes from 41% to 27% at 5°C.min^{-1} and 10°C.min^{-1} respectively. However, even at 10 °C.min^{-1}, the crystalline ability of PLLA was enhanced by the dispersion of the PEA phase. Indeed, the incorporation of PEA decreased cold crystallization temperature by approximate 15°C and narrowed the peak width. Moreover estimated values of crystallinity were higher for the blends than for neat PLLA (15% for neat PLLA to 29% for the blend comprising 20wt% of PEA).

Table 9.2. Cold-crystallization and melting parameters of neat PLLA and blends at different heating rates

	5 °C.min^{-1}					10 °C.min^{-1}				
PEA content (wt%)	Tcc (°C)	ΔHcc (J.g^{-1})	Tm (°C)	ΔHm (J.g^{-1})	χc (%)	Tcc (°C)	ΔHcc (J g^{-1})	Tm (°C)	ΔHm (J g^{-1})	χc (%)
0	111.4	22.8	177.6	38.6	17	129.2	19.2	176.3	32.9	15
5	98.6	1.9	177.3	43.0	46	107.7	21.5	177.4	41.9	23
10	-	-	177.8	34.2	41	105.6	13.0	177.3	36.0	27
15	-	-	177.4	32.3	41	104.7	11.2	176.7	32.6	27
20	-	-	177.6	31.6	42	105.0	10.4	176.8	32.4	29

Tcc and Tm are the cold crystallization temperature and the melting temperature of PLLA phase respectively. ΔHcc and ΔHcc are the corresponding enthalpy values. χ_c is the crystallinity of PLLA phase.

The improvement of the crystalline ability of PLLA by dispersion of polymers into the matrix has been observed by several research groups. It was claimed that the additives proceed by two manners. In a first case the increase of the crystallinity of PLLA is due to an increase in nucleus number while the growth rate (G) of the spherulites remains unchanged. In a second case the nucleus number is lowered while the growth rate increases.[32] To determine which of these phenomena is occurring with the dispersion of PEA, we investigated the formation of crystallinity during non-isothermal cold-crystallization studies. Neat PLLA and the PLLA/PEA (90/10: w/w) blend were molten at 200°C for 3 minutes to fully erase the thermal history. The samples were then quenched leading to amorphous materials and subsequently cold-crystallized at a heating rate of 10°C.min^{-1}. Figure 27.2 shows polarized optical images of the samples during heating.

Regarding neat PLLA, cold-crystallization seems to start around 110°C as seen from the spherulites formation in Figure 27.2.e. The spherulites density at this temperature is quite low indicating the beginning of the cold-crystallization process. At higher temperature (Figure 27.2.g), the spherulites density stayed low however an increase in their size was noticed. In the case of the blend, cold-crystallization started at lower temperature as seen from the first crystallites distinguished at 100°C. This observation is in agreement with the lowering of the cold-crystallization temperature by dispersion of PEA during DSC experiments (See Figure 26.2 and Table 9.2). The size of the crystallites did not seem to increase significantly with the temperature; nevertheless their density became quite important. It is also noteworthy that no distinguishable spherulites were observed for the blend contrary to neat PLLA.

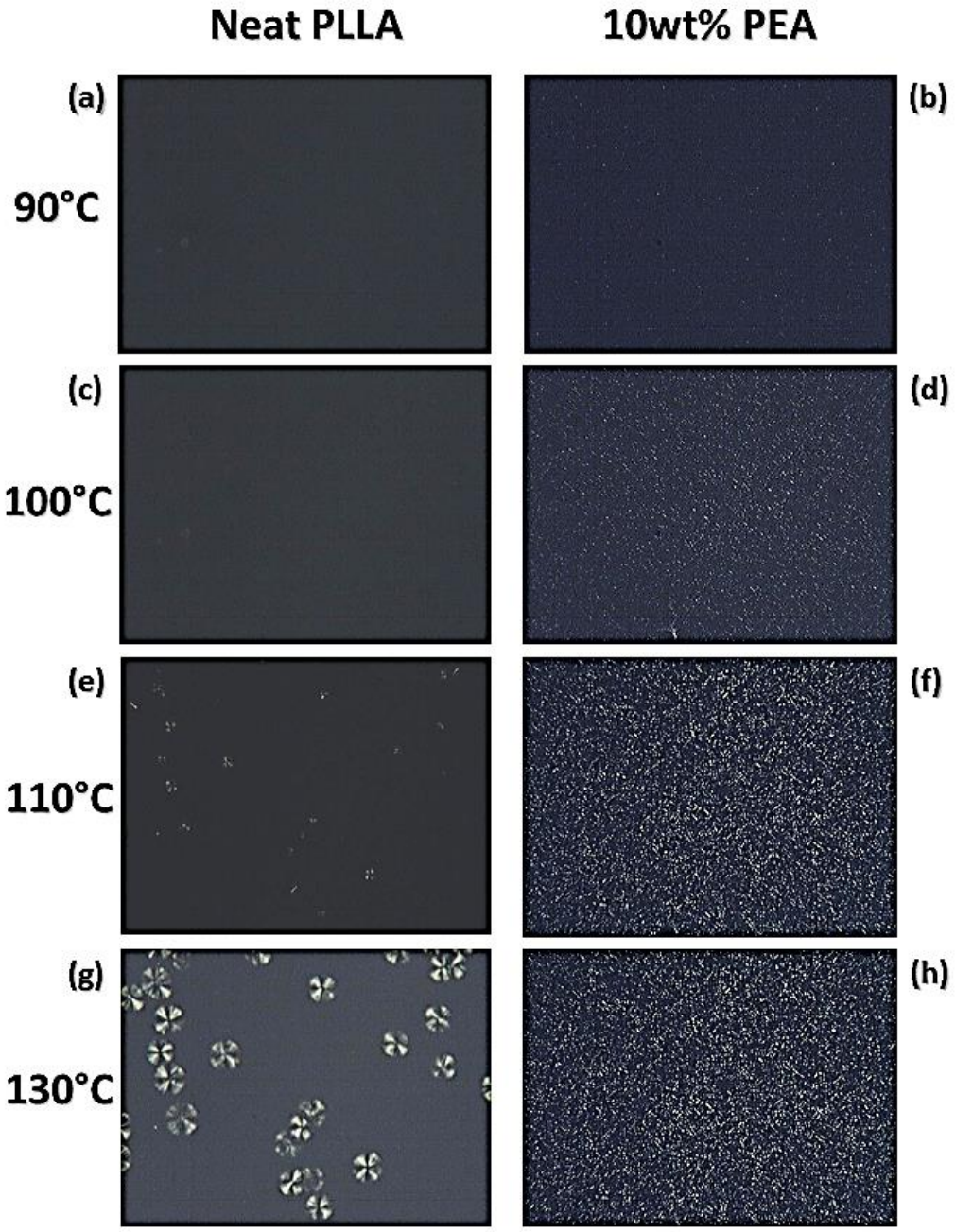

Figure 27.2. Cold-crystallization of neat PLLA and the PLLA/PEA (90/10: w/w) blend during heating at 10°C.min^{-1} the samples that were previously molten for 3 minutes at 200°C and subsequently quenched. Photos taken under polarized microscope.

From these images, we can conclude that improvement of the cold-crystallization occurred via an increase in nucleus number and not from an enhancement of the growth rate. The crystalline surface area was measured on optical images taken for neat PLLA and the blend at different temperatures (Figure 28.2). While for neat PLLA, the crystalline surface area at 110°C counts for 0.4% of the total area, the crystalline surface area of the blend represents 10.5% of the total area. This observation confirms the enhanced cold-crystallization of PLLA by addition of PEA which acts as a nucleating-assisting agent of PLLA.

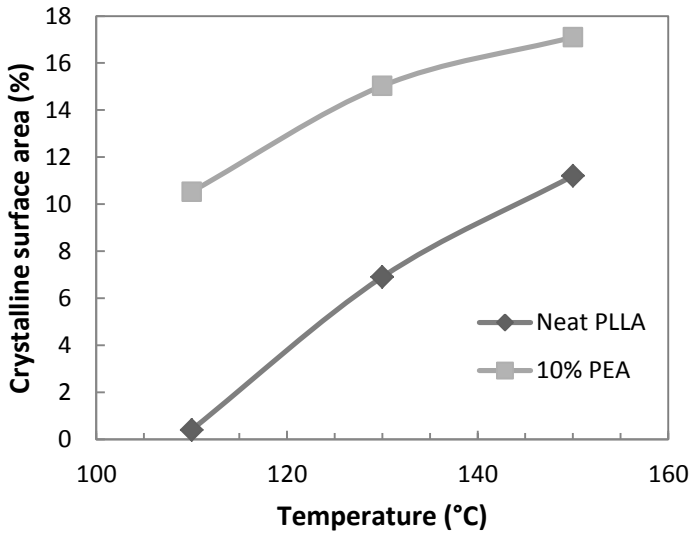

Figure 28.2. Relative crystalline surface area measured by Image J on optical microscopy images taken during non-isothermal crystallization of neat PLLA and the PLLA/PEA (90/10 : wt/wt) blend.

IV.2. Isothermal crystallization behavior by DSC

To further confirm the enhancement of PLLA crystallization rate, isothermal crystallization investigation was conducted by DSC analyses. To that aim, samples were melted at 200°C for 3 minutes and subsequently cooled at 110°C (note: this corresponds to the maximum of PLLA crystallization determined by DSC). The isothermal crystallization data were then fitted to the Avrami equation (3.2).[33]

$$\alpha_c = 1 - exp(k.t^n) \quad \textit{(eq 3.2)}$$

where, α_c is the relative crystalline volume fraction of the polymer as a function of time, k the rate constant of crystallization and n the Avrami index. α_c is the degree of crystallinity at time t and is obtained from dividing the area under exothermic peak in DSC isothermal crystallization analysis at a crystallization time t by the total area. By taking the double logarithm of equation (3.2), equation (4.2) was obtained:

$$log[-ln(1-\alpha_c)] = logk + nlogt \quad \textit{(eq 4.2)}$$

From the intercepts and the slopes of log[-ln(1-α_c)] versus log t, the values of k and n were calculated respectively (Figure 29.2 and Table 10.2). The crystallization half-time was also determined from equation (5.2).

$$t_{1/2} = \left(\frac{ln\,2}{k}\right)^{1/n} \quad \textit{(eq 5.2)}$$

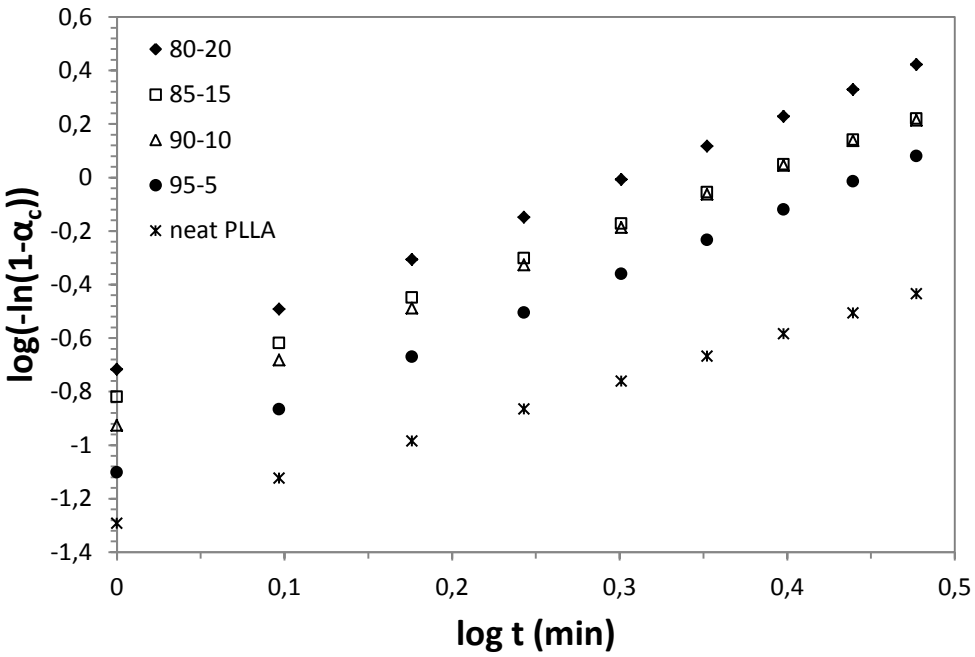

Figure 29.2. Avrami plot - Effect of the PEA amount on isothermal crystallization (110°C) of PLLA phase.

The plots of log[-ln(1-α_c)] versus log t for the different samples showed good linear relationship in agreement with Avrami equation. The half-time of crystallization $t_{1/2}$, the time at which the relative degree of crystallization is 0.5, was calculated for each sample from equation (5.2). The values are summarized in Table 10.2. It is noticeable that the half-time of crystallization of PLLA phase is significantly decreased by the incorporation of PEA. Indeed $t_{1/2}$ for neat PLLA is 6.12 min while for the PLLA/PEA (95/5: w/w) blend this value dropped to 2.41 min. The addition of more PEA in PLLA matrix then only slightly reduces the half-time of crystallization. This observation is in accordance with the observations made during non-isothermal crystallization studies. The enhancement of the crystallinity and the crystallization rate of PLLA for physical blends are well known and have been previously described for other systems.[27, 34] This phenomenon has been attributed to interactions which are taking place at the interface of the phase-separated domains and which create favorable nucleation sites for crystallization. We could then hypothesize that PEA creates interactions with the PLLA phase thus lowering the nucleation barrier. By using the Arrhenius' law and by making the hypothesis that the pre-exponential factor is not influenced by the amount of PEA, it is then possible to calculate an activation energy of crystallization difference between neat PLLA and the blends that is determined from equation (6.2)

$$\Delta E_a = ln\frac{k_1}{k_2} \times R.T \qquad \textit{(eq 6.2)}$$

Where ΔE_a is a difference of activation energies, k_1 and k_2 the rate constants of crystallization, R the gas constant and T the temperature.

A difference of -3.4 $kJ.mol^{-1}$ was calculated between neat PLLA and the PLLA/PEA (95/5: w/w) blend thus confirming the lowering of the nucleation barrier by addition of a small amount of PEA in the matrix.

Table 10.2. Isothermal crystallization parameters of neat PLLA and the blends (110°C).

PLA/PEA	n	k (min^{-n})	t1/2 (min)
100/0	1.80	0.027	6.12
95/5	2.48	0.078	2.41
90/10	2.40	0.122	2.06
85/15	2.20	0.148	2.02
80/20	2.39	0.189	1.72

V. MECHANICAL PROPERTIES

The processability of the blends was first confirmed by TGA and rheological measurements, and then crystallization investigation suggested an improvement of the crystallization rate of PLLA phase in the blends. However the main goal of this study was to induce the toughening of PLLA by dispersion of the PEA elastomer. To evaluate our approach, mechanical testing and dynamic mechanical analysis were carried out.

V.1. Dynamic mechanical analysis

Dynamic mechanical analysis (DMA) was performed on each sample in order to evaluate the viscoelasticity of the blends. In Figure 30.2 is represented the storage modulus and the loss tangent as a function of the temperature. DMA results of pristine PEA showed two primary relaxations in the temperature range examined. One was labeled to the amorphous α-relaxation, which is characteristic of the obvious enhancement in motion of large segments of the macromolecular chains with increasing temperature, and one was identified as the crystalline relaxation. From the maximum of tanδ versus temperature curve was measured a glass transition of -19.9°C. The thermo-mechanical behavior of neat PLLA was more complex. Indeed, the tensile storage modulus (E') dropped abruptly at 55-70°C due to glass transition and then started to increase from 80-90°C. The rising of E' was assigned to cold crystallization due to enhanced mobility of the polymer chains above the Tg. Finally a last transition was observed at around 170°C which is assigned to the crystallization relaxation of PLLA. DMA of all the blends revealed a typical two-phase system, showing two glass

transitions, one for PEA at around -20°C and one for PLLA at around 64°C. No significant difference in the values of amorphous α-relaxation temperature was noticed, in comparison to the values of neat PEA and PLLA. This feature suggests incompatibility of the two polymers, in agreement with the rheological properties and the morphologies observed by SEM. Based on the non-isothermal and isothermal crystallization data, we have seen that crystalline ability of PLLA was enhanced by the dispersion of PEA. However, the important drop of the storage modulus at 55-70°C, even for the blends, suggests incomplete crystallization during cooling (cooling from the melt to room temperature) of the samples prepared by melt compression. It is assumed that the cooling rate was too high to allow PLLA phase crystallization. However, it is noteworthy that the cold crystallization, characterized by the rise of the storage modulus, moved down to lower temperatures with the incorporation of PEA. This observation confirms the enhanced cold crystallization ability of the PLLA phase which was highlighted in the non-isothermal crystallization part. In view of these results and despite the slight enhancement of the crystallization rate of PLLA phase by the addition of PEA, the insufficient elastic modulus at temperatures above the glass transition limits the applications of these materials to the low temperatures.

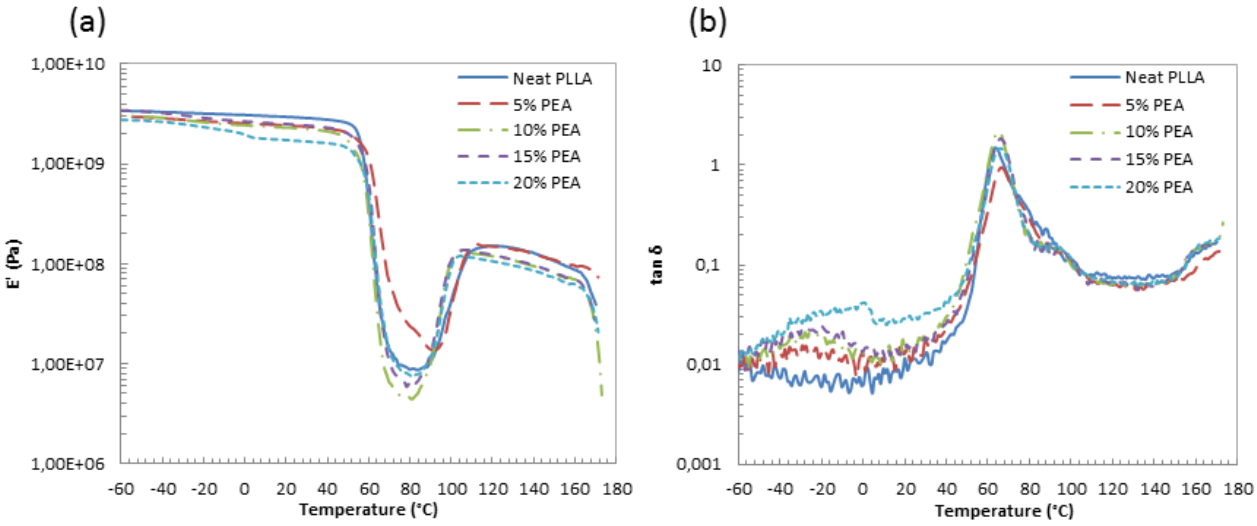

Figure 30.2. (a) Storage modulus and (b) tanδ as a function of temperature for neat PLLA and the blends.

V.2. Toughening evaluation of the blends

Since the main purpose of the PLLA blending with PEA is to improve the flexibility and impact strength of PLLA, tensile experiments as well as impact testing were realized on PLLA and the blends. As seen from the tensile stress-strain curves displayed in Figure 31.2, the fracture behavior of the specimen changed from brittle fracture of the neat PLLA to

ductile fracture of the blends. The yield behavior was not obvious during stretching of neat PLLA and sample is thought to break by neck instability resulting in low elongation at break value (only 3.8%). On the contrary, all the blends showed distinct yielding (stress yield) and stable neck growth. After the yield point, there is a competition between the orientation of PLLA chains and crack formation. Even at 5wt% of PEA, the elongation of the blend was significantly increased (>100%) (Table 11.2). This suggests that large energy dissipation occurred owing to the presence of PEA. Further increase in elongation at break value was noticed up to 10wt% of PEA (155%). However, for higher amounts of dispersed phase, the elongation of the blend dropped tremendously to 6.4% for the PLLA/PEA (80/20: w/w) blend. The poor mechanical properties of the blends for higher contents of PEA can be explained by bigger dispersed phase particles coupled with high heterogeneity of the domain size (See Table 8.2 and Figure 24.2). This observation shows the important effect of the microstructure of the blend on its mechanical properties. The desired beneficial effect of rubber toughening does not always come without some negative consequences. Indeed, the incorporation of rubber into the PLLA matrix generally reduces the modulus in proportion to the amount added.

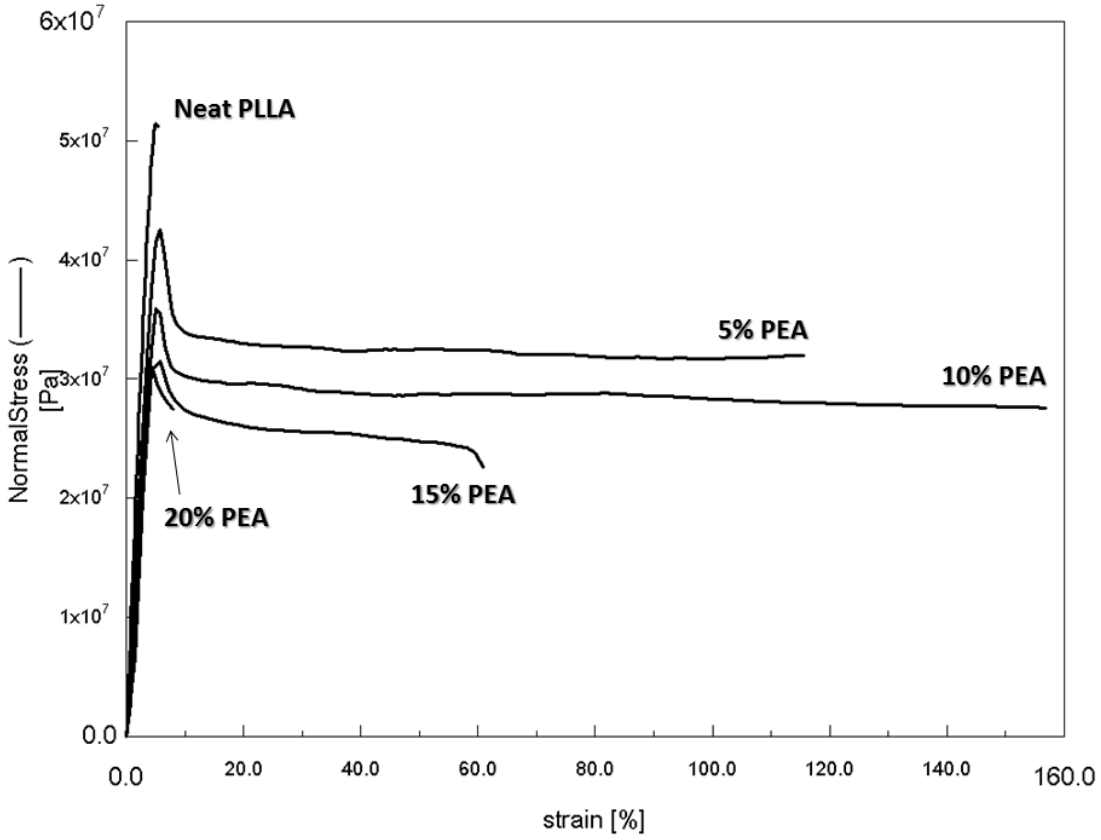

Figure 31.2. Stress-strain curves for neat PLLA and the blends. v=10 mm.min^{-1}.

In this study we also observed a decrease in the Young's modulus by addition of PEA into the PLLA matrix. Indeed while neat PLLA shows a Young's modulus of 1.51 GPa, the blend comprising 5wt% of PEA exhibits a value of 0.84 GPa. Surprisingly, further addition of PEA phase resulted in a slight increase of the Young's modulus up to 0.98 GPa. This may be attributed to higher crystallinity of the PLLA phase for higher contents of PEA due to enhanced crystalline ability given by the incorporation of PEA into the PLLA matrix. Yield stress was decreasing with the addition of PEA. Yield stress changed from 47.1MPa for neat PLLA to 30.1MPa for the blend with 20wt% of PEA.

Impact toughness of the blends was then measured by notched IZOD impact strength test. As seen from Table 11.2, incorporation of 5wt% of PEA resulted in no changes in the impact strength value (2.45 $kJ.m^{-2}$). However from 10wt% to 15wt% of PEA in the material, impact strength increased up to 3.68 $kJ.m^{-2}$. For higher contents of dispersed phase, the impact strength value decreased due to bigger rubber particles in the matrix that did not dissipate impact energy efficiently. For this system, an optimum blend composition for which the impact strength reached a maximum should exist. In terms of mechanical properties, it seems that the blends containing 10wt% and 15wt% of PEA are the most promising materials for the toughening of PLLA. Indeed for these materials, only limited depression of the Young's modulus and the yield stress values were observed compared to neat PLLA and significant improvement in the strain at break and the impact strength were noticed.

Table 11.2. Mechanical properties of neat PLLA and the blends.

wt% PEA	E Modulus (Mpa)	Yield Stress (Mpa)	Strain at break (%)	Notched IZOD IS ($kJ.m^{-2}$)
0%	1510 ± 304	47.1 ± 6.0	3.8 ± 1.4	2.45 ± 0.25
5%	840 ± 138	36.2 ± 5.6	105.5 ± 68.3	2.45 ± 0.31
10%	905 ± 129	36.4 ± 3.3	155.2 ± 66.1	3.37 ± 0.00
15%	985 ± 108	33.4 ± 1.2	65.9 ± 34.4	3.68 ± 0.43
20%	920 ± 49	30.1 ± 2.0	6.4 ± 1.2	3.07 ± 0.53

V.3. Toughening mechanism

In order to identify the main toughening mechanisms occurring during impact testing, the impact-fractured surfaces were observed by SEM. The micrographs of all the blends are displayed in Figure 33.2 and Figure 34.2. Plastic deformation in rubber-toughened polymers can occur through several mechanisms including crazing, cavitation of the rubber phase and shear yielding.[35] It is now well-established that dispersed rubber phase allows control over nucleation and growth of crazes thus decreasing the brittleness of the matrix. Cavitation of the

rubber phase is thought to be the initial step leading to plastic deformation and there exists two types of cavitation.

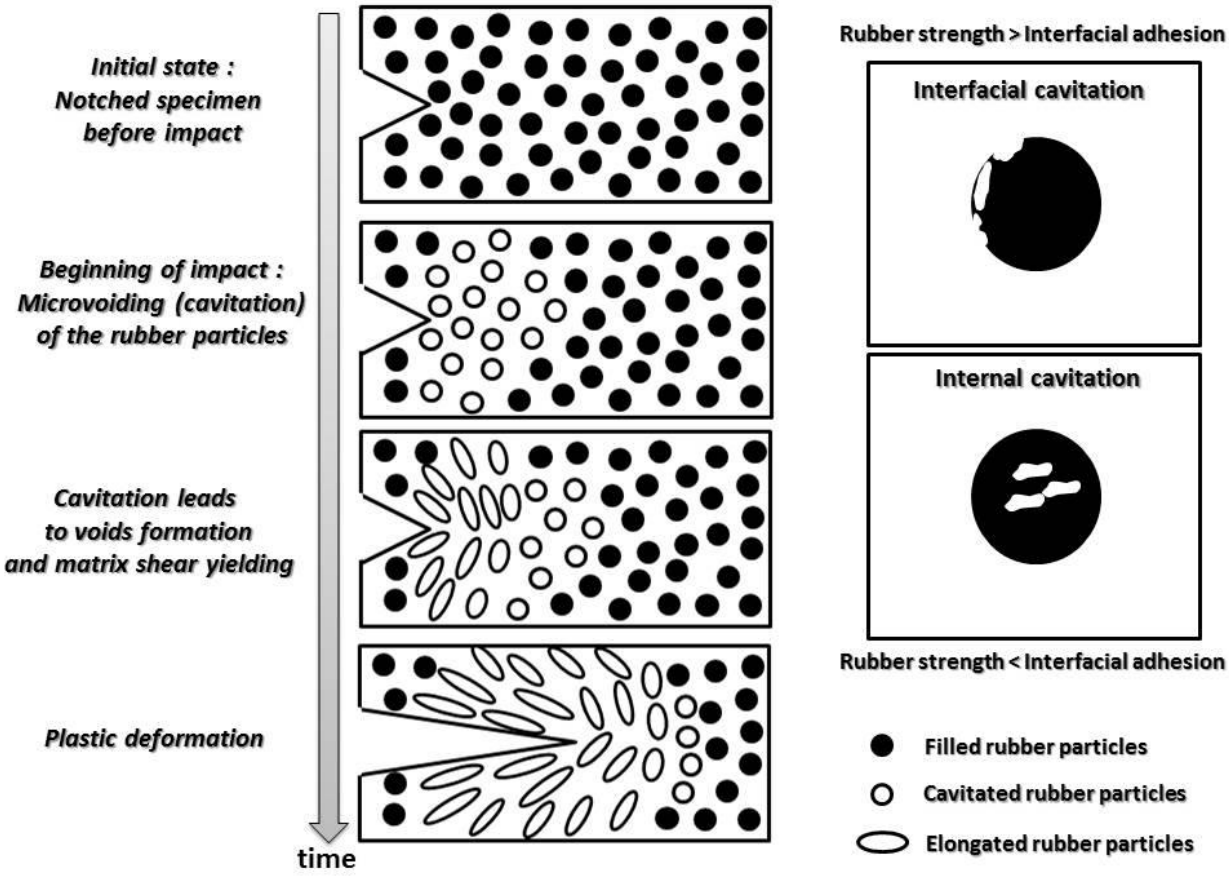

Figure 32.2.Schematic representation of toughening mechanism during impact.

In a first case, when a strong interfacial adhesion is observed between the two phases and when a weak strength of rubber phase is noticed, cavitation occurs through holes formation within the cores of rubber particles. In a second case, when the interfacial adhesion is not sufficient, interfacial debonding takes place (Figure 32.2). SEM microgaphs of the blends showed different fracture morphologies depending on the amount of dispersed phase in the material.[36] For the blend comprising 5wt% of PEA, a relatively smooth surface is observed with a little amount of fibrils and matrix deformation. The formation of fibrils was more important when higher content of PEA was dispersed in the matrix. For an amount of 15wt% of PEA, the morphology of the fractured surface was characteristic of a toughened system with plastic deformation in the stress direction. Indeed it is noteworthy that the matrix is highly elongated close to the notch with the presence of voids and fibrils.

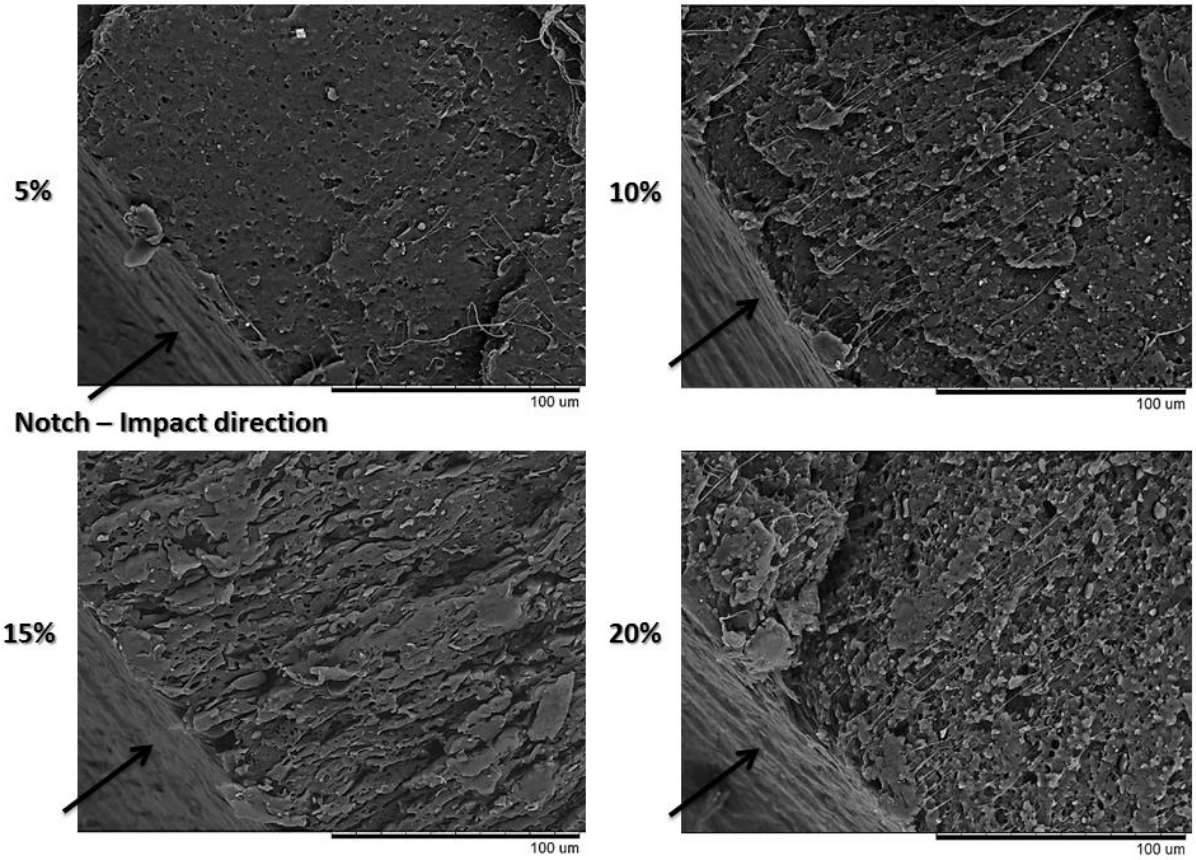

Figure 33.2. SEM images of the impact fractured surfaces of the blends. Images were taken close to the notch.

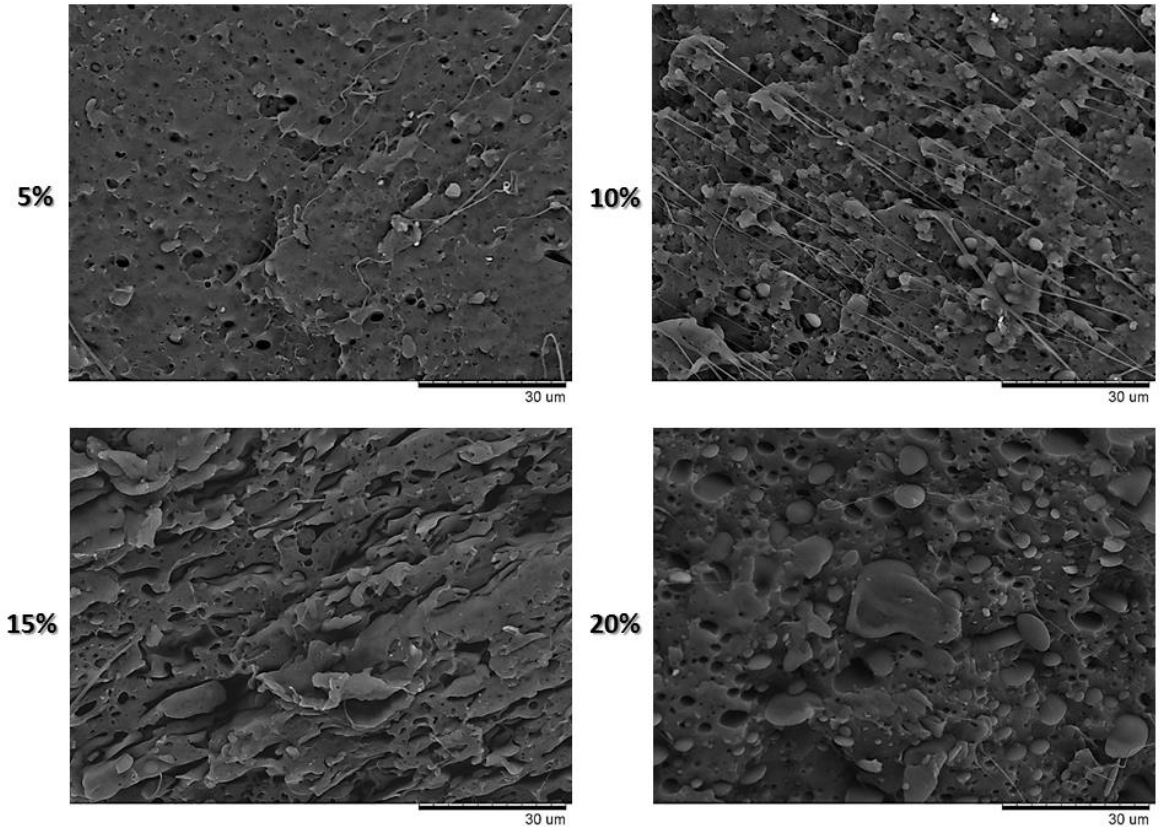

Figure 34.2. zoomed-up SEM images of Figure 34.2.

The large voids might be formed by the coalescence of neighboring small cavities. The deformation of the matrix was less important when higher amount of PEA was used, in accordance with the impact testing results (Table 11.2).

To further investigate the toughening mechanism of such a system, SEM images were taken at various positions on the fractured surface. Two images are displayed in Figure 35.2. The first image corresponds to the morphology of the blend close to the notch and thus at the part of the material that received the maximum impact energy. The other SEM picture was taken at a higher distance from the notch. We can distinguish a more pronounced plastic deformation of the matrix when close to the notch. Far from the notch, the sample is also highly deformed however the voids are smaller. An important observation that needs to be taken into account is the important deformation of the PEA particles along the stress direction. This suggests that cavitation is occurring by the formation of holes into the core of the particles. Indeed cavitation by debonding at the interface generally leads to discrete deformation of the rubber particles. To summarize, the rubber particles, when subjected to triaxial stress, cavitate to produce voids which grow along the crack propagation and release the stress permitting shear yielding.

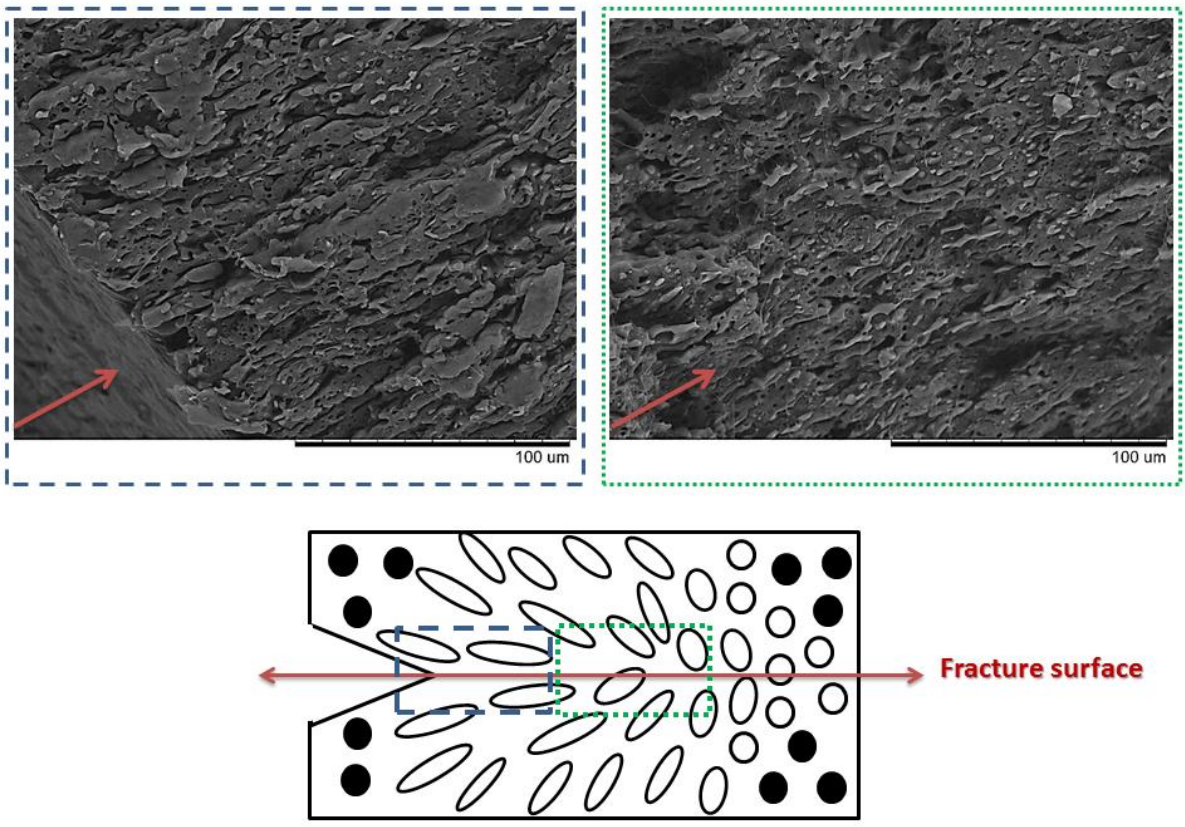

Figure 35.2. SEM images of the PLLA/PEA (85/15: w/w) blend taken at different positions on the fractured surface.

VI. CONCLUSION

A novel poly(ester-amide) (PEA) rubber derived from renewable resources (mainly fatty acids feedstock) was synthesized and subsequently used as impact modifier of PLLA. The PEA fulfilled all the requirements for effective toughening of PLLA as seen from its low Tg (-28°C), its low elastic modulus (191 MPa), its thermal stability at the processing temperature of PLLA as well as its theoretical immiscibility with PLLA. PEA was then melt-blended with PLLA by twin-screw extrusion resulting in typical two-phase polymer alloys. The processability of the blends was evaluated by thermal stability investigations that revealed no significant thermal degradation in the PLLA processing temperature window as well as by rheological measurements that showed improved melt elasticity of the blends in comparison to neat PLLA. The immiscible morphology of the blends predicted by the solubility parameters of the two components was confirmed by SEM images, rheological investigations as well as DMA measurements. Very interestingly, the crystallization behavior of the blends was also improved by the addition of PEA as seen from the higher crystallization rates observed both during non-isothermal and isothermal crystallization studies. Indeed, during isothermal crystallization at 110°C, the half-time of crystallization dropped from 6.12 min for neat PLLA to 1.72 min for the blend with a PEA content of 20wt%. Finally the toughening efficiency of this system was verified by tensile experiments as well as notched IZOD impact testing. A transition from brittle fracture to ductile fracture was observed during tensile tests with PEA contents as low as 5wt%. Maximum elongation at break was observed for 10wt% of PEA (155%) without severe loss in tensile strength and modulus. Notched IZOD impact strength also increased with the incorporation of PEA rubber particles. The toughening mechanism, evaluated by SEM imaging of the fractured surfaces, was relevant to a combination of cavitation of the cores of the rubber particles, voids formation and release of the stress by plastic deformation. Clearly, this study opens new pathways for the rubber-toughening of PLLA by fatty-acid based elastomers.

In this work, only a limited improvement in the impact strength was noticed by the dispersion of the PEA into the PLLA matrix. However, the obtained values (up to 3.7 $kJ.m^{-2}$) are quite similar to those generally obtained for the binary blends realized with some second generation impact modifiers such as PCL, PBS, PBAT, PHAs that rarely showed notched impact strengths higher than 4-5 $kJ.m^{-2}$ for additive contents in the range 5-20wt%.[37-42] For this reason, a third component is generally added such as a reactive molecule (or polymer) or block copolymers which enhance the interfacial adhesion thus resulting in improved toughness. The addition of such third components should definitely improve the mechanical

properties of the PLLA/PEA blends. However, in this thesis project, we were more interested in tuning the properties of fatty acid-based additives in order to select the best candidates for the toughening of PLLA. When regarding the similitudes between the developed PEA thermoplastic elastomer and the mainstream second generation impact modifiers, we can cite their semi-crystalline behaviour. Indeed, both PEA and mainstream impact modifiers such as PCL, PBS, PBAT, PHAs are semi-crystalline with quite high melting points and melting enthalpies. Recently, NatureWorks has defined the key-parameters of impact modifiers useful for toughening PLLA in which low (or absence) of crystallinity was cited.[43] Thus it is thought that limited enhancement of the impact strength of PLLA for the previously mentioned rubbers as well as for the PEA we developed, could come from their too high crystallinity. Consequently, we were interested in investigating the correlation between the crystallinity of the additive and the properties of the resulting PLA materials.

VII. EXPERIMENTAL AND SUPPORTING INFORMATION

1.Poly(ester-amide) (PEA) synthesis

Both UndBdA-diol and the Dimerized fatty acid (DFA-Pripol 1009) were dried at 70°C under vacuum overnight prior to use. A mixture of UndBdA-diol (6.750 g), DFA (7.047 g) and titanium tetra-n-butoxide (84 mg) was stirred at 160°C under dynamic vaccum. After 1h, the temperature was raised to 180°C for 5 hours and then to 200°C for 2 hours. After completion of the reaction, the polymer was dissolved in dichloromethane, precipitated into methanol, filtered and dried under reduced pressure.

Figure S1.2.Picture of a PEA film prepared by compression.

Figure S2.2.Picture of the same PEA film than in Figure S1.2.

2.Blend preparation

Prior to extrusion, PLLA pellets and PEA were dried at least 12h at 80°C in an oven under reduced pressure. Melt-blending of PEA with PLLA was realized using a DSM twin-screw micro-compounder (5cc) at 190°C and 50 rpm for 5 minutes. Impact test bars (dimensions 12.7 × 50 × 3.2 mm) were prepared by injection molding at 200°C.

Figure S3.2. From left to right, picture of injection molded specimen of neat PLLA, and blends containing 5wt%, 10wt%, 15wt% and 20wt% of PEA.

REFERENCES

1. O. Türünç, L. Montero de Espinosa and M. A. R. Meier, *Macromolecular Rapid Communications*, 2011, **32**, 1357-1361.
2. W. Lu, J. E. Ness, W. Xie, X. Zhang, J. Minshull and R. A. Gross, *Journal of the American Chemical Society*, 2010, **132**, 15451-15455.
3. J. Trzaskowski, D. Quinzler, C. Bährle and S. Mecking, *Macromolecular Rapid Communications*, 2011, **32**, 1352-1356.
4. J. Zuo, S. Li, L. Bouzidi and S. S. Narine, *Polymer*, 2011, **52**, 4503-4516.
5. A. Kozlowska and R. Ukielski, *European Polymer Journal*, 2004, **40**, 2767-2772.
6. H. Mutlu and M. A. R. Meier, *European Journal of Lipid Science and Technology*, 2010, **112**, 10-30.
7. T. M. Lammens, J. Le Nôtre, M. C. R. Franssen, E. L. Scott and J. P. M. Sanders, *ChemSusChem*, 2011, **4**, 785-791.
8. R. K. Saxena, P. Anand, S. Saran and J. Isar, *Biotechnology Advances*, **27**, 895-913.
9. H. Biebl, K. Menzel, A. P. Zeng and W. D. Deckwer, *Applied Microbiology and Biotechnology*, 1999, **52**, 289-297.
10. C. Della Pina, E. Falletta and M. Rossi, *Green Chemistry*, 2011, **13**, 1624-1632.
11. F. Fenouillot, A. Rousseau, G. Colomines, R. Saint-Loup and J. P. Pascault, *Progress in Polymer Science*, 2010, **35**, 578-622.
12. L. Maisonneuve, T. Lebarbe, T. H. N. Nguyen, E. Cloutet, B. Gadenne, C. Alfos and H. Cramail, *Polymer Chemistry*, 2012, **3**, 2583-2595.
13. C. Sabot, K. A. Kumar, S. Meunier and C. Mioskowski, *Tetrahedron Letters*, 2007, **48**, 3863-3866.
14. R. N. Butler, C. B. O'Regan and P. Moynihan, *Journal of the Chemical Society, Perkin Transactions 1*, 1978, 373-377.
15. H. Ngo, K. Jones and T. Foglia, *Journal of the American Oil Chemists' Society*, 2006, **83**, 629-634.
16. F. Jerome, G. Kharchafi, I. Adam and J. Barrault, *Green Chemistry*, 2004, **6**, 72-74.
17. P. A. M. Lips, R. Broos, M. J. M. van Heeringen, P. J. Dijkstra and J. Feijen, *Polymer*, 2005, **46**, 7834-7842.
18. S. Liu, C. Li, J. Zhao, Z. Zhang and W. Yang, *Polymer*, 2011, **52**, 6046-6055.
19. C. Regaño, A. Alla, A. Martínez de Ilarduya and S. Muñoz-Guerra, *Macromolecules*, 2004, **37**, 2067-2075.
20. Z. Qian, S. Li, Y. He, C. Li and X. Liu, *Polymer Degradation and Stability*, 2003, **81**, 279-286.
21. H. Ebata, K. Toshima and S. Matsumura, *Macromolecular Bioscience*, 2007, **7**, 798-803.
22. Z. Gan, H. Abe and Y. Doi, *Biomacromolecules*, 2001, **2**, 313-321.
23. J. P. Parker and P. H. Lindenmeyer, *Journal of Applied Polymer Science*, 1977, **21**, 821-837.
24. C. Ramesh and E. B. Gowd, *Macromolecules*, 2001, **34**, 3308-3313.
25. P. A. M. Lips, R. Broos, M. J. M. van Heeringen, P. J. Dijkstra and J. Feijen, *Polymer*, 2005, **46**, 7823-7833.
26. J. Cai, C. Liu, M. Cai, J. Zhu, F. Zuo, B. S. Hsiao and R. A. Gross, *Polymer*, 2010, **51**, 1088-1099.
27. H. Kang, B. Qiao, R. Wang, Z. Wang, L. Zhang, J. Ma and P. Coates, *Polymer*, 2013, **54**, 2450-2458.
28. H.-K. Chuang and C. D. Han, *Journal of Applied Polymer Science*, 1984, **29**, 2205-2229.
29. C. D. Han, *Journal of Applied Polymer Science*, 1988, **35**, 167-213.
30. K. Lamnawar, F. Vion-Loisel and A. Maazouz, *Journal of Applied Polymer Science*, 2010, **116**, 2015-2022.
31. U. Sundararaj and C. W. Macosko, *Macromolecules*, 1995, **28**, 2647-2657.
32. H. Tsuji, M. Sawada and L. Bouapao, *ACS Applied Materials & Interfaces*, 2009, **1**, 1719-1730.
33. A. T. Lorenzo, M. L. Arnal, J. Albuerne and A. J. Müller, *Polymer Testing*, 2007, **26**, 222-231.
34. M. Shibata, Y. Inoue and M. Miyoshi, *Polymer*, 2006, **47**, 3557-3564.

35. W. G. Perkins, *Polymer Engineering & Science*, 1999, **39**, 2445-2460.
36. S. Wu, *Polymer*, 1985, **26**, 1855-1863.
37. T. Semba, K. Kitagawa, U. S. Ishiaku and H. Hamada, *Journal of Applied Polymer Science*, 2006, **101**, 1816-1825.
38. J. Odent, J.-M. Raquez, E. Duquesne and P. Dubois, *European Polymer Journal*, 2012, **48**, 331-340.
39. R. Wang, S. Wang, Y. Zhang, C. Wan and P. Ma, *Polymer Engineering & Science*, 2009, **49**, 26-33.
40. M. Harada, T. Ohya, K. Iida, H. Hayashi, K. Hirano and H. Fukuda, *Journal of Applied Polymer Science*, 2007, **106**, 1813-1820.
41. K. M. Schreck and M. A. Hillmyer, *Journal of Biotechnology*, 2007, **132**, 287-295.
42. L. Jiang, M. P. Wolcott and J. Zhang, *Biomacromolecules*, 2005, **7**, 199-207.
43. *NatureWorks. Technology Focus Report: Toughened PLA, http://www.natureworksllc.com/*

CHAPTER 3:

Tailoring impact toughness of poly(L-lactide)/biopolyester blends by controlling the structure-properties of the impact modifier.

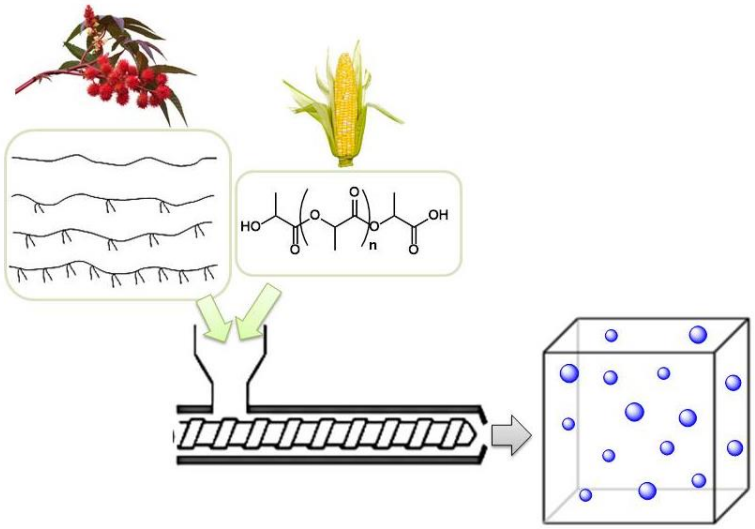

Keywords: fatty acids, castor oil, sebacic acid, dimerized fatty acids, polycondensation, impact modifier, crystallinity, rubber-toughening, melt-blending, PLLA, polyester.

Mots clés: acides gras, huile de ricin, acide sébacique, dimère d'acides gras, polycondensation, modificateur d'impact, cristallinité, renfort au choc, mélange de polymères, PLLA, polyester.

I. INTRODUCTION

In the previous chapter, we have seen that a novel poly(ester-amide) thermoplastic elastomer was used as an additive for the rubber-toughening of PLLA. However, similarly to most of the semi-crystalline second generation impact modifiers (PCL, PBS, PHAs…) for PLLA, the improvement in impact toughness of the final material was limited, even for additive content as high as 20 wt%.

The limited number of examples describing the correlation between the impact strength of PLLA based materials and the structure-properties (e.g. crystallinity) of the impact modifier prompted us to investigate the toughening of PLLA by a series of aliphatic polyesters rubbers having various thermal and mechanical properties. The monomers used for the synthesis of the rubbers need to be cheap, commercially available and preferentially biobased in order to propose an economically viable and environmentally friendly solution to the toughness of PLLA.

Examples of commercially available fatty acid derivatives include azelaic acid, sebacic acid, 10-undecenoic acid, brassylic acid, dimerized fatty acid… For the development of new biobased rubbers, we selected sebacic acid and hydrogenated dimer fatty acid as precursors. Indeed both monomers present a low cost, are commercially available, and present carboxylic acid functions that enable the synthesis of polyesters by polycondensation. Sebacic acid (SA), which is obtained industrially by alkali fusion of ricinoleic acid at 250°C,[1] was used as hard segment in the polyester, while dimerized fatty acid (DFA), which is obtained by dimerizing unsaturated fatty acids on clay catalysts and subsequent hydrogenation, was used as soft segment in the polyester structure.[2-4] These diacid monomers (used in various amounts) were copolymerized with 1,10-decanediol (obtained by reduction of SA) resulting in a series of aliphatic polyesters (Figure 1.3).

In this work, we propose to evaluate the influence of the polyester structure on the properties of the materials obtained by compounding these additives with PLLA. In particular, the morphology, thermal behavior, rheological properties and mechanical properties of the blends will be extensively investigated.

II. SYNTHESIS AND CHARACTERIZATION OF THE RUBBERS

II.1. Synthesis and macromolecular characteristics

In most of the studies dealing with the rubber-toughening of PLLA, the glass transition is taken as the main criterion for effective impact modification of the matrix. In this work a special emphasis was made on the influence of the crystallinity of the impact modifier on the toughness of the final material. To that aim, a set of polyesters was synthesized by varying the amount of dangling alkyl chains in order to tune the crystallinity of the polyester (similarly to the variation of the crystallinity in olefin elastomers by incorporation of octane or hexane dangling chains).The rubbers were synthesized by polycondensation using titanium isopropoxide as a catalyst with various feed ratios between the linear SA and the branched DFA diacids (Figure 1.3).

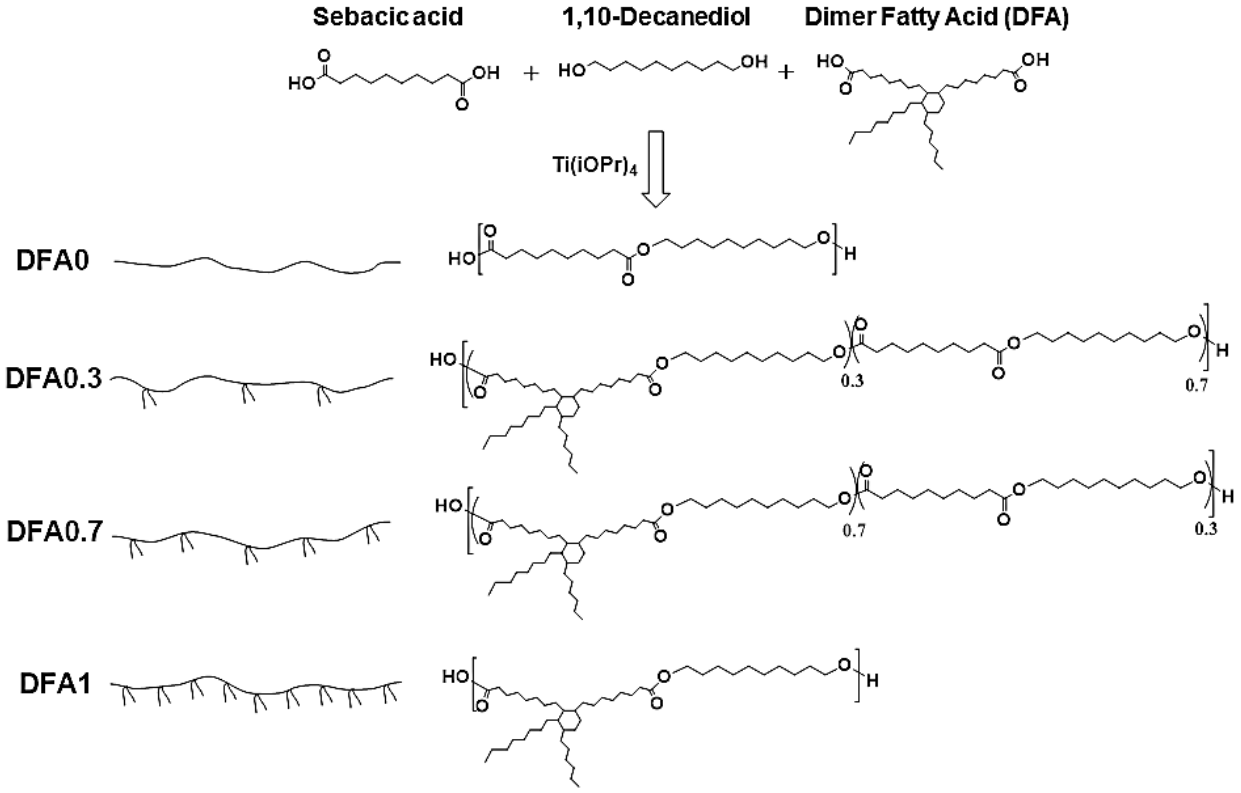

Figure 1.3. Synthetic strategy to polyester rubbers

Bulk polymerization was adapted as a chosen process. This was allowed by the relatively high molar masses of all the monomers which prevent their volatility under reduced pressure at high temperature during the early stages of the polymerization. After completion of the polymerization, the polymers were cooled down to room temperature and characterized. First, the polyesters were analyzed by ^{1}H-NMR in order to confirm their chemical structure. In

Figure 2.3 is displayed the ^{1}H-NMR spectrum of the synthesized rubbers. Formation of ester functions can be underlined by the characteristic peaks at 4.04 and 2.28 ppm attributed to the protons of the methylene group adjacent to the oxygen atom of the ester function and the protons of the methylene group adjacent to the carbonyl linkage of the ester function respectively.

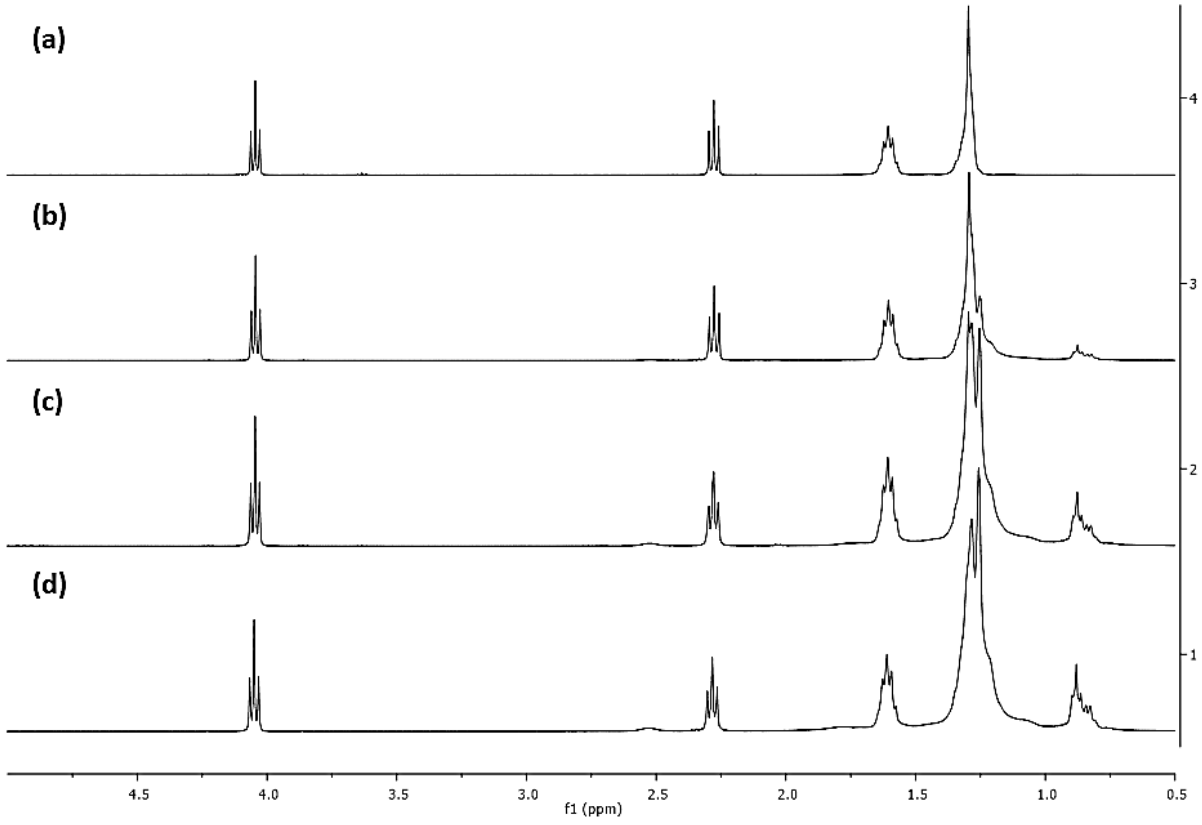

Figure 2.3. ^{1}H-NMR stacked spectra of (a) DFA0 (b) DFA0.3 (c) DFA0.7 (d) DFA1 in $CDCl_3$.

The absence of characteristic peaks of hydroxyl and carboxylic acid functions demonstrates the high conversion of the monomers and the formation of high molecular weight polymers. The multiplet figuring at 0.88 pm is assigned to the methyl group of the dangling alkyl chains thus confirming the incorporation of DFA units in the polyester structure. The ratio between sebacic acid and DFA units in the structure of the polyesters was calculated from the ratio of the 0.88 ppm to 2.28 ppm peak normalized integrals. The chemical composition of the polyesters was slightly different from the feed ratio of the monomers (Table 1.3). Indeed, for DFA0.3, the calculated composition in DFA units was 0.4 of the total diacid composition while the feed composition was 0.3 (0.78 in comparison to 0.7 for the feed composition in the case of DFA0.7). The slight difference between the feed and the calculated composition can be explained by a few distillation of SA. Table 1.3 displays the molecular weights as well as

the dispersities of the polyesters measured by SEC in THF. The molecular weights were found in the range 36-64 kg.mol^{-1} with dispersities in the range 1.8-2.1, which should attest of the sufficient structural integrity and sufficient incompatibility of the rubbers with PLLA.

II.2. Thermal stability

TGA experiments were carried out to evaluate the degradation temperature of the polyesters. It is noteworthy from Figure 3.3 and Table 1.3, that the synthesized polyester rubbers present higher thermal stabilities than neat PLLA thus allowing their use as impact modifier.

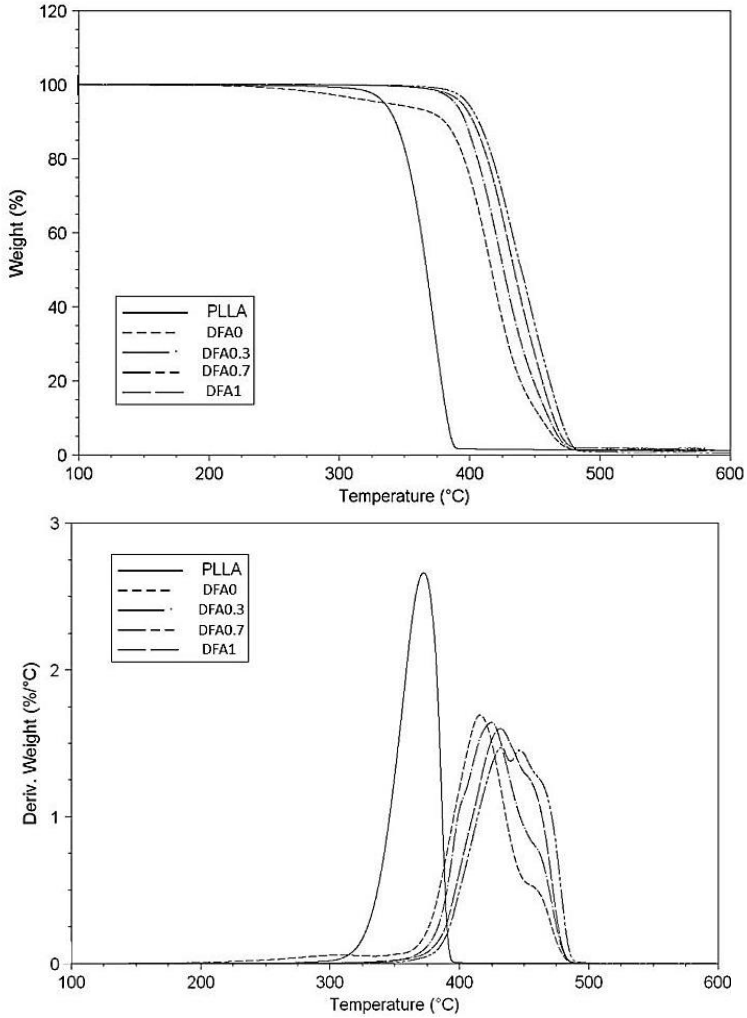

Figure 3.3. TGA curves (up) and TGA derivative curves (bottom) of neat PLLA and the polyesters (DFA0-DFA1) recorded from 20°C to 700°C at 10°C.min^{-1} under a nitrogen atmosphere.

Indeed the first weight loss (temperature corresponding to 5% weight loss) is observed near 390°C and 335°C for polyester rubbers and PLLA respectively. Only DFA0 showed a lower degradation temperature than the other polyesters (338°C for 5% weight loss); DFA inducing a better thermal stability in comparison to the purely linear polyester (DFA0).

II.3. Correlation between structure and crystallinity of the rubbers

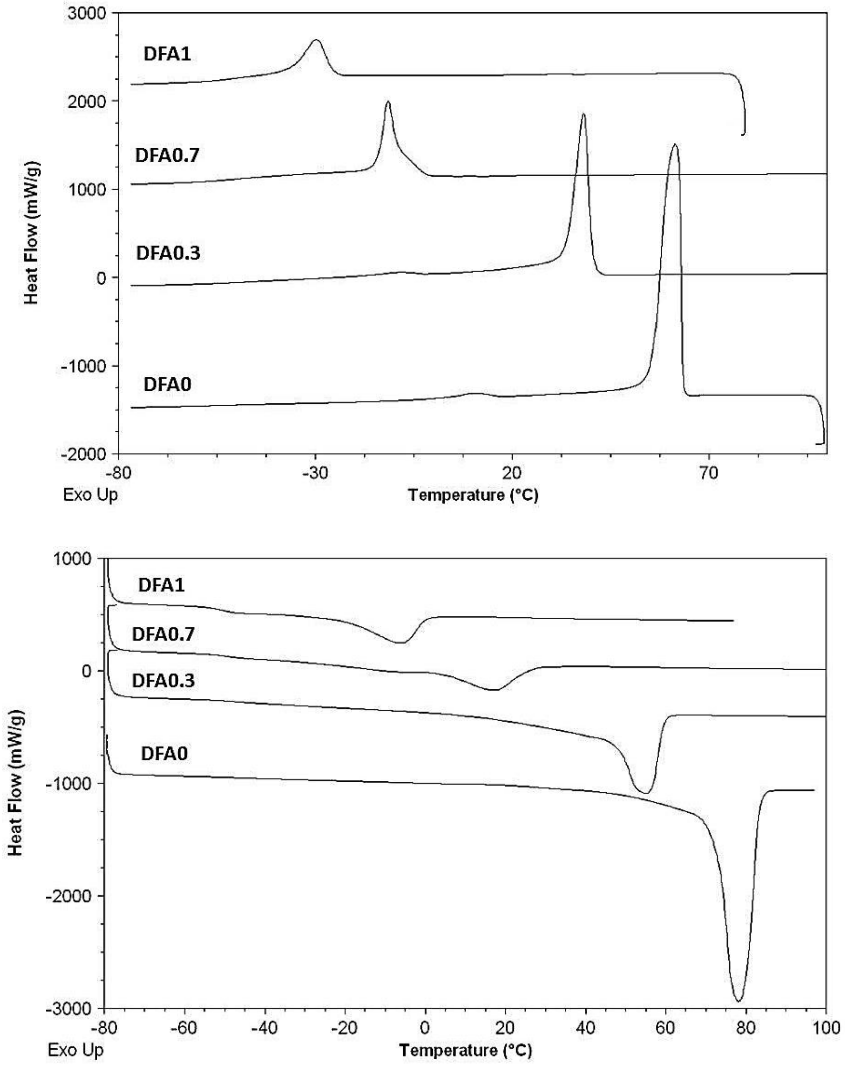

Figure 4.3. Cooling (up) and heating (bottom) curves of neat PLLA and the blends – 10°C.min^{-1} from -80°C to 120°C.

Thermo-mechanical analysis of the polyesters was then carried out by DSC to better evaluate the influence of the dangling alkyl chains density on the melting temperature and enthalpy of the polymers. The glass transition (Tg) of the polyesters was first measured to ensure that these polyesters can be used as toughening agents of PLLA. Tg values well below room temperature were measured (between -50°C and -46°C) suggesting potential application for rubber toughening of PLA. Interestingly, the Tg value was only slightly impacted by the DFA amount showing that the dangling chains have limited influence on the macromolecular mobility of the polyesters. However significant influence of the DFA amount on the crystalline behavior of the polyesters was observed. As expected, an obvious decrease in melting points was noticed with an increase in DFA amount (Figure 4.3, Figure 5.3 and Table

1.3). Indeed, while the purely linear polyester (DFA0) showed a melting point at 78°C, DFA1 presented a melting point at -6°C. Similar trend was observed for the melting enthalpies which varied from 101 $J.g^{-1}$ for DFA0 to 16 $J.g^{-1}$ for DFA1. It can be logically attributed to the internal plasticization by the alkyl dangling chains that resulted in a lack of chain packing for high contents of DFA units.

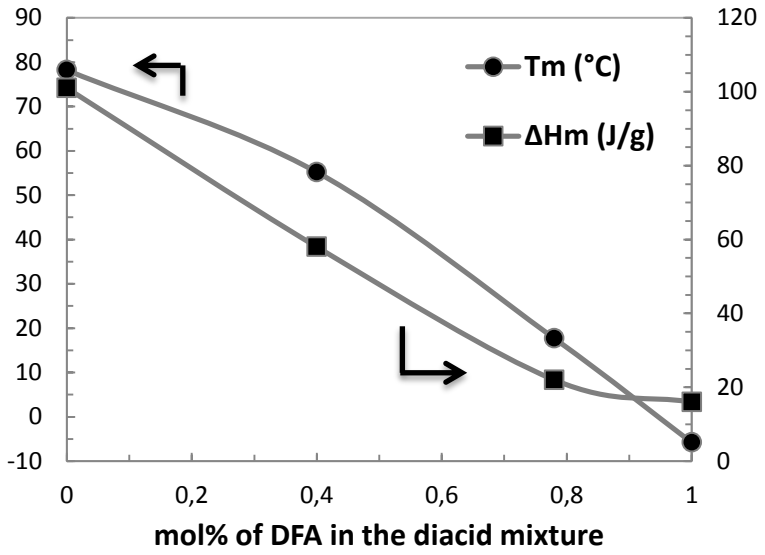

Figure 5.3. Melting parameters as a function of the amount of DFA units in the polyester structure.

Table 1.3. General parameters of the polyester rubbers and neat PLLA.

	mol% DFA/total diacid[a] (feed)	$\bar{M}_n$ (kg.mol^{-1})[b]	$Đ$ [b]	Tg (°C)[c]	Tc (°C)[c]	ΔHc (J.g^{-1})[c]	Tm (°C)[c]	ΔHm (J.g^{-1})[c]	δ (cal.cm^{-3})$^{1/2}$	$T_{5\%}$(°C)[d]
DFA0	0 (0)	59	2.1	- 48.6	61.4	96.9	78.2	100.9	9.11	338
DFA0.3	0.40 (0.3)	44	1.8	- 45.9	38.1	55.1	55.2	57.7	9.24	389
DFA0.7	0.78 (0.7)	64	2.0	- 49.0	- 11.5	25.9	17.7	22.4	9.31	399
DFA1	1 (1)	36	2.0	- 50.0	- 29.8	16.5	- 5.8	16.2	9.34	394
PLLA	-	121	1.5	61	104.2	1.4	176.3	32.9	11.40	335

(a) ^{1}H-NMR (b) SEC in THF, PS calibration (c) DSC – 10°C.min^{-1}(d) TGA – 10°C.min^{-1}/ δ was calculated using Hoftyzer-Van Krevelen method

II.4. Calculation of the solubility parameters

As mentioned above, to consider efficient energy release during impact, the additive compounded with PLLA has to be immiscible with the matrix and dispersed as fine particles (typically 0.1-1.0µm). The Hoftyzer-Van Krevelen method was used in this study to calculate the solubility parameter of the polyesters.[5] In this method, the cohesive energy is separated into three contributions which are the non-polar (dispersion) (d), the polar (permanent) (p)

and the hydrogen bonding forces (h) contributions. Therefore, the total solubility parameter is estimated from the equation 1.3:

$$\delta = \sqrt{\delta_d^2 + \delta_p^2 + \delta_h^2} \qquad (eq\ 1.3)$$

The three increments may be predicted from group contributions using the following equations:

$$\delta_d = \frac{\sum_i F_{di}}{V} \quad (eq\ 2.3)$$

$$\delta_p = \frac{\sqrt{\sum_i F^2_{pi}}}{V} \quad (eq\ 3.3)$$

$$\delta_h = \sqrt{\frac{\sum_i E_{hi}}{V}} \quad (eq\ 4.3)$$

where F_{di}, F_{pi} and E_{hi} are given molar attraction constants of the repeating unit and V the molar volume. The calculated solubility parameters are displayed in Table 1.3 and suggest immiscibility of PLLA with all the polyesters as seen from the difference in the values of the solubility parameter of PLLA (11.40 $(cal.cm^{-3})^{1/2}$) and the one of each polyesters which is higher than 0.5 $(cal.cm^{-3})^{1/2}$.[6] It is noteworthy that the solubility parameter is increasing with an increase in DFA unit amount indicating enhanced interactions between the two phases when higher amounts of DFA were used.

To summarize, a set of aliphatic polyesters were synthesized by polycondensation. These polyesters showed very low Tg values (around -50°C) and a semi-crystalline behavior which was varying with the dangling alkyl chains density in the polymer structure. The thermal stability of these polyesters was high enough to consider their use as additives in blends with PLLA. Finally, their potential immiscibility with PLLA should lead to typical two phase systems while in blends with PLLA, morphology which is mandatory for the efficient toughening of PLLA. All these preliminary characterizations on the polyesters prompted us to investigate their melt-blending with PLLA.

III. INFLUENCE OF THE RUBBER TYPE ON THE PROPERTIES OF THE BLENDS

Similar processing conditions (temperature, time, shear rate) than in chapter 2 were retained for the compounding of the PLLA/polyester blends. For each polyester, an amount of 10 and 20wt% was added into PLLA using a twin-screw micro-compounder.

III.1. Processability and Morphology

III.1.1. Thermal stability of the blends

The thermal stability of the PLLA/Polyesters blends under non-oxidative conditions was first investigated by thermal gravimetric analysis in order to evaluate their processability.

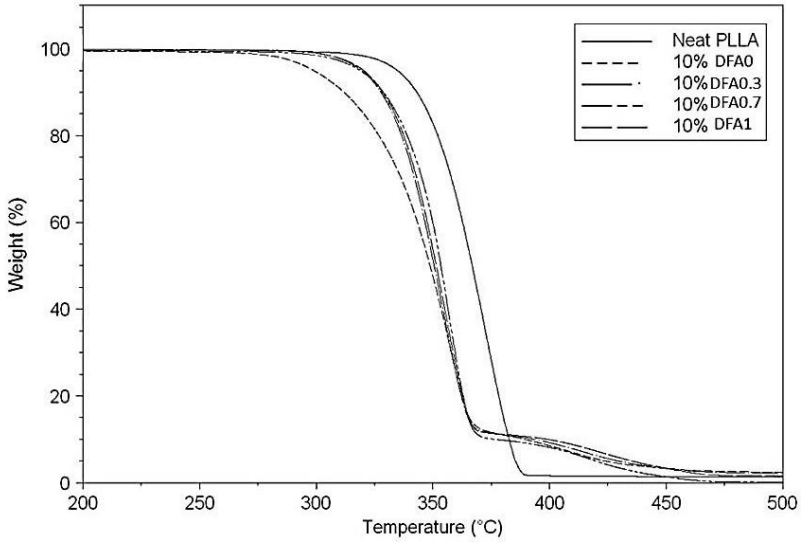

Figure 6.3. TGA curves of neat PLLA and the blends comprising 10wt% of additive recorded from 20°C to 700°C at 10°C.min^{-1} under a nitrogen atmosphere.

Figure 6.3 shows the TGA curves of neat PLLA and the blends comprising 10wt% of additive. The decomposition parameters are given in Table 2.3. As observed in Figure 6.3, the thermal decomposition of the blends is occurring in two steps. A first weight loss is happening near 320°C and can be assigned to the degradation of the PLLA phase. A second weight loss occurring at higher temperatures (around 370°C) is assigned to the degradation of the dispersed polyester phase. Interestingly, a slight decrease in initial degradation temperature was noticed when the polyester impact modifier was added into the PLLA matrix. Indeed, the temperature corresponding to 5wt% loss shifted from 335°C for neat PLLA to around 320°C when 10wt% of polyester was added. This decrease was more pronounced in the case of DFA0 in accordance with the lower thermal stability of the purely linear polyester in comparison to the other polyesters (Figure 3.3). Increasing amount of polyester in the blends (20 wt%) did not resulted in further decrease in initial degradation temperature (Figure 7.3). The two-step thermal decomposition allowed the measurement of the weight composition of the blends (Table 2.3). Good agreement with the feed ratio was observed.

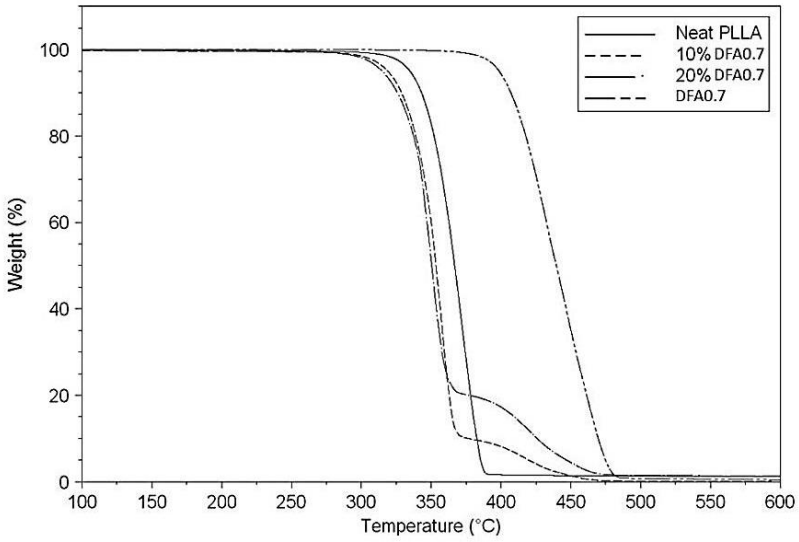

Figure 7.3. TGA curves of the neat PLLA, DFA0.7 and PLLA/DFA0.7 blends– 10°C.min^{-1}.

Table 2.3. Thermal properties, weight compositions of the blends and mean diameter size of the rubber particles.

		wt% Rubber[a]	$T_{5\%}$(°C)[a]	$\bar{d}$ (µm)[b]
	PLLA	-	334.9	-
10wt%	**DFA0**	12.0	298.9	0.34 ± 0.13
	DFA0.3	11.9	319.6	0.54 ± 0.27
	DFA0.7	10.8	319.1	0.48 ± 0.16
	DFA1	11.7	320.3	0.69 ± 0.32
20wt%	**DFA0**	22.7	292.2	0.92 ± 0.46
	DFA0.3	21.8	319.7	0.99 ± 0.61
	DFA0.7	20.7	315.0	0.64 ± 0.36
	DFA1	22.0	314.2	1.35 ± 0.63

(a) TGA, 20 to 700°C, 10°C/min (b) calculated from SEM images using Image J

III.1.2. Melt processability

The melt processability was also evaluated by dynamic melt rheological analysis of neat PLLA and the blends at 190°C. In Figure 8.3.a is displayed the storage modulus of neat PLLA and of the blends containing 10wt% of rubber versus the angular frequency. From these curves, an increase in the G' of the blends at low frequencies is observed in comparison to neat PLLA. It is ascribed to an enhancement in blend elasticity with the addition of the rubber additives due to the relaxation of the dispersed phase under slight shear deformation. At higher frequencies, only a slight decrease in the G' was noticed which means that no or little plasticization of the dispersed particles occurred for a rubber amount of 10wt%. Contrary to G', the loss modulus (G") remains mostly unaffected by the type of rubber (Figure 8.3.b).

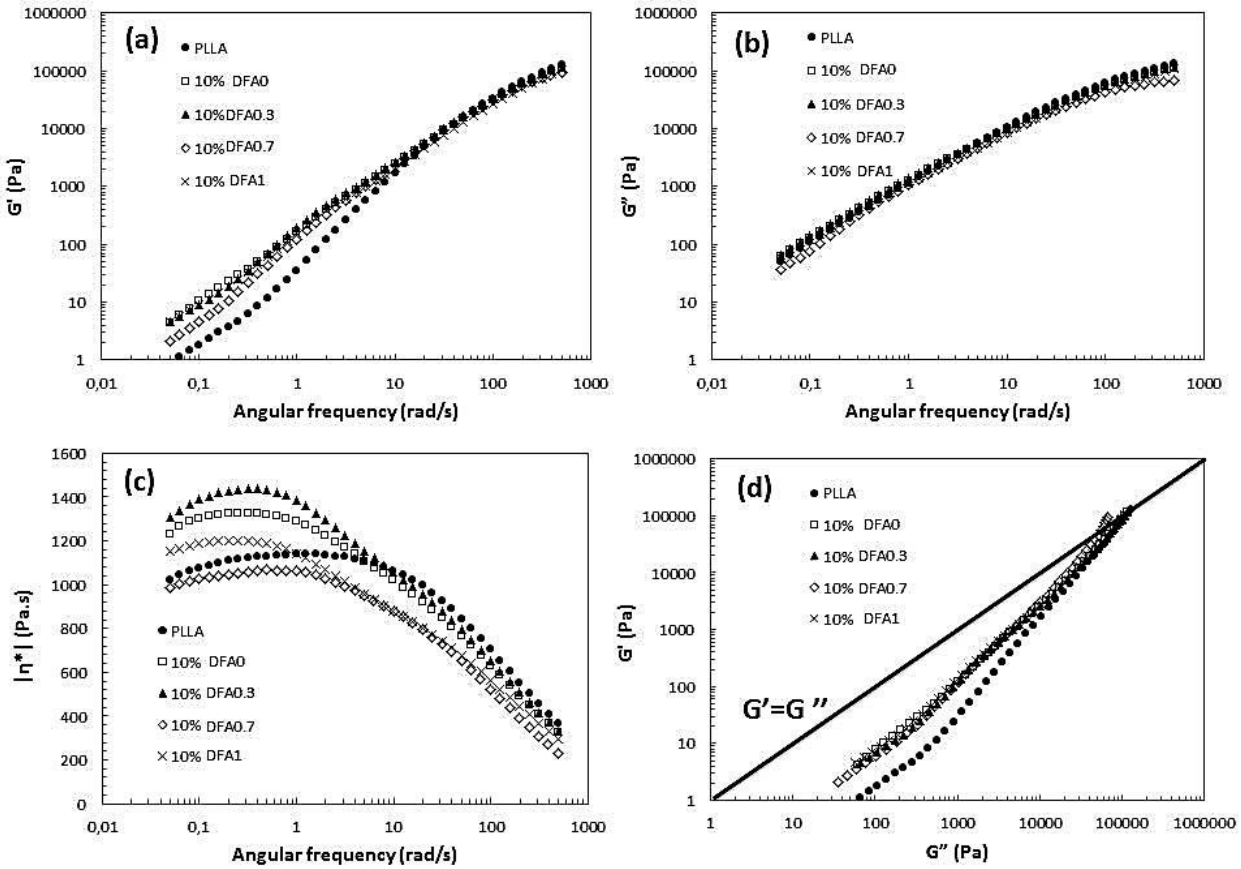

Figure 8.3. (a) Storage modulus, (b) loss modulus, (c) complex viscosity of neat PLLA and the PLLA/Rubber (90/10: w/w) blends as a function of angular frequency. (d) Han plot showing the storage modulus versus the loss modulus. All measurements were performed at 190°C using a strain deformation of 5%.

The complex viscosities, η*, of neat PLLA and PLLA/Rubber (90/10: w/w) blends as a function of the angular frequency, ω, are shown in Figure 8.3.c. For all the blends, a typical Newtonian behavior can be observed in the low-frequency region while shear thinning occurs at higher frequencies. It is noteworthy that the Newtonian region for the blends is narrower than for neat PLLA. Also, all the blends (except the blend with DFA0.7 as a rubber) showed a higher viscosity at low frequencies in comparison to neat PLLA while this behavior reversed at higher frequencies. It can be ascribed to the higher elasticity of the blends at low frequencies, probably due to chemical interactions between the dispersed phase and the matrix which are lowered with an increase in frequency. Enhancement of the elasticity at low frequencies by incorporation of 10wt% rubber was also confirmed by the Han plot (Figure 8.3.d) as evidenced by the shift to the straight line for all the curves corresponding to the blends.

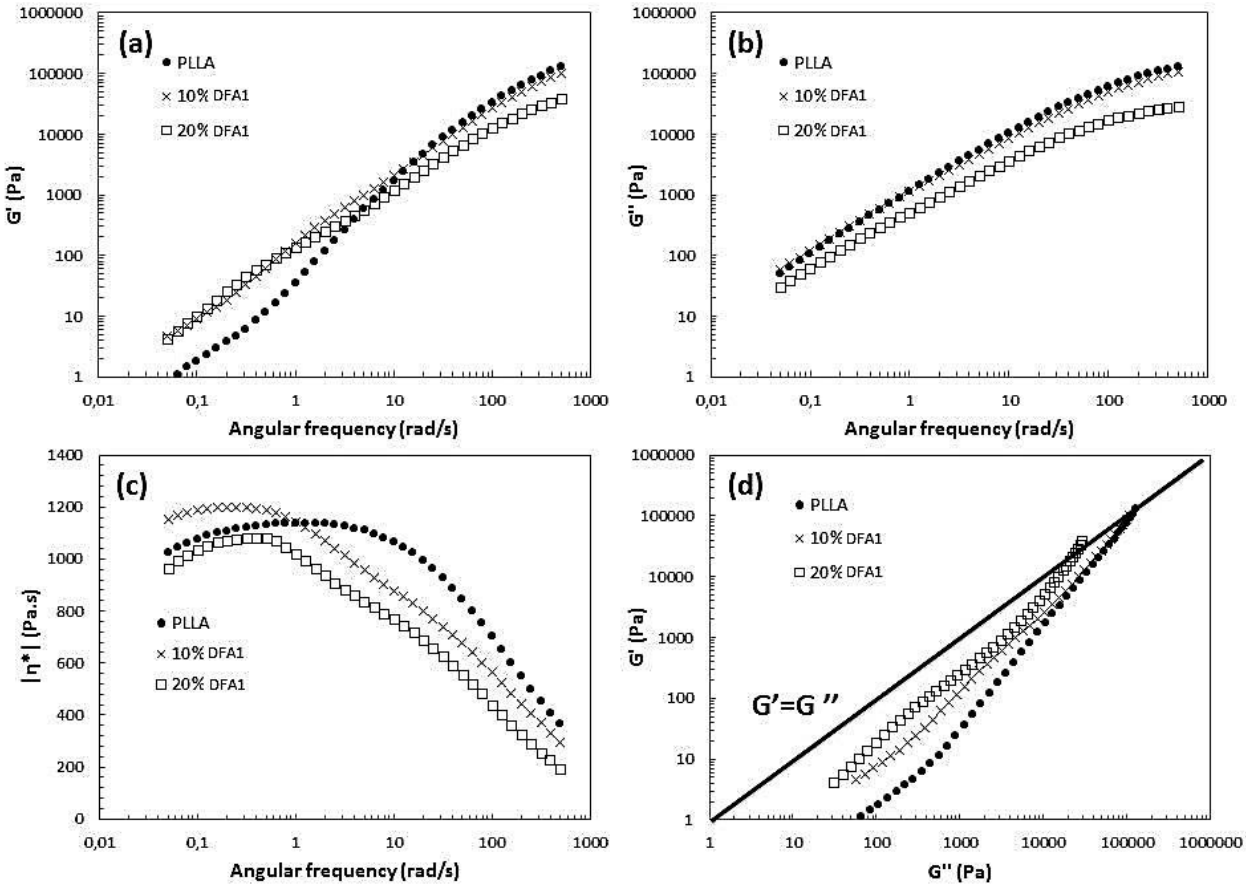

Figure 9.3. (a) Storage modulus, (b) loss modulus, (c) complex viscosity of neat PLLA and the PLLA/DFA1 blends as a function of angular frequency. (d) Han plot showing the storage modulus versus the loss modulus. All measurements were performed at 190°C using a strain deformation of 5%.

An increase in the amount of dispersed phase (20wt%) was investigated in the case of DFA1, and resulted in a significant lowering of the G' values at high frequencies (see Figure 9.3.a) while only slight increase (in comparison to the blend with 10wt% of DFA1) was noticed at low frequencies. Thus, when the PLLA/DFA1 (80/20: w/w) was subjected to high frequencies, some plasticization of the dispersed particles occurred due to their highly elongated shape. Interestingly, for the (80/20: w/w) blends, the lowering of the G' at high frequencies was less significant when the dangling chain density of the rubber decreased (Figure 10.3). The lowering of plasticization with a decrease in dangling chain density can be correlated to the higher incompatibility and the higher viscosity at high frequencies of DFA-poor polyesters with the PLLA matrix (in agreement with the solubility parameters). The effect of the rubber amount, investigated in the case of DFA1, also showed a lowering of G" (Figure 9.3.b), a decrease in the complex viscosity as well as a narrowing in the Newtonian region with an increase in rubber content (Figure 9.3.c).

To conclude from this rheological study, all the blends showed good melt processability with some variations of the elasticity and the viscosity of the blend depending on the rubber type as well as on the rubber content.

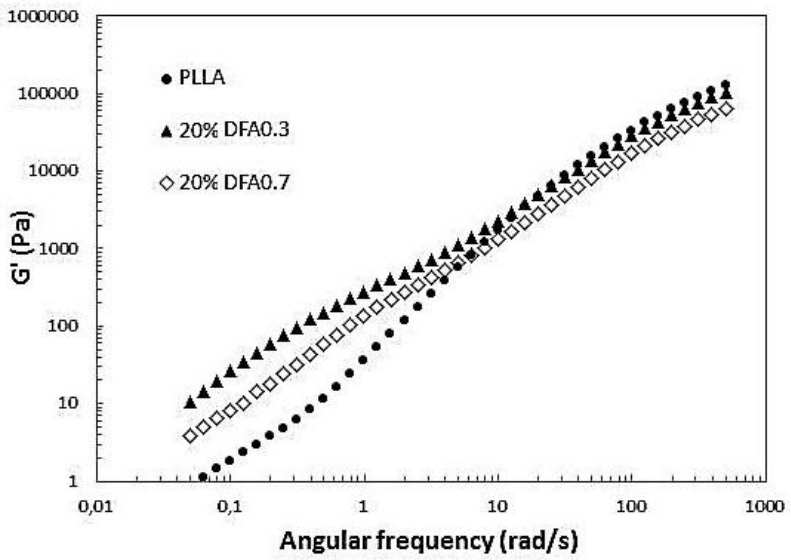

Figure 10.3. Storage modulus of neat PLLA, PLLA/DFA0.3 (80/20: w/w) and the PLLA/DFA0.7 (80/20: w/w) blends as a function of angular frequency.

III.1.3. Morphology of the blends

Calculation of the solubility parameters of PLLA and of the polyesters indicated a theoretical phase segregation of the two phases due to structural incompatibility. To confirm this statement, Han plot was used as an experimental tool. Indeed, on Figure 8.3.d, the upturning of the curves for the blends at low modulus (on the contrary to the curve of neat PLLA) indicates the immiscibility of the matrix and the dispersed phase.[7, 8]

To ensure this, the different samples were cryo-fractured and the surfaces were observed using scanning electron miscroscopy (SEM). For all the samples, the morphologies were characterized by spheres and holes of rubber phase dispersed into the PLLA matrix. Statistics from 200 randomly selected particles at each sample showed that the number-average particle diameter was in the range 0.34-1.35µm (Table 2.3). Thus, the fine dispersion obtained was in accordance with the requirement concerning optimal particles size which was defined in the range 0.1-1.0µm. The small particle size of dispersed phase can be attributed to some interactions occurring at the interphase thus lowering the surface tension. As expected, the mean size diameter of the particles increased with an increase in the rubber amount in the blend. For instance, when DFA1 was used as a rubber, the number-average diameter of the particles increased from 0.69 to 1.35 µm for the blends comprising 10 wt% and 20 wt% of

rubber respectively. However the increase in particles size remains limited due to good interfacial adhesion.

Dynamic mechanical analysis was then performed on each blend to study the interactions between the two phases. The DMA samples were all prepared by compression (using a hot press) without controlling the cooling rate of the samples. Nevertheless, all samples were prepared by the same manner in order to compare their DMA traces. Figure 11.3 displays the tensile storage modulus (E') as well as the tan δ versus the temperature for neat PLLA and the blends containing 10wt% of rubber. DMA data showed three primary relaxations in the temperature range examined. Two were labelled to amorphous α-relaxations of the polyesters and PLLA at around -45°C and 65°C respectively and one was labelled to crystallization relaxation of PLLA at around 170°C. No crystallization relaxation was distinguished for the rubbers due to their low amount in the blends. The distinct glass transitions observed by DMA confirm the immiscibility of the two phases and the establishment of a typical two-phase system in which rubber particles are dispersed into the PLLA matrix. Moreover no significant difference in the values of amorphous α-relaxation temperature was noticed compared to the values of the pristine polymers, suggesting no partial miscibility of the two phases. Thus, partial miscibility of the two polymers at the interface does not seem to be responsible for the good interfacial adhesion between the two phases postulated from the small particles mean diameter measured by SEM. Chemical interactions due to the presence of numerous ester functions both in the PLLA matrix and in the polyester dispersed phase may be the reasons for good interfacial adhesion.

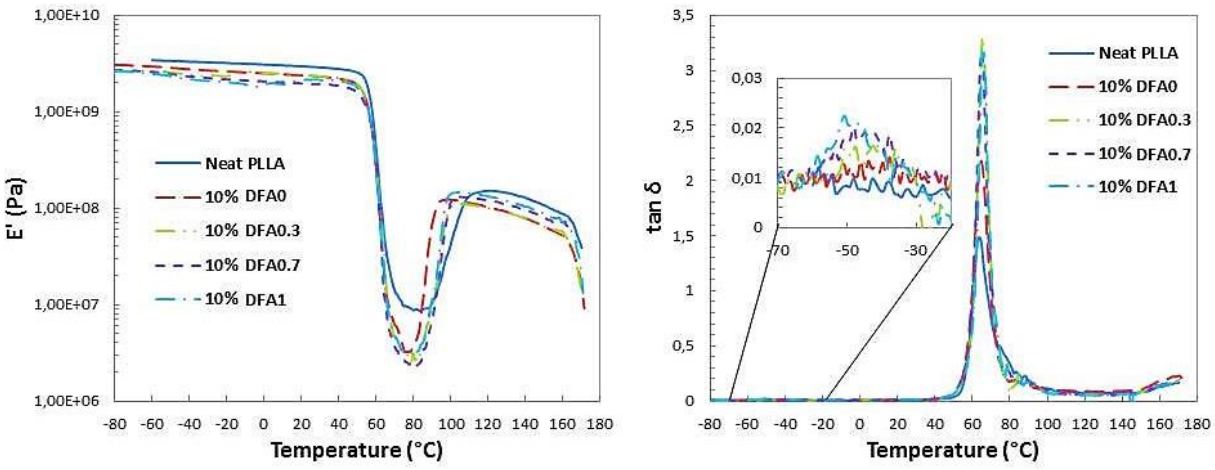

Figure 11.3. Storage modulus and tanδ as a function of temperature for neat PLLA and the PLLA/Rubber (90/10: w/w) blends.

The curves showing the storage modulus (E') versus the temperature can also give some information relative to the mechanical strength and the crystallization of the material. Indeed,

below the Tg, the tensile storage modulus of the blends decreases with the addition of the rubber due to incorporation of a soft phase. The E' then dropped abruptly at 55-70°C due to glass transition and started to increase from 80-90°C. This drastic fall of E' provides evidence of insufficient mechanical strength above the Tg and incomplete crystallization of the material during cooling of the samples from the melt. The increase in E' from 80-90°C is assigned to cold-crystallization enabled by the enhanced mobility of the polymer chains above the Tg. Interestingly, this cold-crystallization transition occurred at lower temperatures for the blends in comparison to neat PLLA. This clearly indicates that rubber polyesters enhance the cold-crystallization ability by lowering the activation energy of crystallization. When cold-crystallization was completed, neat PLLA demonstrated higher modulus than PLLA/rubber blends due to a lower part of amorphous soft phase.

III.2. Crystallization behavior

Further investigations of the crystallization behavior of these blends were realized both during non-isothermal and isothermal crystallization experiments to confirm the enhanced crystallization ability of PLLA when blended with polyester rubbers.

III.2.1. Non -isothermal crystallization

Non-isothermal crystallization was first investigated at a heating rate of 10°C.min^{-1} by cooling the samples from the melt to -80°C and subsequently heating to 200°C. DSC cooling and heating curves are shown in Figure 12.3. The crystallization peak of neat PLLA, when cooled from the melt, was rather small in comparison to the ones of PLLA phase in the blends. However, even in the case of the blends, the peak was not consistent with a fully relative crystallization. This suggests that PLLA phase did not have enough time to crystallize at 10°C.min^{-1}. The glass transition of PLLA phase in the blends was readily identified and was similar to the one of neat PLLA suggesting that the matrix and the rubbers were phase-separated during cooling from the melt. By further cooling, crystallization of the dispersed phase was observed at various temperatures depending on the rubber used. By subsequent heating of the samples, melting of the rubbers, characterized by slight variations of the heat flow, occurred at different temperatures depending on the rubber (Figure 12.3). The melting transition of the dispersed phase was more pronounced as the amount of rubber in the blend increased (See the endothermic peak around -6°C in Figure 13.3). The phase separation between the matrix and the rubbers was also confirmed by measuring the Tg of the PLLA phase during heating (Table 3.3). Indeed, similar Tg values were observed for neat PLLA and

PLLA phase in the blends. Dispersion of more rubber into the matrix did not change the Tg values (Figure 13.3). Further heating of the samples led to cold-crystallization of the PLLA phase as seen from the exothermic peaks figuring at around 100°C. The cold-crystallization peak of neat PLLA was found at higher temperature (129°C) and was much broader suggesting enhanced cold-crystallization ability of PLLA by dispersion of the rubbers in agreement with DMA data (Figure 11.3).

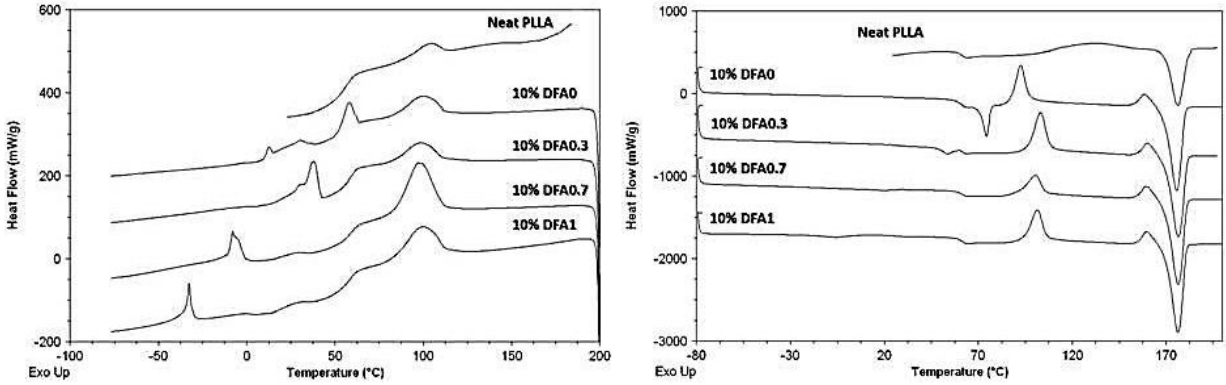

Figure 12.3. (a) Cooling curves and (b) heating curves of neat PLLA and the blends – 10°C.min^{-1} from -80°C to 200°C.

Interestingly, the melting point of PLLA phase remained unchanged (Tm around 176°C) when 10 and 20 wt% of rubber were added. It is however noteworthy that a small exothermic peak (around 162°C) was observed just before the melting transition of PLLA. This peak is assigned to a solid-solid transition explained by the transformation of the meta-stable and disordered α'-crystals into more stable α-crystals.[9]

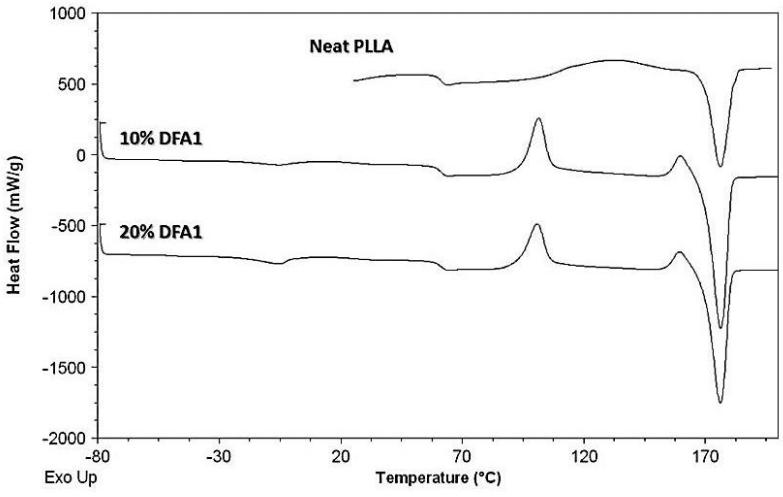

Figure 13.3. Heating curves of neat PLLA and the blends with DFA1 as a rubber – 10°C.min^{-1} from -80°C to 200°C.

For all the blends, except with 10 wt% of DFA0.3, a significant increase in crystallinity was noticed. The most noticeable difference was measured with 20 wt% of DFA0.7. Indeed, for

this sample, the crystallinity of PLLA phase reached 49% while neat PLLA showed a crystallinity value of 15%. It was also observed that the crystallinity of the PLLA phase was enhanced by an increase of the rubber amount in the blend. In the case of the blends with DFA0.3 as a rubber, the crystallinity changed from 17% to 28% for a rubber amount of 10 wt% and 20 wt% respectively. From non-isothermal crystallization studies, we can then ensure that polyester rubbers act as nucleating assisting agents.

Table 3.3. Thermo-mechanical properties of neat PLLA and the blends. Measured by DSC at 10°C.min^{-1}.

		Tg(°C)	Tcc(°C)	ΔHcc(J.g^{-1})	Tm(°C)	ΔHm(J.g^{-1})	χ_c(%)
	PLLA	60.9	129.2	19.2	176.3	32.9	15
10wt%	**DFA0**	61.2	92.6	19.6	175.7	44.2	29
	DFA0.3	60.7	103.1	24.6	176.5	38.7	17
	DFA0.7	61.4	100.5	14.3	176.4	45.3	37
	DFA1	61.7	101.4	19.2	176.4	45.4	31
20wt%	**DFA0**	61.3	92.8	16.8	175.3	40.1	31
	DFA0.3	61.1	102.9	20.1	176.3	41.3	28
	DFA0.7	63.8	-	-	177.0	36.8	49
	DFA1	61.7	100.8	15.5	176.2	40.1	33

III.2.2. Isothermal crystallization

Isothermal crystallization kinetics were also carried out by DSC to evaluate the isothermal crystallization behavior of the blends. The procedure was the following: the samples were first melted at 200°C for 3 minutes to erase the thermal history and were subsequently cooled rapidly at 110°C (this temperature corresponds to the maximum of PLLA crystallization determined by DSC) and kept at this temperature for 30 minutes. The isothermal crystallization data were then fitted to the Avrami equation (Table 4.3 and Figure 14.3).

Table 4.3. Isothermal crystallization parameters of neat PLLA and the blends (110°C).

		n	k (min^{-n})	$t_{1/2}$ (min)
	PLLA	1.80	0.027	6.12
10wt%	**DFA0**	3.53	0.021	2.70
	DFA0.3	3.73	0.014	2.85
	DFA0.7	3.81	0.116	1.60
	DFA1	4.20	0.015	2.48
20wt%	**DFA0**	3.92	0.011	2.86
	DFA0.3	3.42	0.044	2.23
	DFA0.7	3.80	0.384	1.17
	DFA1	3.47	0.033	2.41

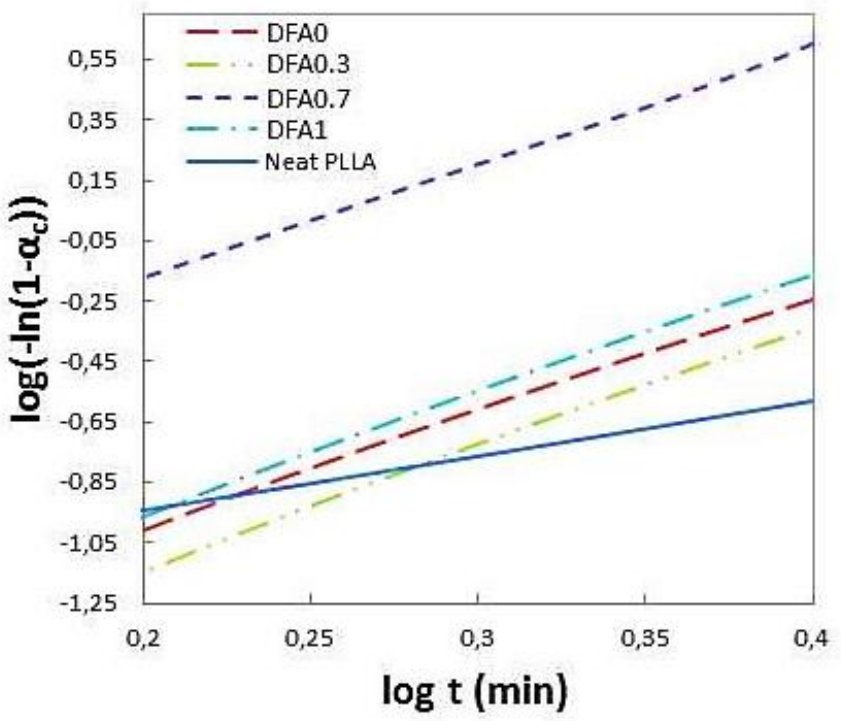

Figure 14.3. Avrami plot - Effect of the rubber type on isothermal crystallization (110°C) of PLLA phase in 10wt% blends.

As seen from Figure 14.3, a good linear relationship was obtained for the curves log[-ln(1-α_c)] versus log t, in agreement with Avrami equation. The Avrami index n was in the range 3.4-4.2 suggesting a three-dimensional crystal growth in accordance with what is generally described for such systems.[10] It is noteworthy that the crystallization half-time was significantly decreased by the incorporation of 10wt% of rubber. Indeed the value changed from 6.12 min for neat PLLA to 1.60 min for the blend containing 10 wt% of DFA0.7. For the other rubbers, $t_{1/2}$ values were in the range 2.48-2.85 min. Similarly to the non-isothermal crystallization experiments, DFA0.7 seems to be the most effective rubber for the enhancement of the PLLA crystallization rate. Addition of more rubber into the PLLA matrix did not resulted in significant changes of the $t_{1/2}$ values. The enhancement of the crystallization rate is thought to arise from the incorporation of flexible rubber chains which increases the PLLA chains mobility thus enhancing the crystallization ability. Interestingly, the most effective nucleating assisting agents (DFA0.7 and DFA1) were the rubbers that presented the best affinity (and lower melting points) with the PLLA matrix as seen from the calculated solubility parameters (Table 1.3). Thus, the higher crystallization rates could be linked to the increased mobility of PLLA chains at the matrix/rubber particle interface due to improved compatibility between the two phases.

III.3. Influence of the polyester structure on the toughening efficiency

III.3.1. Tensile properties

Since the main purpose of this study was to evaluate the influence of the rubber crystallinity on the mechanical properties of the blends, tensile tests were first performed. Figure 15.3 shows the stress-strain curves of neat PLLA and the blends containing 10wt% of additive. Neat PLLA showed a distinct maximum load with subsequent brittle failure at low elongation (only 3.8%) without yielding. When 10wt% of rubber was added, the failure changed from a brittle to a ductile behavior as seen from the distinct yielding which was followed with stable neck growth. An elongation at break value as high as 385 % was obtained when 10wt% of DFA0 was dispersed into the PLLA matrix. This constitutes a 100 fold increase compared to neat PLLA. The fracture of the material happened at different elongation depending on the rubber used.

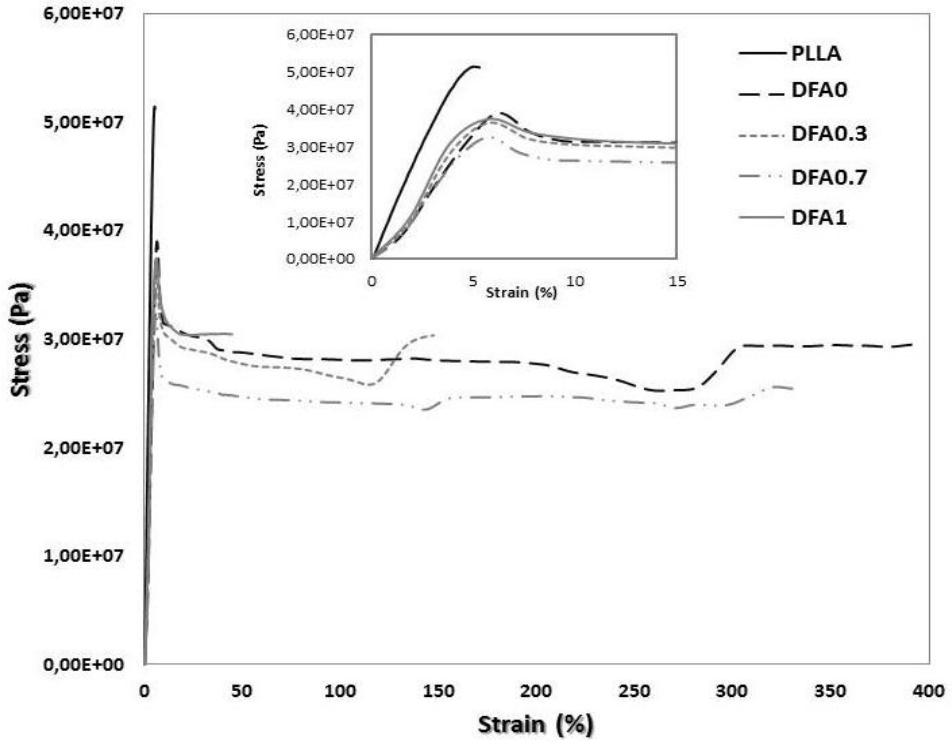

Figure 15.3. Stress-strain curves for neat PLLA and the blends containing 10wt% of rubber. v= 10 mm.min^{-1}.

As seen from the molecular characteristics of the rubbers (Table 1.3) and the mean size diameter of the dispersed particles (Table 2.3), a correlation between the molecular weight of the rubber as well as the mean size of the rubber particles in the matrix and the elongation at break of the blends may be established. Indeed the maximum elongation at break was

obtained with DFA0 which exhibited the higher molecular weight and the smaller particles size. Addition of DFA1, which presented the lower molecular weight and the higher particles size, gave rise to the smaller value of elongation at break of the blend. Further addition of rubber (20 wt%) resulted in a lowering of the elongation at break for all the samples. The most significant decrease of the elongation at break was observed for the samples with DFA0 as additive; values from 385 to 21% were obtained for DFA0 amount of 10 and 20 wt% respectively. Regarding the stiffness of the blends, the incorporation of rubber into the PLLA matrix reduced both the Young's modulus and the yield stress. This is generally observed for rubber-toughened materials and is logically attributed to the lower modulus and tensile strength of the polymeric additives.[11] The Young's modulus decreased from 1.5 GPa for neat PLLA to values in the range 0.7-1 GPa for the blends containing 10 wt% of rubber. The addition of higher amount of rubber did not yield to further significant decrease of the elastic modulus. Similar trend was observed for the yield stress that changed from 47 MPa for neat PLLA to around 30-40 MPa for the PLLA/Rubber blends.

III.3.2. Impact strength evaluation

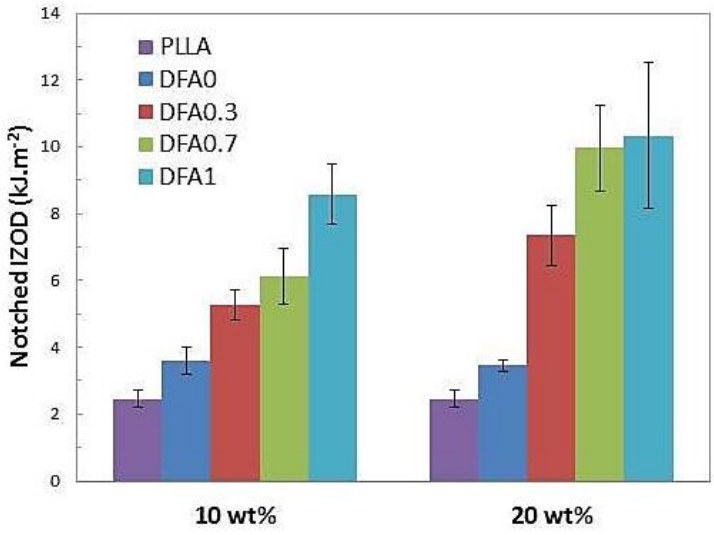

Figure 16.3. Notched IZOD impact strength of PLA-based materials containing 10 and 20wt% of rubber.

Tensile tests allow good evaluation of the improved toughness of rubber-toughened materials, nevertheless measurement of the notched impact strength (IS) represents a more accurate and useful method for the observation of fracture energy absorption during high loading. Thus notched IZOD impact strength tests were realized with all the samples.

The results are displayed in Figure 16.3 and in Table 5.3. An obvious correlation of the crystallinity degree of the rubbers with the impact strength of the blends can be established.

Indeed, in the case of the highly crystalline DFA0 rubber (Tm of 78°C and ΔHm of 101 $J.g^{-1}$), very limited enhancement in notched IZOD IS was observed (3.60 $kJ.m^{-2}$ for 10wt% of DFA0 compared to 2.45 $kJ.m^{-2}$ for neat PLLA). Moreover, in this case (DFA0), no improvement in IS was noticed when higher amount of rubber was added (3.45 $kJ.m^{-2}$ for 20wt% of DFA0). A decrease in crystallinity degree of the rubber resulted in a gradual enhancement of the IS value. For a rubber amount of 10wt%, the lowering of the melting point and the melting enthalpy from 78°C to -5.8°C and from 101 $J.g^{-1}$ to 16.2 $J.g^{-1}$ respectively led to an increase in IZOD impact resistance from 3.60 $kJ.m^{-2}$ to 8.58 $kJ.m^{-2}$. Moreover, in opposition to DFA0, an increase in the rubber amount for DFA0.3, DFA0.7 and DFA1 resulted in a significant enhancement in IS. The higher value of IS (10.34 $kJ.m^{-2}$) was obtained when DFA1 (in the melted state at room temperature) was used with an amount of 20wt%. Regarding the notched IZOD IS value of neat PLLA (2.45 $kJ.m^{-2}$), it corresponds to an increase by a factor of 4.2.

Table 5.3. Mechanical properties of neat PLLA and the blends.

		EModulus (Mpa)	Yield stress (Mpa)	Strain at break (%)	Notch IZOD IS ($kJ.m^{-2}$)
	PLLA	1510 ± 304	47.1 ± 6.0	3.8 ± 1.4	2.45 ± 0.25
10wt%	**DFA0**	788 ± 61	39.7 ± 4.1	385.3 ± 124.2	3.60 ± 0.39
	DFA0.3	888 ± 97	36.2 ± 1.7	143.2 ± 42.7	5.28 ± 0.46
	DFA0.7	709 ± 61	33.4 ± 0.9	358.7 ± 94.8	6.12 ± 0.83
	DFA1	988 ± 42	38.5 ± 1.9	62.6 ± 31.7	8.58 ± 0.90
20wt%	**DFA0**	765 ± 128	33.9 ± 3.9	21.2 ± 8.2	3.45 ± 0.16
	DFA0.3	880 ± 61	31.8 ± 1.4	126.0 ± 47.6	7.35 ± 0.90
	DFA0.7	857 ± 56	30.0 ± 1.9	251.5 ± 127.3	9.96 ± 1.27
	DFA1	809 ± 54	28.2 ± 1.6	17.2 ± 7.1	10.34 ± 2.19

III.3.3. Toughening mechanism

It is now well established, that in addition to the microstructure of the blend and the thermo-mechanical properties of the rubber, interfacial adhesion between the two phases plays a key role in the toughening efficiency of brittle materials.[11, 12] Due to the different chemical structures of the polyesters that were used in this study, interfacial adhesion has to be taken into account in the toughening evaluation. Indeed, it was demonstrated previously that the solubility parameter of the rubbers is becoming closer to the one of PLLA when higher amounts of DFA units are introduced in the chemical structure of the polyester. Thus, in addition to the lowering of the crystallinity induced by the presence of alkyl dangling chains, the higher compatibility of the DFA rich rubbers with PLLA is thought to also act toward high toughening efficiency due to a reinforced interface between the two phases.

In order to identify the main toughening mechanisms occurring during impact testing, the impact-fractured surfaces were observed by SEM. The micrographs of all the blends are displayed in Figure 17.3 and the micrographs of the blends containing 20wt% of rubber are displayed in Figure 18.3 and Figure 19.3.

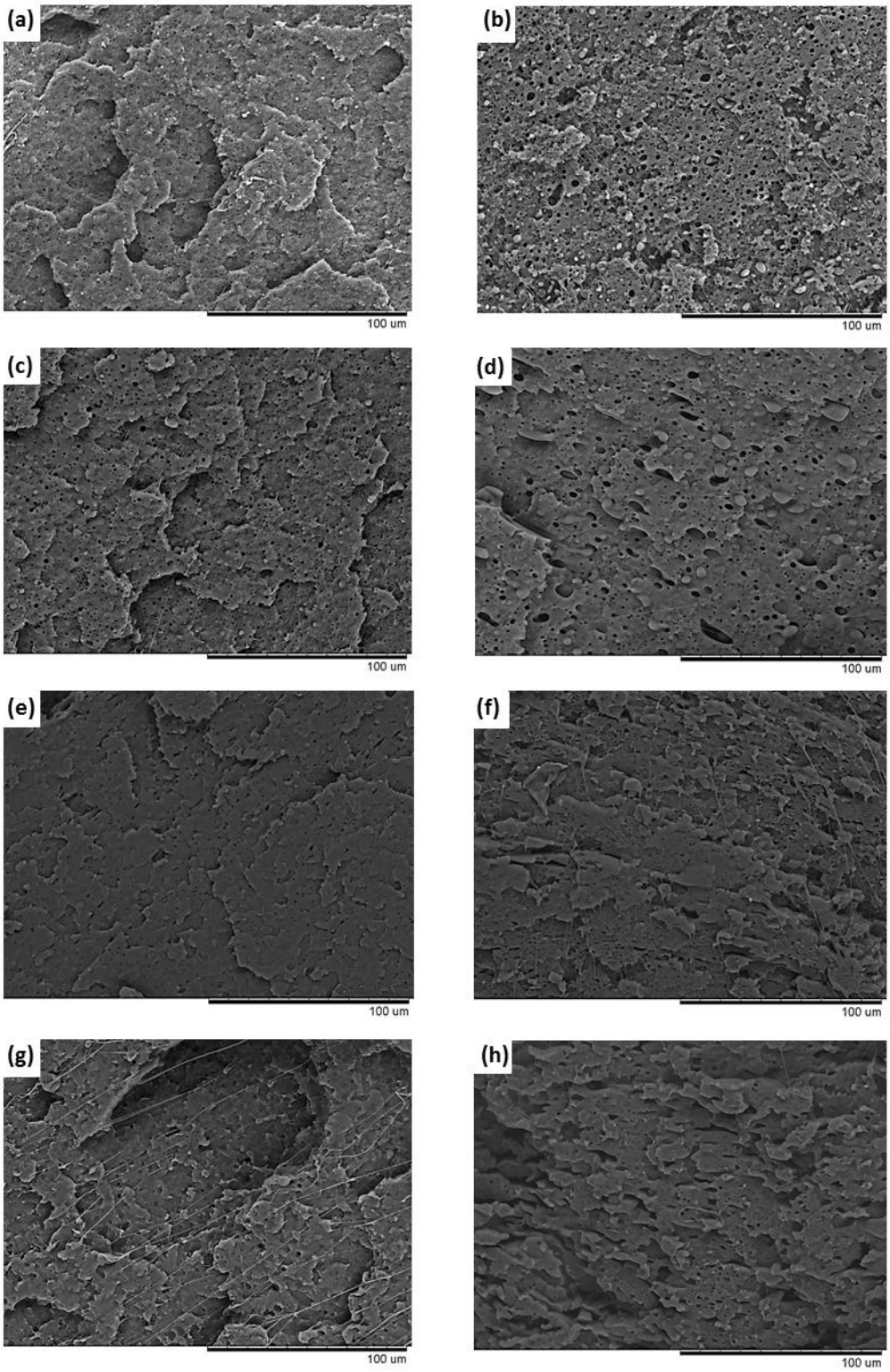

Figure 17.3. SEM images of the impact fractured surfaces of the blends. (a) 10% DFA0 (b) 20% DFA0 (c) 10% DFA0.3 (d) 20% DFA0.3 (e) 10% DFA0.7 (f) 20% DFA0.7 (g) 10% DFA1 (h) 20% DFA1.

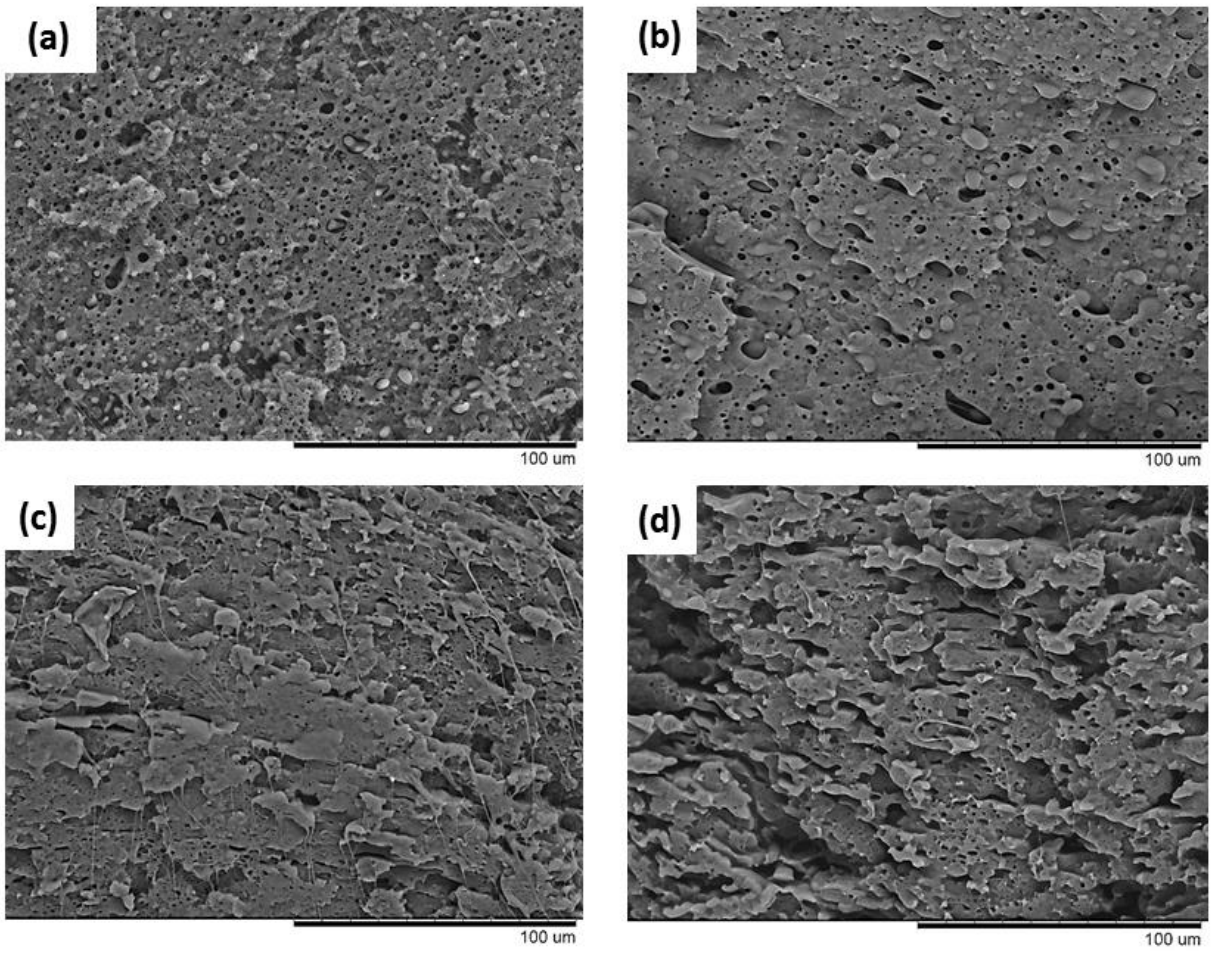

Figure 18.3. SEM images of the impact fractured surfaces of the blends with 20wt% of rubber (a) DFA0 (b) DFA0.3 (c) DFA0.7 (d) DFA1

As discussed in chapter 2, the rubber-toughening mechanism is now well elucidated and is linked to the lower strength of the dispersed rubber phase in comparison to the PLLA matrix. The rubber particles, when subjected to impact stress, cavitate to produce voids which grew along the crack propagation and induce matrix shear yielding by stress concentration then leading to plastic deformation.[13-16] Optimal impact strength of the blend is generally occurring when sufficient interfacial strength is observed and thus when internal cavitation is preferred as an initial step of the rubber-toughening mechanism. Interfacial debonding generally results in rapid and catastrophic crack propagation. From Figure 18.3, various fractured surface morphologies can be observed. For the blend comprising 20wt% of DFA0 (Figure 18.3.a), a relatively smooth surface is observed with a little amount of fibrils and matrix deformation. The holes and spheres representing the DFA0 particles were only slightly deformed. The microvoiding mechanism in this material is clearly typical of interfacial debonding with poorly deformed particles which debonded to the matrix/rubber interface due to superior rubber strength in comparison to the interfacial strength.

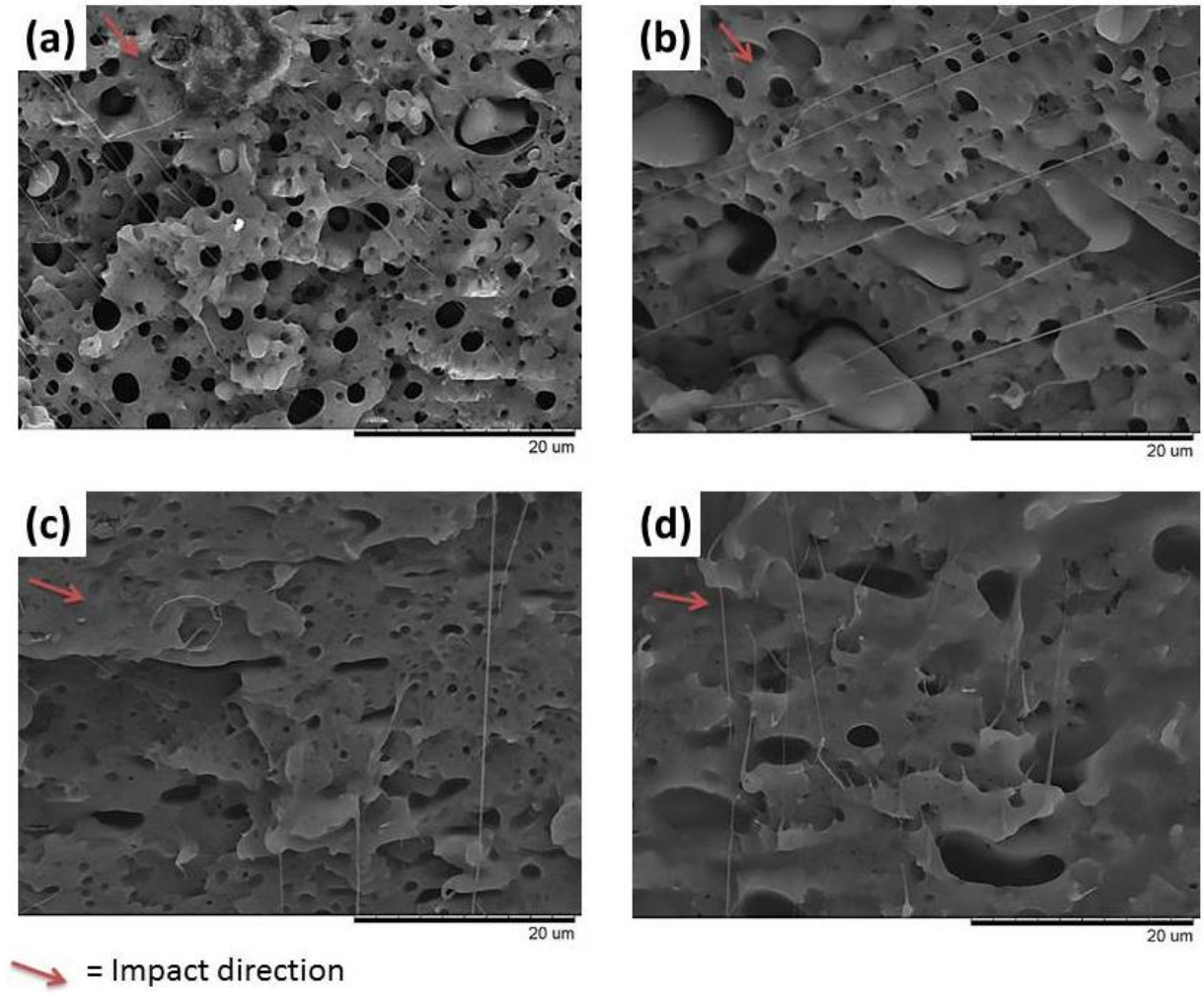

Figure 19.3. Zoomed-up SEM images of Figure 18.3

From Figure 20.3 which shows one image of the fractured surface close to the notch (left) and one far from the notch (right), it is noteworthy that interfacial debonding is much more pronounced close to the notch due to higher impact energy. The scheme of Figure 20.3 clearly illustrates the toughening mechanism as a function of the distance from the notch. Close to the notch, the particles largely cavitate at the matrix/rubber interface to start producing elongated voids. When the image is taken far from the notch, particles only slightly cavitate and elongation of the voids is less pronounced. Finally, very far from the notch, only a small amount of particles cavitate due to a lower impact energy.

For the blends with DFA0.3 as a rubber (Figure 17.3.c and d, Figure 18.3.b and Figure 19.3.b), the toughening mechanism seems to be quite different as the rubber particles are more elongated and more bonded to the matrix. However some debonded particles can be observed which suggest the competition between internal and interfacial cavitation mechanisms.

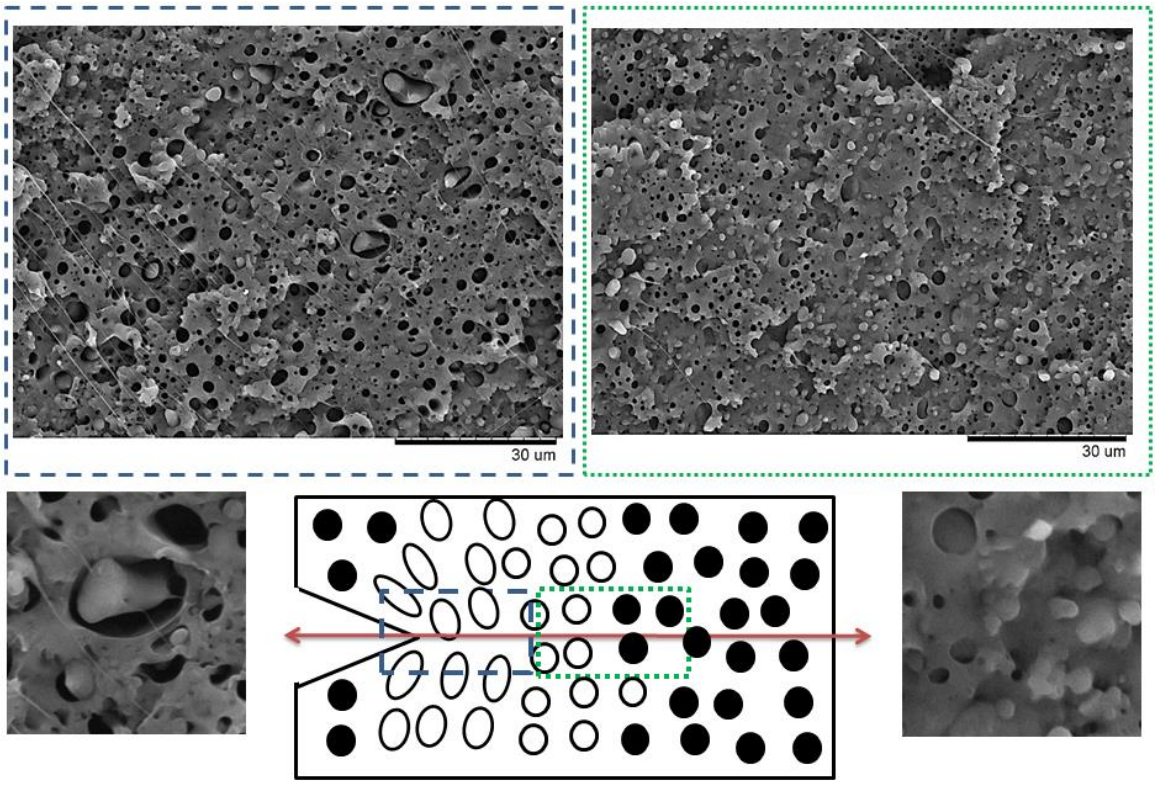

Figure 20.3. SEM images of the PLLA/DFA0 (80/20: w/w) blend taken at different positions on the fractured surface.

These observations are in agreement with the calculated solubility parameters and the measured IS values. The fractured surfaces of the blends with DFA0.7 and DFA1 as rubbers, showed higher deformation of the matrix with particles and voids more difficult to identify. This is logically attributed to the important plastic deformation and the coalescence of the largely elongated voids. Therefore internal cavitation is thought to be the predominant toughening mechanism for these samples in accordance with the low strength of DFA0.7 and DFA1 rubbers (in the melted state at the impact test temperature) and their better compatibility with PLLA (See solubility parameters in Table 1.3). This resulted in the optimum IS in our PLLA blend systems.

To summarize, two effects were investigated in the toughening of PLLA by the developed polyester rubbers. Indeed, the invariant glass transition of the different rubbers used allowed us to evaluate the influence of both the crystallinity degree of the rubbers and their compatibility with the PLLA matrix on the impact resistance of the blends. It was shown that the selection of a rubber showing low or no crystallinity and having good affinity with the PLLA matrix is needed to obtain optimal IS of the blends. By selecting the appropriate rubber, internal cavitation is predominant over interfacial cavitation which allows higher matrix shear yielding and thus higher ductility of the material.

IV. CONCLUSION

A set of novel aliphatic polyesters were prepared from plant oils based building blocks, namely sebacic acid (SA), 1,10-decanediol and hydrogenated dimer fatty acid (DFA). By varying the alkyl dangling chains (provided by DFA units) density, a large range of thermo-mechanical properties were obtained similarly to the tuning of the properties for commercial olefin elastomers (ethylene-hexene and ethylene-octene copolymers). By this way, polyesters with melting points in the range -6 to 78°C were obtained. Calculation of the solubility parameters of the rubbers suggested immiscibility of the two phases but an improved compatibility with the PLLA matrix as the DFA units increased in the polyester structure. The invariant glass transition with the rubber type allowed us to evaluate the influence of two factors on the impact resistance of binary blends of the different rubbers with PLLA: the crystallinity of the rubber and its affinity with the PLLA matrix.

First of all, thermal stability of the blends was investigated to judge about the feasibility of such toughened PLLA systems. A slight lowering of the initial degradation temperature was noticed in comparison to neat PLLA; however, the sufficient thermal stability prompted us to consider further investigations of these blends. Both non-isothermal and isothermal crystallization studies revealed an improved crystallization rate of PLLA phase in the blends compared to neat PLLA. It was attributed to an enhancement of the PLLA chains mobility caused by dispersion of highly flexible rubbers into the matrix.

Tensile tests performed with the blends showed a ductile to brittle transition as seen from the distinct yielding which was followed with stable neck growth. Elongation at break as high as 385 % was obtained for the blend containing 10wt% of DFA0 (compared to 3.8% for neat PLLA). Improvement in the elongation at break was observed for all the blends; however an amount of 10wt% seems to be optimal as seen from the lowering of the ultimate strain with further addition of rubber. As expected, a decrease in the stiffness of the material was observed with the incorporation of the rubbers, however the lowering was limited.

Impact resistance of the blends was evaluated by notched IZOD impact tests. At similar composition, impact strength (IS) gradually increased with a decrease in crystallinity degree of the rubber. It was attributed to differences in the toughening mechanisms which were linked to the strength of the rubber. Highly crystalline rubbers resulted in interfacial cavitation when subjected to impact due to higher strength of the rubber in comparison to adhesion strength between the two phases. On the contrary, melted rubbers or poorly crystalline rubbers dispersed in the PLLA matrix reacted to high loading by internal cavitation. In all cases,

cavitation was followed by void formation, growing along the crack propagation and matrix shear yielding. Nevertheless optimal IS was obtained for the less crystalline rubbers which showed internal cavitation as initial step in the toughening mechanism. An increase in the amount of rubber into the material led to further improvement of the IS.

This study proved the importance of the rubber properties, which can be controlled with the crystallinity and the affinity of the rubber with the matrix, for the toughening of PLLA. The importance of these criteria were illustrated by using potentially biodegradable and biobased aliphatic polyesters that were obtained from the polycondensation of cheap and commercially available plant oil-based building blocks. This work might open other opportunities for the development of efficient and environmental friendly second-generation impact modifiers for PLLA. Indeed, as discussed in chapter 1, fatty acids offer numerous possibilities for the design of amorphous or poorly crystalline polyesters.

V. EXPERIMENTAL

Polyester synthesis

All monomers were dried at 70°C under vacuum overnight prior to use. A mixture of SA, DFA, 1,10-decanediol and titanium isopropoxide (0.1 wt%) was stirred at 180°C under a dynamic nitrogen flow. After 1h, dynamic vacuum was applied. After 1h, the temperature was then raised to 200°C for 4 hours and subsequently raised to 220°C for 2 hours. After completion of the reaction, the polymer was cooled down to room temperature.

REFERENCES

1. H. Mutlu and M. A. R. Meier, *European Journal of Lipid Science and Technology*, 2010, **112**, 10-30.
2. C. Bueno-Ferrer, E. Hablot, F. Perrin-Sarazin, M. C. Garrigós, A. Jiménez and L. Averous, *Macromolecular Materials and Engineering*, 2012, **297**, 777-784.
3. E. Hablot, B. Donnio, M. Bouquey and L. Avérous, *Polymer*, 2010, **51**, 5895-5902.
4. C. Bueno-Ferrer, E. Hablot, M. d. C. Garrigós, S. Bocchini, L. Averous and A. Jiménez, *Polymer Degradation and Stability*, 2012, **97**, 1964-1969.
5. V. K. DW and t. N. K, *Properties of polymers. 4nd ed*, 2008, 190.
6. H. Kang, B. Qiao, R. Wang, Z. Wang, L. Zhang, J. Ma and P. Coates, *Polymer*, 2013, **54**, 2450-2458.
7. C. D. Han, *Journal of Applied Polymer Science*, 1988, **35**, 167-213.
8. K. Lamnawar, F. Vion-Loisel and A. Maazouz, *Journal of Applied Polymer Science*, 2010, **116**, 2015-2022.
9. J. Zhang, K. Tashiro, H. Tsuji and A. J. Domb, *Macromolecules*, 2008, **41**, 1352-1357.
10. T. Miyata and T. Masuko, *Polymer*, 1998, **39**, 5515-5521.
11. H. Liu and J. Zhang, *Journal of Polymer Science Part B: Polymer Physics*, 2011, **49**, 1051-1083.
12. S. Wu, *Polymer*, 1985, **26**, 1855-1863.
13. A. S. Argon and R. E. Cohen, *Polymer*, 2003, **44**, 6013-6032.
14. C. B. Bucknall, *Journal of Polymer Science Part B: Polymer Physics*, 2007, **45**, 1399-1409.
15. D. K. Mahajan and A. Hartmaier, *Physical Review E*, 2012, **86**, 021802.
16. M. Kowalczyk and E. Piorkowska, *Journal of Applied Polymer Science*, 2012, **124**, 4579-4589.

CHAPTER 4:

Novel poly(L-lactide)-b-poly(ricinoleic acid)-b-poly(L-lactide) triblock copolyesters: Investigation of solid-state morphology and thermo-mechanical properties.

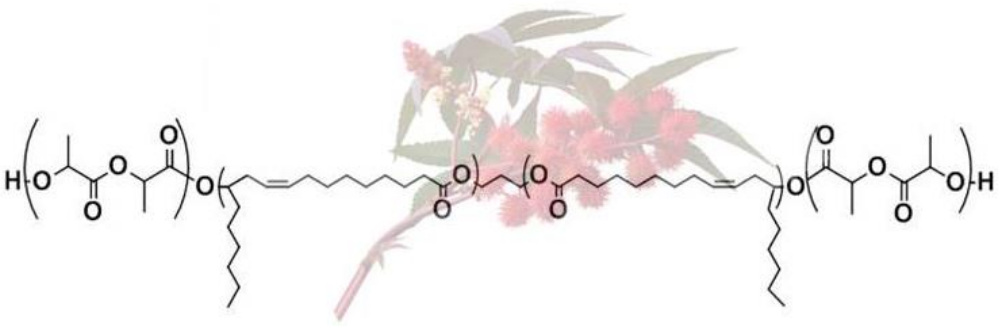

poly(L-lactide)-*b*-poly(ricinoleic acid)-*b*-poly(L-lactide)

Keywords: fatty acids, castor oil, ricinoleic acid, polycondensation, lactide, ROP, block copolymer, ductility, PLLA.

Mots clés: acides gras, huile de ricin, acide ricinoléique, polycondensation, lactide, polymérisation par ouverture de cycle, copolymère à bloc, ductilité, PLLA.

I. INTRODUCTION

Among the triglyceride oils, castor oil has attracted much attention as it contains approximately 85-90% of ricinoleic acid, a naturally hydroxylated fatty acid. [1, 2] In the previous chapters we employed castor oil platform to synthesize novel polyester impact modifiers for PLLA. To that aim, methyl 10-undecenoate and sebacic acid were used as building blocks. However, industrially, these molecules are obtained from castor oil by a two-step procedure. On the contrary, methyl ricinoleate (obtained from castor oil by a simple transesterification step) can directly react by self-condensation to yield an economically viable low Tg amorphous poly(ricinoleic acid), (PRic) (Tg= -70°C).[3-5] In addition to its thermo-mechanical properties similar to polybutadiene or polyisoprene, PRic is biodegradable and thus represents a potential 'green', rubbery, toughness modifier for PLLA.[4 6] Interesting features of PRic have been exploited in polyurethane synthesis [4] as well as for cross-linked elastomers.[5] Copolyesters of ricinoleic acid with lactic acid were also reported by Domb and coll.; however, completely random copolymers were obtained which resulted in the loss of the thermal properties of PLLA.[7,8] Hillmyer and coll. used dispersed castor oil directly as an impact modifier in a PLLA matrix. Nonetheless, the incompatibility between the dispersed and continuous phases necessitated the use of a compatibilizer to enhance adhesion forces between the two phases. For that purpose, poly(ricinoleic acid)-*b*-poly(L-lactide) diblock copolymers were used. While the method was found to be efficient for PLLA toughening, no real investigations on the properties of the synthesized block copolymers were implemented.[9]

All these studies based on ricinoleic acid derivatives for PLLA toughening prompted us to investigate the design and the use of novel poly(L-lactide)-*b*-poly(ricinoleic acid)-*b*-poly(L-lactide) (PLLA-*b*-PRic-*b*-PLLA) triblock copolymers as thermoplastic elastomers and high-impact PLLA. The synthetic strategy selected for this work was to design di-hydroxy telechelic poly(ricinoleic acid) (HO-PRic-OH) as macro-initiator for the ring-opening polymerization of L-lactide. The addition of a small amount of bio-based 1,3-propanediol during methyl ricinoleate self-polycondensation enabled the preparation of hydroxyl telechelic HO-PRic-OH with high yield.[10] ROP of L-lactide initiated by HO-PRic-OH was then performed to give the targeted triblock copolymers, PLLA-*b*-PRic-*b*-PLLA. The synthesis of such PLLA-*b*-PRic-*b*-PLLA triblock copolymers and the study of their physico-chemical properties with respect to the copolymer composition are discussed in this chapter.

II. SYNTHESIS

II.1. Synthesis of the α,ω-dihydroxy prepolyester

The synthesis of PLLA-*b*-PRic-*b*-PLLA triblock copolymers was realized in two steps (Scheme 1.4). The macroinitiator, α,ω-dihydroxy-poly(ricinoleic acid) (HO-PRic-OH), was prepared by self-polycondensation of methyl ricinoleate with a very low amount of biobased 1,3-propanediol.[11]

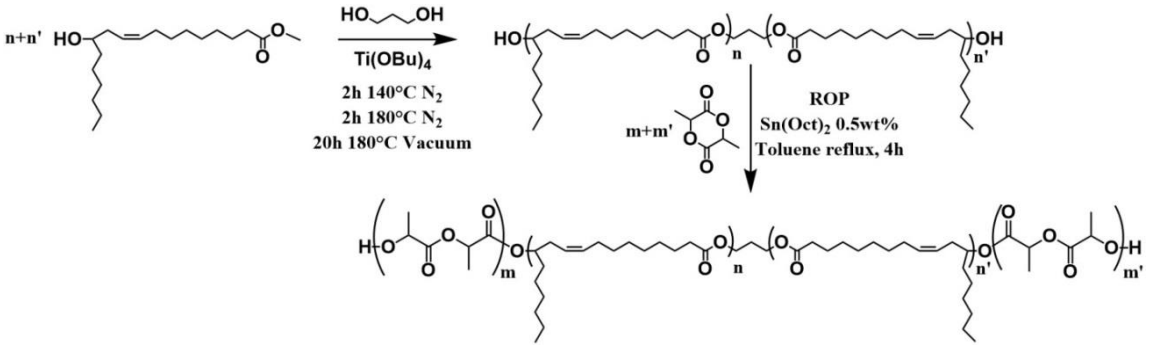

Scheme 1.4. Two-step procedure to PLLA-b-PRic-b-PLLA triblock copolymers

Heating the reaction mixture at a temperature of 140°C under a flow of nitrogen in the presence of a transesterification catalyst ($Ti(OBu)_4$, 1 mol%) permitted the easy removal of the methanol condensate without distilling the less volatile 1,3-propanediol.

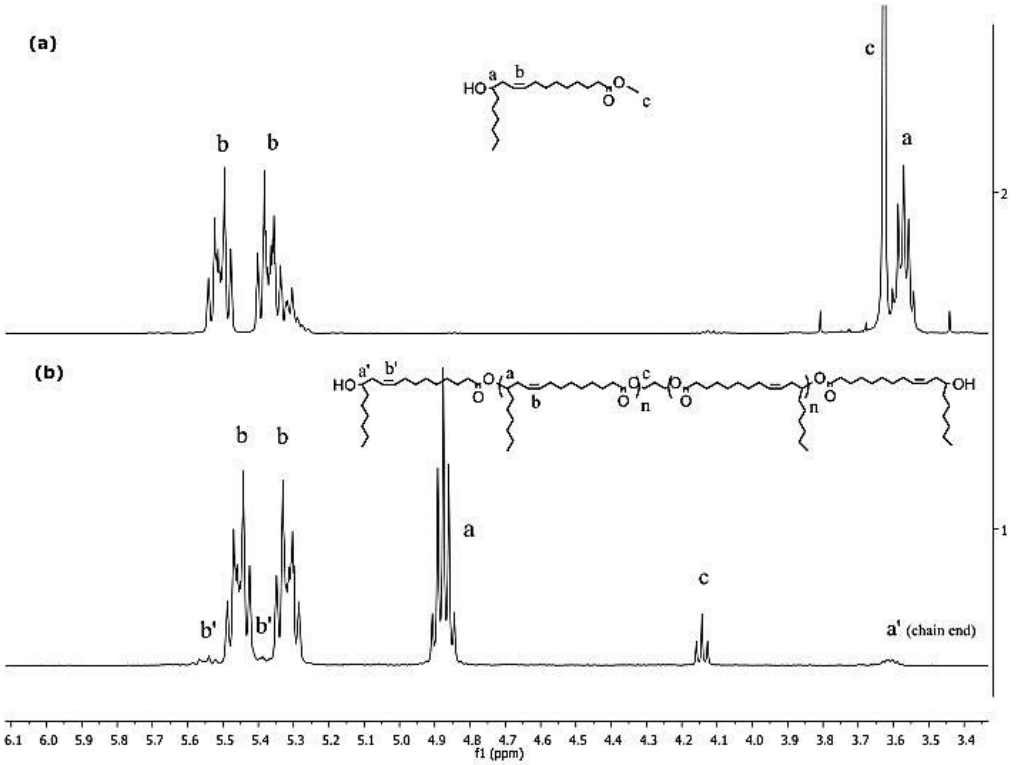

Figure 1.4.Stacked ^{1}H-NMR spectra of (a) methyl ricinoleate and (b) HO-PRic-OH in $CDCl_3$

A higher temperature (180°C) was then applied under dynamic vacuum to ensure the full conversion of methyl ester functions. The formation of HO-PRic-OH was first verified by ^{1}H-NMR spectroscopy (Figure 1.4).

The characteristic peak of the proton linked to the carbon bearing the hydroxyl function in methyl ricinoleate (See Figure 1.4.a, H_a proton) is shifted downfield as the conversion of methyl ricinoleate increases, confirming the formation of ester functions. The double bond protons (See Figure 1.4.a and b, H_b protons), are also shifted upfield as the transesterification proceeds. The total disappearance of the methyl ester peak proves that all methyl ester functions have reacted with hydroxyl functions of methyl ricinoleate or 1,3-propanediol. Furthermore, the appearance of a triplet at 4.15 ppm characteristic of the protons linked to the carbon adjacent to the ester function in the propanediol unit (See Figure 1.4.b, H_c protons), clearly confirms that the hydroxyl functions of 1,3-propanediol efficiently reacted with the ester moieties of methyl ricinoleate or poly(ricinoleic acid) chain ends. The ratio of 1,3-propanediol units *vs* methyl ester chain ends was determined by ^{1}H-NMR to evaluate the percentage of HO-PRic-OH chains. A very high percentage (96 %) of HO-PRic-OH was obtained (Table 1.4) allowing the use of this pre-polymer for the ring-opening polymerization of L-lactide.

Table 1.4.Molecular characteristics of the synthesized HO-PRic-OH

	Ric/Prop [a]	$\bar{M}_n$ (g.mol^{-1}) [b]	$\bar{M}_n$ (g.mol^{-1}) [c]	Đ [c]	%HO-PRic-OH [b]
HO-PRic-OH	100/6	10 800	19 050	1.7	96

(a) Molar ratio Methyl Ricinoleate/1,3-propanediol in feed (b) ^{1}H-NMR (c) SEC, THF, PS calibration

^{1}H-NMR end-group analysis was used to determine the molecular weight of the HO-PRic-OH pre-polyester. An $\bar{M}_n$ value of 11 kg.mol^{-1} was calculated (Table 1.4) which is slightly higher than the theoretical value, due to partial distillation of 1,3-propanediol during polymerization.

The HO-PRic-OH sample was also characterized by SEC. Figure 2.4 shows SEC traces of methyl ricinoleate and HO-PRic-OH samples. The shift of the SEC trace to lower elution times after reaction revealed the efficiency of the AB type self-polycondensation. The $\bar{M}_n$ value relative to PS calibration was 19 kg.mol^{-1} with a dispersity of 1.7 (Table 1.4). A significant difference was noticed between the molecular weight evaluated by SEC and the absolute molecular weight calculated by ^{1}H-NMR. It is attributed to the calibration used for SEC analysis.

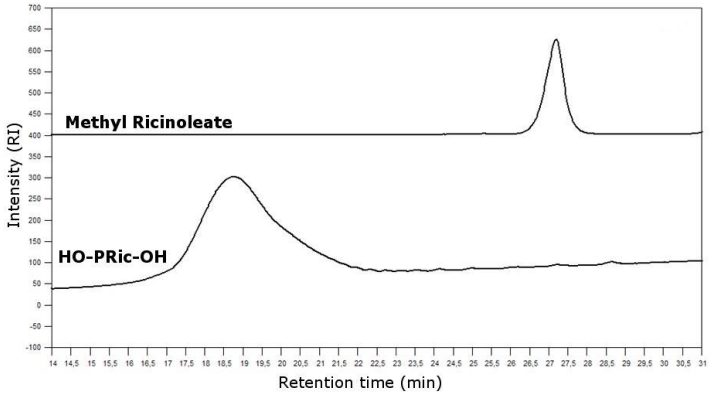

Figure 2.4.SEC traces of Methyl Ricinoleate and HO-PRic-OH.

II.2. Synthesis of PLLA-*b*-PRic-*b*-PLLA triblock copolymers

The HO-PRic-OH prepolyester was then used as macroinitiator for the ring-opening of L-Lactide. Because of the high viscosity of the prepolyester, polymerizations were carried out in toluene. The toluene reflux temperature was selected in order to avoid transesterification reactions and thus the formation of random copolyester. The completion of the polymerization was monitored by ^{1}H-NMR and SEC.

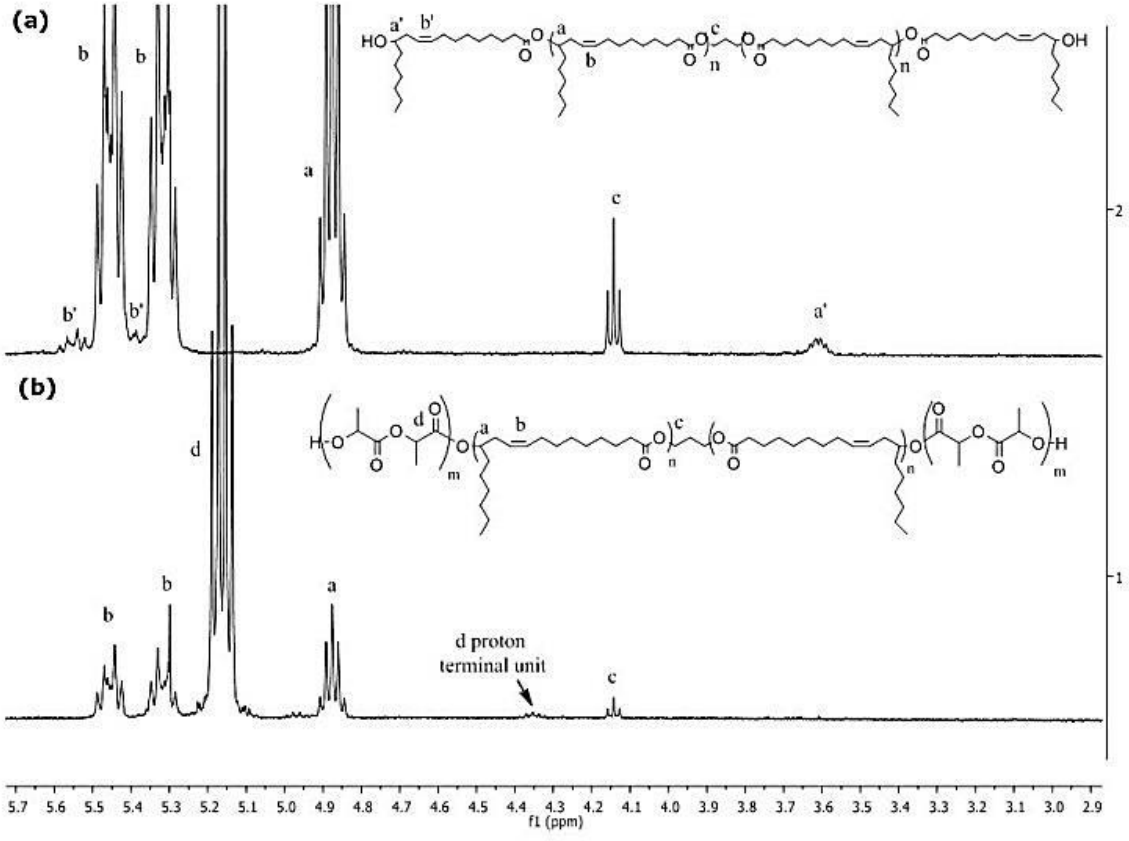

Figure 3.4.Stacked ^{1}H-NMR spectra of the reprecipitated (a) HO-PRic-OH and (b) PLLA-b-PRic-b-PLLA (H63). $CDCl_3$

Polymerizations were stopped before full conversion of L-lactide (in the range 85-92% at the end of the polymerization) to avoid transesterification reactions that generally occurred at long reaction times and/or high monomer conversions. This non-quantitative conversion partially explained the differences in weight composition of the triblock copolymers from the theoretical values.

A series of triblock copolymers were synthesized for different L-lactide to HO-PRic-OH ratios enabling the preparation of block copolymers with various compositions ranging from 35 to 83 wt% of PLLA (Table 2.4). The nomenclature used to identify the copolymers is based on the experimental weight percentage of the hard block (PLLA) in the copolymer. For instance H83 means that the weight composition of the PLLA (Hard) block in the copolymer is 83 wt%.

Table 2.4.Molecular features of PLLA-b-PRic-b-PLLA triblock copolymers

	$[M]_0/[I]_0$	$Wt\ \%_{PLLA}^{feed}$	$Wt\ \%_{PLLA}$ [a]	Conversion(%) [a]	$\bar{M}_n$ (kg.mol^{-1}) [a]	$Đ$ [b]
H83	677/1	0.90	0.83	90	61	1.2
H71	306/1	0.80	0.71	90	49	1.3
H63	179/1	0.70	0.63	92	31	1.3
H53	115/1	0.60	0.53	86	28	1.2
H45	68/1	0.50	0.45	85	14	1.2
H35	46/1	0.40	0.35	86	13	1.2

(a) ^{1}H-NMR (b) SEC, THF, PS calibration . [M] : L-lactide, [I] : HO-Pric-OH.

As can be seen from the ^{1}H-NMR spectra (see Figure 3.4), a quadruplet, assigned to the proton linked to the tertiary carbon of lactic acid repeat units, appears at 5.17 ppm (See Figure 3.4.b, H_d proton), confirming the ring-opening of L-lactide. In addition, the characteristic peaks of the terminal units of HO-PRic-OH macro-initiator are shifted in agreement with the lactide polymerization from hydroxyl end groups of HO-PRic-OH. The protons of the double bonds are shifted upfield (from 5.39 ppm to 5.33 ppm and from 5.54 ppm to 5.44 ppm) (See Figure 3.4, $H_{b'}$ proton) while the proton close to the hydroxyl function shifts from 3.65 ppm to 4.87 ppm (See Figure 3.4, $H_{a'}$ proton). The absence of peaks between 5.0 ppm and 5.10 ppm, characteristic of ricinoleic acid-lactic acid and lactic acid-ricinoleic acid sequences, confirmed that polymerization occurred without transesterification (or very limited transesterification). The weight composition of the triblock copolymers was evaluated by ^{1}H-NMR and was in accordance with the expected values (Table 2.4). The total molar mass of the copolymers was also calculated by ^{1}H-NMR taking into account the molar mass of HO-PRic-OH macroinitiator; $\bar{M}_n$ values were in the range 13-60 kg.mol^{-1} depending on the

percentage of PLLA in the copolymer structure. DOSY-NMR experiments were performed to give additional evidence of block copolymer formation (Figure 4.4). DOSY experiments on dilute solutions of H63 and HO-PRic-OH in $CDCl_3$ revealed two distinct diffusion coefficients at 39.10^{-12} $m^2.s^{-1}$ and 104.10^{-12} $m^2.s^{-1}$ respectively. The unique diffusion coefficient of H63 is lower than that of HO-PRic-OH in agreement with the higher molecular weight of the block copolymer.

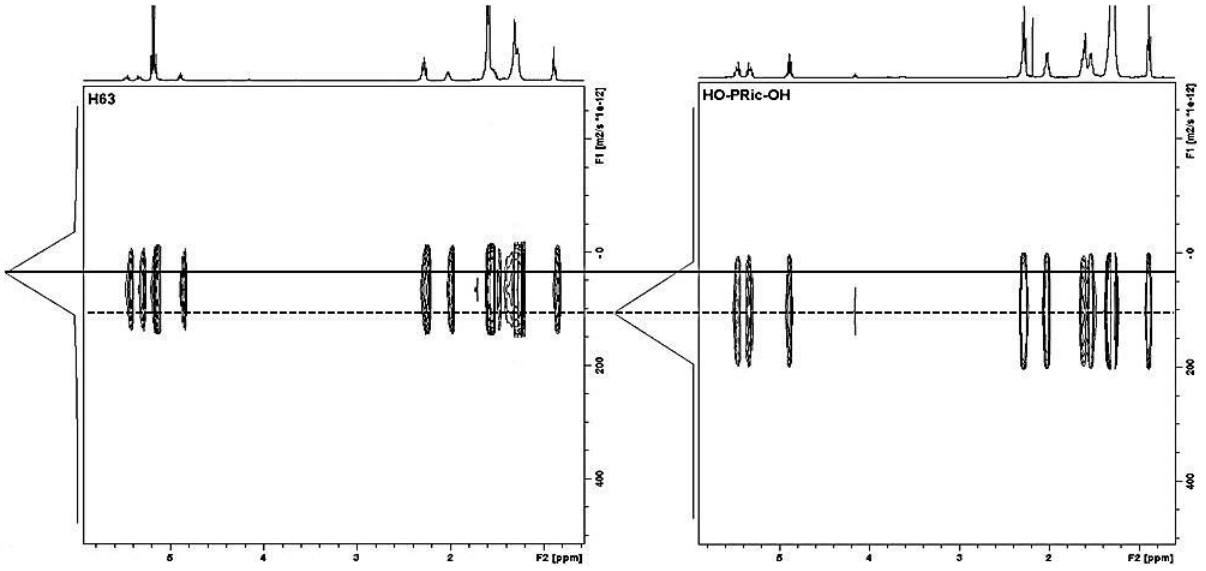

Figure 4.4.^{1}H DOSY-NMR spectra of H63 and HO-PRic-OH obtained in dilute $CDCl_3$ solution.

All the copolymers were characterized by SEC in THF. The shift of the copolymer traces to lower elution times in comparison to that of the HO-PRic-OH macro-initiator confirms the efficiency of the ring-opening polymerization of lactide (see Figure 5.4).

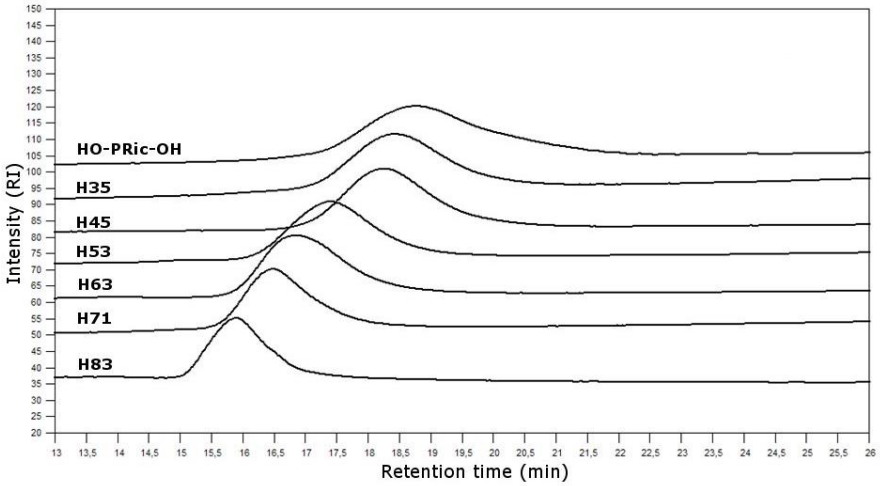

Figure 5.4. SEC traces of HO-PRic-OH , H35, H45, H53, H63, H71 and H83.

The total disappearance of the macro-initiator trace after polymerization reveals the complete initiation of lactide. The dispersities measured by SEC were in the range 1.2-1.3 showing a

narrow distribution of the block copolymer chains in agreement with the controlled polymerization of lactide. After the confirmation of the triblock structure of these copolymers with the help of ^{1}H-NMR, DOSY-NMR and SEC techniques, the thermal and thermo-mechanical properties as well as the crystallographic data of these block copolymers were further investigated.

III. INFLUENCE OF COMPOSITION ON THE PROPERTIES

III.1. Thermal stability

The thermal stability of the PLLA-*b*-PRic-*b*-PLLA block copolymers under non-oxidative conditions was investigated by thermal gravimetric analysis (TGA) in order to evaluate the processability of these materials into molded articles using traditional techniques such as extrusion and injection. TGA also allowed to validate the weight fraction of each block. Thermal decomposition data are given in Table 3.4 and illustrated in Figure 6.4.

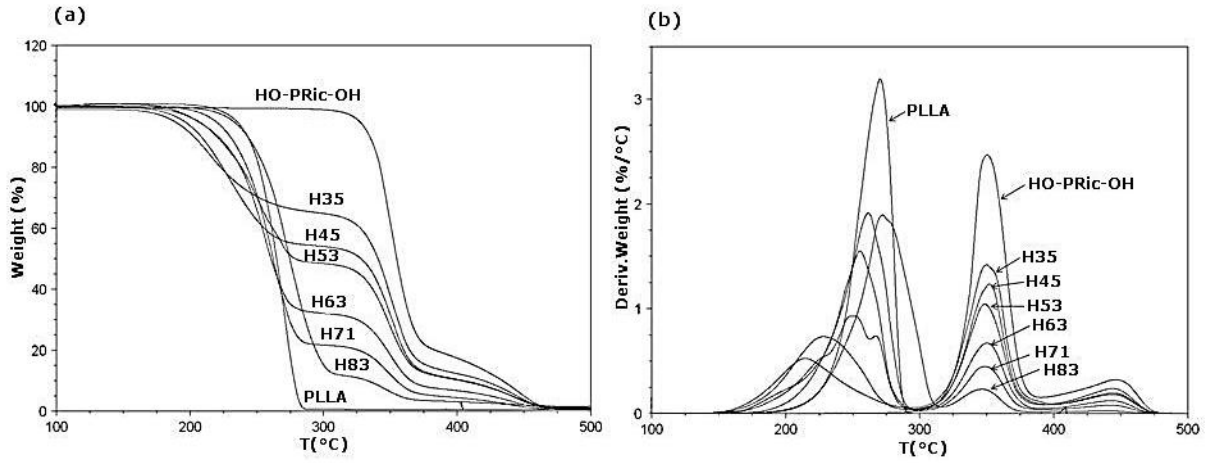

Figure 6.4.(a) TGA curves and (b) TGA derivative curves of HO-PRic-OH, PLLA and triblock copolymers thereof at a heating rate of 10°C.min^{-1} under nitrogen atmosphere.

As expected, PLLA-*b*-PRic-*b*-PLLA copolymers present a multi-step thermal decomposition. A first weight loss is observed at a temperature in the range 175-225°C followed by another significant weight loss at around 325°C, which corresponds to the degradation of PLLA and PRic respectively. A third degradation occurs at higher temperature (around 400°) and can also be assigned to the decomposition of PRic as the amount of material degraded at this temperature increases with the PRic content. This thermal decomposition allowed us to calculate the weight percentage (proportional to the weight loss) of each block in the copolymer. As can be observed in Table 3.4, the weight percentages match with the values calculated by ^{1}H-NMR. The drastic effect of the incorporation of the PRic moiety in the

copolymer on the initial degradation temperature of PLLA must be underlined. The higher the weight fraction of PRic in the copolymer, the lower the temperature PLLA starts to degrade.

Table 3.4.Thermal and thermo-mechanical properties of HO-PRic-OH, PLLA and triblock copolymers thereof.

	Wt PLLA[a]	Wt PLLA[b]	Tm (PLLA)[c] (°C)	ΔHm[c] (J.g^{-1})	Xc[c] (%)	$T_{5\%}$[b] (°C)
PLLA	1	1	175	55	59	235
H83	0.83	0.85	179	51	66	233
H71	0.71	0.77	170	37	56	219
H63	0.63	0.66	167	35	60	206
H53	0.53	0.51	160	28	57	206
H45	0.45	0.45	147	19	45	196
H35	0.35	0.32	138	13	40	189
HO-PRic-OH	0	0	-	-	-	327

(a) 1H-NMR, (b) TGA, N2 atmosphere-10°C.min^{-1}, (c) DSC-10°C.min^{-1} after annealing at 120°C for 2 hours.

While the temperature corresponding to 5% weight loss of PLLA homopolymer is 235°C, this value drops to 189°C for the copolymer containing 35wt% of PLLA (H35). For all samples, the temperature corresponding to the final degradation was nearly the same at around 460°C. Moreover, all the polymers presented negligible weight residues (less than 3%). To conclude, as PLLA processing conditions involve the use of high temperatures (around 180°C), PLLA-*b*-PRic-*b*-PLLA copolymers with a high PLLA weight fraction are preferable.

III.2. Thermo-mechanical properties

The phase transitions of PLLA-*b*-PRic-*b*-PLLA copolymers were determined by DSC analyses. All samples were heated at 190°C for 3 minutes in order to convert all the chains into their molten state. The samples were then annealed for 2 hours at 120°C in order to produce maximum crystallinity. Melting points and corresponding enthalpies were then recorded while heating at 10°C.min^{-1} from -100°C to 200°C. The crystallinity of the annealed PLLA blocks in the copolymer was also calculated by taking into account the weight fraction of PLLA calculated from the molar composition obtained using ^{1}H-NMR. DSC traces in the range 100°C-200°C of all the PLLA-*b*-PRic-*b*-PLLA copolymers are illustrated in Figure 7.4. As expected, the primary effect of the copolymer composition on the thermo-mechanical properties is a decrease in the melting temperature with an increase in the PRic weight fraction, except for H83 containing only 17wt% of PRic (Table 3.4).

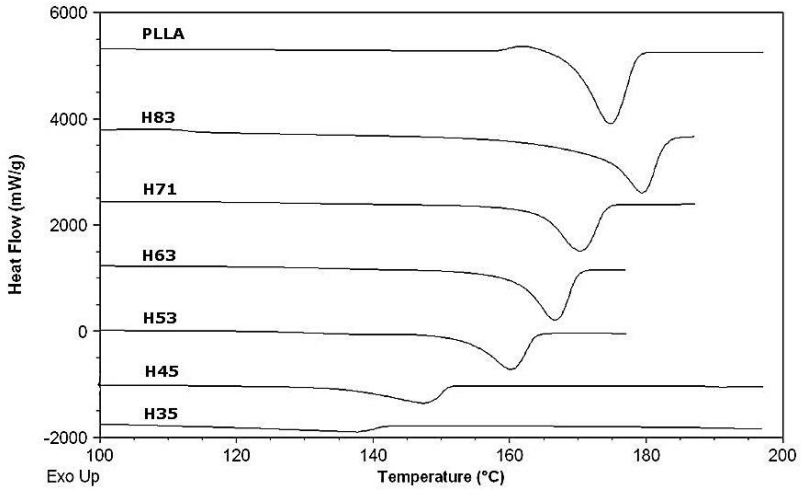

Figure 7.4. DSC traces of PLLA and PLLA-b-PRic-b-PLLA block copolymers –heating scan at 10°C.min^{-1} after annealing at 120°C for 2 hours.

Indeed, PLLA-*b*-PRic-*b*-PLLA block copolymers containing high weight percentages of PLLA (up to 63wt%, H63) melt at a temperature close to the melting point of PLLA homopolymer (175°C). However, when incorporating 65wt% of PRic in the copolymer structure (H35), Tm drops to 138°C (Figure 8.4).

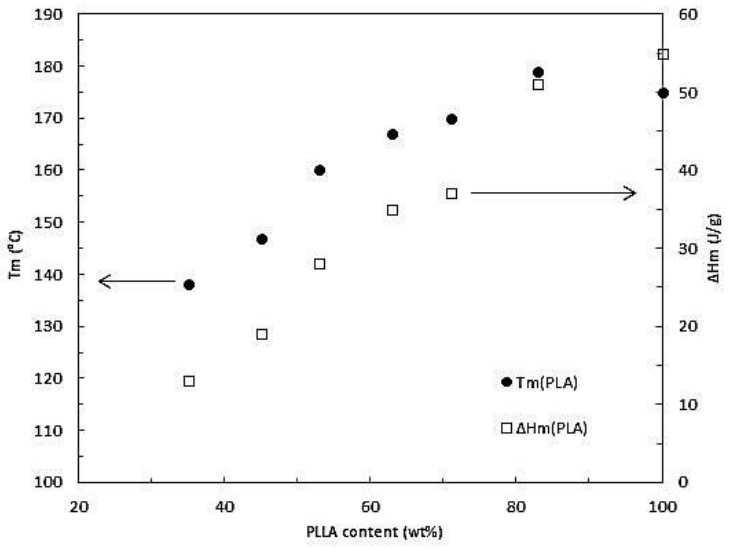

Figure 8.4.Melting parameters of PLLA and PLLA-b-PRic-b-PLLA block copolymers as a function of PLLA weight content calculated by ^{1}H-NMR.

One can also notice that the melting endotherms broaden considerably with the presence of high amounts of PRic (Figure 7.4). These observations can be correlated with a nanoconfinement of the crystallization coupled with shorter PLLA block chains that cannot easily crystallize and that produce crystallites of different size. In the particular case of H35 the partial miscibility, which will be discussed in the solid state morphology, can be one of the reasons for the broadening and the large decrease in the melting peak. In Figure 8.4 the

melting enthalpy is displayed as a function of the PLLA weight content in the block copolymers. The value of ΔH_m decreases linearly with decreasing PLLA hard block content. The linear relationship between ΔH_m and PLLA content ω can be described as

$$\Delta H_m\,(J.g^{-1}) = 0.543\,\omega \qquad (eq\ 1.4)$$

after extrapolation to ΔH_m=0 for 100% PRic, consistent with the totally amorphous character of PRic. This equation was established by making the supposition that PLLA blocks can nucleate and crystallize at all copolymer compositions. The calculated crystallinity (χ_c) of annealed PLLA in the block copolymer decrease slightly with decreasing PLLA content (see Table 3.4). The crystallinity of PLLA phase in triblock copolymer H35 is 40% while PLLA homopolymer exhibits a crystallinity of 59%, indicating that PRic moderately disturbs the PLLA crystallinity when there is a low amount of hard block as in the structure of H35. This decrease in the crystallinity of PLLA in the copolymer can be attributed to nanoconfinement and/or partial miscibility that disfavor the crystallization process. These thermo-mechanical analyses confirmed that incorporation of a relatively high amount of soft block (PRic) in PLLA-*b*-PRic-*b*-PLLA block copolymers only moderately affects PLLA melting point and crystallinity values, in contrast to the large effect observed with random copolymers.[7, 8]

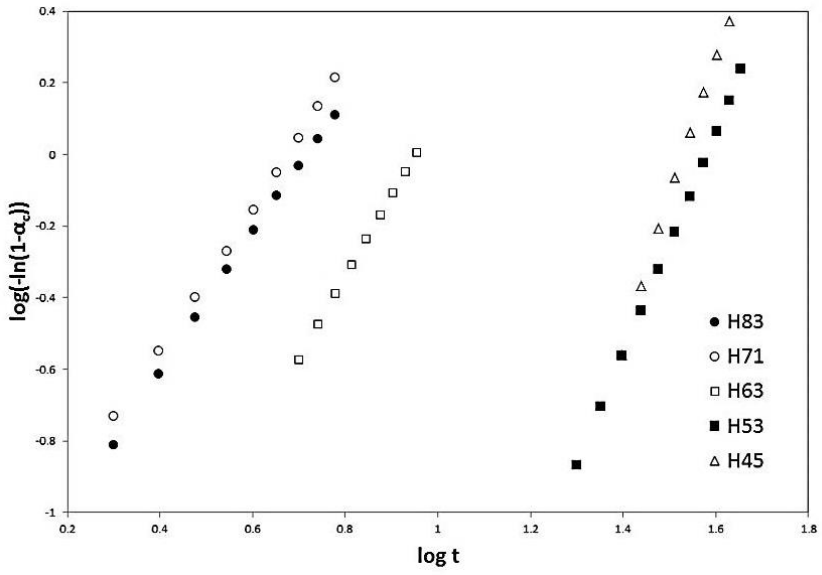

Figure 9.4.Avrami plots for isothermal crystallization of PLLA-b-PRic-b-PLLA block copolymers.

The overall isothermal crystallization kinetics of the PLLA phase for the different triblock copolymers were determined by DSC experiments at 120°C after the copolymers were melted at 190°C for 3 minutes. The isothermal crystallization data was fitted to the Avrami equation using a reported procedure.[12] From the intercepts and the slopes of the plots of log[-ln(1-α_c)]

versus log t, the values of k and n were calculated respectively (Figure 9.4) (see also Table 4.4). In the case of the PLLA-*b*-PRic-*b*-PLLA block copolymers, the values of n were lower than expected (around 4) but higher than the value of neat PLLA. Moreover, n values increased for higher PRic weight fractions in the copolymer (see Table 4.4). Because neat PLLA crystallizes into spherulites in a homogeneous fashion, the block copolymers are thought to also crystallize with a similar behavior.

Table 4.4.Isothermal crystallization parameters (120°C).

	n	$k.10^{-3}$ (min^{-n})	$t_{1/2}$ (min)
PLLA	1.72	14.1	9.62
H83	1.93	41.5	4.29
H71	1.98	45.7	3.94
H63	2.26	7.1	7.59
H53	3.11	0.012	33.81
H45	4.02	0.0007	31.04
H35	-	-	-

The crystallization half-time ($t_{1/2}$) significantly increases with increasing PRic content. In addition, the copolymers exhibit different molecular weights (from 13 to 61 $kg.mol^{-1}$), a feature that can affect PLLA crystallization kinetics. Indeed, it has been reported that an increase in PLLA molecular weight yields a lower crystallization ratio. [13] However, the opposite behavior was observed in our case. In fact, the higher the PLLA content in the copolymer, the higher the molecular weight. Thus, the decrease in the crystallization rate was attributed to the presence of the amorphous PRic segment. Nevertheless, it is noteworthy that when limited amount of PRic is incorporated into the block copolymer (<37wt%), the crystallization rate of the PLLA phase in the block copolymer is higher than for neat PLLA. A small amount of PRic thus improves the crystalline ability of the PLLA phase.

III.3. Crystallographic structure

PLLA can crystallize in α-, β-, or γ-forms depending on the processing conditions.[14-19] Wide-angle X-ray diffraction (WAXD) at room temperature after annealing PLLA-*b*-PRic-*b*-PLLA samples for 2 hours at 120°C was used to obtain information about the crystalline structure of PLLA. The annealing temperature was fixed at 120°C to avoid the formation of the α'-form and to favor the crystallization into the more stable α-form. Figure 10.4 shows the WAXD patterns of PLLA-*b*-PRic-*b*-PLLA and of native PLLA. An expansion of the profiles for the weaker reflections is depicted in Figure 10.4.b.

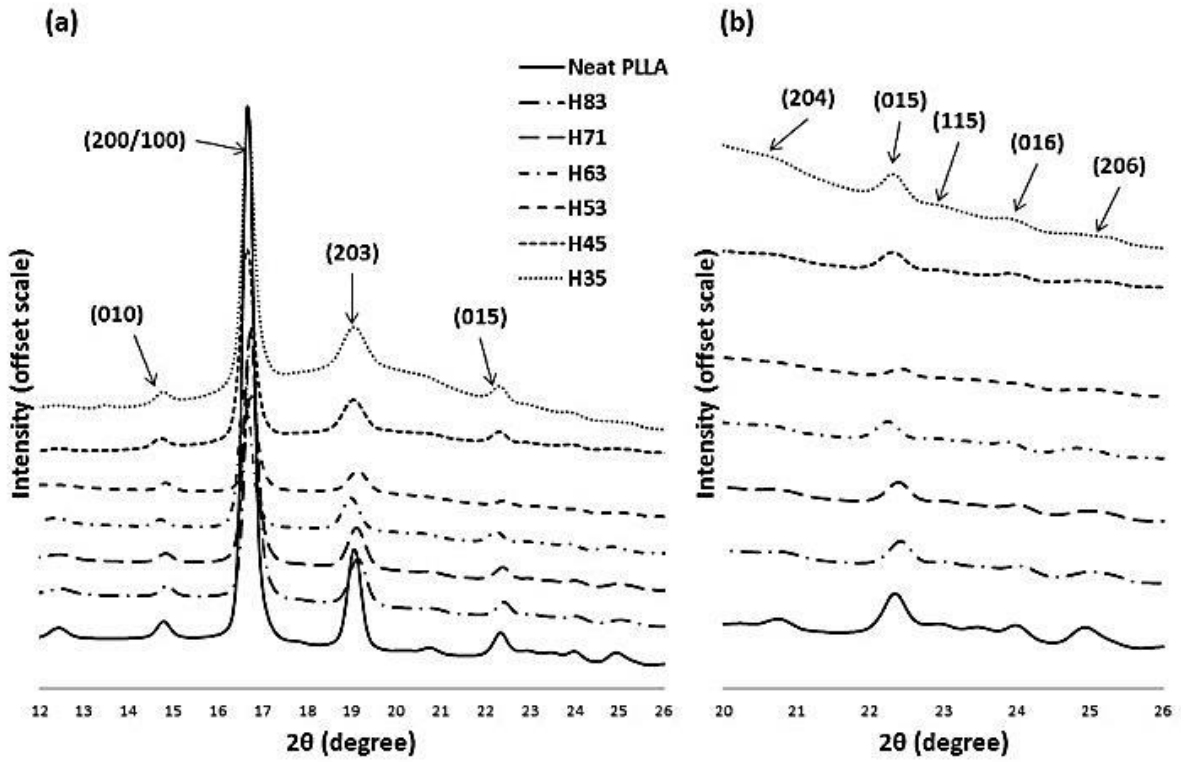

Figure 10.4.(a) Global and (b) enlarged WAXD patterns of PLLA and of PLLA-b-PRic-b-PLLA block copolymers.

As expected, typical reflections of the α-form were identified such as (010), (110/200), (203), (204), (015), (115), (016) and (206). Moreover no α'-crystals coexisted with α-crystals as no reflection was discernible at nearby 2θ = 24.5°. This observation is consistent with the DSC analyses because the existence of α'-crystals in the material generally leads to a small exotherm just before the melting transition; no such exothermic peak was detected except for neat PLLA.[20] This crystalline structure investigation demonstrates the passive role of PRic on PLLA crystallization in terms of crystalline phase. Nevertheless, variations were found regarding the crystallite size. Indeed, the width at half-height of the reflection peak is directly linked to the crystallite size (the larger the width the smaller size of the crystallites). By observing the width at half-height of the (203) reflection peak, an obvious increase in the peak width with an increase in the PRic content is noticed. Consequently, high contents of PRic in the copolymer structure tend to lower the crystallite size of the PLLA phase. This observation is in agreement with the DSC traces displayed in Figure 7.4.

III.4. Solid-state morphology

It is well established that two blended polymers of different chemical nature generally tend to segregate due to interfacial tensions that can be evaluated by the Flory-Huggins interaction

parameter, χ.[21, 22] This thermodynamic repulsion is also valid for block copolymers between the covalently bonded chains which provokes microphase segregation below the order-disorder transition temperature (T_{ODT}). This phase segregation can lead to various morphologies depending on the temperature, the molar mass of the copolymer and the ratio of the different blocks. However some parameters can disturb these characteristic morphologies. For instance, crystallization can highly affect the nano-organization of these materials leading to crystalline lamellae, notably for weak-segregated semi-crystalline copolymers.[23-26] The morphology of PLLA-*b*-PRic-*b*-PLLA triblock copolymers was first investigated in the melted state to avoid crystallization. To that aim, the samples were heated for 3 minutes at 10°C above the melting point of PLLA blocks and then quenched in liquid nitrogen to study the melted state morphology. Copolymer samples were then analyzed by small-angle X-ray scattering. Diffractograms are displayed in Figure 11.4 and revealed different morphologies depending on the copolymer composition. H83 and H71 exhibited phase-separated morphologies consisting of cylindrical domains rich in PRic surrounded by a matrix of PLLA. The first- and higher- order diffraction peaks show the position ratio of 1:√3:√7 for H83 and 1:2:√7:√9 for H71. When increasing PRic wt% in the copolymer, the morphology changes from cylindrical to lamellar, as seen from the periodic behavior of the diffraction peaks. Indeed SAXS curves of H63 and H53 show three shoulders with the position ratio of 1:2:3:4. This observation is in accordance with the phase diagram predicted by self-consistent field theory.[27] Concerning H45, we were not able to conclude about the melt morphology because the only higher-order diffraction peak was broad. However, this peak was in the range between the peak ratios 1:√7 and 1:3 suggesting a cylindrical or lamellar phase. Finally, H35 displays no significant diffraction peaks for higher orders probably due to the molecular weight being too low to allow clear segregation in defined morphologies. The principal domain spacing was qualitatively evaluated by the value of q for each sample. The principal domain spacing increased (q decreased) with an increase in the PLLA content (except for H83 where q increased compared to H71) which is consistent with variation in morphological transitions and enhancement of PLLA molecular weight.[28, 29] In order to investigate how crystallization of PLLA can disturb the copolymer phase segregation, the samples were crystallized at 120°C for 2 hours. This annealing temperature was chosen to favor α-crystal formation.

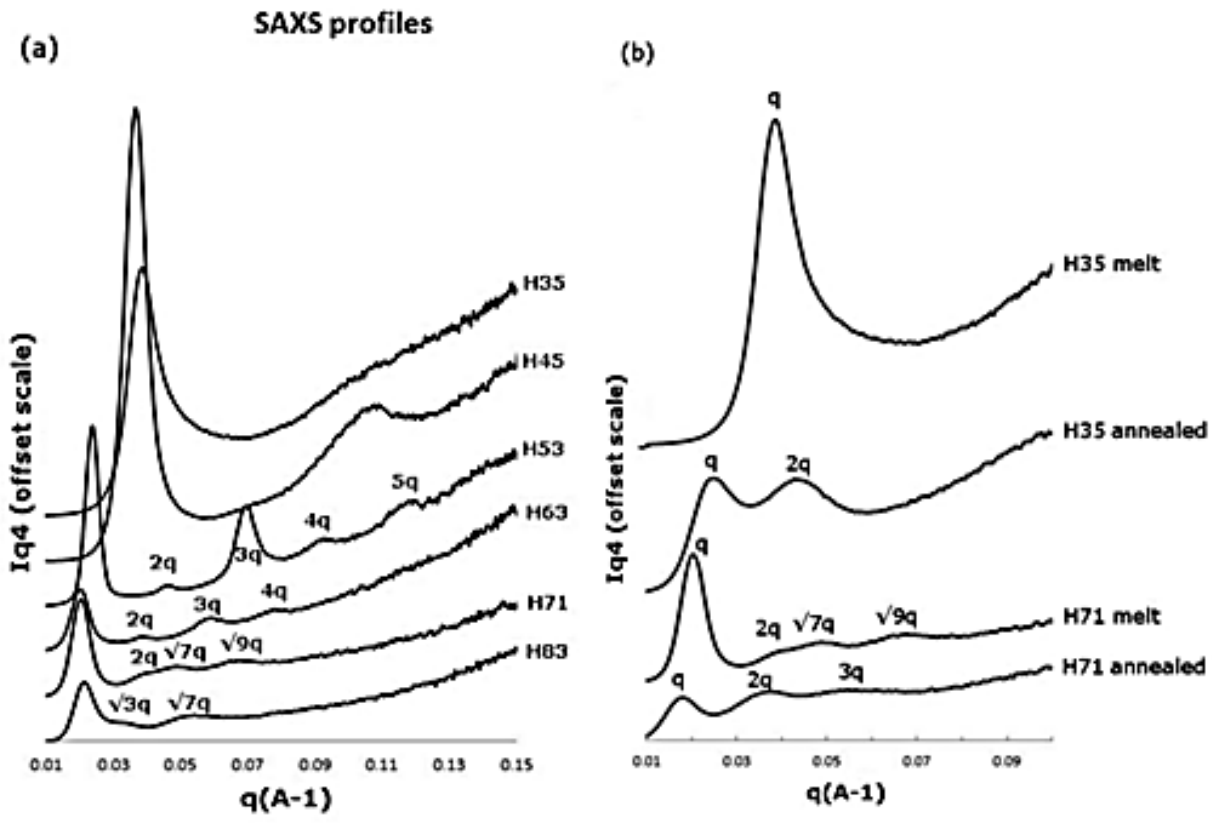

Figure 11.4.SAXS diffractograms of PLLA-b-PRic-b-PLLA block copolymers (a) in the melted state and (b) after annealing.

Figure 11.4b displays the SAXS profiles of H35 and H71 that were annealed as well as the profiles of the samples in the melted state. It can be seen for H71 that the periodic diffraction peaks of the cylindrical phase were absent in the case of the annealed samples, suggesting a dramatic change of the copolymer nano-organization. The position ratio of the diffraction peaks changes to 1:2:3, indicating the crystallization of PLLA into lamellar crystallites. H35 showed similar behavior when annealed at 120°C with diffraction peaks at position 1:2. This investigation demonstrated that all these samples exhibited low segregation strength because the driving force of crystallization overwhelmed phase segregation. Concerning the periodic spacing of the annealed samples, its value increased with an increase in PLLA content which is logically attributed to the enhancement of the total molecular weight of the copolymers. To further investigate PLLA crystallization in the copolymer, all samples were observed by polarized optical microscopy. To that aim, thin films were produced from copolymer solutions in dichloromethane. These films were completely melted at a temperature 10°C higher than the melting point, and were then cooled to 120°C for isothermal crystallization during 2 hours. The morphologies of some samples are shown in Figure 12.4.

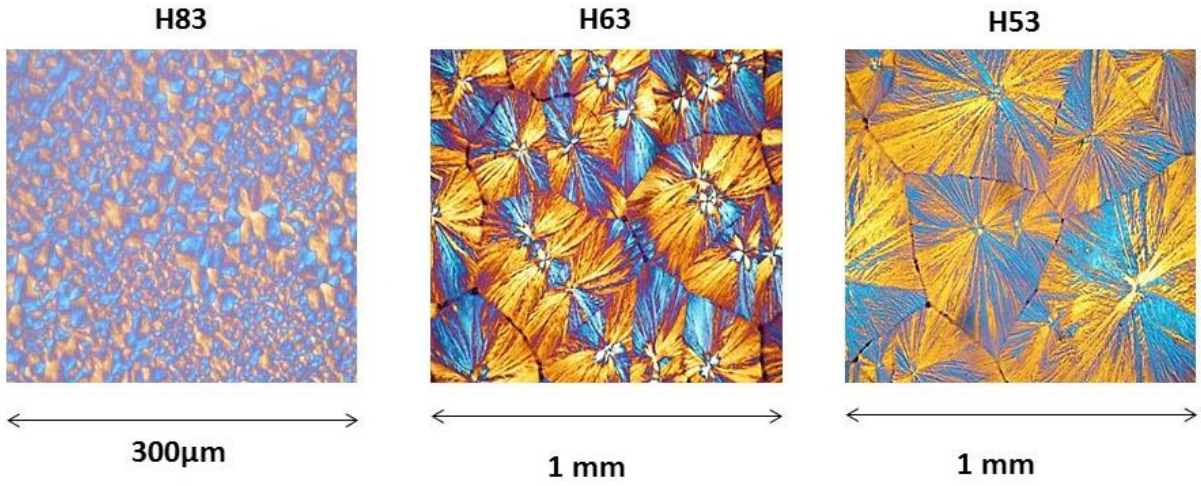

Figure 12.4.Polarized optical micrographs of PLLA-b-PRic-b-PLLA block copolymers H83, H63 and H53.

For all copolymers, spherulitic morphologies were observed in accordance with literature data for PLLA and its copolymers. However, we noticed some variations in the mean size of spherulites depending on the copolymer composition. The diameter of the spherulites increases with a decrease in PLLA weight percentage in the copolymer. This observation suggests that a larger number of nuclei are generated when the weight percentage of PLLA is high, giving rise to a larger quantity of spherulites.

We were also interested in evaluating the morphological differences inside the spherulite structures in order to evaluate the influence of the PRic segment on the space filling. To that aim, we used atomic force microscopy (AFM) on annealed samples. AFM phase images are shown in Figure 13.4 and revealed lamellar structures in all the copolymers even in the case of H35 and H45 in which high amounts of amorphous segments are present. Moreover, the predominantly radial orientation of the lamellas confirmed the birefringence pattern observed by optical microscopy. Highly packed lamellas were observed for neat PLLA, H83 and H71 with the presence of spiral terraces (flat on) indicative of screw dislocations which are one of the factors that lead to space filling in spherulites.[30] However, these twisted lamellas were irregular and disappeared from H63 to H35 suggesting a lower crystallinity for a high content of soft segments in the copolymer. The internal morphologies of spherulites for H83, H71, H63 and H53 were interpreted as PLLA crystalline lamellas separated by interlamellar amorphous PLLA and PRic segments. This behavior is in accordance with what is generally observed for weak-segregated systems. AFM images of H45 show the coexistence of crystalline domains characterized by clear lamellas and nano-segregated domains with non-organized spheres or cylinders (Figure 14.4.a).

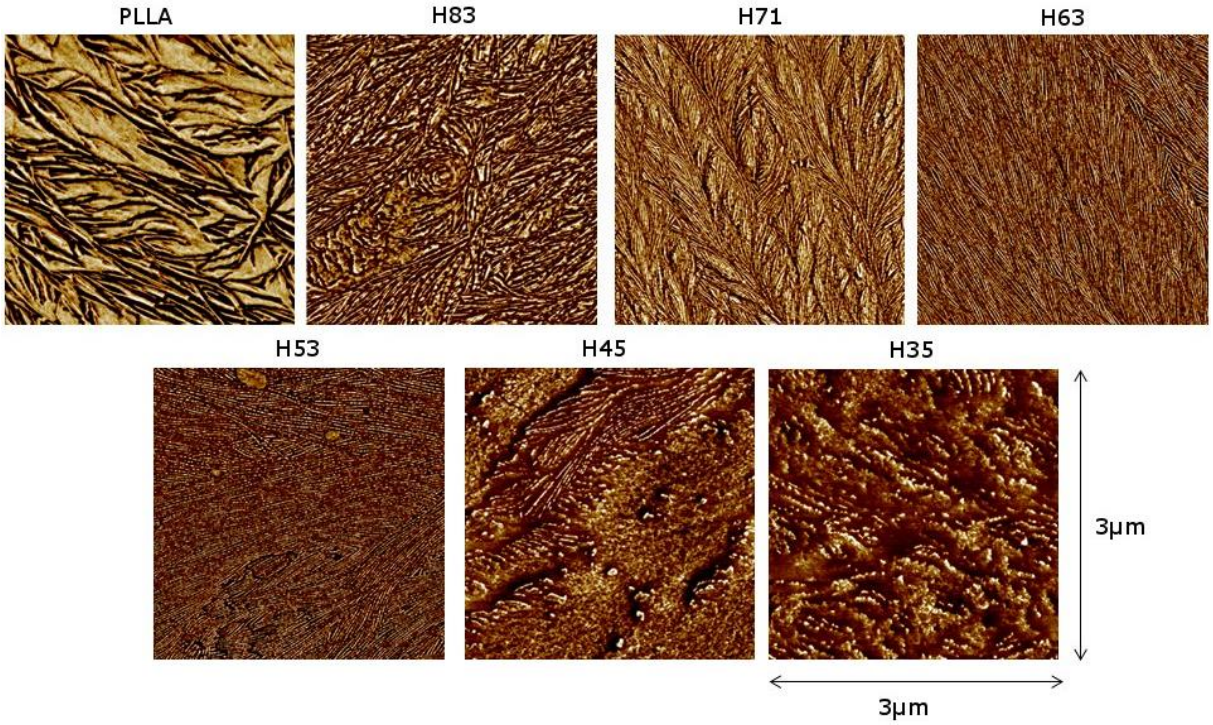

Figure 13.4.AFM images of annealed PLLA and PLLA-b-PRic-b-PLLA block copolymers.

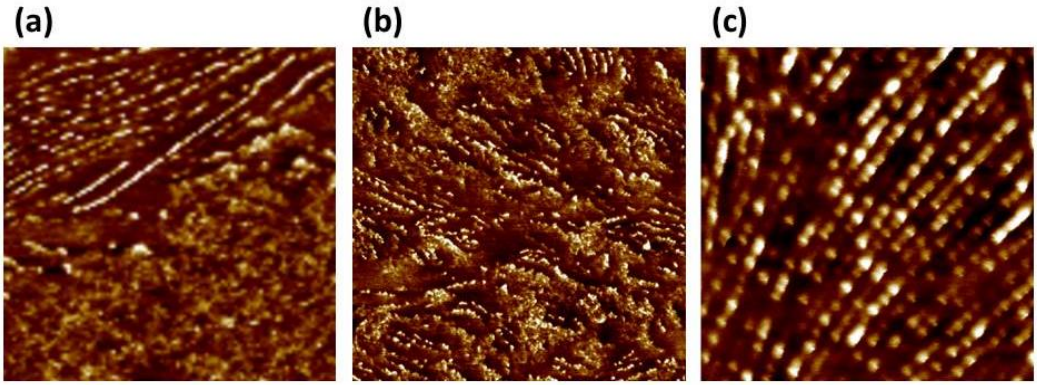

Figure 14.4.AFM images of (a) annealed H45 (1µm*1µm), (b) annealed H35 (3µm*3µm), and (c) annealed H53 (500nm*500nm).

This is due to the low crystallinity of PLLA blocks in the H45 sample, coupled with a weak-segregated system. A similar morphology was observed for H35, with in addition some partially miscible domains (Figure 14.4.b). Furthermore, the lamellae of H53, H45 and H35 were more fragmented and acquired a segmented appearance like a string of beads (Figure 14.4.c)**.** This behavior was not investigated; however one can make the hypothesis of lamellae twisting or bending due to the effect of high amorphous content in the central block of the copolymer.[31] The high resolution of the AFM allowed us to measure the lamella thickness by making the estimation that all lamellae were on the edge. Graphs of phase as a function of distance are displayed in Figure 15.4 with the corresponding AFM images that reveal an increase in the packing density of the lamellae with an increase in hard block content in the copolymer.

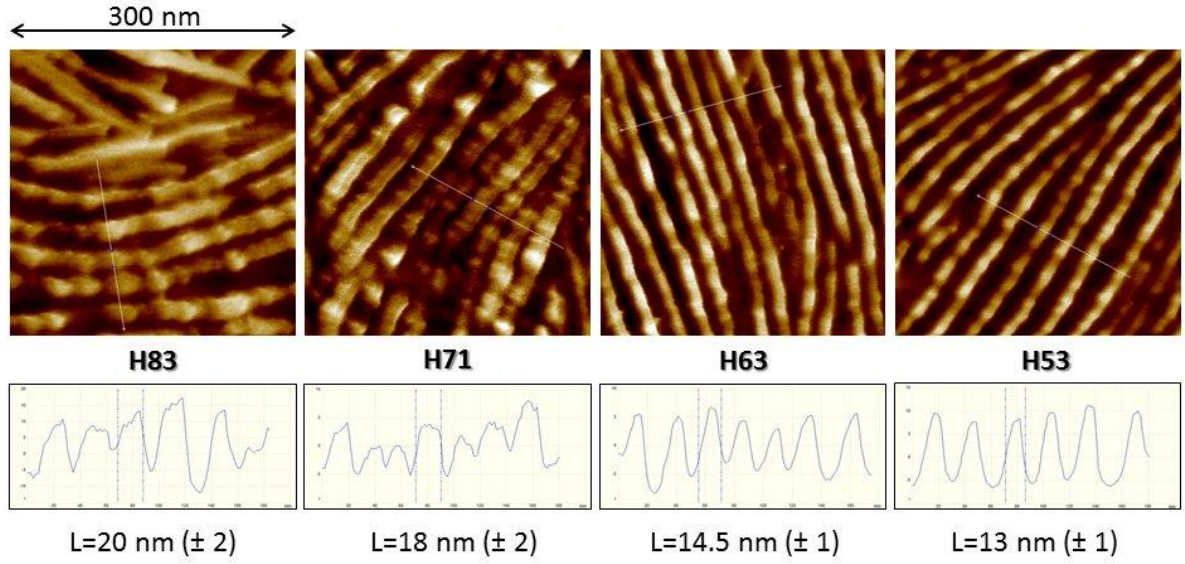

Figure 15.4.Phase profiles and AFM images of annealed H83, H71, H63 and H53.

Lamellar thickness values range from 20 nm for H83 to 13nm for H53. This observation is in accordance with what was expected due to the accommodation of a larger fraction of amorphous material in the interlamellar regions for higher soft block content. However, special care has to be taken when interpreting these data due to heterogeneity in lamellar orientations for highly crystalline block copolymers (H83 and H71) that can induce error in the measurement.

III.5. Dynamic-mechanical analysis

Dynamic mechanical analysis was performed on each annealed sample in order to evaluate the viscoelasticity of these copolymers. In Figure 16.4, the storage modulus and the loss tangent are represented as a function of temperature.

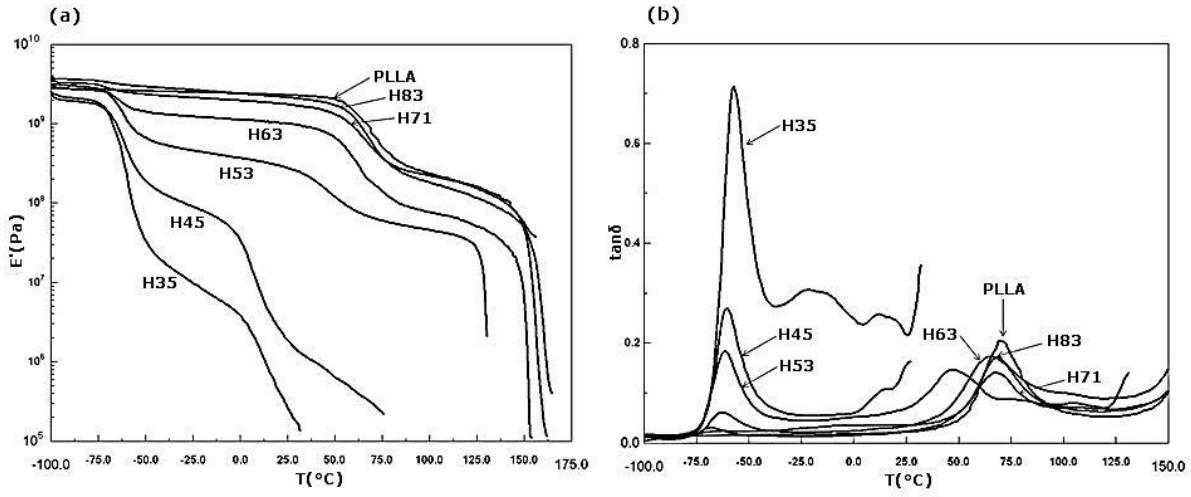

Figure 16.4.(a) Storage modulus and (b) tanδ as a function of temperature for annealed (2h at 120°C) PLLA and PLLA-b-PRic-b-PLLA block copolymers.

Three primary relaxations were observed in the temperature range examined. Two were assigned to the amorphous α-relaxation of each block and one was identified as the crystalline relaxation of PLLA blocks. A first variation of storage modulus at around -60°C was assigned to the α-relaxation of the PRic segment. The intensity of this α-relaxation increases with the amount of PRic, as observed on the intensity of tanδ corresponding to this temperature (Figure 16.4.b). The temperature value corresponding to this transition was not significantly shifted to higher temperature when a higher amount of PLLA hard block was fixed, except for H45 and H35 which shows a slight increase in the value of this temperature. This observation shows that soft block mobility was not reduced by the restrictions imposed by the crystalline phase.[24] However, in the case of the second variation of storage modulus corresponding to PLLA α-relaxation, a decrease in the transition temperature was noted for high contents of PRic in the copolymer structure. This suggests that the PLLA block mobility was enhanced due to both effects of partial miscibility of the different blocks and diminution of the molecular weight of the copolymers with a higher content of PRic. The intensity of the α-relaxation of the PLLA segment varied with the composition of the copolymer. In fact, for high amounts of PLLA, the storage modulus decreases moderately suggesting that the PLLA content in the amorphous phase was quite low. However, for low amounts of PLLA, the storage modulus is lowered, suggesting a low crystallinity of PLLA blocks. This confirms the crystallinity ratios measured by DSC. The last transition related to the crystalline relaxation of PLLA blocks was observed around 150°C which corresponds to the beginning of the PLLA crystalline lamellas melting process. This temperature value was revealed to decrease with higher amounts of PRic due to a decrease in lamellar thickness.

III.6. Tensile properties

Tensile analyses were performed using a strain rate of 1 $mm.min^{-1}$ (Figure 17.4). The tensile properties listed in Table 5.4 include the Young's modulus, the yield stress, the ultimate stress and the ultimate strain. As a blank, neat PLLA was analyzed and stress-strain curves showed brittle behavior with an elongation at break of 5.2%. By increasing the PRic soft block content in the copolymer, the Young's modulus decreased as well as the yield stress. The Young's Modulus dropped from 749 MPa for H83 to 3 MPa for H35. Elongation at break increased drastically for H83 and H71 in comparison to neat PLLA showing the efficiency of soft block incorporation to toughen PLLA. By incorporation of 17wt% of PRic in the triblock structure, the ultimate strain increased from 5% to 98%. H71 also exhibits a high elongation

at break. However for samples with higher soft block content, ultimate strain decreases to values between 10 and 20%.

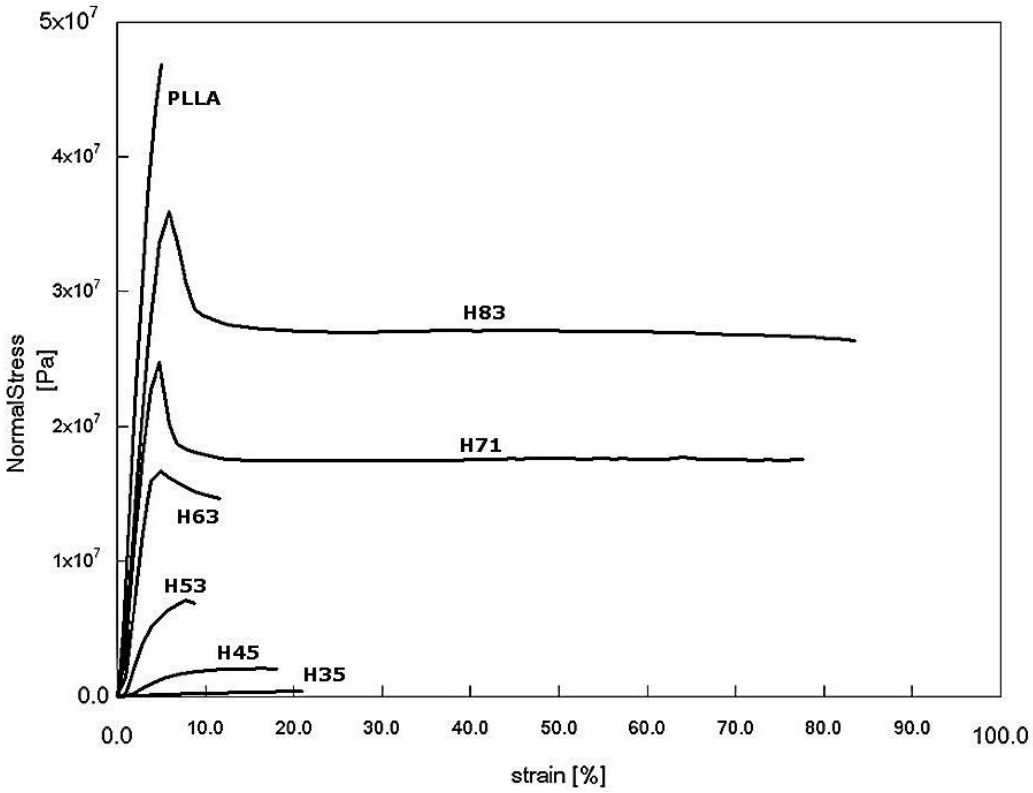

Figure 17.4.Stress-strain curves of PLLA and PLLA-b-PRic-b-PLLA block copolymers – 1 mm.min^{-1}.

This behavior can be explained by the dependency of mechanical properties on the molar mass.[32] By increasing the total molar mass of the copolymer while maintaining a similar block ratio, we could expect higher elongations at break. Thus, the toughening of PLLA proved to be efficient considering the elongation at break obtained for H83 and H71.

Table 5.4.Tensile properties of PLLA and PLLA-b-PRic-b-PLLA block copolymers-1mm.min^{-1}.

	E modulus (Mpa)	Yield stress (Mpa)	Stress at break (Mpa)	Strain at break (%)
Neat PLLA	1062 ± 128	43 ± 6	43 ± 6	5.2 ± 0.9
H83	749 ± 47	36 ± 3	25 ± 2	97.9 ± 33.4
H71	827 ± 93	27 ± 2	19 ± 1	94.8 ±24.3
H63	670 ± 90	19 ± 2	14 ± 2	15.8 ± 5.2
H53	147 ± 49	6 ± 1	6 ± 1	9.3 ± 1.3
H45	42 ± 6	2.4 ± 0.3	2.4 ± 0.3	17.0 ± 4.2
H35	3 ± 1	0.4 ± 0.2	0.4 ± 0.2	21.5 ± 2.5

IV. CONCLUSION

In summary, new entirely bio-based PLLA-*b*-PRic-*b*-PLLA triblock copolymers were obtained by a two-step procedure: self-polycondensation of methyl ricinoleate in the presence of a low amount of 1,3-propanediol leading to a hydroxyl-telechelic prepolyester HO-PRic-OH, followed by ring-opening polymerization of L-lactide from the hydroxyl functions. The number average molar mass of the copolymers so-formed was in the range 13 to 61 $kg.mol^{-1}$ and the thermo-mechanical properties were highly dependent on the chemical composition of the copolymer. The thermal degradation of the polymers was found to occur in the range 190 to 235°C for the temperature corresponding to 5% weight loss. For this reason, copolymers with a high amount of PLLA are preferable due to their better thermal stability. DSC analyses showed that the soft segment had a moderate effect on the thermal properties of the PLLA end blocks. The block structure of the copolymer enabled conservation of relatively high PLLA crystallinity and melting point after annealing. However, the PLLA crystallization kinetics were rather slow for high contents of soft block in the copolymer indicating a significant effect of PRic on the nucleation step. The crystalline structures of the copolymers were investigated by WAXD, which revealed no influence of the PRic block content on the PLLA crystalline phase. SAXS analyses showed different morphologies for melted and annealed samples. While the incompatibility of the different blocks dictates the phase segregation in the melt, after annealing the segregation of the non-crystallizable PRic blocks into the interlamellar regions is governed by crystallization of PLLA hard blocks. This behavior was confirmed by AFM images as seen from intern spherulite lamellar structures. A high degree of separation of hard and soft phases in the solid state for all the block copolymers was confirmed by distinct and separate α-relaxations, as demonstrated by dynamic mechanical analyses. Tensile properties range from thermoplastic to elastomeric depending on the block copolymer composition. This study proves the feasibility of environmentally friendly solutions for PLLA toughening by using castor oil derived polyester.

In the bibliographic chapter, we mentioned the high cost of production as the main limitation to the use of block copolymers as commodity and specialty plastics (they are generally used for high performance applications). Nevertheless, past researches focusing on the reactive extrusion of lactide yielded promising results in term of monomer conversion, polymerization control and reaction time.[33-35] Consequently we could think about the formation of economically viable PLLA-based materials by reactive extrusion of blends between PRic macroinitiator and lactide. Moreover, the highly hydrophobic behavior of PRic could help

preventing side reactions in the extruder caused by moisture. This strategy would lead to nano-structured PLLA materials showing unique properties (improved ductility).

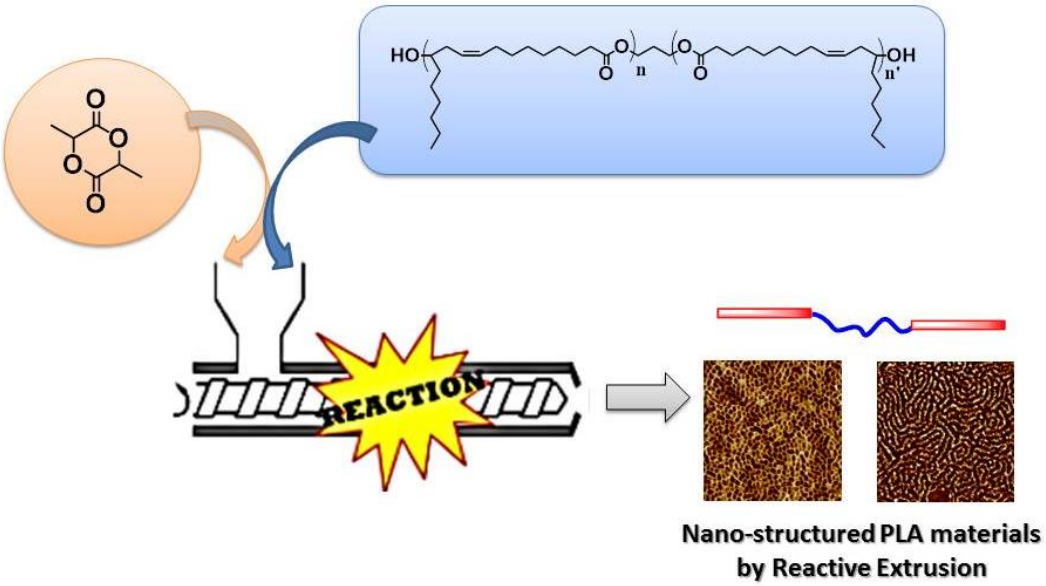

Figure 18.4. Possible reactive extrusion of lactide with PRic macroinitiator as a perspective to cheaper materials.

V. EXPERIMENTAL

1. Synthesis of hydroxy telechelic poly(ricinoleic acid) (HO-PRic-OH) macro-initiator.

A mixture of purified methyl ricinoleate (5g, 16mmol), 1,3-propanediol (73mg, 0.96mmol) and titanium tetra-n-butoxide (54mg, 0.16mmol) was stirred at 140°C under nitrogen atmosphere. After 1h, a dynamic nitrogen flow was applied followed by 2 hours under dynamic vacuum. The temperature was then raised to 180°C for 20 hours. After completion of the reaction, the polyester was dissolved in dichloromethane, precipitated into methanol, filtered and dried under reduced pressure. Di-hydroxy poly(ricinoleic acid), HO-PRic-OH, was obtained as a yellowish viscous liquid.

2.Synthesis of poly(L-lactide)-*b*-poly(ricinoleic acid)-*b*-poly(L-lactide) triblock copolymers (PLLA-*b*-PRic-*b*-PLLA).

The triblock copolymers PLLA-*b*-PRic-*b*-PLLA were synthesized by ring-opening polymerization of L-lactide using dihydroxyl-telechelic poly(ricinoleic acid) HO-PRic-OH as macro-initiator. HO-PRic-OH was dried at 70°C under dynamic vacuum overnight. The desired amounts of HO-PRic-OH and L-lactide were added to a two-necked round bottom flask equipped with a condenser, a nitrogen inlet and a mineral oil bubbler. The solution polymerization in dry toluene (0.1g/mL) proceeded at reflux under nitrogen atmosphere for 2 to 4 hours upon addition of tin octoate (0.5 wt%). After completion of the reaction, toluene

was removed under reduced pressure and the copolymer was recovered by precipitating a concentrated dichloromethane solution into cold methanol and drying overnight at 50°C under reduced pressure.

3. Synthesis of neat PLLA.

PLLA was synthesized by ring-opening polymerization of L-lactide using 1,3-propanediol and tin octoate as initiating system. 1,3-propanediol (12mg, 0.16mmol) and L-lactide (15.7g, 109mmol) were added to a two-necked round bottom flask equipped with a condenser, a nitrogen inlet and a mineral oil bubbler. The solution polymerization in dry toluene proceeded at reflux under nitrogen atmosphere for 2 to 4 hours upon addition of tin octoate (0.5wt%). After completion of the reaction, toluene was removed under reduced pressure and the copolymer was recovered by precipitating a concentrated dichloromethane solution into cold methanol and drying overnight at 50°C under reduced pressure.

REFERENCES

1. D. S. Ogunniyi, *Bioresource Technology*, 2006, **97**, 1086-1091.
2. H. Mutlu and M. A. R. Meier, *European Journal of Lipid Science and Technology*, 2010, **112**, 10-30.
3. Y. Xu, Z. Petrovic, S. Das and G. L. Wilkes, *Polymer*, 2008, **49**, 4248-4258.
4. Z. S. Petrović, I. Cvetković, D. Hong, X. Wan, W. Zhang, T. Abraham and J. Malsam, *Journal of Applied Polymer Science*, 2008, **108**, 1184-1190.
5. H. Ebata, K. Toshima and S. Matsumura, *Macromolecular Bioscience*, 2007, **7**, 798-803.
6. Z. Petrović, Y. Xu, J. Milić, G. Glenn and A. Klamczynski, *Journal of Polymers and the Environment*, 2010, **18**, 94-97.
7. R. Slivniak and A. J. Domb, *Macromolecules*, 2005, **38**, 5545-5553.
8. R. Slivniak and A. J. Domb, *Biomacromolecules*, 2005, **6**, 1679-1688.
9. M. L. Robertson, J. M. Paxton and M. A. Hillmyer, *ACS Applied Materials & Interfaces*, 2011, **3**, 3402-3410.
10. R. K. Saxena, P. Anand, S. Saran and J. Isar, *Biotechnology Advances*, **27**, 895-913.
11. H. Biebl, K. Menzel, A. P. Zeng and W. D. Deckwer, *Applied Microbiology and Biotechnology*, 1999, **52**, 289-297.
12. A. T. Lorenzo, M. L. Arnal, J. Albuerne and A. J. Müller, *Polymer Testing*, 2007, **26**, 222-231.
13. P. Pan, W. Kai, B. Zhu, T. Dong and Y. Inoue, *Macromolecules*, 2007, **40**, 6898-6905.
14. W. Hoogsteen, A. R. Postema, A. J. Pennings, G. Ten Brinke and P. Zugenmaier, *Macromolecules*, 1990, **23**, 634-642.
15. J. Kobayashi, T. Asahi, M. Ichiki, A. Oikawa, H. Suzuki, T. Watanabe, E. Fukada and Y. Shikinami, *Journal of Applied Physics*, 1995, **77**, 2957-2973.
16. B. Eling, S. Gogolewski and A. J. Pennings, *Polymer*, 1982, **23**, 1587-1593.
17. J. Puiggali, Y. Ikada, H. Tsuji, L. Cartier, T. Okihara and B. Lotz, *Polymer*, 2000, **41**, 8921-8930.
18. L. Cartier, T. Okihara, Y. Ikada, H. Tsuji, J. Puiggali and B. Lotz, *Polymer*, 2000, **41**, 8909-8919.
19. P. Pan and Y. Inoue, *Progress in Polymer Science*, 2009, **34**, 605-640.
20. J. Zhang, K. Tashiro, H. Tsuji and A. J. Domb, *Macromolecules*, 2008, **41**, 1352-1357.
21. E. Helfand and Y. Tagami, *The Journal of Chemical Physics*, 1972, **56**, 3592-3601.
22. E. Helfand, S. M. Bhattacharjee and G. H. Fredrickson, *The Journal of Chemical Physics*, 1989, **91**, 7200-7208.
23. C.-H. Ho, G.-W. Jang and Y.-D. Lee, *Polymer*, 2010, **51**, 1639-1647.
24. H. P. Wang, D. U. Khariwala, W. Cheung, S. P. Chum, A. Hiltner and E. Baer, *Macromolecules*, 2007, **40**, 2852-2862.
25. W.-N. He and J.-T. Xu, *Progress in Polymer Science*, 2012, **37**, 1350-1400.
26. H. C. Moon, D. Bae and J. K. Kim, *Macromolecules*, 2012, **45**, 5201-5207.
27. M. W. Matsen and R. B. Thompson, *The Journal of Chemical Physics*, 1999, **111**, 7139-7146.
28. M. W. Matsen and F. S. Bates, *The Journal of Chemical Physics*, 1997, **106**, 2436-2448.
29. L. M. Pitet and M. A. Hillmyer, *Macromolecules*, 2009, **42**, 3674-3680.
30. M. Kanchanasopa, E. Manias and J. Runt, *Biomacromolecules*, 2003, **4**, 1203-1213.
31. C.-C. Chao, C.-K. Chen, Y.-W. Chiang and R.-M. Ho, *Macromolecules*, 2008, **41**, 3949-3956.
32. J. Cai, C. Liu, M. Cai, J. Zhu, F. Zuo, B. S. Hsiao and R. A. Gross, *Polymer*, 2010, **51**, 1088-1099.
33. S. Jacobsen, H. G. Fritz, P. Degée, P. Dubois and R. Jérôme, *Polymer*, 2000, **41**, 3395-3403.
34. S. Jacobsen, H. G. Fritz, P. Degée, P. Dubois and R. Jérôme, *Polymer Engineering & Science*, 1999, **39**, 1311-1319.
35. J.-M. Raquez, P. Degée, Y. Nabar, R. Narayan and P. Dubois, *Comptes Rendus Chimie*, 2006, **9**, 1370-1379.

CHAPTER 5:

Fatty acids as raw materials for the design of novel block copolymers and "LLDPE like" polyesters by ADMET. Evaluation of their potential as PLLA impact modifiers.

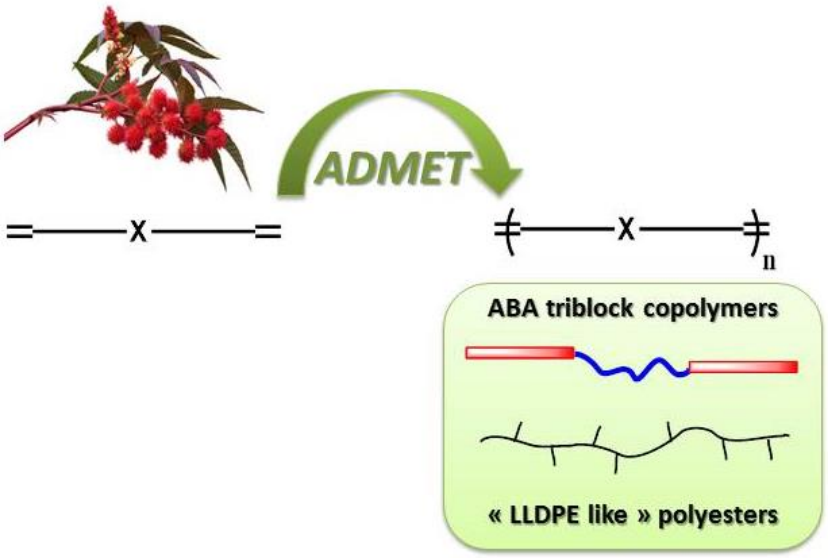

Keywords: fatty acids, castor oil, α,ω-diene, ADMET, block copolymer, green solvent, urethane, ester, carbonate, ether, amide, PLLA, LLDPE, VLDPE, polyester.

Mots clés: acides gras, huile de ricin, dienes α,ω, ADMET, copolymère à bloc, solvant vert, uréthane, ester, carbonate, éther, amide, PLLA, polyéthylène linéaire basse densité, polyéthylène très basse densité, polyester.

In the previous chapters, we reported the development of low Tg polyesters by the classical route, namely the polycondensation of hydroxyacids or the polycondensation of diols with diacids (or diesters). In this chapter, we investigated the use of metathesis polymerization as an alternative to most common synthetic routes to polyesters.

Since its first reports in the mid-1950s, olefin metathesis has shown a constant development especially thanks to the discovery of the reaction mechanism by Chauvin and coll. in 1971 and the development of efficient metathesis catalysts by the groups of Schrock and Grubbs in the 1990s.[1-5] Since then, a multitude of chemical transformations were developed and applied to various substrates by self-metathesis (SM), cross-metathesis (CM), ring-closing metathesis (RCM) and ring-opening metathesis (ROM). Metathesis was also applied to polymerization methods such as ring-opening metathesis polymerization (ROMP) and acyclic diene metathesis polymerization (ADMET).[6-8] In this chapter, special attention has been paid to the ADMET approach for the formation of fatty acid-based polymers. ADMET is a step-growth polymerization driven by the release of a condensate which is generally ethylene (easy to remove); thus monomers bearing terminal olefins are needed.

Herein, two strategies were employed for the potential toughening of PLLA by using ADMET polymerization. In a first study, ABA triblock copolymers formation was investigated. Various α,ω-dienes were first prepared from the 10-undecenoic acid platform. The versatility of ADMET methodology allowed us to synthesize polyesters, polyurethanes, polycarbonates, polyethers and polyamides. The use of these functional polymers as middle soft segment in ABA block copolymers where A block is PLLA was then investigated.

In a second study, ADMET polymerization was used to develop aliphatic polyesters which mimic the structure of linear low-density polyethylene (LLDPE), the latter being commonly used for the rubber-toughening of PLLA. Castor oil and vernonia oil platforms were used to synthesize two α,ω-diene monomers, one linear and one bearing an hexyl branch. Their copolymerization in various amounts allowed us to develop a series of “LLDPE like” polyesters.

PART A. INVESTIGATION OF PLLA-BASED TRIBLOCK COPOLYMERS FORMATION WITH TUNABLE MIDDLE SOFT SEGMENT

I. INTRODUCTION

In the first chapter, block copolymer strategy was mentioned as an efficient methodology to toughen PLLA. Various synthetic approaches were used in the literature to design PLLA block copolymers covering a large range of mechanical properties (from elastomeric to stiff materials). The most commonly used synthetic route is undoubtedly the sequential ROP of lactones and lactide. However, this approach does not enable the easy incorporation of organic functionalities in the backbone of the central block, necessary to tune the properties of the final material.

The emergence of highly tolerant metathesis catalysts in the 1990's enabled the use of functional monomers in ADMET polymerization and afforded new pathways to various polymeric systems.[9] ADMET polymerization was already reported for the synthesis of fatty-acid based polyesters, polyamides, polyethers and polycarbonates, which shows the great versatility of this polymerization method.[6, 10-13] Thus, it is thinkable that ADMET methodology could be a convenient way to synthesize ABA triblock copolymers where B would be a soft middle block and A would be PLLA.

The synthesis of functional α,ω-diene monomers and their subsequent polymerization were first performed by varying the reaction conditions. Once the reaction conditions established, block copolymerization was then investigated by two different approaches; either by the synthesis of dihydroxyl telechelic prepolymers or by direct chain transfer by a terminal alkene-functionalized PLLA.

II. SYNTHESIS OF BIOBASED α,ω-DIENES

In order to develop a set of novel triblock copolymers with a tunable middle soft segment, α,ω-dienes bearing various central organic functions were synthesized as ADMET precursors. The 10-undecenoic acid platform (10-undecenoic acid, 10-undecenol and 11-bromo-undecene) was employed to synthesize various α,ω-diene precursors ranging from urethane, ester, carbonate, ether and amide ones.

II.1. α,ω-diene urethane (1)

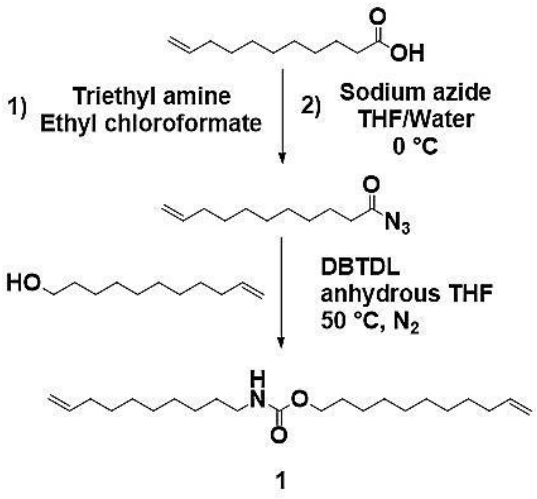

Scheme 1.5. Synthetic pathway to α,ω-diene urethane monomer

A two-step methodology was applied for the synthesis of the urethane monomer (Scheme 1.5). First, 10-undecenoic acid was reacted with ethyl chloroformate in the presence of triethylamine to form *in-situ* anhydride which then reacted with sodium azide to obtain the acyl azide compound. Completion of the reaction was monitored by FTIR-ATR (Figure 1.5).

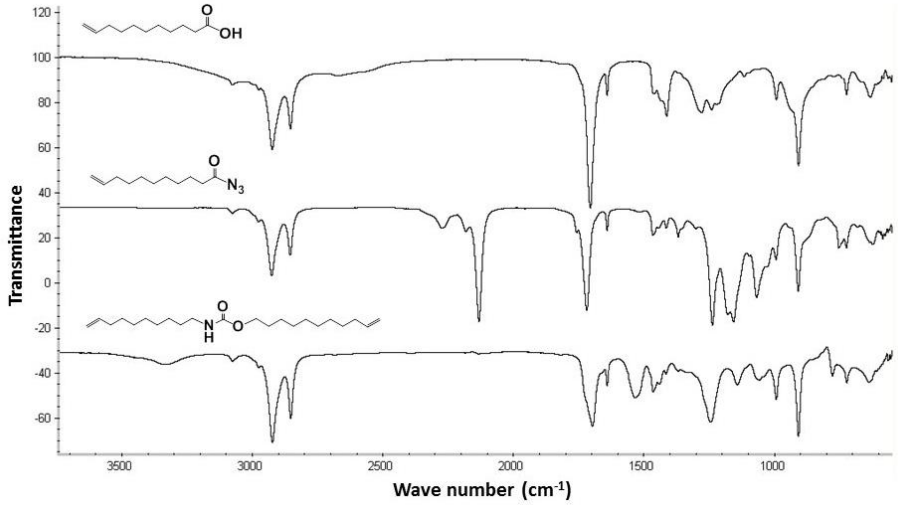

Figure 1.5. FTIR-ATR stacked spectra of 10-undecenoic acid, 10-undecenoyl azide and bis-unsaturated urethane.

The spectrum revealed the appearance of bands at 1720cm^{-1}, 2120cm^{-1} and 2300cm^{-1} which are attributed to acyl azide C=O stretching, N_3 bending, and isocyanate N=C=O stretching modes. This analysis shows that a small fraction of the acyl azide intermediate rearranged into the isocyanate compound (26% - determined by ^{1}H-NMR) by a Curtius-rearrangement. It was also confirmed by ^{1}H-NMR spectroscopy with the appearance of a signal at 3.28 ppm related to protons near the isocyanate group (Figure 2.5). However the presence of isocyanate does

not disturb our synthetic strategy as the latter will be also converted in the second step to the expected urethane.

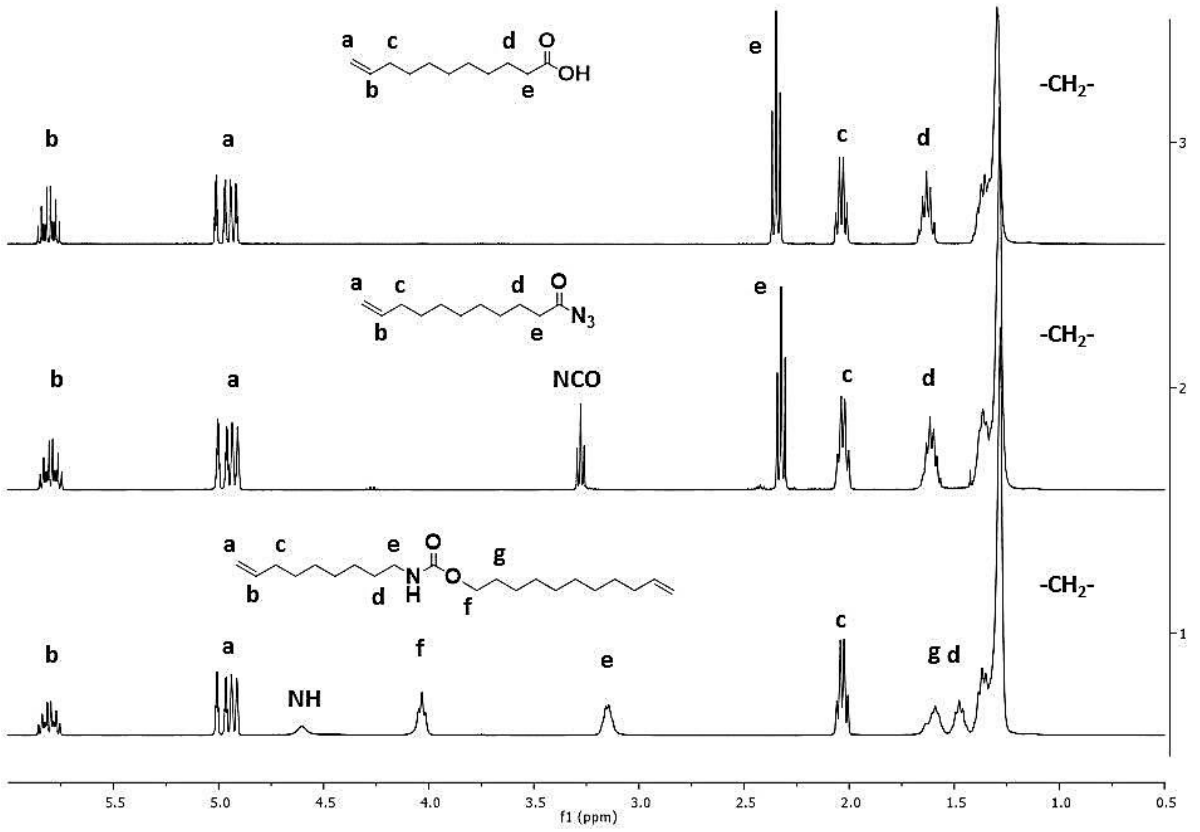

Figure 2.5. ^{1}H-NMR stacked spectra of 10-undecenoic acid, 10-undecenoyl azide and bis-unsaturated urethane (1) in $CDCl_3$.

The α,ω-diene urethane monomer (**1**) was then obtained by Curtius rearrangement with 10-undecenol. Its structure was confirmed by FTIR-ATR analysis (Figure 1.5) as well as NMR spectroscopy (Figure 2.5). FTIR spectrum of (**1**) displays one band at 1700cm^{-1} related to the C=O stretching of urethane function and a broad band at 3300cm^{-1} related to NH bending. Regarding ^{1}H-NMR spectrum of (**1**), neither acyl azide nor isocyanate has been observed after purification. New peaks appeared at 3.08, 3.97 and 4.54 ppm which are assigned respectively to the protons in α position of the urethane linkage as well as to the proton attached to the nitrogen atom. GC analysis was not possible on this compound; however, ^{1}H-NMR spectra shows good purity as evidenced by the absence of side products thus allowing the ADMET polymerization of this α,ω-diene monomer.

II.2. α,ω-diene ester (2)

An α,ω-diene ester (**2**) was also synthesized by a simple transesterification of methyl 10-undecenoate with 10-undecenol in bulk catalysed by TBD as reported by Meier and coll.[10]

After completion of the transesterification and after purification by column chromatography, the structure of (**2**) was confirmed by ^{1}H-NMR spectroscopy (Figure 3.5). Indeed, the appearance of a peak at 4.05 ppm assigned to the protons in α position of the oxygen atom of the ester function is observed. This clearly demonstrated the formation of ester linkage between 10-undecenol and methyl 10-undecenoate. The purity obtained by GC was 99% thus allowing the ADMET polymerization of this monomer.

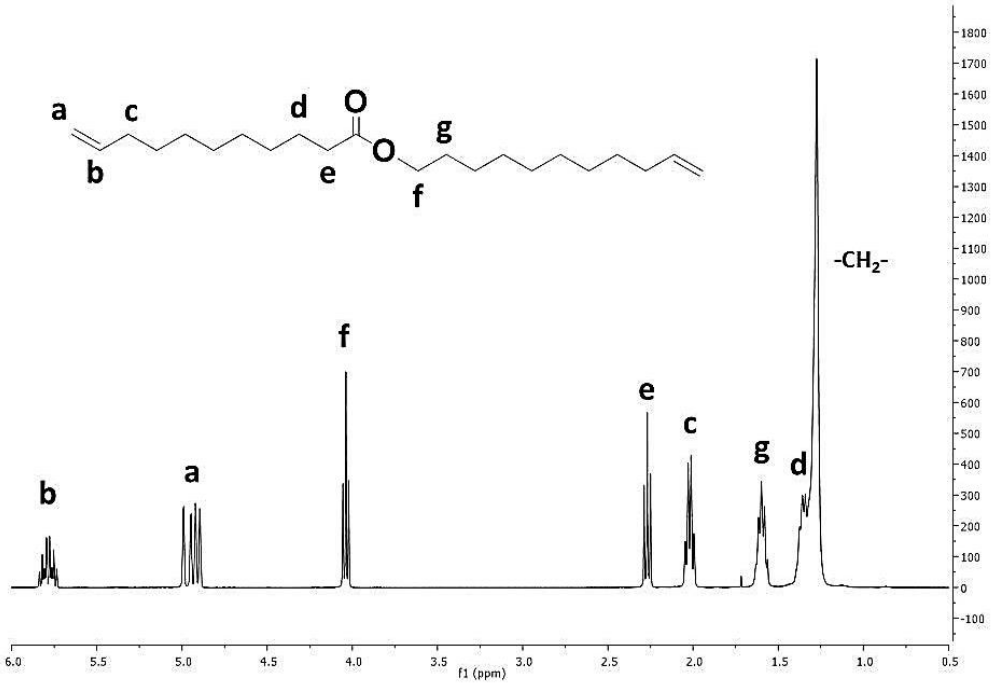

Figure 3.5. ^{1}H-NMR spectra of the bis-unsaturated ester (2) in $CDCl_3$.

II.3. α,ω-diene carbonate (3)

Recently, Meier and coll., described the synthesis of various carbonate molecules by using a TBD catalyzed transcarbonation.[14] From these carbonates, one was formed by reaction of 10-undecenol with dimethyl carbonate resulting in a α,ω-diene carbonate. In order to compare the properties of the polycarbonate obtained by ADMET of this compound with the other polymers that will be discussed in this part, we synthesized this ADMET precursor by using the same reaction conditions than Meier and coll.

The transcarbonation reaction led to a mixture of 86.5% of the desired product (bis-unsaturated) and 13.5% of the mono-unsaturated compound. Thus purification by column chromatography was performed in order to remove the mono-unsaturated molecule that would act as a chain-stopper during ADMET polymerization.

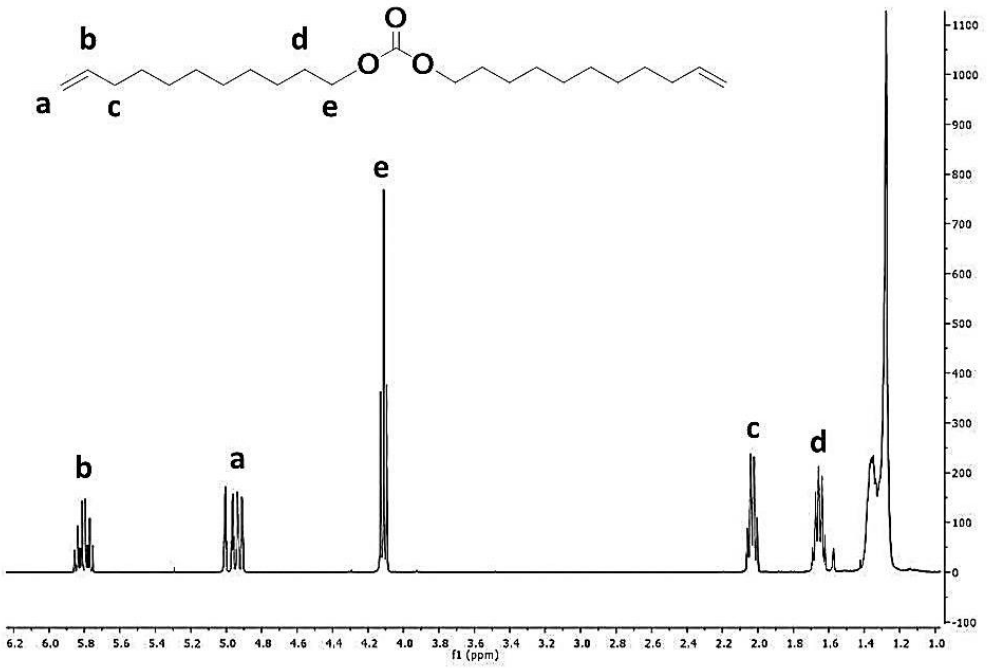

Figure 4.5. ^{1}H-NMR spectra of the bis-unsaturated carbonate (3) in $CDCl_3$.

The structure of the carbonate monomer (**3**) obtained from ^{1}H-NMR spectroscopy (Figure 4.5) on the purified product was in accordance with the expected structure. Indeed, the formation of the carbonate function was confirmed by the appearance of a peak at 4.11 ppm which is assigned to the protons in α position of the carbonate function. Analysis of (**3**) by GC showed a polymerization grade purity of 99% .

II.4. α,ω-diene ether (4)

The ether monomer (**4**), previously described by Meier and coll.[15], was synthesized by a two-step procedure. First 1-tosyl-10-undecene was formed from 10-undecenol to introduce a good living group. Subsequent reaction with 10-undecenol yielded to the expected ether compound in good yield (88%). ^{1}H-NMR characterization confirmed the expected structure of both the intermediate and the final products (Figure 5.5). Formation of the tosylated intermediate was confirmed by the shift of the peak of the protons in α position of the hydroxyl group of 10-undecenol to lower field after tosylation but also by the characteristic peaks of the aromatic moiety (See Figure 5.5 protons e, f and g). The removal of the tosylate leaving group after reaction with 10-undecenol was confirmed by the disappearance of the aromatic peaks but also by the shift of the protons e (See Figure 5.5) to upper field. The purity of the final ether monomer measured by GC was 99% thus allowing its polymerization by ADMET.

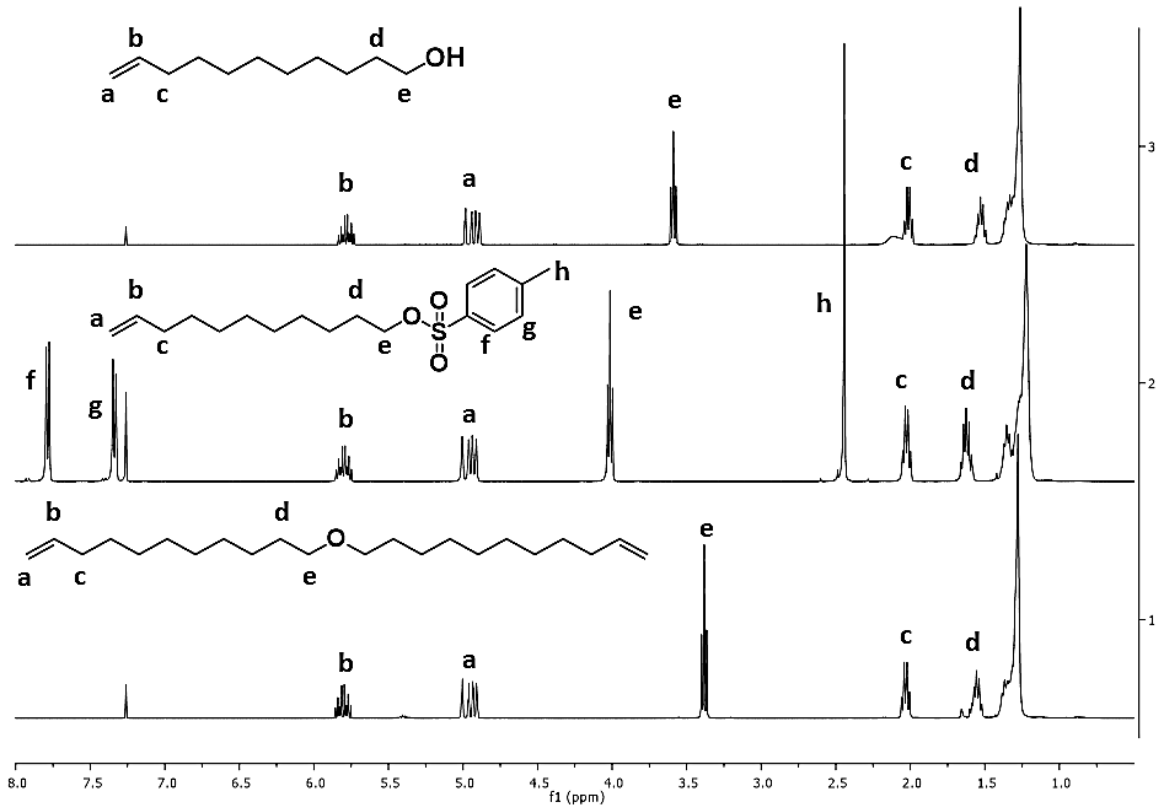

Figure 5.5. ^{1}H-NMR stacked spectra of 10-undecenoic acid, 1-tosyl-10-undecene and bis-unsaturated ether (4) in $CDCl_3$.

II.5. α,ω-diene amide (5)

A monomer bearing amide function (**5**) was synthesized by formation of 10-azidoundecene from 10-bromoundecene followed by reduction of the azido compound into the amine counterpart and then subsequent amidation by reaction with 10-undecenoyl chloride. ^{1}H-NMR spectroscopy was used to confirm the expected structures of all the intermediates and the final product. After completion of the first reaction step which consisted in the formation of the azide compound, a slight shift to upper field of the peaks corresponding to the protons in α and β positions of the bromine and azide functions was noticed (See Figure 6.5 protons e and d). Further reduction of the azide compound to the amine by using zinc dust, revealed a more pronounced shift of the peaks of α and β protons. Amidation of 1-amino-10-undecene with 10-undecenoyl chloride in the presence of triethylamine was then carried out to synthesize the α,ω-diene monomer. ^{1}H-NMR spectroscopy shows the appearance of a peak at 3.24 ppm assigned to the protons in α position of the amide function in the side of the nitrogen atom. The protons in α position of the carbonyl of the amide function displayed a peak at 2.14 ppm. The integrations of the characteristic peaks of (**5**) were consistent with the expected structure.

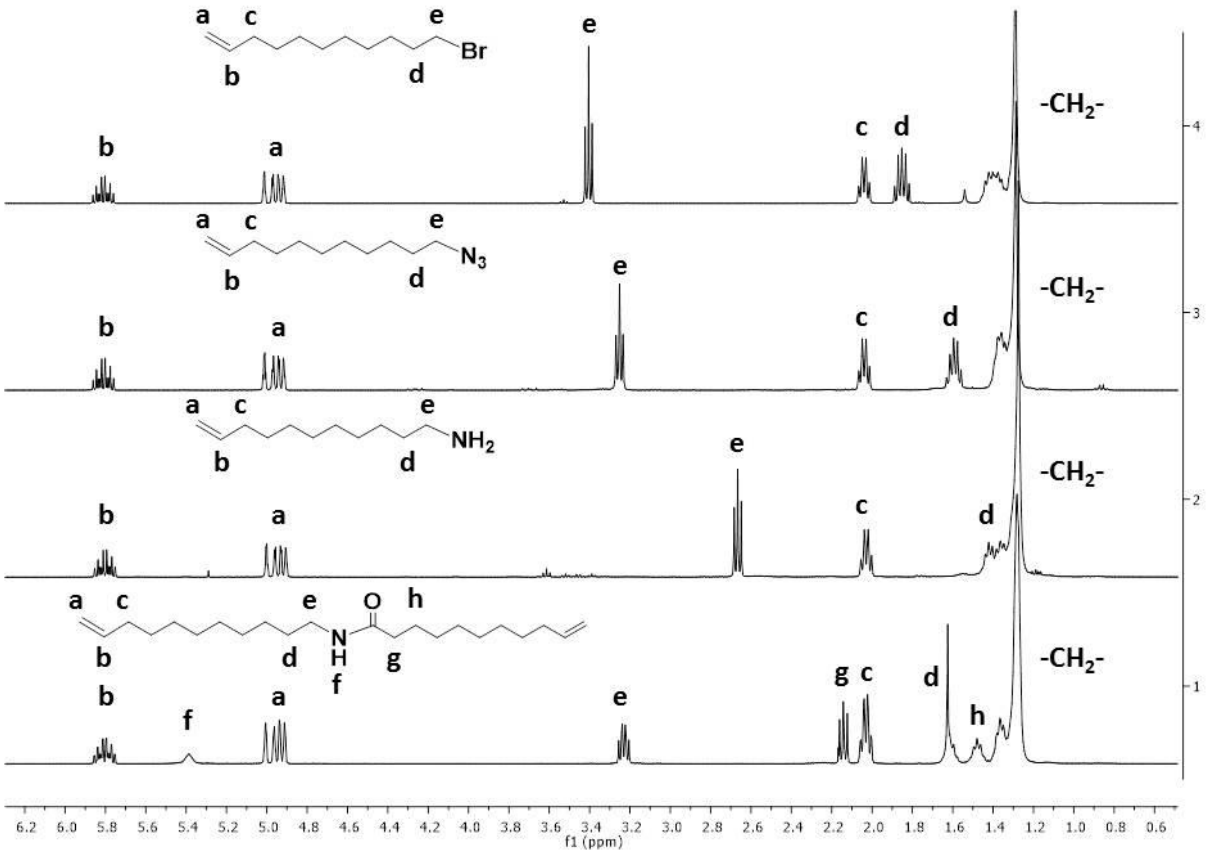

Figure 6.5. ^{1}H-NMR stacked spectra of 1-bromo-10-undecene, 1-azido-10-undecene, 1-amino-10-undecene and bis-unsaturated amide (5) in $CDCl_3$.

GC analysis was not possible on this compound; however, ^{1}H-NMR spectra shows good purity as evidenced by the absence of side products thus allowing the ADMET polymerization of this α,ω-diene monomer.

III. ADMET POLYMERIZATIONS IN BULK AND SOLUTION

III.1. Tolerance investigation of the catalysts toward Polarclean®

ADMET is generally conducted in bulk when the melting points of both monomers and polymers are not too high (<100°C). All of the previously described α,ω-diene monomers show melting points below 80-100°C thus allowing their polymerization in bulk. Nevertheless, our aim in this part is to synthesize block copolymers with PLLA by using an alkene-terminated PLLA that will act as chain stopper during ADMET polymerization of the different α,ω-dienes. Consequently, a solvent is needed as the melting point of PLLA is around 170-180°C. ADMET in solution will therefore be investigated with all the α,ω-dienes in order to evaluate the feasibility of such a pathway to PLLA-based block copolymers.

In the case of ADMET in solution, a high boiling point solvent is generally needed to fit with the reaction conditions (temperature around 80°C with dynamic vacuum to eliminate the ethylene condensate). Solvents such as o-xylene or DMF fulfill the ADMET requirements while their relative toxicity limits their use. Methyl-5-(dimethylamido)-2-methyl-5-oxopentanoate (Polarclean®) is an eco-friendly water soluble and polar solvent which presents a high boiling point and a lower toxicity than o-xylene or DMF.[16] Moreover this solvent can be easily removed from the reaction mixture by washing with methanol or water.

To the best of our knowledge Polarclean® was never employed in metathesis reactions. The first step was thus to evaluate the tolerance of frequently used ruthenium-based metathesis catalysts (Figure 7.5) toward Polarclean®. To that aim, the α,ω-diene ester monomer (**2**) was used as a model in solution ADMET.

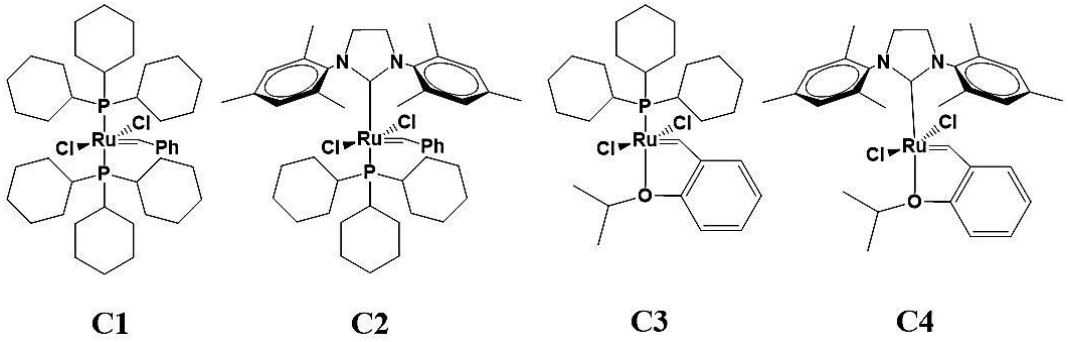

Figure 7.5.Chemical structures of the first and second generation ruthenium metathesis catalysts.

The monomer (**2**) was first reacted in bulk with Grubbs 1st (**C1**), Grubbs 2nd (**C2**), Hoveyda-Grubbs 1st (**C3**) and Hoveyda-Grubbs 2nd (**C4**) generation catalysts. In all cases, the monomer feed was reacted with 0.5mol% of catalyst at 80°C for 24h under dynamic vacuum. When **C2** and **C4** were used, 5mol% of 1,4-benzoquinone was added to limit isomerization.[17, 18] As expected, for all the reactions launched in bulk, good molecular weights were obtained suggesting good tolerance of the catalysts toward (**2**) (Table 1.5, entries 5^{a}, 6^{a}, 7^{a} and 8^{a}). Interestingly, despite their lower reactivity in comparison to 2nd generation catalysts, 1st generation catalysts led to higher molecular weights. It was ascribed to limited isomerization with these catalysts.

ADMET polymerizations of (**2**) in Polarclean® in the same reaction conditions were then launched. In the case of **C1** and **C2** (Table 1.5, entries 5^{b} and 6^{b}), only oligomers were achieved which suggested poor tolerance of these catalysts for the Polarclean® solvent. Moreover, low yields of around 20% were achieved which shows that the oligomers poorly precipitated in methanol.

Table 1.5. Summary of the macromolecular characteristics of the polymers synthesized (a) in bulk or (b) in solution. Data obtained by SEC in THF using PS calibration.

			$\bar{M}_n$ (g.mol^{-1}) (Đ)	
Entry	**Monomer**	**Catalyst**	**Bulk[a]**	**Polarclean®[b]**
1	**(1)**	**C1**	17 100 (1.7)	-
2		**C2**	9 300 (1.6)	-
3		**C3**	22 600 (1.9)	-
4		**C4**	25 400 (2.4)	20 500 (1.6)
5	**(2)**	**C1**	43 700 (1.9)	1 500(1.2)
6		**C2**	10 800 (1.7)	1 300 (1.1)
7		**C3**	37 000 (2.2)	52 600 (1.8)
8		**C4**	15 700 (1.5)	24 900 (1.5)
9	**(1)+(2)**	**C4**	-	28 500 (1.6)
10	**(3)**	**C4**	34 400 (1,8)	50 800 (1.6)
11	**(4)**	**C4**	nd	3 900 (1.7)
12	**(5)**	**C4**	nd	nd

The use of **C3** and **C4** (Table 1.5, entries 7[b] and 8[b]) was much more adapted regarding the higher molecular weights obtained in comparison to the other catalysts. It is noteworthy that solution polymerization of (**2**) by using **C3** and **C4** gave a polyester of higher molecular weight than the same polymerization launched in bulk. It is ascribed to higher homogenization of the reaction mixture.

III.2. Tolerance investigation of the catalysts toward urethane function

To the best of our knowledge, this is the first example of ADMET polymerization with a fatty acid-based urethane monomer. Consequently, the monomer (**1**) was first polymerized in bulk while screening the metathesis catalysts to evaluate their tolerance toward the urethane function. As shown in Table 1.5 (entries 1[a] and 2[a]), **C1** led to higher molecular weight than **C2**. It can be correlated with the amount of isomerization, despite the presence of p-benzoquinone, more important in the case of the polymer synthesized with **C2** as shown from the ^{1}H-NMR spectrum (See the peaks between 0.8 and 1 ppm in Figure 8.5b). **C3**, yielded higher molecular weight than **C1**. Finally, **C4** yielded polyurethane with comparable molecular weight than with **C3**. Interestingly, lower molecular weights were obtained in the case of bulk ADMET of (**1**) in comparison to ADMET of (**2**), except for **C4** which appears to be more suitable than the other catalysts. Consequently, we retained **C4** as a catalyst in the following.

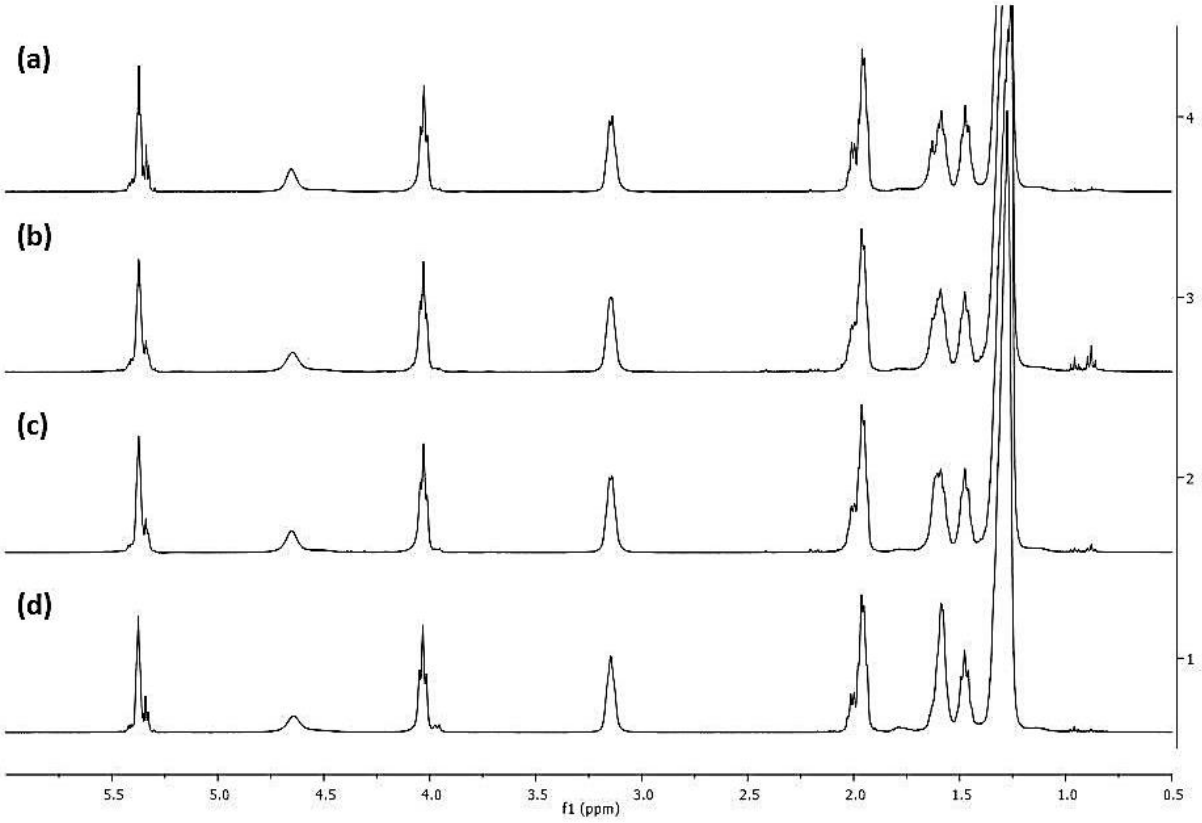

Figure 8.5. ^{1}H-NMR stacked spectra of the polyurethanes synthesized in bulk from (a) C1, (b) C2, (c) C3 and (d) C4. $CDCl_3$.

III.3. Solution ADMET polymerizations of the α,ω-dienes

The monomer (**1**) was then polymerized in Polarclean® which led to a homogeneous reaction mixture. SEC analysis in THF showed a molecular weight of 20 500 g.mol^{-1}. The completion of the polymerization was confirmed by ^{1}H-NMR spectroscopy as seen from the decrease in the integration of the terminal olefin protons and the appearance of a multiplet at 5.37 ppm (Figure 9.5). All peaks were easily assigned except the end-groups which should be terminal double bonds. The appearance of undesirable signals between 0.85 ppm and 1.00 ppm suggests that some isomerization reactions took place, even in the presence of 1,4-benzoquinone, and that some chain ends may consist in methyl groups. The introduction of ester functions in the polyurethane backbone was also carried out by copolymerizing (**1**) and (**2**), in equimolar ratio, with **C4** as a catalyst (Table 1.5, entry 9^b). The obtained copolymer exhibited a $\bar{M}_n$ of 28 500 g.mol^{-1} by SEC analysis with a dispersity of 1.6. Chemical composition of the copolymer, calculated from ^{1}H-NMR analysis (Figure 9.5), was in agreement with the feed ratio.

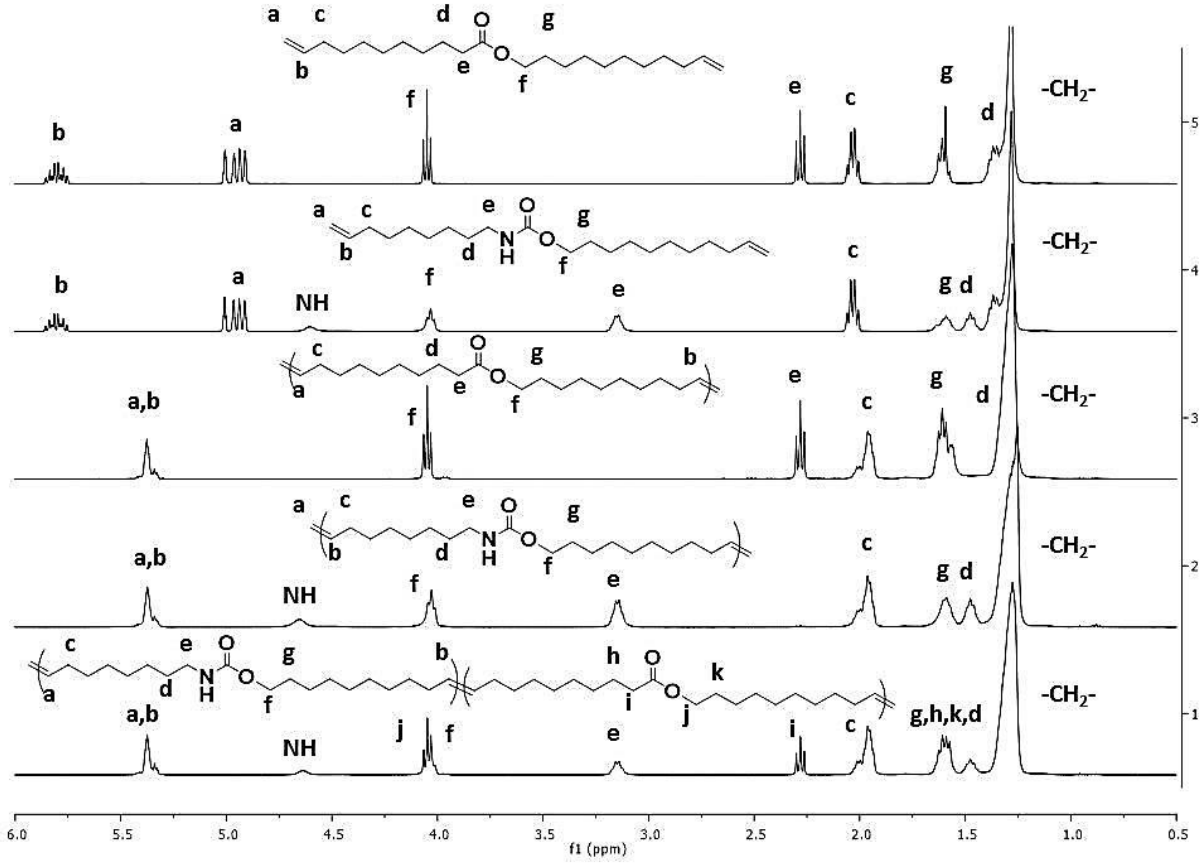

Figure 9.5. ^{1}H-NMR stacked spectra of (2), (1), their respective polymers and the poly(ester-urethane) copolymer synthesized in solution using C4. $CDCl_3$.

The monomers bearing carbonate (**3**), ether (**4**) and amide function (**5**), were also polymerized. ADMET polymerizations of (**3**), (**4**) and (**5**) were first conducted in bulk by using **C4** as a catalyst (Table 1.5, entries 10[a], 11[a] and 12[a]). An obvious increase in the viscosity of the reaction mixture was noticed in all cases; however the polyamide and the polyether so-formed were insoluble in all the solvents generally used for SEC and NMR analysis, impeding their molecular characterization. The SEC analysis of the polycarbonate in THF showed a molecular weight of 34 400 g.mol^{-1} with a dispersity of 1.8. Polymerizations in Polarclean® were then launched and showed evidence of polymer formation in all cases. The polycarbonate, analyzed by SEC in THF, presented a molecular weight of 50 800 g.mol^{-1} which is significantly higher than in bulk. Unlike the solution polymerizations of (**1**), (**2**) and (**3**) where the reaction mixtures were homogeneous, the polymerizations of (**4**) and (**5**) led to the precipitation of the polymers in Polarclean® after a certain reaction time. Contrary to the polyether formed in bulk, the one synthesized in solution showed good solubility in THF thus allowing its molecular characterization. A low molecular weight of 3 900 g.mol^{-1} was formed which explains the better solubility of the polymer in THF. This low molecular weight value was ascribed to the precipitation of the polymer in Polarclean® during its formation which limited the accessibility of the reactive sites. The polyamide was still not soluble in THF.

To summarize, Polarclean® was revealed to be an effective green solvent for ADMET polymerizations of (**1**), (**2**) and (**3**) while it does not dissolve properly the polymers resulting from (**4**) and (**5**).

III.4. Influence of organic functions on the properties of the resulting polymers

In order to anticipate the thermo-mechanical properties of the potential block copolymers, all the polymers synthesized by ADMET were analyzed by DSC and TGA. Due to precipitation of the polyether and the polyamide during the early stage of solution polymerizations, thermal investigations were performed on the polymers synthesized in bulk. Various thermal and thermo-mechanical behaviors were observed depending on the type of organic functions present in the polymer backbone (Table 2.5). The lower thermal stability, determined by TGA, was observed for the polyurethane with an initial degradation temperature (temperature corresponding to 5wt% loss: $T_{5\%}$) of 307°C (value in the range of commercially available polyurethanes). The polycarbonate showed quite similar thermal stability ($T_{5\%}$=321°C). As expected, the polyamide, polyester and polyether presented higher thermal stability with initial degradation temperatures of 343°C, 386°C and 409°C respectively.

Table 2.5. Thermal and thermo-mechanical characteristics of the polymers.

Monomer	Polymer	Tc (°C)[a]	Tm (°C)[a]	ΔHm (J.g^{-1})[a]	$T_{5\%}$ (°C)[b]
1	**Polyurethane**	21	48	38	307
2	**Polyester**	43	53	89	386
1+2	**Poly(ester-urethane)**	35	55	55	325
3	**Polycarbonate**	36	36-49	13-39	321
4	**Polyether**	50	60	99	409
5	**Polyamide**	45	78	11	343

Determined by (a) DSC-10°C.min^{-1} (b) TGA-10°C.min^{-1}

Regarding the thermo-mechanical properties evaluated by DSC analysis, the novel polyurethane showed a very low Tg (around -50°C). This low value was attributed to the purely aliphatic nature of the polymer. In the case of the polyurethane, which was never described yet, a melting point was noticed with a corresponding temperature of 48°C. The melting enthalpy was quite low (38 J.g^{-1}) due to the remaining double bonds in the polymer structure which restrict the chain packing and thus the crystallinity. Interestingly, the polyester showed higher melting temperature (53°C) and corresponding enthalpy (89 J.g^{-1}) in comparison to the polyurethane. The copolymer from (**1**) and (**2**) showed intermediate thermo-mechanical properties in comparison to the polyester and the polyurethane respectively (Figure 10.5).

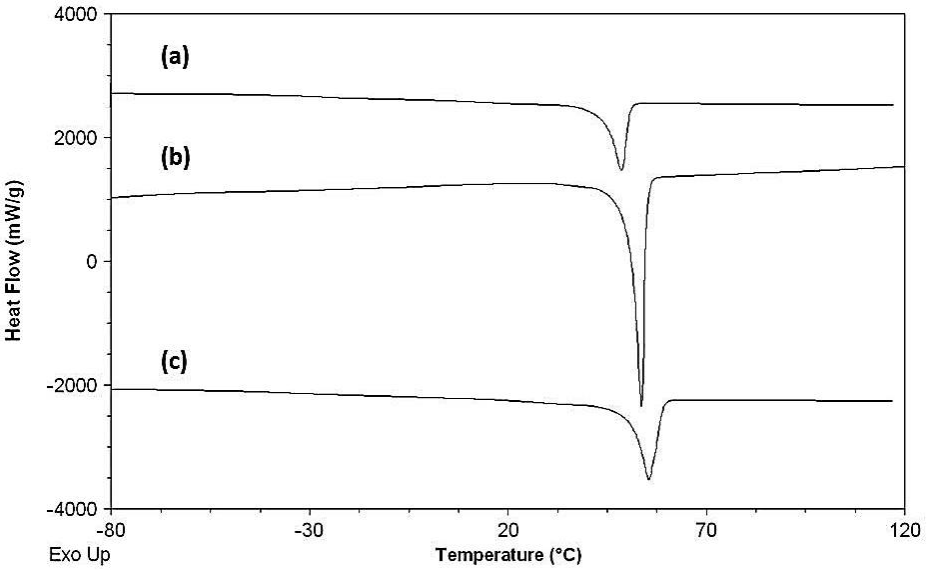

Figure 10.5. DSC 2nd heating curves of (a)polyurethane, (b)polyester, and (c)poly(ester-urethane)-10°C.min^{-1}.

In the case of the polycarbonate, a complex melting pattern was observed with two melting peaks (36°C and 49°C respectively) on heating the sample, most probably ascribed to polymorphism or to melting-recrystallization processes (Figure 11.5).

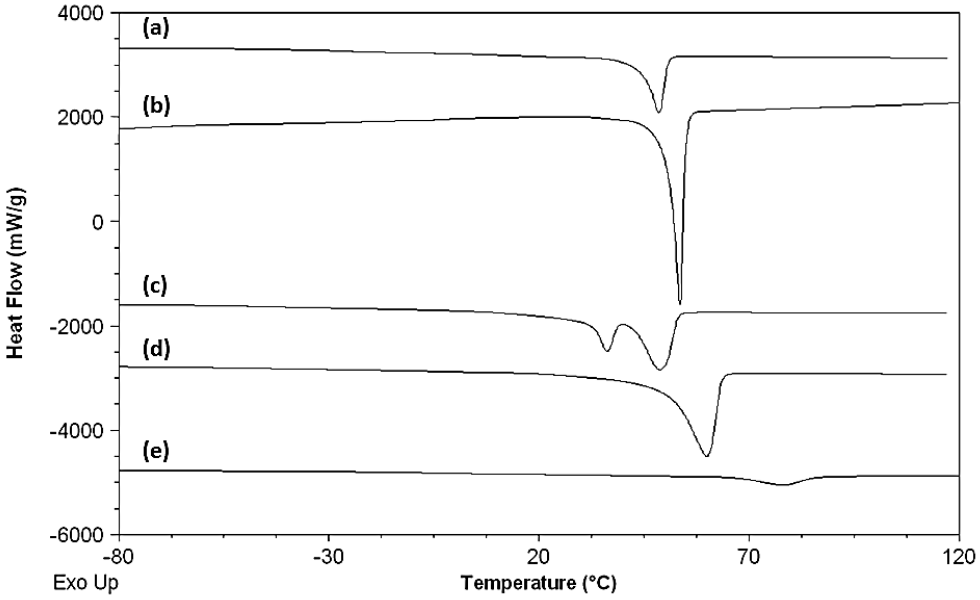

Figure 11.5. DSC 2nd heating curves of (a)polyurethane, (b)polyester, (c)polycarbonate, (d)polyether and (d)polyamide. 10°C.min^{-1}.

The DSC curve of the polyether showed a melting temperature of 60°C with the higher melting enthalpy of 99 J.g^{-1}. The high crystalline ability of the polyether is given by the conformational flexibility of the ether linkage which promotes chain packing. As expected, of all the investigated polymers, the polyamide showed the highest melting temperature (78°C) due to the high cohesion (and thus to the high stability of the crystals) that amide functions confer to the material.

IV. SYNTHESIS OF BLOCK COPOLYMERS

Once the ADMET polymerization conditions established, we investigated the formation of ABA block copolymers. In the few studies reported in the literature concerning the synthesis of block copolymers by ADMET methodology, two approaches are generally used. In a first route, terminal alkene-functionalized polymers or oligomers are acting as chain stopper during the polymerization resulting in block copolymers. In another approach, functionalized telechelics (mono-, di-) are generated by using chain stoppers during the polymerization or by depolymerisation with functional alkenes. Subsequent polymerization of a distinct polymer is then initiated from these functionalized telechelics.[6] The following part described these two pathways to block copolymers applied to PLLA.

IV.1. Triblock copolymers formation by ADMET with a terminal alkene-functionalized PLLA

The synthesis of a terminal alkene-functionalized PLLA was necessary prior to the ADMET polymerization. Consequently, 10-undecenol was chosen as an initiator with $Sn(Oct)_2$ for the ROP of L-lactide (Scheme 2.5).

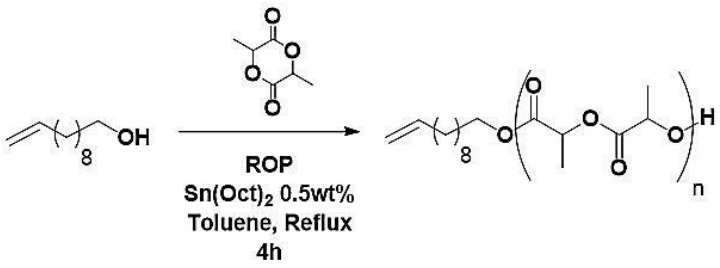

Scheme 2.5.ROP of lactide initiated by a 10-undecenol/Sn(Oct)$_2$ system.

The polymerization was carried out in toluene at reflux for 4h. The completion of the reaction was monitored by ^{1}H-NMR and SEC in THF. As can be seen from the ^{1}H-NMR spectra (see Figure 12.5), a quadruplet, assigned to the proton linked to the substituted carbon of lactide unit, appears at 5.17 ppm (See Figure 12.5, H_d proton), confirming the ring-opening of L-lactide with a conversion of 91%. In addition, the characteristic peaks of the 10-undecenol initiator are shifted in agreement with the lactide polymerization from hydroxyl end groups. The protons close to the hydroxyl function shifted downfield from 3.6 ppm to 4.1 ppm. Moreover, the calculated integrations of the peak at 4.1 ppm and those of the olefin peak at 5.8 ppm were in accordance with a nearly quantitative initiation by 10-undecenol. The molecular weight values calculated from SEC in THF (PS calibration) and from ^{1}H-NMR by end-group analysis were $\bar{M}_n$= 10 300 g.mol^{-1} (Đ=1.4) and 5 300 g.mol^{-1} respectively.

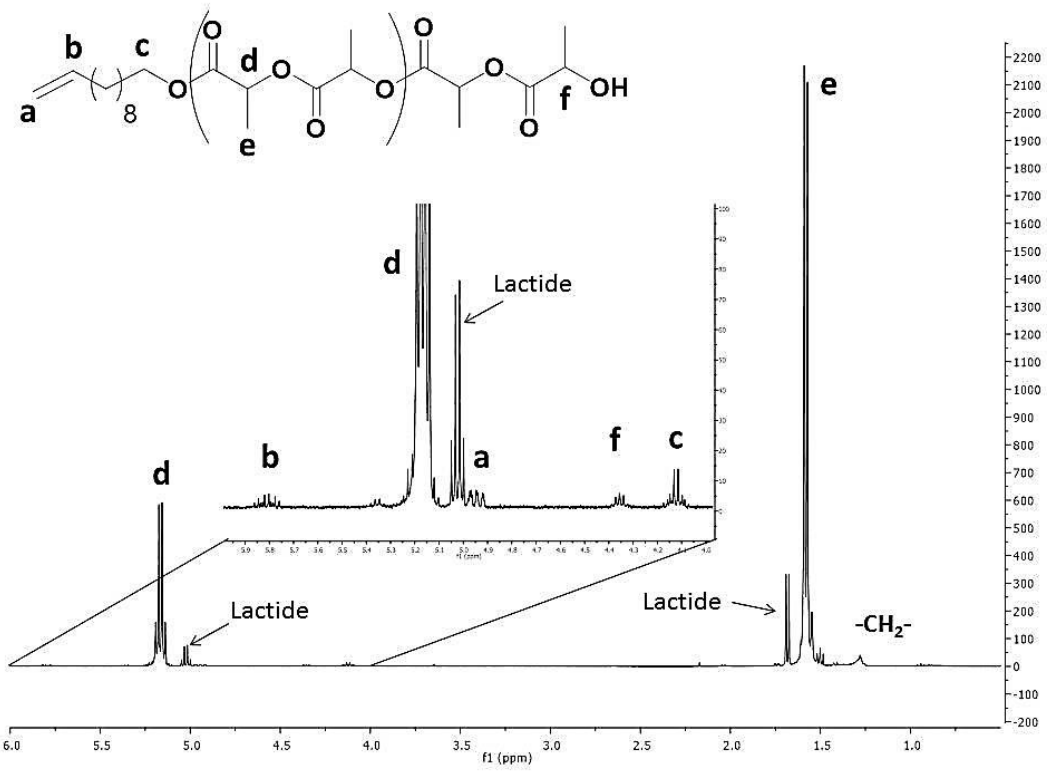

Figure 12.5. ^{1}H-NMR spectrum of the alkene-terminated PLLA in $CDCl_3$

In order to confirm the feasibility of our synthetic strategy to triblock copolymers, a solubility test of the alkene-terminated PLLA in Polarclean® was carried out at the ADMET fixed temperature (80°C). Good solubility was observed which should attest of the sufficient reactivity of the terminal alkene of the macromolecular chain stopper. ADMET polymerization of the monomers (**2**) and (**3**) were then carried out in Polarclean® in the presence of 5wt% (0.33mol%) of the PLLA chain stopper (relative to the mass of α,ω-diene) . The reaction was performed at 80°C under dynamic vacuum with 0.5mol% of **C4** and 5mol% of 1,4-benzoquinone.

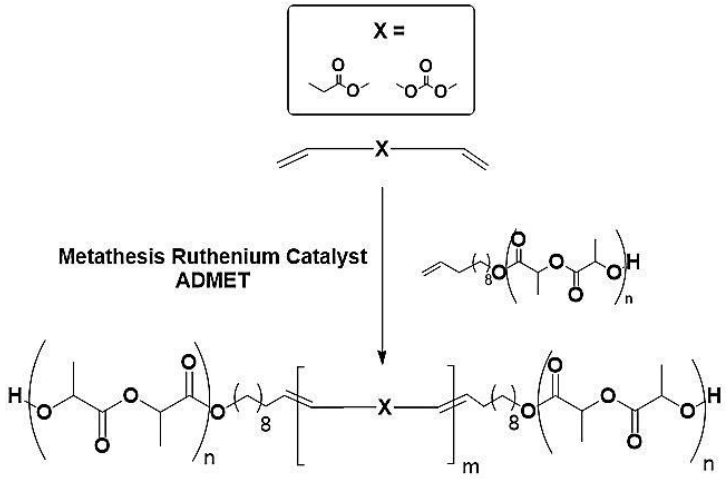

Scheme 3.5.Triblock copolymer synthesis by the chain transfer approach with alkene-terminated PLLA.

Aliquots of the so-formed polymers were analyzed by SEC in THF at different reaction times and it was found that a time of 96h was necessary to observe efficient shifting of the SEC traces to higher molecular weight and stabilization of this value. Figure 13.5 displays the SEC traces of the alkene-terminated PLLA (blue), the polyester (**P1**) reacted with 5wt% of chain stopper (green) and the polycarbonate (**P2**) reacted with 5wt% of chain stopper (red).

Table 3.5. Macromolecular characteristics of the triblock copolymers obtained by SEC in THF-PS calibration.

Entry	Monomer	wt% PLLA	$\bar{M}_n$ (g.mol^{-1})	Đ
P1	2	5	29 300	1.9
P2	3	5	25020	2.1
P3	2	33	8 390	3.2
P4	3	33	43 700	3.1

It is obvious that ADMET polymerization of both ester and carbonate monomers occurred as evidenced by the relatively high molecular weight values obtained (29 300 and 25 020 g.mol^{-1} respectively). The completion of the reaction was also noticeable as seen from the values of dispersity close to 2 (1.9 and 2.1 respectively). From SEC traces, it was not possible to conclude about the efficiency of chain transfer of the polymers with the alkene-terminated PLLA chain stopper as the latter was introduced in the reaction mixture with a low content of 5wt%. However no clear evidence of remaining chain stopper traces was noticed and monomodal distribution was obtained which let us think that transfer with the unsaturated polymers occurred.

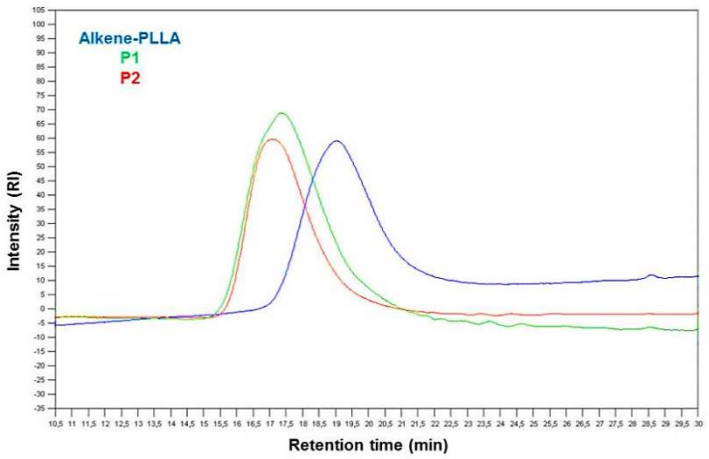

Figure 13.5. SEC traces of the PLLA chain stopper and the copolymers containing 5wt% of PLLA (P1 and P2).

In order to obtain copolymers with a higher weight fraction of PLLA, ADMET polymerizations of the ester (**2**) and the carbonate (**3**) monomers were carried out in similar conditions than previously while increasing the weight fraction of chain stopper in the feed to

33wt%. After 96h of reaction, the resulting polymers were analyzed by SEC in THF and ^{1}H-NMR. The SEC traces (Figure 14.5) of the two polymers (**P3** and **P4**) showed multimodal distributions in both cases with remaining chain stopper. This indicates that for higher contents of chain stopper, the reversible feature of the metathesis reaction impedes the good control of the macromolecular architecture.

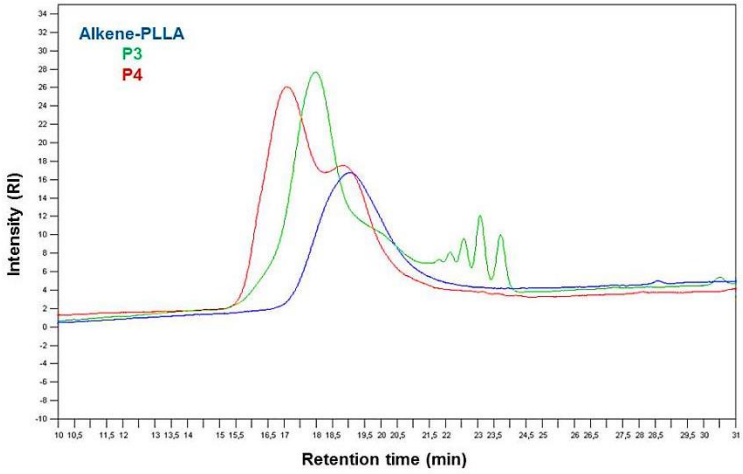

Figure 14.5. SEC traces of the PLLA chain stopper and the copolymers containing 33wt% of PLLA (P3 and P4).

Figure 15.5 displays the ^{1}H-NMR spectrum of the P4 polymer. The bimodal SEC trace observed on Figure 14.5 could suggest no conversion of the olefin of PLLA chain stopper, however, the total disappearance of the terminal olefin protons peaks on the ^{1}H-NMR spectrum gives evidence of chain transfer with the alkene functionalized PLLA. This is emphasized by the low amount of isomerization when regarding the low intensity of the peaks below 1 ppm.

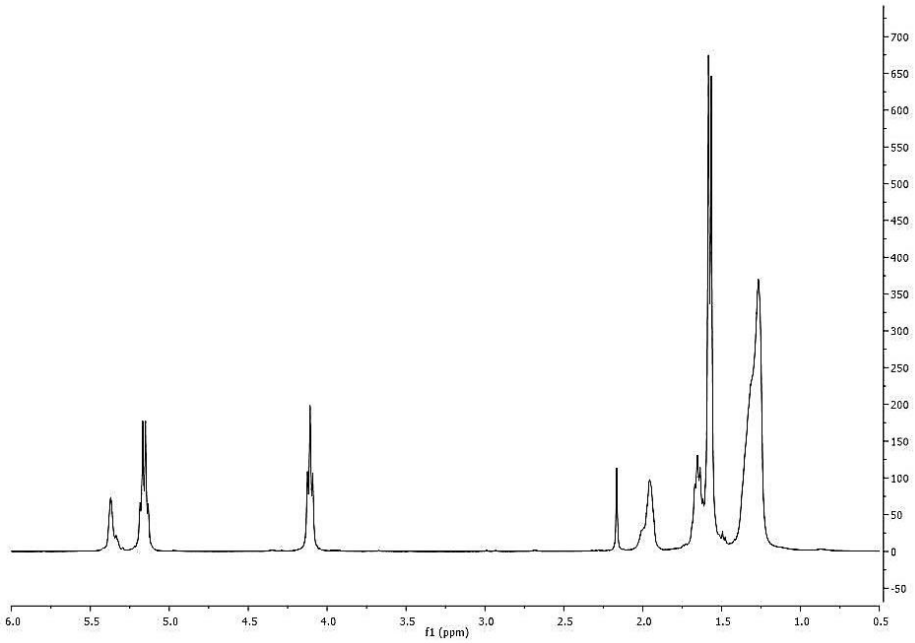

Figure 15.5.^{1}H-NMR spectrum of P4 in $CDCl_3$

Consequently we can conclude about an efficient chain transfer of the polycarbonate with the chain stopper. However, the high heterogeneity of the polymer chains, observed from the bimodal distribution of the SEC traces, constitutes an important drawback to the utilization of such polymeric materials. Consequently, no further investigation or application of the materials developed in this part has been carried out.

IV.2. Triblock copolymers formation by the dihydroxy-telechelic pre-polymer approach

Due to the poor control obtained by the first approach, the dihydroxy-telechelic pre-polymer methodology was studied by ADMET of α,ω-dienes with 10-undecenol as a chain stopper. In a subsequent step, these pre-polymers were used to initiate the ROP of L-lactide (Scheme 4.5).

IV.2.1. Dihydroxy-telechelic pre-polymer synthesis

The synthesis of polyurethane, polyester and polycarbonate pre-polymers was first investigated by solution ADMET of the respective α,ω-dienes with 5mol% of 10-undecenol. **C3** was used as a catalyst and 5mol% of 1,4-benzoquinone was added to limit isomerization.

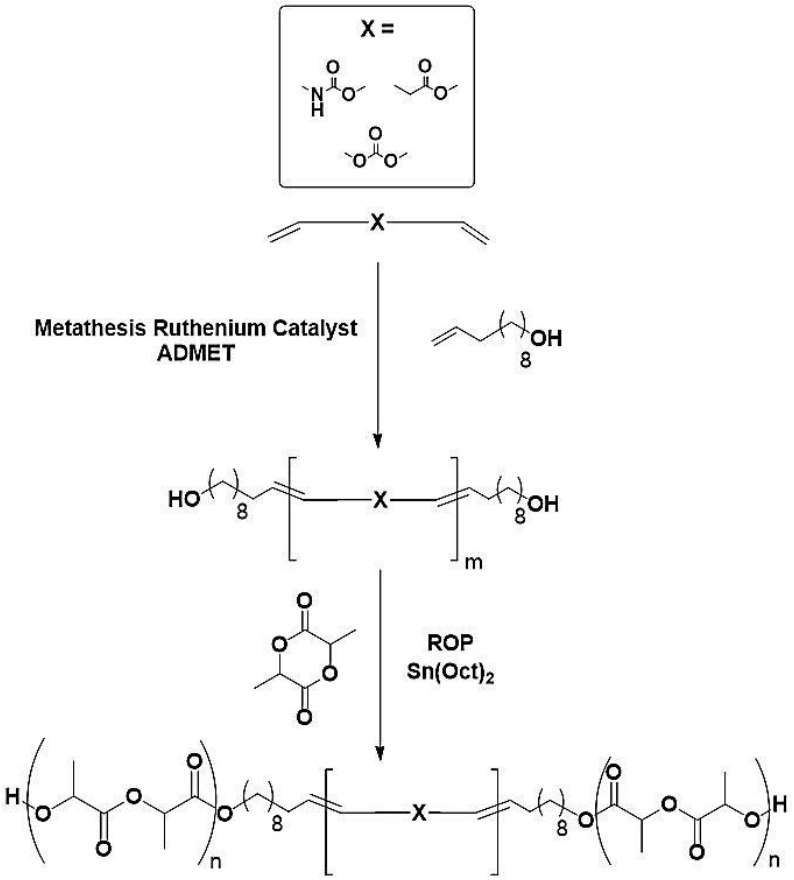

Scheme 4.5. Triblock copolymer synthesis by the dihydroxy-telechelic pre-polymer approach.

For all polymerizations, after 24 hours of reaction at 80°C under dynamic vacuum, the catalyst was deactivated with ethyl vinyl ether, and the polymer was precipitated into methanol. The so-formed pre-polymers were then analyzed by ^{1}H-NMR and SEC in THF. Regarding the molecular weights of the three pre-polymers, it is noteworthy that chain transfer occurred. Indeed, lower molecular weights were obtained when chain stopper was added in comparison to the corresponding homopolymers obtained without chain stopper (See Table 4.5.).

Table 4.5. Macromolecular characteristics of the polyurethane, polyester and polycarbonate synthesized with or without 10-undecenol as chain stopper. Data obtained by SEC in THF-PS calibration.

	Without chain stopper		2mol% 10-undecenol	
Monomer	$\bar{M}_n$ (g.mol^{-1})	Đ	$\bar{M}_n$ (g.mol^{-1})	Đ
1	20 500	1.6	7 340	1.3
2	24 900	1.5	9 510	1.7
3	50 800	1.6	15 920	1.6

^{1}H-NMR spectrum of the so-formed polyurethane pre-polymer (Figure 16.5) shows complete conversion of the terminal double bonds into internal ones as seen from the absence of terminal olefin peaks at 5.8 ppm and 4.9 ppm. This demonstrates the efficient chain transfer.

However, ^{1}H-NMR also shows that chain transfer occurred not only with 10-undecenol but also with isomerized side products. Indeed, some peaks appeared below 1 ppm and were ascribed to methyl protons peaks. Isomerization of terminal olefins yield internal ones that can, after metathesis reactions, lead to condensed hydrocarbons that act as non-functionalized chain stoppers. Chain ends composed of hydroxyl functions were also noticed as evidenced by the appearance of a triplet at 3.6 ppm, nevertheless the desired chain ends were in minor amount (28%) in comparison to methyl chain ends (72%). Methyl chain ends were also observed in the case of the polyester and polycarbonate pre-polymers, which constitutes an important hindrance to the formation of controlled architecture such as block copolymers as only partial amount of chain ends will effectively initiate the ROP of L-lactide.

Some attempts to limit isomerization reactions were carried out by playing on the reaction conditions (vacuum/N_2, time, temperature…), the nature of the isomerization inhibitor (various 1,4-benzoquinones), the nature of the chain stopper and the catalyst. Nevertheless, the ratio between methyl and hydroxyl chain ends still remained too high to consider effective formation of ABA block copolymers.

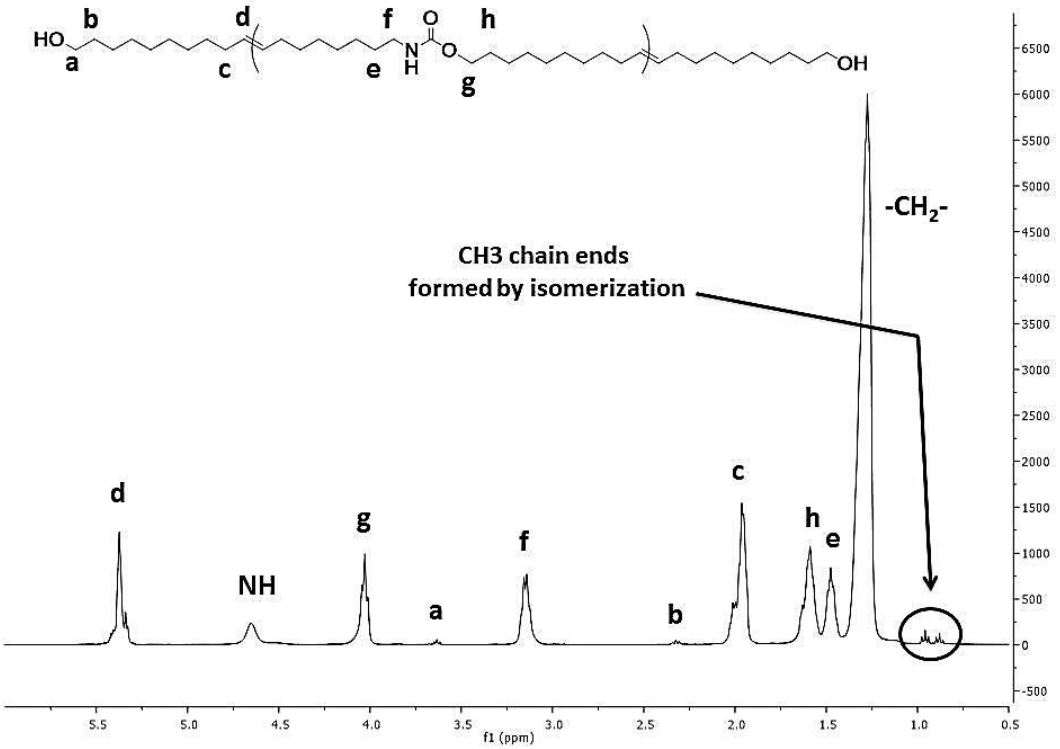

Figure 16.5.^{1}H-NMR spectrum of the polyurethane pre-polymer in $CDCl_3$.

IV.2.2. Synthesis of PLLA-b-Polyurethane-b-PLLA

Even if high amounts of isomerization were noticed for all the synthesized pre-polymers (Table 4.5), ROP of L-lactide was nonetheless carried out using polyurethane and polyester pre-polymers having in mind that the obtained materials should not be well-defined and thus should not be used for PLLA applications. The ROP was carried out in toluene at reflux for 4h. First, the polyurethane pre-polymer was used as a macroinitiator. Two copolymers were synthesized for different L-lactide to macroinitiator ratios enabling the preparation of block copolymers with compositions of 60wt% (PLLA-*b*-PU-*b*-PLLA 1) and 80wt% (PLLA-*b*-PU-*b*-PLLA 2) of PLLA. The completion of the reaction was monitored by ^{1}H-NMR and SEC in THF. As can be seen from the ^{1}H-NMR spectra (see Figure 17.5.b and c), a quadruplet, assigned to the proton linked to the tertiary carbon of lactide repeating units, appears at 5.17 ppm, confirming the ring-opening of L-lactide with a conversion of 92% (PLLA-*b*-PU-*b*-PLLA 1) and 84% (PLLA-*b*-PU-*b*-PLLA 2).

The SEC traces of the polyurethane pre-polymer (HO-PU-OH) and the two copolymers are displayed in Figure 18.5. The shift of the SEC traces toward the lower elution times indicates the efficiency of the initiation of L-lactide ROP by the hydroxyl chain ends of the macroinitiator. However, regarding the SEC trace of PLLA-b-PU-b-PLLA 1, it is noteworthy that a mixture of homopolymer, diblock copolymer and triblock copolymer constitutes the

final material. Consequently, the properties (thermal and mechanical) of these polymers were not investigated as their chaotic structure hinders their potential applications.

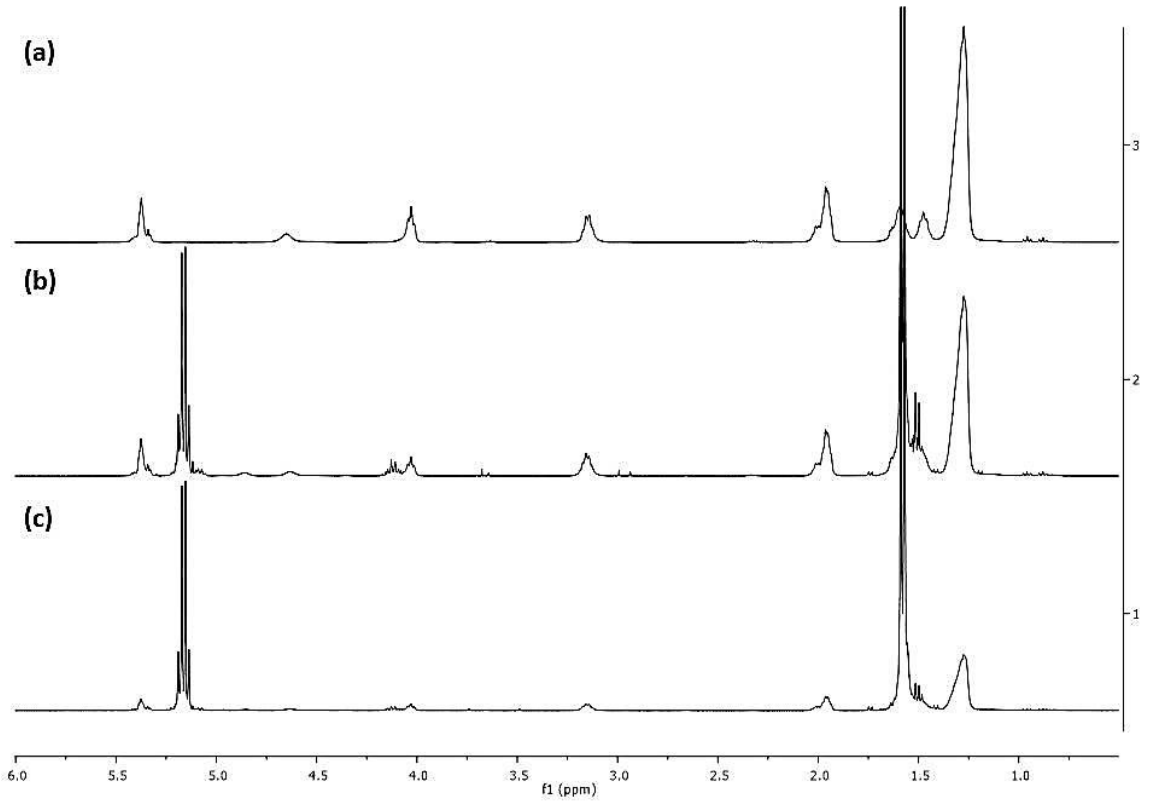

Figure 17.5. ^{1}H-NMR stacked spectra of (a) HO-PU-OH, (b) PLLA-b-PU-b-PLLA 1 and (c) PLLA-b-PU-b-PLLA 2 in $CDCl_3$.

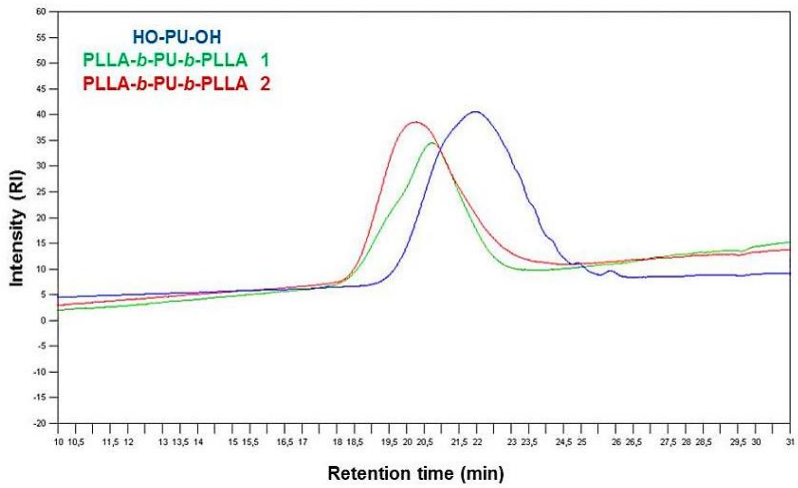

Figure 18.5. SEC traces in THF of HO-PU-OH, PLLA-b-PU-b-PLLA 1 and PLLA-b-PU-b-PLLA 2.

IV.2.3. Synthesis of PLLA-b-Polyester-b-PLLA

ROP of L-lactide was also carried out with the polyester pre-polymer (HO-PE-OH) by fixing the weight amount of PLLA to 60%. Similarly to the copolymers with polyurethane as a soft segment, the SEC trace of the copolymer differs from a Gaussian distribution (Figure 19.5).

The trace of the unreacted pre-polymer can be clearly seen at high elution times which attest from a partial initiation by the polyester prepolymer. Thus the obtained product is also composed of a mixture of homopolyester, diblock and triblock copolymers hindering its applications.

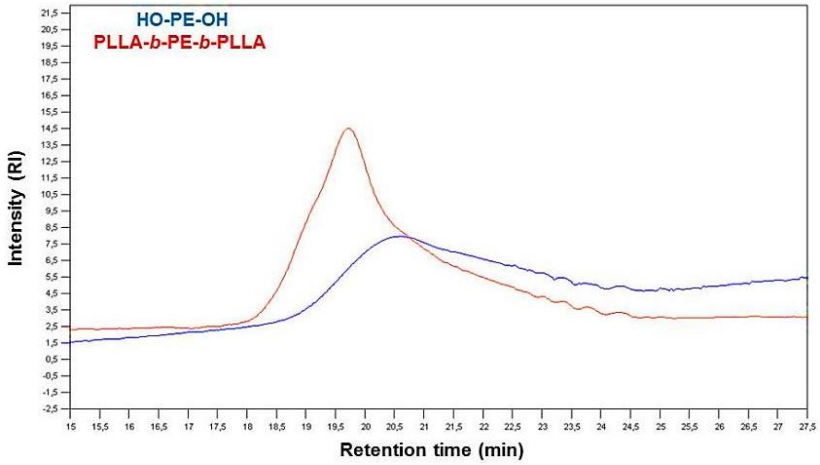

Figure 19.5. SEC traces in THF of HO-PE-OH and PLLA-b-PE-b-PLLA.

V. CONCLUSION

In summary, we have demonstrated that ADMET polymerization of a α,ω-diene urethane monomer could be readily achieved in bulk and in Polarclean®. This methodology thus offers "greener" reaction conditions for polyurethane synthesis in comparison to the classical route (polyaddition of polyols and polyisocyanates) or to transurethanisation pathway. Moreover, the use of Polarclean® constitutes a greener alternative to common high boiling solvents employed in ADMET polymerizations. Other biobased α,ω-diene monomers bearing various organic functions can also be polymerized by ADMET which resulted in good efficiency of Polarclean® as a polymerization solvent when carbonate and ester monomers were used. An overview of the thermomechanical properties of these polymers showed significant variations in the melting temperature and melting enthalpy values depending on the organic function present in the polymer backbone.

Investigation of two approaches to the synthesis of triblock copolymers by ADMET was then performed. In a first pathway, the formation of block copolymers by chain transfer of a polyunsaturated polymer with an alkene-functionalized PLLA was carried out. However it resulted in a poor control of the macromolecular architecture as seen from the multimodal shape of the SEC curves. In a second approach, dihydroxy-telechelic pre-polymers formation was investigated by chain transfer with a hydroxyl-functionalized alkene. However, even by

changing the reaction conditions, isomerization side reactions hindered the control of the chain ends and thus the control of the macromolecular architecture.

To conclude, this explorative study on block copolymerization using ADMET methodology did not show the expected results. The synthesized materials were thus not retained as efficient PLLA materials due to their heterogeneity of chemical structure. Nevertheless, independently from the block copolymer formation, we described for the first time the ADMET polymerization of a fatty acid-based α,ω-diene urethane in a green solvent.

VI. EXPERIMENTAL

1. Synthesis of monomers.

10-undecenoyl azide To a suspension of 10-undecenoic acid (8.9 g, 48.3 mmol) in tetrahydrofuran:water (50:15 mL) was added triethylamine (9.77 g, 96.6 mmol). The clear solution obtained was then cooled to 0 °C and then ethyl chloroformate (10.48 g, 96.6 mmol) was added drop-wise over a period of 10 min. The reaction mixture was stirred for 2 h and then NaN_3 (15.69 g, 241.5 mmol) in water (10 mL) was added drop-wise for 10 min and the stirring continued at 0 °C for 4 h. Icecold-water (20 mL) was added to the crude product which was then extracted with DCM (2 x 75 mL). The DCM solution was washed with water (3 x 40 mL), dried over sodium sulphate and filtered. The solvent was evaporated under reduced pressure at room temperature to obtain 10-undecenoyl azide as viscous oil. Yield: 82%.

Bis-unsaturated urethane (1) To a solution of undecylenic acyl azide (4.18 g, 20 mmol) in anhydrous THF, under nitrogen stream was slowly added 10-undecen-1-ol (**3**) (3.41 g, 20 mmol) and a drop of DBTDL. The reaction mixture was heated at 50 °C for overnight. After completion of reaction, the THF was evaporated under reduced pressure and to the crude product was added petroleum ether. The solid separated was filtered off and the filtrate concentrated on rotavapor to give bis-unsaturated urethane compound (**2**). The further purification was carried out using flash column chromatography (Pentane/ethyl acetate: 80/20). Yield: 63%.

Bis-unsaturated ester (2) Methyl 10-undecenoate (15.00 g, 75.6mmol), 10-undecenol (12.87 g, 75.6mmol) and TBD (1: 1: 0.05) were stirred under nitrogen flow at 120 °C (4 h), at 160 °C (2 h) then under vacuum at 160 °C (1 h). After completion of the reaction, the product was purified using flash column chromatography (Heptane/diethyl ether: 80/20). Yield: 81%. Purity by GC: 99%.

Bis-unsaturated carbonate (3) 10-undecenol (20.8 g, 122.1mmol), dimethyl carbonate (5.50 g, 61.1mmol) and TBD (1: 0.5: 0.05) were stirred under nitrogen atmosphere at 80 °C (2 h), and then under nitrogen flow at the same temperature (4 h) then under vacuum at 80°C (1 h). After completion of the reaction, the product was purified using flash column chromatography (Heptane/ethyl acetate: 90/10). Yield: 75%. Purity by GC: 99%.

1-tosyl-10-undecene Into a two necked round bottom flask equipped with magnetic stirrer and additional funnel, 10-undecen-1-ol (10 g, 58.82 mmol) and triethylamine (5.95 g, 58.82 mmol) were dissolved in dichloromethane (100 mL). The solution was cooled at 0 °C in an ice bath. Solution of 4-toluenesulfonyl chloride (11.17 g, 58.82 mmol) in dichloromethane (25 mL) was slowly added to the cooled solution through additional funnel. The reaction mixture was stirred at 0 °C for 2 h and at room temperature overnight. The reaction mixture was filtered and the organic layer was washed with 5% $NaHCO_3$ (3 x 100 mL) and water (3 x 100 mL). The organic layer was dried over anhydrous sodium sulphate, filtered and chloroform was evaporated under reduced pressure. The crude product was purified by silica gel column chromatography using a mixture of ethyl acetate: petroleum ether (10:90, v/v) as eluent. The removal of the solvent yielded 18.70 g (98 %) of 1-tosyl-10-undecene as a pale yellow liquid.

Bis-unsaturated ether (4) Into a two necked round bottom flask equipped with magnetic stirrer, slurry of sodium hydride (0.576 g, 23.52 mmol) in dimethylsulfoxide (25 mL) was formed. Solution of 10-Undecen-1-ol (1.0 g, 5.88 mmol) in dimethylsulfoxide (10 mL) was slowly added. The reaction mixture was stirred at room temperature for 10 minutes. To this, 1-tosyl-10-Undecene (1.81 g, 5.88 mmol) was added slowly. After 12h, dimethylsulfoxide was removed under reduced pressure and excess sodium hydride was deactivated by aqueous solution of ammonium chloride. Dichloromethane (50 mL) was added. The organic layer was washed with 5% $NaHCO_3$ (3 x 100 mL) and water (3 x 100 mL). The organic layer was dried over anhydrous sodium sulphate, filtered and chloroform was evaporated under reduced pressure. The crude product was purified by silica gel column chromatography using a mixture of ethyl acetate: petroleum ether (5:95, v/v) as eluent. Yield: 88%. Purity by GC: 99%.

1-azido-10-undecene To a 250mL, round-bottom flask equipped with a stirring bar, sodium azide (9.56 g, 147mmol) and 40mL of dimethylformamide (DMF) were transferred. To the stirred solution, 1-bromo-10-undecene (8.57 g, 37mmol) was added dropwise, and the entire mixture was allowed to stir for 12h. The azide mixture was then transferred to a separating funnel and extracted with ether and water at a ratio 1:1. The ether layer was washed with

water three times to remove DMF, dried over anhydrous sodium sulphate and concentrated under reduced pressure to end-up with 1-azido-10-undecene compound. Yield: 81%.

1-amino-10-undecene Reduction of azide to amine was performed by following reported procedures.[19] To a solution of azide (6 g, 30.7mmol) and ammonium chloride (7.49 g, 140mmol) in ethyl alcohol and water (150: 50/v: v), zinc dust (3.9 g, 60mmol) was added, the mixture was stirred vigorously at refluxing for 1h. After the reaction is over, ethyl acetate and aqueous ammonia (20mL) was added. The mixture was filtered, and the filtrate was washed with brine, dried over anhydrous sodium sulfate and concentrated under reduced pressure. Yield: 63%.

Bis-unsaturated amide (5) To a 500mL, round-bottom flask equipped with a stirring bar, a solution of triethylamine (2.69 g, 26.6mmol) and 1-amino-10-undecene (3 g, 17.75mmol) in THF was transferred. 10-undecenoyl chloride (3.60 g, 17.75mmol) was added dropwise to the solution at 0°C. After addition, the reaction mixture was stirred for 24h at room temperature under nitrogen atmosphere. After completion of the reaction, the obtained suspension was filtered to remove triethylamine salt and THF was removed under reduced pressure. The product was purified by column chromatography using a mixture of cyclohexane: ethyl acetate (90:10 / v: v). The bis-unsaturated amide was obtained as a light yellow solid. Yield: 69%.

2. Polymerization reactions.

Polymerizations in solution. Typical procedure for the solution polymerization in Polarclean® was as follow. Monomers were dried under vacuum at 70°C overnight prior to use. In a round-bottom flask was transferred a solution of the monomer (and in some cases a chain stopper) with 0.5mol% of metathesis catalyst (and 5mol% of 1,4-benzoquinone in the case of ruthenium 2nd generation catalysts) in polarclean®. The reaction mixture was stirred at 80°C for 24h under dynamic vacuum (96h when PLLA chain stopper was used). After completion of the reaction, ethylvinyl ether was added and the mixture was stirred at room temperature for 30 minutes under nitrogen atmosphere to deactivate metathesis catalyst. Dynamic vacuum was then applied to remove excess ethylvinyl ether. The reaction mixture was then precipitated in methanol in order to remove all the polarclean® solvent. Polymers were finally dried overnight at 70°C under dynamic vacuum.

Polymerizations in bulk. All monomers were dried under vacuum at 70°C overnight prior to reaction. In a round-bottom flask was transferred the monomer feed, with 0.5mol% of metathesis catalyst (and 5mol% of 1,4-benzoquinone in the case of ruthenium 2nd generation

catalysts). The reaction mixture was stirred at 80°C for 24h under dynamic vacuum. Tetrahydrofuran (THF) and ethylvinyl ether were then added and the mixture was stirred at room temperature for 30 minutes under nitrogen atmosphere. Dynamic vacuum was then applied. The reaction mixture was dissolved in dichloromethane and the polymer was precipitated in methanol and dried overnight at 70°C under vacuum.

All polymerizations in bulk and in solution led to a yield between 50 and 75%. Only the polyesters synthesized in solution from (**2**) by using **C1** and **C2** were obtained with a lower yield of around 20% and the polyether synthesized in Polarclean® which was obtained with a 38% yield.

Synthesis of the alkene-terminated PLLA. PLLA was synthesized by ring-opening polymerization of L-lactide using 10-undecenol and tin octoate as initiating system. 10-undecenol (170mg, 1mmol) and L-lactide (5.0g, 347mmol) were added to a two-necked round bottom flask equipped with a condenser, a nitrogen inlet and a mineral oil bubbler. The solution polymerization in dry toluene proceeded at reflux under nitrogen atmosphere for 4 hours upon addition of tin octoate (0.5wt%). After completion of the reaction, toluene was removed under reduced pressure and the copolymer was recovered by precipitating a concentrated dichloromethane solution into cold methanol and drying overnight at 50°C under reduced pressure.

Polymerization of L-lactide initiated by the pre-polymers.

The block copolymers were synthesized by ring-opening polymerization of L-lactide using HO-PU-OH or HO-PE-OH and tin octoate as initiating system. The pre-polymer and L-lactide were added in various amounts to a two-necked round bottom flask equipped with a condenser, a nitrogen inlet and a mineral oil bubbler. The solution polymerization in dry toluene proceeded at reflux under nitrogen atmosphere for 4 hours upon addition of tin octoate (0.5wt%). After completion of the reaction, toluene was removed under reduced pressure and the copolymer was recovered by precipitating a concentrated dichloromethane solution into cold methanol and drying overnight at 50°C under reduced pressure.

PART B. DEVELOPMENT OF A SERIES OF SUSTAINABLE "LLDPE LIKE" POLYESTERS BY ADMET METHODOLOGY

I. INTRODUCTION

In this part we focused our research on the development, by ADMET, of soft polymers that could mimic existing polymeric impact modifiers for PLLA. In the first chapter, we identified several polymer families as efficient additives for the modification of PLLA mechanical properties. From these, polyethylene-based materials appeared to be the most widely used impact modifiers for PLLA. Several reasons for that can be explained.

Targeted applications for PLLA range from commodity to specialty, thus the price of the additives used to improve the performance of PLLA need to be as low as possible in order for the final material to be competitive with other commodity polymers. Yet, polyethylene (PE) is the top manufactured polymer with readily available primary materials at the lowest prices. Another evidence of the success of PE-based polymers as PLLA additives resides in their unique properties. Indeed, the chemistry of PE is well established and it is thus possible to cover a wide range of thermo-mechanical properties by playing on the chemistry of polymerization that will dictate the microstructure of the so-formed PE. It is possible to identify four types of PE (HDPE, LDPE, LLDPE and VLDPE) which possess different properties depending on their morphological characteristics (Figure 20.5).

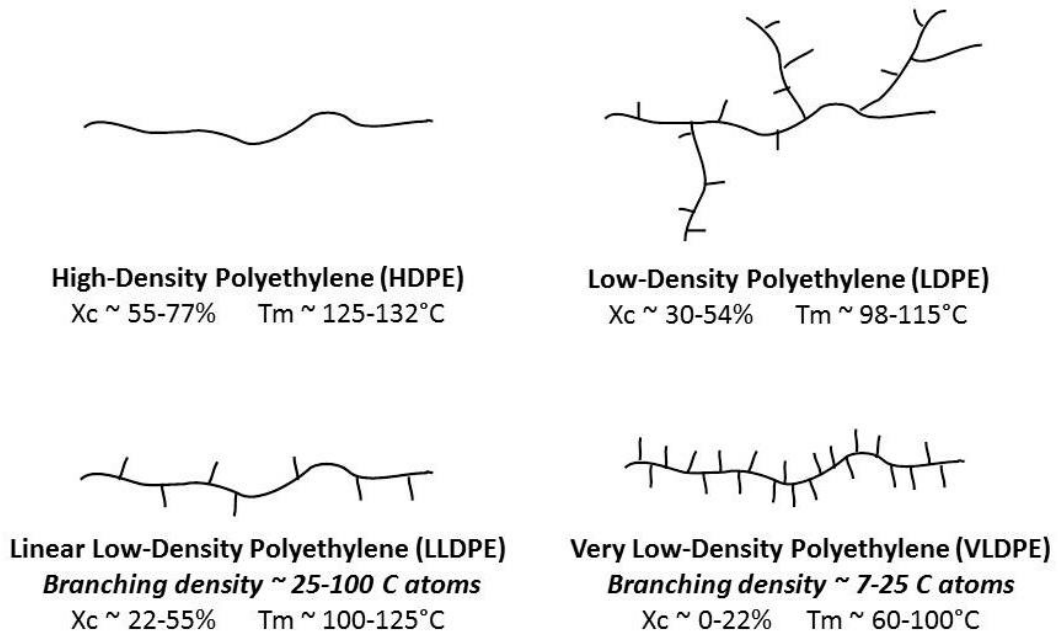

Figure 20.5. Schematic representation of polyethylene classes and corresponding properties

Regarding the properties of the different classes of PE, it appears that LDPE, LLDPE and VLDPE are the best candidates for the rubber- toughening of PLLA as evidenced by their lower degrees of crystallinity. This is the reason why many groups investigated the use of these materials in blends with PLLA.[20-22] Nevertheless the use of such polymers doesn't constitute a sustainable solution as evidenced by their lack of hydrolytical degradability thus impeding the compostability of the resulting PLLA materials. With the aim to introduce hydrolytically degradable segments to a polyethylene backbone while keeping the good characteristics of PE, a lot of efforts have been carried out these last years to design sustainable "polyethylene like" polyesters.[23-28] It was generally achieved by chemical modification of fatty acids yielding long chain aliphatic monomers bearing hydroxyl, acid or ester groups. After polymerization, aliphatic polyesters were obtained with various ester function densities incorporated in a polyethylene backbone. Nonetheless, most of the studies carried out on the development of "PE like" from fatty acids resulted in materials showing high crystallinity in the range of those achieved with HDPE.

On the contrary, very few investigations were carried out to mimic "LDPE", "LLDPE" and "VLDPE like" polyesters from plant oils. Some relevant examples include the works of Matsumura and coll. In a first study, the authors used hydrogenated methyl ricinoleate (methyl 12-hydroxystearate) and 12-hydroxydodecanoic acid (obtained from vernolic acid) as AB type monomers for the synthesis of aliphatic polyesters by enzyme-catalyzed polycondensation. By varying the amount between the two monomers, a series of high molecular weight copolyesters with versatile properties were obtained. Melting points of the so-formed polyesters were localized in a temperature window similar to LLDPE and VLDPE. The same group used a similar approach based on the copolymerization of methyl 12-hydroxystearate with pentadecalactone by an enzyme catalysis. Polyesters ranging from stiff to elastomeric thermoplastics were obtained depending on the feed composition. However the use of very high quantities of enzymes coupled with the high price of these catalysts limit the industrial potential of such materials.

In this part we aimed to develop, in a similar way than Matsumura and coll., new LLDPE and VLDPE like polyesters by using ADMET polymerization of castor oil and vernonia oil-based α,ω-dienes.

II. MONOMERS SYNTHESIS

The aim of this study being to mimic the structure of LLDPE, two monomers (one linear and one branched) were synthesized. Methyl 10-undecenoate and 12-hydroxystearic acid, obtained by steam cracking and hydrogenation of ricinoleic acid respectively were employed for the synthesis of the branched α,ω-diene. A second monomer showing a linear structure (with the same main chain structure than for the branched monomer) was also synthesized from methyl 10-undecenoate and 1,12-dodecanediol (obtained by oxidative cleavage of vernolic acid) (Figure 21.5).

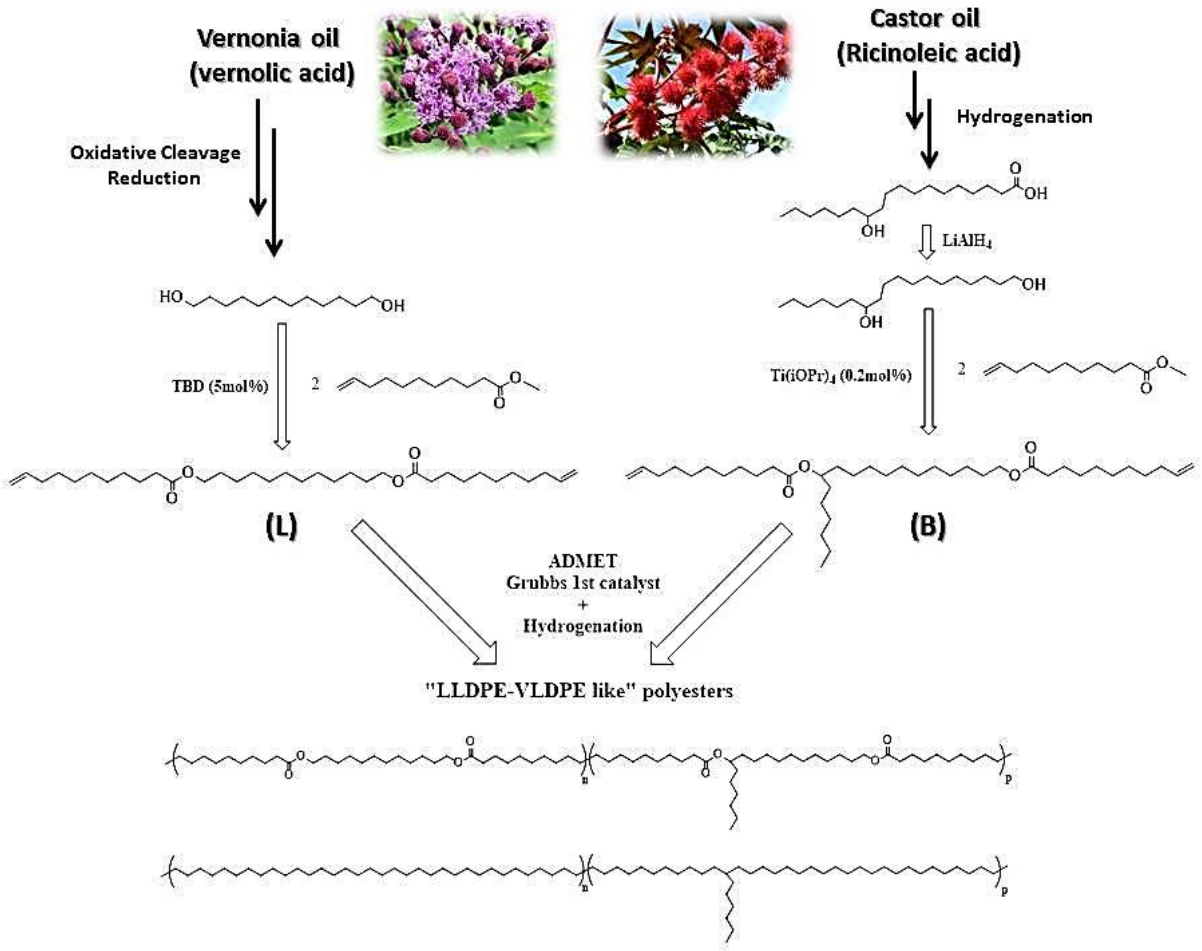

Figure 21.5 Synthetic strategy to « LLDPE like » polyesters.

II.1. Synthesis of the linear α,ω-diene (L)

The formation of the linear monomer (**L**) was carried out by a simple transesterification of two equivalents of methyl 10-undecenoate with one equivalent of 1,12-dodecanediol. The reaction was catalysed by TBD and carried out at 120°C-160°C under nitrogen atmosphere and then at 160 °C under vacuum. The progress of the transesterification reactions was monitored by ^{1}H-NMR spectroscopy.

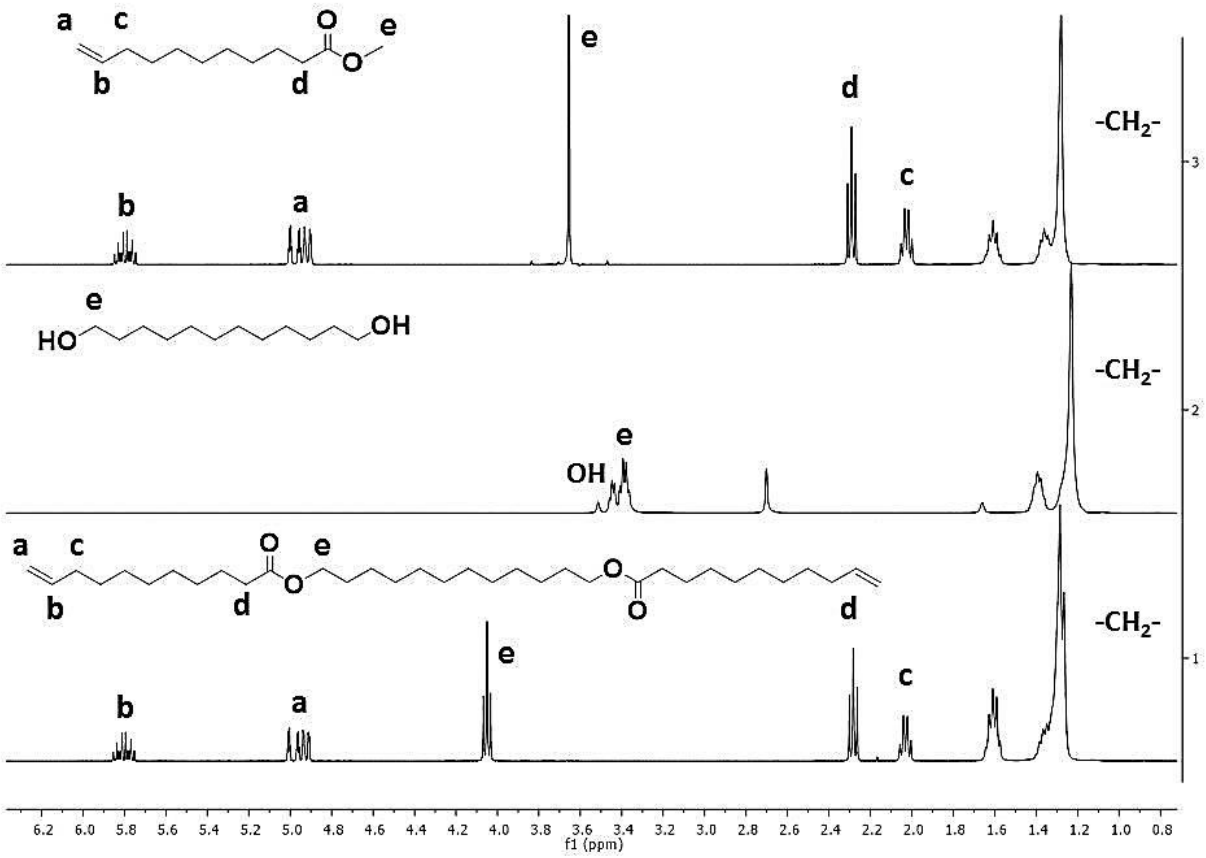

Figure 22.5. ^{1}H-NMR stacked spectra of methyl 10-undecenoate ($CDCl_3$), 1,12-dodecanediol (DMSO-d_6) and linear α,ω-diene ($CDCl_3$).

The ester linkage methyl protons in methyl 10-undecenoate (See Figure 22.5, H_e protons at 3.6 ppm) disappeared as a function of time. After transesterification and purification by column chromatography, a triplet corresponding to the methylene protons nearby the ester oxygen (See Figure 22.5, H_e protons) appeared at 4.1 ppm. The integrations of the peaks were in agreement with the expected structure. The purified product, obtained with a yield of 62% was analysed by GC and showed a purity of 97%, thus allowing its polymerization.

II.2. Synthesis of the branched α,ω-diene (B)

For the branched monomer (**B**), the synthetic strategy was the same than for the linear one, however, a reduction step of 12-hydroxystearic acid into 12-hydroxystearyl alcohol was needed prior to transesterification as the latter was not commercially available. The reduction of 12-hydroxystearic acid was carried out with $LiAlH_4$ yielding the corresponding diol with a conversion of 83.5%. The purification of the product was carried out by dissolving the reaction mixture into THF and by adding LiOH. The precipitate formed by addition of LiOH, which corresponds to the lithium salt of the unreacted 12-hydroxystearic acid, was then

removed from the solution yielding, after concentration of THF, the desired product with a sufficient purity as evidenced by ^{1}H-NMR spectroscopy (Figure 23.5).

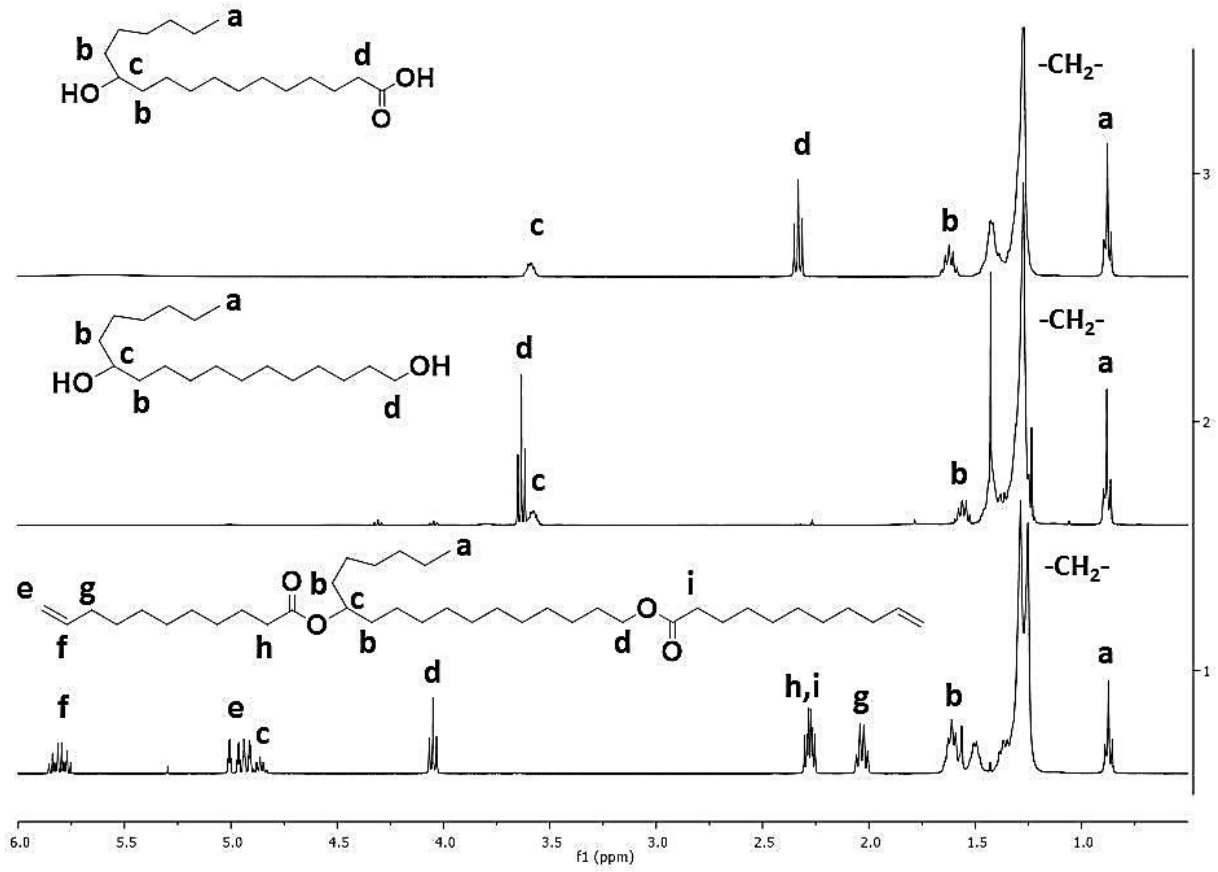

Figure 23.5. ^{1}H-NMR stacked spectra of 12-hydroxystearic acid, 12-hydroxystearyl alcohol and branched α,ω-diene in $CDCl_3$.

The diol was then reacted with methyl 10-undecenoate by transesterification catalyzed with titanium isopropoxide. After purification by column chromatography, the structure of the monomer was confirmed by ^{1}H-NMR spectroscopy (Figure 23.5). It is noteworthy that transesterification efficiently occurred as seen from the peaks at 4.86 ppm and 4.05 ppm assigned to the proton of the tertiary carbon in α position of the ester function in the side of the oxygen atom and to the protons in α position of the other ester function (in the side of the oxygen atom) respectively. The polymerization grade of the branched monomer was confirmed by GC analysis regarding the high purity obtained (99%).

III. POLYESTERS SYNTHESIS

III.1. ADMET polymerizations

Once the α,ω-diene monomers synthesized, it was then possible to develop a series of polyesters by ADMET copolymerization of the two monomers. The well-defined structure of

the monomers allowed to precisely control the branching density by varying the ratio between the two monomers. All the polymerizations were launched at 80°C in bulk under dynamic vacuum due to the non-volatile character of the monomers. Grubbs 1st generation catalyst (**C1**) was employed in this study in order to limit olefins isomerization. Indeed such side reactions would hinder the control of the microstructure by changing the methylene spacer length between the alkyl branches. The feed ratio between the two monomers was changed from 100% of purely linear monomer (**L**) to 100% of branched monomer (**B**) resulting in a number of atoms of the main chain between two branching points in the range 34-136 as shown in Table 5.5.

Table 5.5. Macromolecular characteristics of the unsaturated polyesters.

Entry	mol% (B) $_{theo}$	mol% (B) $_{exp}$ [a]	Branching density[b]	$\bar{M}_n$ (kg.mol^{-1})[c]	Đ[c]
B0	0	0	-	62	1.5
B25	25	22	136	20	1.7
B50	50	47	68	22	1.6
B75	75	74	45	14	1.6
B100	100	100	34	22	1.6

(a) ^{1}H-NMR, (b) average number of atoms of the main chain between two branching points, (c) SEC in THF, PS calibration.

After 24h of polymerization, the catalyst was deactivated with ethyl vinyl ether and the polyesters were precipitated into methanol. The resulting polyesters were analyzed both by ^{1}H-NMR and SEC in THF. Figure 24.5 shows the ^{1}H-NMR spectra of all the unsaturated polyesters after ADMET polymerization. The disappearance of the peaks at 5.8 and 4.9 ppm and the appearance of a multiplet at 5.4 ppm provide evidence of polyester formation by formation of internal olefins. ^{1}H-NMR analysis also gave information about the composition of the copolymers. Indeed, by incorporation of branched units, some peaks appeared such as the one assigned to the methyl protons of the alkyl dangling chain at 0.9 ppm and the one assigned to the proton of the tri-substituted carbon in α position of the ester function at 4.9 ppm. On the other hand, the integration of the peak at 4.1ppm characteristic of the protons in α position of the other ester functions (on the side of the oxygen atom) decreases with an increase in the branching density. Calculation of the experimental composition of the polyesters was then performed by integration of the characteristic peaks and showed good accordance with the expected compositions (See Table 5.5). From these values, it was then possible to calculate the average number of atoms of the main chain between two branching points. Values ranging between 34 and 136 atoms were found which show good agreement with the number of carbon atoms generally found for commercial LLDPE (See Table 5.5 and Figure 20.5).

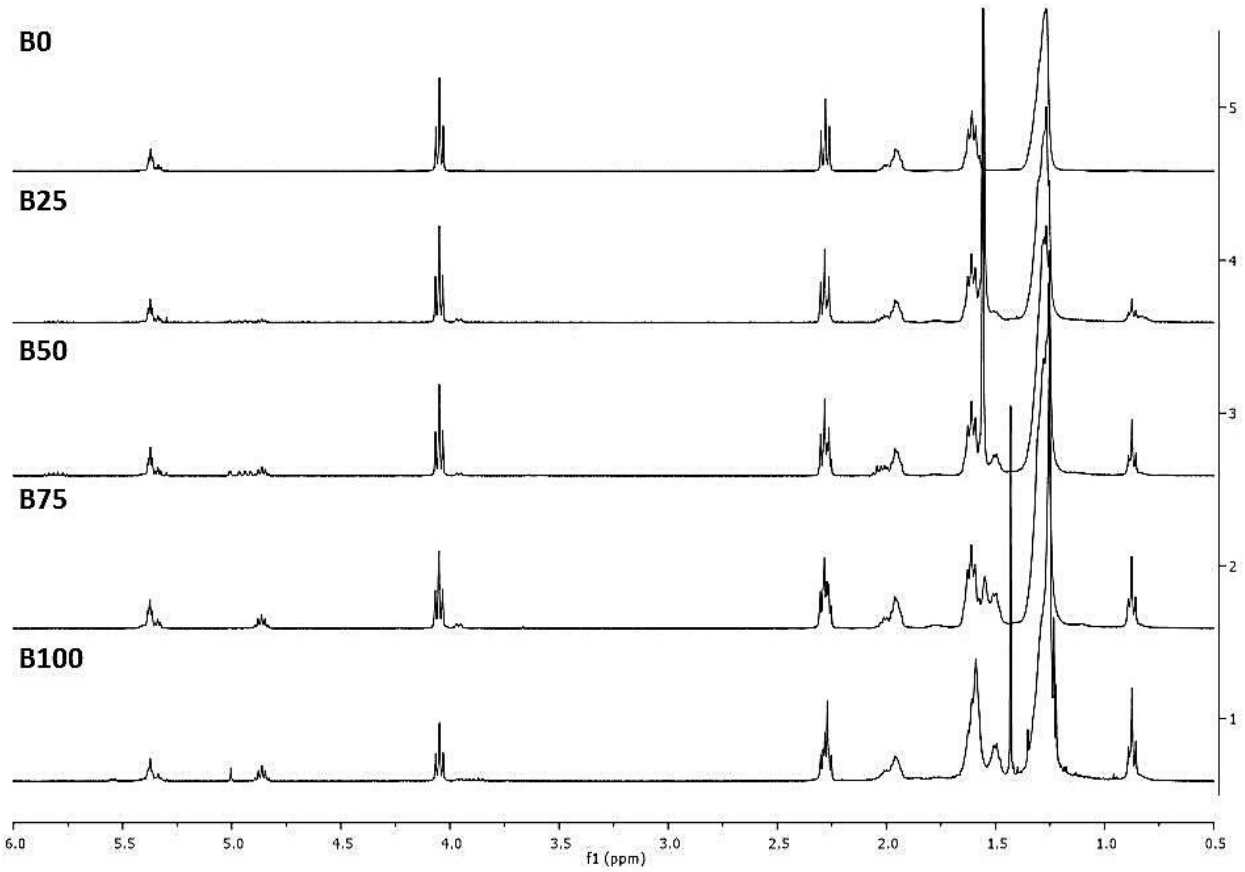

Figure 24.5. ^{1}H-NMR stacked spectra of the unsaturated polyesters in $CDCl_3$.

The unsaturated polyesters were then analyzed by SEC in THF using a PS calibration. Except for B0 (62 kg.mol^{-1}) which was synthesized using mechanical stirring (contrary to the other polyesters which were synthesized under magnetic stirring), the obtained molecular weight values were in the range 14-22 kg.mol^{-1}.

III.2. Hydrogenation of the unsaturated polyesters

In certain circumstances, it is desirable to keep unsaturation in the polymer backbone for further functionalization or cross-linking. However, in the context of our study, the polyesters must be free from remaining double bonds to avoid oxidation and possible cross-linking during heating of the samples. Reduction of the double bonds of the polyesters proceeded in toluene at 80°C with Pd on charcoal under hydrogen pressure (50bar). Fully saturated polyesters were obtained as evidenced by the disappearance of olefins protons peaks in ^{1}H-NMR spectra (Figure 25.5 and Figure 26.5).

Only HB0 did not show quantitative conversion. It can be attributed to the lower solubility of the polyester, above a certain hydrogenation conversion, which precipitates due to high crystallinity thus impeding quantitative conversion of the double bonds. Nevertheless, a

conversion of 88% was measured by ^{1}H-NMR analysis for HB0 which should provide sufficient improvement of the thermo-mechanical properties.

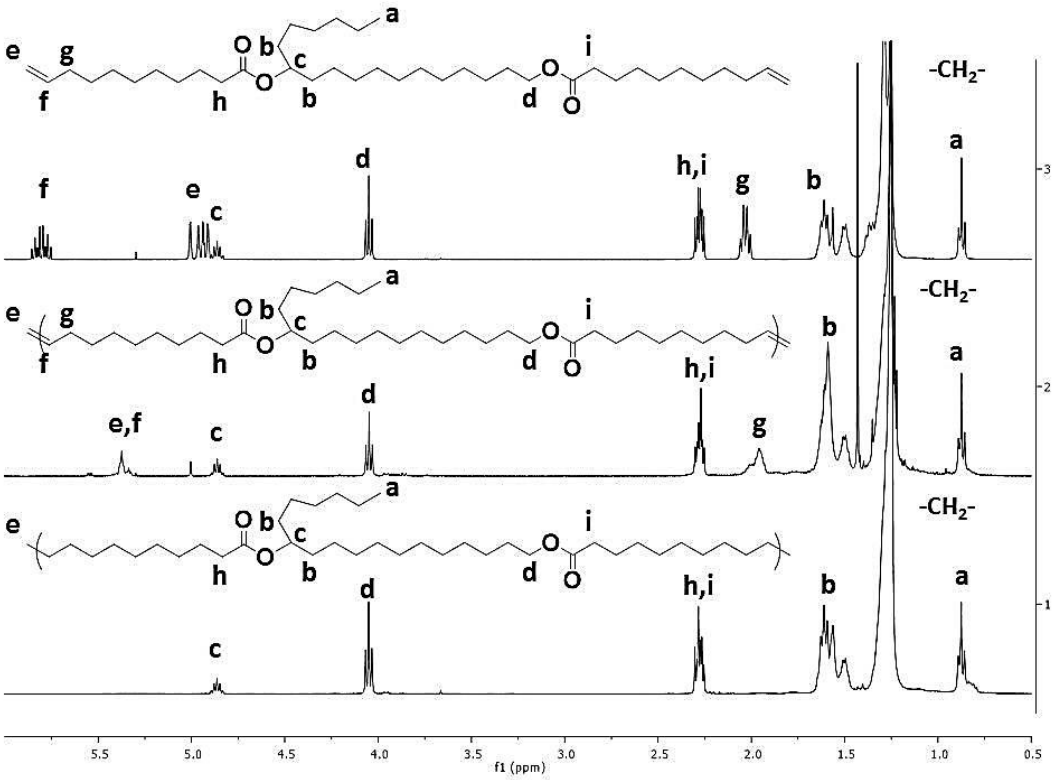

Figure 25.5. ^{1}H-NMR stacked spectra of the branched α,ω-diene, B100 and HB100 in $CDCl_3$.

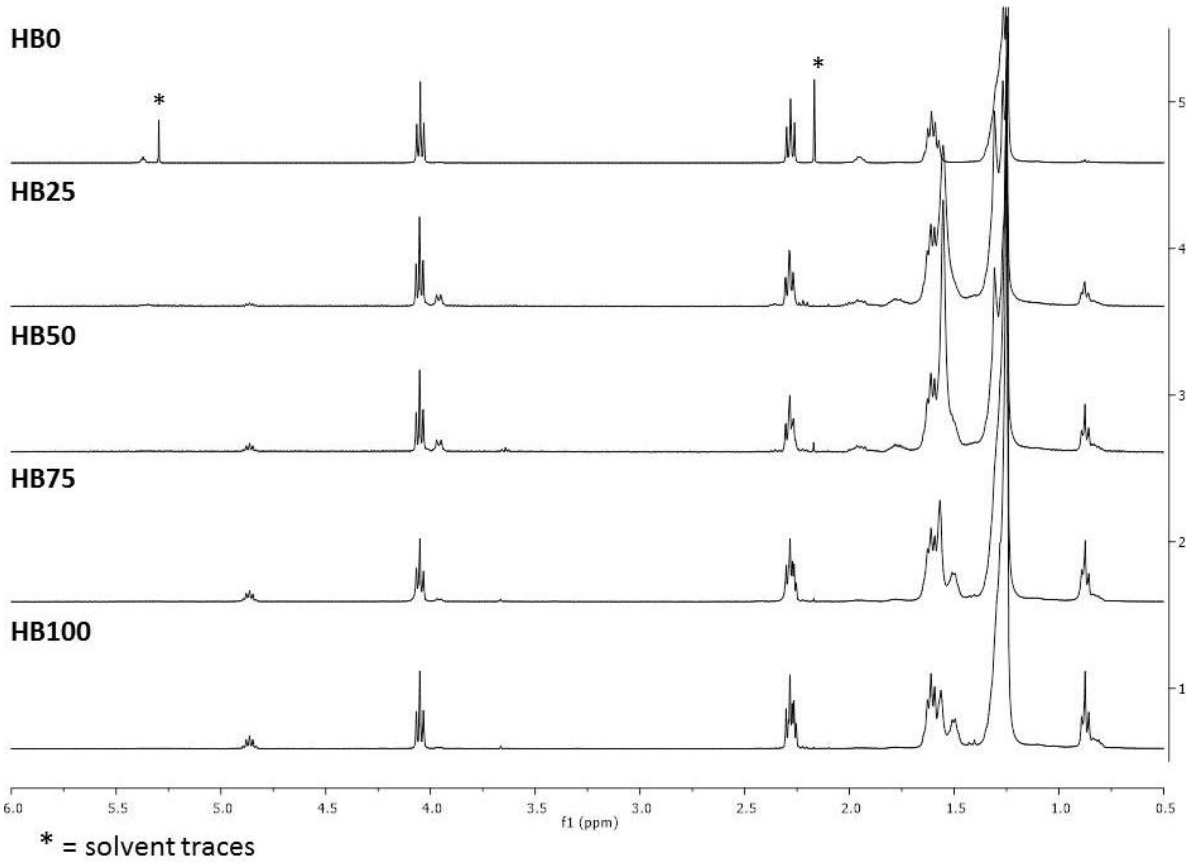

Figure 26.5. ^{1}H-NMR stacked spectra of the hydrogenated polyesters in $CDCl_3$.

IV. THERMAL AND THERMO-MECHANICAL PROPERTIES

IV.1. Thermal stability

In order to establish the structure-properties relationship for these novel polymers, DSC and TGA analyses were carried out. The thermal stability of the saturated polyesters was first investigated by TGA experiments under non-oxidative atmosphere. TGA derivative curves are presented in Figure 27.5 and illustrate the dependence of thermal stability with the amount of branched units.

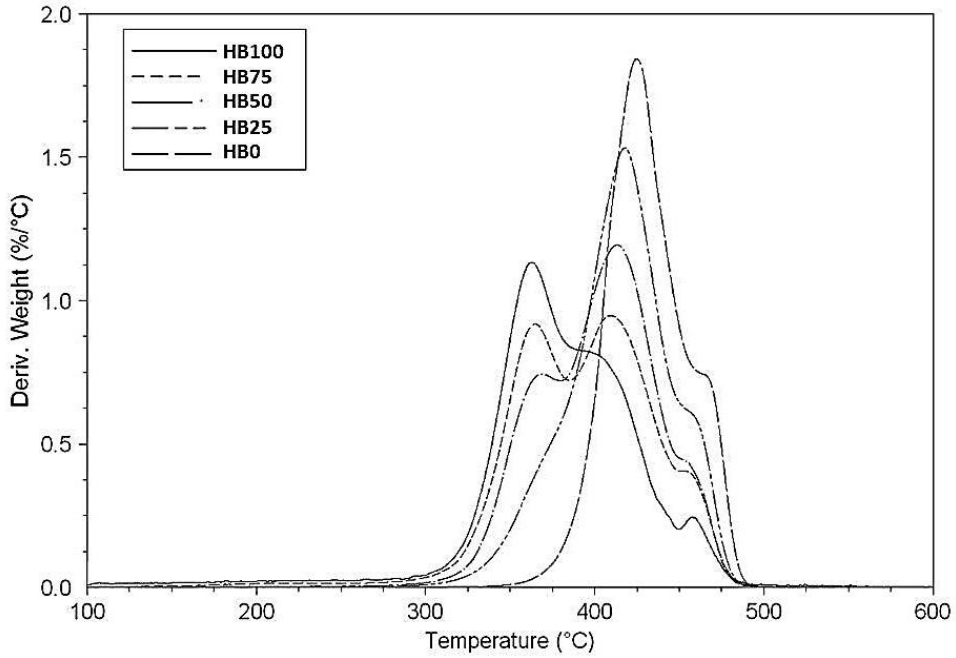

Figure 27.5. TGA derivative curves of the saturated polyesters. 10°C.min^{-1}.

Indeed it is noteworthy that the first weight loss (temperature corresponding to 5% weight loss) occurs at lower temperature when the branches density is higher (Table 6.5). Moreover, the TGA derivative curve clearly point out a multi-state thermal decomposition. A first weight loss is observed near 300°C followed by two other significant weight losses at around 375°C and 450°C. Interestingly, the intensity of the first degradation step increases with an increase in the branching density. Furthermore, the intensity of the other degradation steps decreases with an increase in the branching density. This observation is in agreement with the assignment of the first weight loss to the decomposition of the branches rich segments. In the case of LDPE, it was demonstrated that branching points generally lead to early thermal degradation in comparison to more linear analogues.[29] In this study, the same tendency than LDPE seems to be observed. Nevertheless, it is thought that the degradation mechanism must be different than for LDPE due to the presence of ester functions. The good thermal stability

for all polyesters, illustrated by the large difference between their decomposition temperatures and their melting points, let us consider their easy compression or injection molding and therefore their use for the toughening of PLLA by melt-blending.

IV.2. Melting and crystallization behaviors

In order to evaluate the influence of the alkyl branches on the crystalline ability of the polyesters, DSC analyses were performed. The unsaturated polyesters were first analyzed. From Figure 28.5, it is immediately obvious that hexyl branches significantly reduce the crystalline ability of the polyesters. Indeed both crystallization and melting temperatures (and their corresponding enthalpies) highly decrease with an increase in hexyl branches density. This was attributed to a hindrance of the chain packing by the hexyl branches. The unsaturated polyesters thus cover a large range of thermo-mechanical properties depending on the branching density with Tm in the range 13-69°C (Table 6.5). Melting enthalpy was also highly affected by the presence of hexyl branches as evidenced by the values of 101 $J.g^{-1}$ and 34 $J.g^{-1}$ for B0 and B100 respectively. The relatively low value of melting point and corresponding enthalpy measured for B0 in comparison to other "polyethylene like" polyesters described in the literature is ascribed to the remaining olefins which disrupt efficient crystallites formation due to cis- and tans- conformations which imped sufficient mobility of the chains.[23]

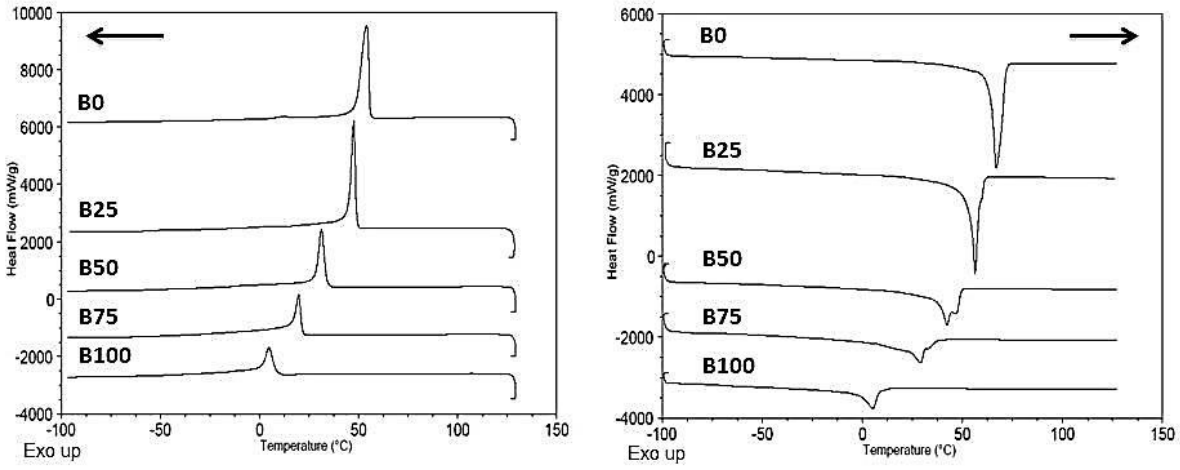

Figure 28.5. DSC cooling and heating curves of the unsaturated polyesters. 10°C.min^{-1}.

Hydrogenation of the unsaturated polyesters resulted in improved thermo-mechanical properties (Figure 29.5 and Table 6.5). Indeed, the fully saturated structure of the resulting polyesters was responsible for improved chain packing and thus enhancement of the crystallization and melting temperatures (and their respective enthalpies). An enhancement of

around 20-30°C was observed for the melting temperature of all the polyesters. On the other hand, the melting enthalpy value was more or less enhanced depending on the sample.

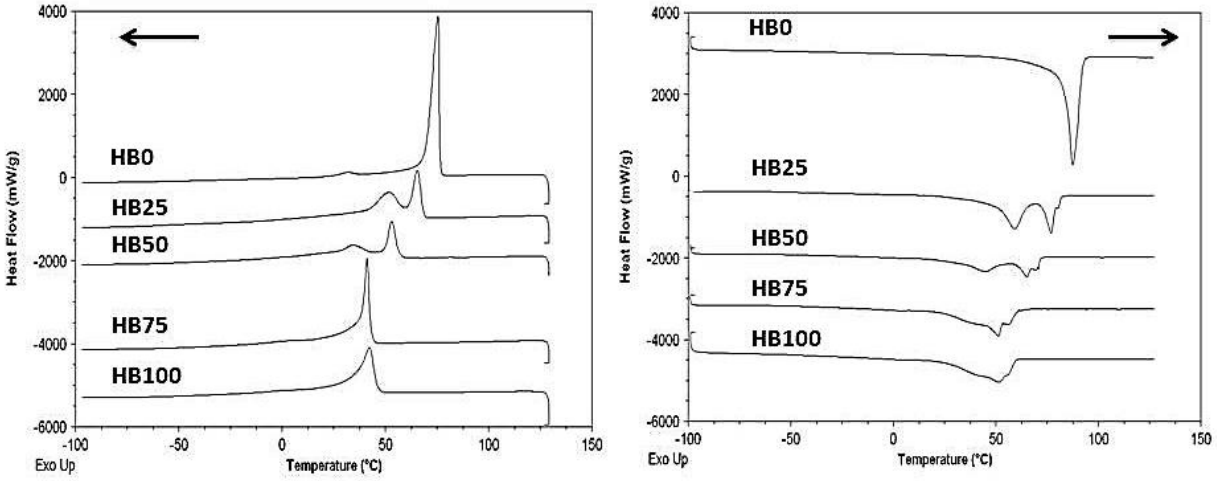

Figure 29.5. DSC cooling and heating curves of the saturated polyesters. 10°C.min^{-1}.

Despite the close average number of atoms between two branching points in comparison to LLDPE (25-100 carbon atoms), the melting points of the branched polyesters (HB25, HB50, HB75 and HB100) in the range 51-77°C, were much lower than for LLDPE (Tm ~ 100-125°C) and were closer to those generally measured for VLDPE (Tm ~ 60-100°C). This deviation to the LLDPE thermo-mechanical properties was logically attributed to the presence of inherent ester functions, in accordance to the previous studies realized on "polyethylene like" polyesters.[24-28, 30] Indeed, Penelle and coll. demonstrated that ester group can be incorporated in the crystallites thus lowering the overall attractive interaction between the polymer chains in comparison to polyethylene.[31]

Table 6.5.Summary of the properties of the unsaturated and saturated polyesters.

Entry	Branching density[a]	$T_{5\%}$ (°C)[b]	Tc (°C)[c]	ΔHc (J.g^{-1})[c]	Tm (°C)[c]	ΔHm (J.g^{-1})[c]
B0	-	-	54.0	103.3	68.9	101.2
HB0		394	75.4	133.3	87.4	135.5
B25	136	-	47.6	88.4	55.9	89.4
HB25		357	51.3 – 65.5	92.6	59.2 – 77.0	98.1
B50	68	-	31.2	62.3	46.3	62.9
HB50		344	34.1 – 53.2	65.3	44.8 – 64.9	66.5
B75	45	-	19.7	40.1	26.3 - 36.6	38.1
HB75		331	41.0	62.9	51.3 – 56.6	65.1
B100	34	-	4.9	32.1	13.2	32.4
HB100		312	42.2	60.3	51.6	63.0

(a) Average number of atoms of the main chain between two branching points, (b) TGA-10°C.min^{-1}, (c) DSC-10°C.min^{-1}.

It is noteworthy that only HB0 showed a narrow endothermic melting peak, while the other saturated polyesters showed complex melting patterns. This was attributed to the highly

regular microstructure of HB0 in comparison to the other saturated polyesters for which hexyl branches are distributed randomly along the "polyethylene like" backbone giving rise to a broader crystalline lamella thickness distribution. In the case of HB25 where the alkyl dangling chain density remains low, two narrow endothermic peaks were observed. To investigate this melting behavior, DSC analysis was performed on a HB25 sample annealed for 15 minutes at 65°C. The obtained DSC heating trace (Figure 30.5) shows evidence of two distinct melting peaks at similar temperatures than without annealing. This information let us consider polymorphism (different crystalline phases or crystallites differing in size) rather than melting of a meta-stable crystalline phase with subsequent crystallization into a more stable phase.

Modulated DSC analysis at a heating rate of 3°C.min^{-1} was then performed on the same sample (HB25) in order to confirm our hypothesis of polymorphism. The DSC traces, displayed in Figure 31.5 gives evidence of polymorphism. Indeed, the reversible heat flow signal shows two endothermic peaks with maxima at 59°C and 78°C related to two melting transitions. On the contrary, the non-reversible heat flow shows no significant variations (crystallization) in the temperature window concerned. Thus, the complex melting pattern is not ascribed to a melting-recrystallization process but to polymorphism.

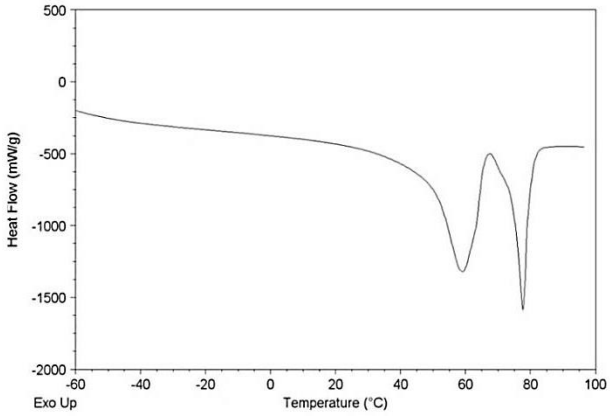

Figure 30.5. DSC heating scan trace of HB25 after annealing at 65°C during 15 minutes. 10°C.min^{-1}.

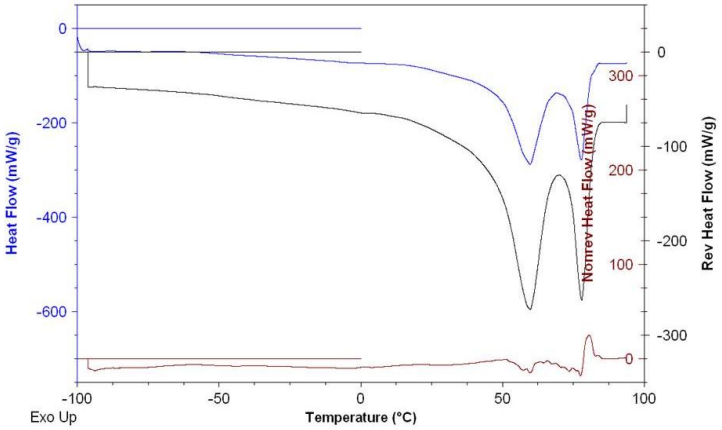

Figure 31.5. Modulated DSC heating scan traces of HB25. 3°C.min^{-1}.

In the case of HB25 and HB50, due to the low branching density and the randomness of the branching point positions along the polyester backbone, it is thought that the melting peak at lower temperature is assigned to crystallites corresponding to segments with high branching content while the melting transition at higher temperature corresponds to the nearly linear segments. It is known that, contrary to ethylene/propylene copolymers, ethylene/octene copolymers display the exclusion of large hexyl branches from the crystal unit cell.[32, 33] In the case of HB75 and HB100, the increased branching density coupled with the hypothetical exclusion of hexyl branches from the crystal unit cell, gave rise to smaller crystallites with a broad size distribution which explains the broad melting peak. Similar melting behavior was reported by Hillmyer and coll with LLDPEs synthesized by random ROMP of 5-hexylcyclooct-1-ene and cyclooctadiene.[34] The synthesis of precision LLDPE in which the hexyl dangling chains would be regularly space separated could lead to a narrower melting and crystallization peak by homogenization of the crystallites size.[35, 36] However, our synthetic strategy based on the restrictive use of biobased building blocks does not allow us to achieve such a control.

V. CONCLUSION

Castor oil plastform was efficiently used to develop a series of "LLDPE like" polyesters by ADMET polymerization. Two biobased α,ω-diene monomers, one linear and one bearing an hexyl dangling chain, were first synthesized by transesterification of methyl 10-undecenoate with 1,12-dodecanediol or 12-hydroxystearyl alcohol respectively. The α,ω-dienes were then copolymerized in different amounts resulting in unsaturated polyesters covering a wide range of thermo-mechanical properties. Their hydrogenation yielded the saturated polyesters that showed close structural similarities with LLDPE regarding their polyethylene backbone with incorporated ester functions and hexyl dangling chains. These copolyesters showed good thermal stability as seen from the initial degradation temperatures above 300°C. Thermo-mechanical properties were closer to VLDPE than LLDPE regarding the melting points in the range 51-77°C. For most of the copolyesters, a broad melting peak with complex pattern was observed which provide evidence of small crystallites formation with a high heterogeneity in size.

Despite the presence of numerous hexyl dangling chains distributed in the backbone of these polyesters, it seems that the rather high melting enthalpies of these polymers could constitute a hindrance to their use as efficient impact modifiers of PLLA. Indeed, in chapter 3, it was claimed that the lower the crystallinity of the additive, the higher the impact strength of the

resulting blends with PLLA. For potential application as impact modifiers of PLLA, the chemical structure of these copolyesters should be adapted by increasing the dangling chain density in order to imped more efficiently their crystalline ability. Nevertheless, independently to the toughening of PLLA, these novel biobased materials constitute good alternatives to petroleum-based LLDPE and VLDPE.

VI. EXPERIMENTAL

1. Synthesis of monomers.

Linear α,ω-diene monomer (L). Compound (**L**) was prepared using methyl 10-undecenoate (15 g, 75.6 mmol) as two molar equivalents and 1,12-dodecanediol (7.65g, 37.8 mmol), representing one equivalent in terms of reactive functions. The reaction was catalyzed by Triazabicyclodecene (TBD) using a 5% mol ratio regarding 10-methylundecenoate. The mixture was flushed with nitrogen at 120°C for 6 h. Then, for the last 2 h, the nitrogen flux was substituted for vacuum. The reaction was eventually stopped and the compound was isolated by (recrystallization at 50°C in dichloromethane) and then on silica-gel column eluted with a mixture of cyclohexane/ethyl acetate (80/20). The process resulted in the isolation of compound (**L**) as a white solid in 61% yield (12.4 g).

Branched α,ω-diene monomer (B). The 12-hydroxy stearyl alcohol first had to be reduced from its carboxylic acid version, the 12-hydroxy stearic acid. This reaction was carried out using 10 g (33 mmol) of 12-hydroxy stearic acid and 3 molar equivalents of $LiAlH_4$ (3.79 g, 100 mmol) catalyst. The 12-hydroxy stearic acid was first dissolved in 100 mL of dry THF, and $LiAlH_4$ was slowly dissolved in 300 mL. The reaction flask with $LiAlH_4$ was put in an ice bath and the dissolved 12-hydroxy stearic acid was slowly added. The mixture was stirred for 16 h under nitrogen, then the ice bath was removed and the mixture was refluxed at 70°C for 6 h. Distilled water was added to deactivate the catalyst followed by 400 mL of 1N HCl. The synthesized compound could not be isolated using a silica-gel column, whatever the solvents or the proportions involved. The 12-hydroxystearic acid was separated from the 12-hydroxystearyl alcohol using Lithium hydroxide in THF. 12-hydroxystearic acid precipitated by forming a complex with the lithium ion whilst on carboxylate form. The 12-hydroxystearyl alcohol is still soluble in THF and can be isolated by simple filtration. Then, compound (**B**) was synthesized by transesterification using 10-methylundecenoate (6.39 g, 32.2 mmol) as 2.5 molar equivalents and 12-hydroxystearyl alcohol (4.37 g, 12.9 mmol) as one molar equivalent. The same conditions were used for the reaction than for compound (**L**) except the catalyst which was substituted by 0.2mol% of titanium isopropoxide. Compound (**B**) was

isolated using silica-gel column eluted with a mixture of n-heptane/ethyl acetate (95/5). The process resulted in the isolation of compound (**B**) as a viscous liquid with a 99% purity determined by gas chromatography.

2. ADMET polymerizations.

The copolymers were synthesised by ADMET polymerization using monomers (**B**) and (**L**) in various combinations. Each reaction was catalyzed using first generation Grubbs catalyst at 1mol%. The reaction was carried out at 85°C for 8h, and vacuum was constantly applied to remove the ethylene formed by the polymerization. The reaction medium was then solubilized in THF and deactivated using a few drops of ethylvinyl ether. Each polymer was then precipitated in methanol and dried to remove solvent traces.

3. Hydrogenation of the polyesters.

Unsaturations in between polymer units were hydrogenated by solubilizing each polymer in toluene with a 15 mL ratio for 500 mg of polymer. The Palladium on charcoal catalyst was added with a 50 mg ratio for 500 mg of polymer. The reaction was carried out under 50 bar H_2 at 80°C for 20h. The resulting solution was filtered on Celite to isolate the saturated polymer.

REFERENCES

1. P. Jean-Louis Hérisson and Y. Chauvin, *Die Makromolekulare Chemie*, 1971, **141**, 161-176.
2. C. J. Schaverien, J. C. Dewan and R. R. Schrock, *Journal of the American Chemical Society*, 1986, **108**, 2771-2773.
3. R. R. Schrock, R. T. DePue, J. Feldman, C. J. Schaverien, J. C. Dewan and A. H. Liu, *Journal of the American Chemical Society*, 1988, **110**, 1423-1435.
4. R. R. Schrock, J. S. Murdzek, G. C. Bazan, J. Robbins, M. DiMare and M. O'Regan, *Journal of the American Chemical Society*, 1990, **112**, 3875-3886.
5. S. T. Nguyen, L. K. Johnson, R. H. Grubbs and J. W. Ziller, *Journal of the American Chemical Society*, 1992, **114**, 3974-3975.
6. H. Mutlu, L. M. de Espinosa and M. A. R. Meier, *Chemical Society Reviews*, 2011, **40**, 1404-1445.
7. K. L. Opper and K. B. Wagener, *Journal of Polymer Science Part A: Polymer Chemistry*, 2011, **49**, 821-831.
8. P. Atallah, K. B. Wagener and M. D. Schulz, *Macromolecules*, 2013, **46**, 4735-4741.
9. G. C. Vougioukalakis and R. H. Grubbs, *Chemical Reviews*, 2009, **110**, 1746-1787.
10. A. Rybak and M. A. R. Meier, *ChemSusChem*, 2008, **1**, 542-547.
11. S. Warwel, F. Brüse, C. Demes, M. Kunz and M. R. g. Klaas, *Chemosphere*, 2001, **43**, 39-48.
12. M. A. R. Meier, *Macromolecular Chemistry and Physics*, 2009, **210**, 1073-1079.
13. H. Mutlu and M. A. R. Meier, *Macromolecular Chemistry and Physics*, 2009, **210**, 1019-1025.
14. H. Mutlu, J. Ruiz, S. C. Solleder and M. A. R. Meier, *Green Chemistry*, 2012, **14**, 1728-1735.
15. O. Türünç, L. Montero de Espinosa and M. A. R. Meier, *Macromolecular Rapid Communications*, 2011, **32**, 1357-1361.
16. *Rhodiasolv web page*, http://www.rhodia.com/fr/markets_and_products/brands/Novecare_Rhodiasolv_polarclean.tcm.
17. S. H. Hong, D. P. Sanders, C. W. Lee and R. H. Grubbs, *Journal of the American Chemical Society*, 2005, **127**, 17160-17161.
18. P. A. Fokou and M. A. R. Meier, *Macromolecular Rapid Communications*, 2010, **31**, 368-373.
19. W. Lin, X. Zhang, Z. He, Y. Jin, L. Gong and A. Mi, *Synthetic Communications*, 2002, **32**, 3279-3284.
20. K. S. Anderson, S. H. Lim and M. A. Hillmyer, *Journal of Applied Polymer Science*, 2003, **89**, 3757-3768.
21. Y. Feng, Y. Hu, J. Yin, G. Zhao and W. Jiang, *Polymer Engineering & Science*, 2013, **53**, 389-396.
22. Z. Su, Q. Li, Y. Liu, G.-H. Hu and C. Wu, *European Polymer Journal*, 2009, **45**, 2428-2433.
23. J. Trzaskowski, D. Quinzler, C. Bährle and S. Mecking, *Macromolecular Rapid Communications*, 2011, **32**, 1352-1356.
24. F. Stempfle, D. Quinzler, I. Heckler and S. Mecking, *Macromolecules*, 2011, **44**, 4159-4166.
25. C. Vilela, A. J. D. Silvestre and M. A. R. Meier, *Macromolecular Chemistry and Physics*, 2012, **213**, 2220-2227.
26. F. Stempfle, P. Ortmann and S. Mecking, *Macromolecular Rapid Communications*, 2013, **34**, 47-50.
27. M. P. F. Pepels, M. R. Hansen, H. Goossens and R. Duchateau, *Macromolecules*, 2013, **46**, 7668-7677.
28. P. Ortmann and S. Mecking, *Macromolecules*, 2013, **46**, 7213-7218.
29. A. Holmström and E. M. Sörvik, *Journal of Applied Polymer Science*, 1974, **18**, 761-778.
30. I. van der Meulen, E. Gubbels, S. Huijser, R. l. Sablong, C. E. Koning, A. Heise and R. Duchateau, *Macromolecules*, 2011, **44**, 4301-4305.
31. C. L. F. De Ten Hove, J. Penelle, D. A. Ivanov and A. M. Jonas, *Nat Mater*, 2004, **3**, 33-37.
32. M. J. Richardson, P. J. Flory and J. B. Jackson, *Polymer*, 1963, **4**, 221-236.
33. R. G. Alamo and L. Mandelkern, *Thermochimica Acta*, 1994, **238**, 155-201.

34. S. Kobayashi, C. W. Macosko and M. A. Hillmyer, *Australian Journal of Chemistry*, 2010, **63**, 1201-1209.
35. B. Inci, I. Lieberwirth, W. Steffen, M. Mezger, R. Graf, K. Landfester and K. B. Wagener, *Macromolecules*, 2012, **45**, 3367-3376.
36. S. Kobayashi, L. M. Pitet and M. A. Hillmyer, *Journal of the American Chemical Society*, 2011, **133**, 5794-5797.

CONCLUSION AND PERSPECTIVES

The aim of this thesis was to develop novel bio-based aliphatic polyesters that can be used as impact modifiers for PLLA. Indeed, a state-of-the-art concerning toughening solutions for PLLA revealed the emergence of a second-generation of impact modifiers which show bio-sourcing and biodegradability as main characteristics in addition to their softness. Plant oils, more precisely fatty acids, were used as a suitable resource to design new low Tg aliphatic polyesters matching with PLLA toughening requirements.

Special attention was paid to this bio-resource due to several factors. Firstly, plant oils are annually renewable and are the most important sustainable raw materials for the chemical industry. Indeed, plant oils are used as a feedstock for an already mature bioplatform composed of several commercially available molecules used in various industrial sectors (surfactants, coatings, cosmetics, resins…). The inherent aliphatic structure of fatty acids, coupled with their high functionality yield by chemical transformation mostly to aliphatic diols and diacids. Thus, it makes fatty acids a tailor-made resource for the synthesis of aliphatic polyesters.

The results obtained by investigating different rubber-toughening systems let us say that we fulfilled the initial goal of this thesis. Indeed by using available and cheap raw materials we succeeded in the synthesis of low Tg aliphatic polyesters. Moreover, simple, safe and efficient chemical transformations such as transesterification, thiol-ene addition and metathesis were mostly used to provide industrial perspectives to this work in accordance with our partners' expectations. Regarding the polyesters synthesis, bulk polymerization was used as much as possible in order to be in line with the green chemistry principles that advocate the use of safe synthetic methods and the limitation of side products and solvents. The modification of PLLA properties with the use of these polyester additives was then carried out using usual industrial methods such as extrusion-injection; also with the aim to provide an industrial reality to the developed materials. Promising results were obtained for the developed PLLA materials in terms of impact strength. Further optimization of these systems should even yield to comparable or better impact strength than current commercially available high impact PLLA materials. This thesis work thus demonstrated the possible rubber-toughening of PLLA by sustainable polyesters synthesized from the plant oils platform.

In the first part of the manuscript, a novel poly(ester-amide) (PEA) thermoplastic elastomer derived from plant oils (mainly castor oil platform) was synthesized and subsequently used as an impact modifier for PLLA. Firstly, various diols bearing ester and/or amide functions were

synthesized in order to evaluate the influence of amide function density on the thermal and mechanical properties of the materials synthesized by polycondensation of these diols with a C20 methyl diester. This investigation showed the beneficial effect of amide functions on the melting-point of the materials; however it was accompanied with a significant increase in the Young's modulus. In order to provide softness to the PEA with the highest melting point, while keeping its high thermal endurance, the diamide diol was polycondensated with a dimerized fatty acid that acted as internal plasticizer thus lowering the Young's modulus. The optimized PEA fulfilled all the requirements for effective toughening of PLLA as seen from its low Tg (-28°C), its low elastic modulus (191 MPa), its thermal stability at the processing temperature of PLLA as well as its theoretical immiscibility with PLLA. The PEA was then melt-blended with PLLA by twin-screw extrusion resulting in typical two-phase polymer alloys. A transition from brittle fracture to ductile fracture was observed during tensile tests with PEA contents as low as 5wt%. The efficient toughening was also evaluated from the obtained notched IZOD impact strength values (up to 3.7 $kJ.m^{-2}$) that were in the range of those generally measured for most of the toughening systems involving PCL, PBS or PHAs as impact modifiers. The limited improvement of the impact strength could be overcome by adding a third component that would act as adhesion promoter at the interface of the matrix and the dispersed phase.

Nevertheless the scope of this thesis being to synthesize the most suitable bio-based polyester impact modifiers, we were more interested to understand how we can tune the efficiency of the impact modifier without adding a third component. We identified crystallinity of the additive as a potential factor of impact strength limitation. Indeed, higher crystallinity of the impact modifier involves higher mechanical strength of the dispersed phase and thus lower energy absorption during impact. To confirm this point, a series of polyesters showing different degrees of crystallinity was developed. Impact resistance of the blends of these rubbers with PLLA was evaluated by notched IZOD impact tests. At similar composition, impact strength gradually increased with a decrease in crystallinity degree of the rubber. It was attributed to differences in the toughening mechanisms which were linked to the mechanical strength of the rubber. In all cases, cavitation was followed by void formation, growing along the crack propagation and matrix shear yielding. Interestingly, the blend realized with 10wt% of the less crystalline rubber showed notched impact strength of 8.6 $kJ.m^{-2}$ (2.4 $kJ.m^{-2}$ for neat PLLA). Biomax® strong 100, a commercial modifier for PLLA from DuPont company, which is said to be an ethylene-acrylate copolymer, was reported to yield notched impact strength of 12.4 $kJ.m^{-2}$ (2.6 $kJ.m^{-2}$ for neat PLLA) when 10wt% was incorporated into PLLA. Blends of PLLA with various amorphous polyester rubbers reported

in the literature showed impact strength values in the range 7-11 $kJ.m^{-2}$. Consequently, the toughening efficiency of the rubbers we developed is in agreement with what is reported both with similar systems and with commercial impact modifiers. To further improve the toughening efficiency and thus being highly competitive with most of impact modifiers currently on the market, we could add adhesion promoter to compatibilize the two phases (matrix and dispersed phase). This work is currently under investigation.

Because ideally amorphous polyesters are needed to toughen PLLA, we then decided to focus our investigations on methyl ricinoleate as a starting material. This molecule can be obtained by a simple transesterification step from castor oil which makes it a cheap and available building block for further chemical transformation. Direct AB-type polycondensation yield poly(ricinoleic acid) (PRic) which is a very low Tg (~ -70°C) amorphous polyester. Rather than melt-blending, we studied the block copolymerization as a rubber-toughening methodology. A dihydroxy-telechelic PRic was thus synthesized by polycondensation of methyl ricinoleate with a low amount of 1,3-propanediol. The obtained polymer was then used as a macroinitiator (in various amounts) for the ROP of L-lactide resulting in a series of PLLA-*b*-PRic-*b*-PLLA copolymers with weight percentages of PLLA block in the range 35-83%. Elastomeric to hard and ductile materials were obtained depending on the weight ratio between the hard and soft blocks. Interestingly, the copolymer with only 17wt% of PRic, showed an elongation at break value of 98% (5% for neat PLLA) with limited lowering of the stiffness. Clearly, this study opens new pathways for the development of economically viable PLLA-based block copolymers showing improved toughness in comparison to neat PLLA. Further investigations need to be carried out regarding the synthetic process of these copolymers. For instance, reactive extrusion could be an interesting perspective to further lowering the cost of production of these materials.

In the last part, we carried out an exploratory work regarding the use of ADMET polymerization for the potential toughening of PLLA. In a first study, ABA triblock formation was investigated. The ADMET conditions were first optimized by using two reaction media (in bulk or in a green solvent) and four types of catalysts. Once the optimal conditions established, the ADMET polymerization of various α,ω-dienes was conducted either in the presence of an alkene-terminated PLLA chain stopper or an hydroxyl-functionalized chain stopper. In the first case, the synthesis of triblock copolymers in one pot did not showed the expected results as an obvious lack of control of the polymer architecture was noticed. In the second case, isomerization side reactions highly impeded the control of the chain ends necessary for the subsequent ROP of L-lactide initiated by the prepolymer synthesized by

ADMET. This work thus demonstrated that the lack of control during ADMET polymerization is an important limitation to the synthesis of valuable PLLA-based block copolymers using this polymerization technique. Nevertheless, ADMET is a powerful technique to mimic the structure of polyethylene as demonstrated in the bibliographic part. Due to the extensive use of polyethylene materials in the toughening of PLLA, we studied the formation of "LLDPE like" fatty acid-based polyesters by ADMET. The structure-properties relationship of the so-formed polyesters was readily established with an obvious effect of the dangling chain density on the crystallinity of the material. Despite the similar structure than LLDPE, these polyesters showed thermo-mechanical properties much closer to VLDPE as evidenced by the low melting point values. The melt-blending of these polyesters with PLLA remains to do, however good toughening efficiency is expected regarding their thermo-mechanical properties.

In this thesis work, we developed a sustainable approach to the toughening of PLLA in agreement with a biorefinery approach. Indeed, the plant oils platform was efficiently used to develop new environmentally friendly additive for the improvement of the mechanical properties of PLLA which is a mature polyester obtained from the ligno-cellulosic and starch platforms. The industrial perspectives of the developed materials were highlighted by the deposit of three patents. Optimization of the synthesis of the additives at a pilot scale is currently undertaken at ITERG.

Nevertheless further developments need to be performed in order to give rise to a highly competitive high-impact PLLA. Regarding the polyesters synthesized in the chapter 3, reactive compatibilization with PLLA (by using dicumyl peroxide, isocyanates or glycidyl methacrylate copolymers) need to be carried out in order to change from tough PLLA to super-tough PLLA (with notched impact strength higher than 20-30 $kJ.m^{-2}$). The use of functionalized polyesters bearing epoxide groups is also a promising alternative to the toughening of PLLA.

Concerning the block copolymers developed in chapter 3, a synthesis adapted to industrial processes is an interesting perspective to lower the production cost of these materials. They could also be used as third components in blends of PLLA with poly(ricinoleic acid) (PRic). Preliminary results concerning binary blends of PLLA with PRic showed encouraging impact strength values (6.3 $kJ.m^{-2}$ with only 10wt% of PRic). Addition of block copolymers should improve the impact strength by enhancing the interfacial adhesion between the two phases.

In summary, this thesis work showed preliminary encouraging results and open new pathways concerning the use of fatty acid-based polyesters as impact modifiers for PLLA.

MATERIALS AND METHODS

1. MATERIALS

Methyl 10-undecenoate (UndME) (>98.0%), 10-undecenoic acid (98%), 2-mercaptoethanol (MCET, 98%), 1,4-diaminobutane (99%) and dianhydro-D-glucitol (isosorbide, >98%) were supplied by TCI, Europe.

1,5,7-triazabicyclo[4.4.0]dec-5-ene (TBD, 98%), 1,3-aminopropanol (99%), azobisisobutyronitrile (AIBN, 98%), triethylamine (99%), ethyl chloroformate (97%), sodium azide (99.99%), calcium hydride (95%), Grubbs 1st generation catalyst (C1), Grubbs 2nd generation catalyst (C2), Hoveyda-Grubbs 1st generation catalyst (C3), Hoveyda-Grubbs 2nd generation catalyst (C4), dimethyl carbonate (99%), 4-toluenesulfonyl chloride (>99%), 11-bromo-1-undecene (95%), zinc dust (98%), 10-undecenoyl chloride (>97%), N-Methyl-2-pyrrolidone (NMP), Titanium tetra-n-butoxide (99%), tin octoate (95%), titanium isopropoxide (99.9%), 1,10-decanediol (98.0%), 1,12-dodecanediol (99%), Palladium on charcoal and L-lactide (98%) were obtained from Sigma-Aldrich. L-lactide was recrystallized in toluene to remove impurities and dried overnight under vacuum prior to reaction.

1,3-propanediol (99%), 10-undecenol (99%) 1,4-benzoquinone (98%), dibutyltin dilaurate (DBTDL, 95%) and Sebacic acid (SA) (98.0%) were purchased from Alfa Aesar.

12-hydroxy stearic acid (99%) was purchased from Nu-chek prep.

Hydrogenated Dimer Fatty Acid (DFA) (Pripol 1009®) and Methyl Ricinoleate (85%) were kindly provided by ITERG (Pessac-France). Methyl Ricinoleate was purified by column chromatography using a mixture of cyclohexane/acetone (v/v: 95/5) permitting to reach 98% purity by GC.

Methyl-5-(dimethylamino)-2-methyl-5-oxopentanoate (polarclean®) was kindly provided by Rhodia. Polarclean® was dried over CaH_2 and cryodistilled prior to use.

Poly(L-lactide) (PLA) was kindly provided by PURAC (Netherlands)($\overline{M}_n$= 121 kg.mol^{-1}, Đ= 1.5 as determined by size-exclusion chromatography in THF).

2. METHODS

2.1. Nuclear Magnetic Resonance (NMR) analysis

All NMR experiments were performed at 298 K in $CDCl_3$ on a Bruker Avance I NMR spectrometer operating at 400MHz and equipped with a Bruker multinuclear z-gradient direct probe head capable of producing gradients in the z direction with strength 53.5 G cm^{-1}.

2.2. Gas chromatography (GC)

The gas chromatography analyses (GC) were performed using a Shimadzu GC equipped with: Flame ionization detectors (FID, 380 °C) and Zebron ZB-5HT (5% phenyl - 95% dimethylpolysiloxane) 15 m x 0.25 mm ID, 0.1 µm thickness capillary column. The carrier gas was hydrogen. The temperature program of the column was initially set at 60 °C (volume injected: 1 µl), then increased to 370 °C at a rate of 10 °C.min^{-1} and held isothermally for 10 min.

2.3. Fourier Transformed Infra-Red-Attenuated Total Reflection (FTIR-ATR)

Infrared spectra were obtained on a Bruker-Tensor 27 spectrometer using the attenuated total reflection (ATR) mode. The spectra were acquired using 16 scans at a resolution of 4 wavenumbers.

2.4. Size exclusion chromatography (SEC)

Size exclusion chromatography (SEC) analyses were performed in THF (40°C) on a PL-GPC 50 plus Integrated GPC from Polymer laboratories-Varian with a series of four columns from TOSOH (TSKgel TOSOH: HXL-L (guard column 6.0mm ID x 4.0cm L); G4000HXL (7.8mm ID x 30.0cm L) ;G3000HXL (7.8mm ID x 30.0cm L) and G2000HXL (7.8mm ID x 30.0cm L)). The elution of the filtered samples was monitored using simultaneous refractive index and UV detection. The elution times were converted to molar mass using a calibration curve based on low dispersity (M_w/M_n) polystyrene (PS) standards.

2.5. Differential Scanning Calorimetry (DSC)

Non-Isothermal crystallization

Differential scanning calorimetry (DSC) thermograms were measured using a DSC Q100 apparatus from TA instruments. Each sample was first melted for 3min at 200°C to remove previous thermal history. Non-isothermal crystallization behaviors were evaluated by cooling the samples from the melt. Measurement of the glass transition temperature (Tg), cold crystallization temperature (Tcc) and melting temperature (Tm) was then performed by heating the sample. The DSC program is specified in the manuscript for each experiment.

Isothermal crystallization

Isothermal crystallization investigation was performed by rapid cooling (50°C.min^{-1}) of the samples from the melt to a fixed temperature and by keeping the samples at this temperature for 30 min. The exothermic curves of heat flow as a function of time were recorded. The DSC program is also specified in the manuscript for each experiment.

2.6. Thermogravimetric analysis (TGA)

Thermogravimetric analyses (TGA) were performed on TGA-Q50 system from TA instruments at a heating rate of 10 °C.min^{-1} under nitrogen atmosphere.

2.7. Dynamic Mechanical Analysis (DMA)

The visco-elastic properties of the copolymers were recorded by a dynamic mechanical analyzer (DMA), a model RSA-III apparatus from TA Instruments equipped with a liquid nitrogen cooling system. Forced strain was used on a rectangular tensile geometry at a frequency of 1 Hz, a strain of 0.1% and a temperature range between -80 °C and T_m +15 °C at a rate of 5 °C.min^{-1}.

2.8. Optical miscroscopy

Optical images were obtained using an Axioskop 40 Zeiss polarizing microscope equipped with a digital camera (Canon Powershot A640) connected to the computer. The spherulite morphology was observed in thin films prepared between microscope coverslips

2.9. Atomic Force Microscopy (AFM)

AFM measurements were performed at room temperature using a Veeco Dimension Icon AFM system equipped with a Nanoscope V controller. Both topographic and phase images of sample films were obtained in Tapping Mode using a rectangular silicon cantilever (AC 160-TS, Atomic Force, Germany) with a spring constant of 26N m^{-1}, a resonance frequency lying in the 270-320 kHz range and a radius of curvature of less than 10 nm. Samples were prepared by solvent casting at ambient temperature from dilute solutions in dichloromethane (10 wt %). Freshly cleaved mica pieces were placed in a spin-coating apparatus (G3P-8 Spin Coater, PI-Kem, UK) and excess solvent was removed by spinning for 300 s at an angular rotation of 500rpm.

2.10. Tensile tests

To determine the mechanical properties of the polymers, tensile stress and tensile strain were obtained using DMA apparatus in traction transient mode at a rate which is specified in the manuscript for each experiment. Tensile tests were performed on polymers processed into films using a simple hot-press technique. The effective length, width, and thickness of the specimens were generally 10, 2.5, and 0.5 mm, respectively. Tensile tests were carried out after the processed specimens were let overnight at room temperature. An average value of seven replicated measurements was taken for each sample

2.11. Rheological measurements

The rheological properties of the blends in the molten state were assessed using a parallel-plate (d = 25 mm) rheometer (AR 2000 rheometer from TA instruments). The sample was loaded between the parallel plates and melted at 190 ° C for 3 min. The parallel plates subsequently compressed the sample to 1.000 mm thick prior to each test. A dynamic frequency sweep test was performed to determine the viscoelastic properties of the blends. The strain and frequency range used during testing were 5% and 500–0.05 $rad.s^{-1}$, respectively. Complex viscosity (η^*), storage modulus (G'), and loss modulus (G'') in the molten state were obtained.

2.12. **X-Ray diffraction**

X-ray diffraction patterns were obtained with a microfocus rotating anode X-ray source (Rigaku MicroMax-007 HF) combined with multi-layer optics and a 3-pinhole collimation that provide an intense X-ray intensity on the sample. The sample, mounted on an X-Y stage, was held in a Lindemann capillary and placed in an oven providing a temperature control of 0.1 K. A 2-dimensional detector (Image plate from Mar Research) collected the scattered radiation. The sample-detector distance was 133mm and the calibration of this distance was performed using silver behenate as reference. Small-angle X-ray scattering (SAXS) experiments were performed using a Nanostar from Bruker. A 2-dimensional detector (HiStar from Bruker) was collected the scattered radiation. The SAXS intensities obtained were plotted against scattering vector $q = (4\pi/\lambda) \sin\theta$, where λ is the wavelength of the X-ray (λ = 0.154 nm) and 2θ is the scattering angle. In order to better distinguish the peaks at high q values, SAXS intensities were multiplied by q^4.

2.13. **Melt-blending**

Prior to extrusion, PLLA pellets were dried at least 12h at 80°C in an oven under reduced pressure. Melt-blending of the rubbers with PLLA was realized using a DSM twin-screw micro-compounder (5cc) at 190°C and 50 rpm for 5 minutes. Impact test bars (dimensions 12.7 × 50 × 3.2 mm) were prepared by injection molding at 200°C in a mold kept at 50°C.

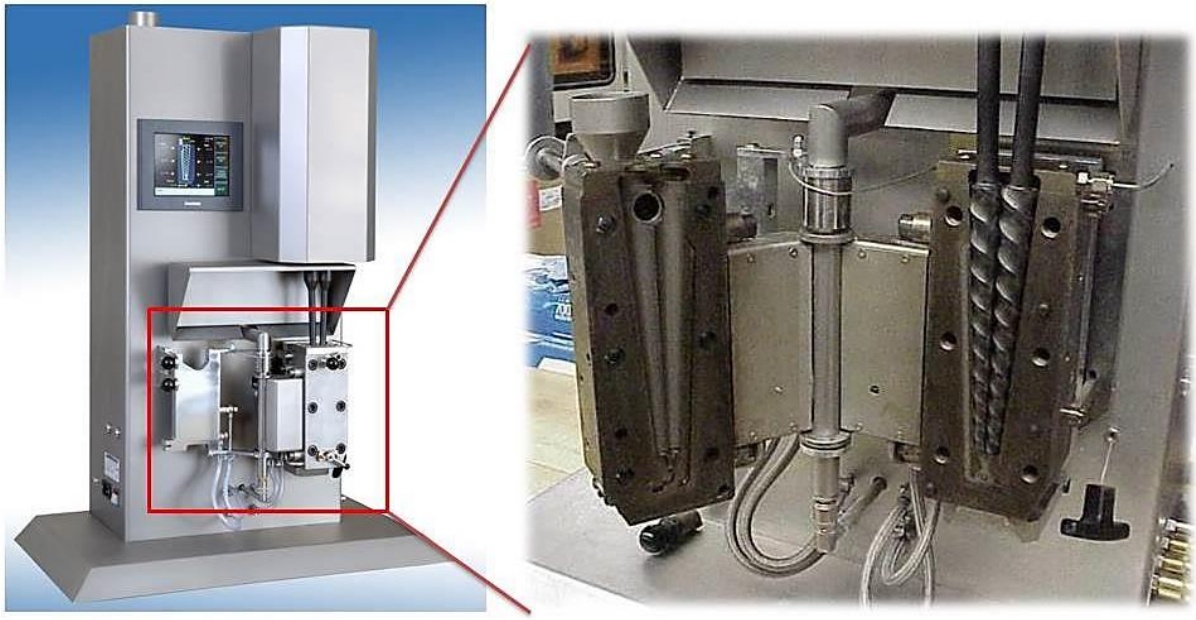

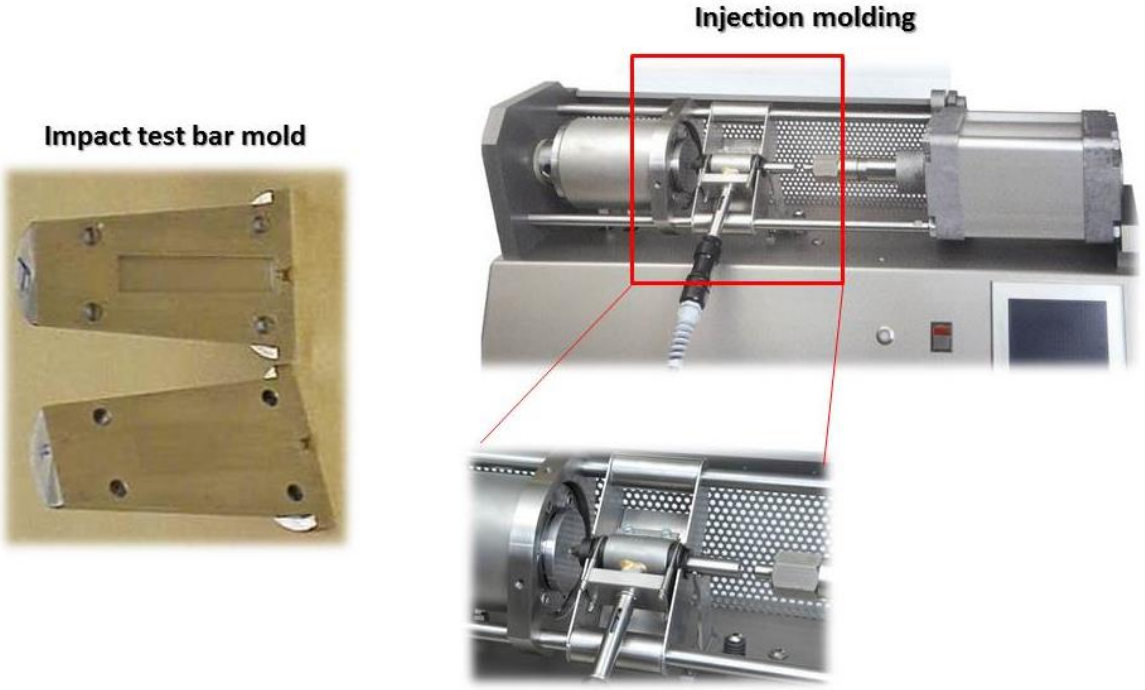

2.14. **Impact testing**

Notched Izod impact tests were performed according to ASTM D256 using an AIS multi impact XJF-5.5 pendulum impact tester.

Pendulum-type machines are used for notched or unnotched specimens that may be of different sizes and clamped as a cantilever (Izod) or as an unclamped bar supported at both ends (Charpy). These tests are also referred to as flexed-beam impact tests, and determine the resistance to breakage by flexural shock, in terms of the difference between the potential energy of the striker before and after impact. A mass is attached to the end of an arm that rotates about a pivot point; a striker is placed near this mass. The arm is raised to a predetermined position, and when released, swings downward and strikes the specimen, which is either supported at both ends or mounted rigidly in a vise or fixture. The precise mounting position and the type of fixture depends on the test. The mass, length of the arm, and angle at the raised position determine the amount of available energy, which must be high enough to give a clean break. After the striker breaks the sample at the bottom of its swing, it continues to swing upward until all the kinetic energy is exhausted. From the height it reaches after impacting the sample, energy expended per unit area can be calculated via either a calibrated dial mounted in the plane of rotation, or through a transducer mounted on the striker or on the mounting block to which the specimen vise is attached. Maximum pendulum velocities (impact speeds) are 300-400 cm/sec.

The notched Izod test is frequently used to determine crack propagation resistance. The test utilizes a cantilever-mounted bar or beam specimen, firmly clamped in a vertical position, with a horizontal notch cut on the side facing the striker, which impacts the sample just above the notch. The material at the tip of the notch is subjected to a highly amplified state of triaxial stress. Farther away from the notch the stress state is one of plane, or biaxial stress, and eventually, if the bar is wide enough, uniaxial tension. It is because of this triaxial stress state that notched Izod test samples usually fail in a brittle manner.

The notched Charpy test utilizes a bar or beam specimen mounted horizontally on a span support, with a vertical notch cut on the side opposite the striker-impact side, and struck centrally by the pendulum, behind the notch. Sample and notch specifications for both tests are given in ASTM test method D256.

2.15. **Scanning Electronic Microscopy (SEM)**

Blend morphologies were observed under scanning electronic microscopy (SEM) analyses on a JEOL JSM 2500 apparatus. Observations were carried out both on cryo-fractures surface or impact-fractures surfaces. The samples were metallized with gold prior to observation.

RESUME:

Dans cette étude, plusieurs voies ont été explorées dans l'objectif d'utiliser des polyesters aliphatiques issus de ressources oléagineuses comme additifs pour le renfort au choc du poly(L-lactide) (PLLA).

Dans un premier temps, des poly(ester-amide)s (PEAs) ont été synthétisés à partir de dérivés de l'huile de ricin. La relation structure-propriétés des PEAs obtenus a été clairement établie. La dispersion des PEAs (à différents taux) par extrusion à l'état fondu dans une matrice de PLLA a ensuite été effectuée, démontrant un accroissement de la résilience de ces mélanges en comparaison au PLLA seul.

Une étude systématique reliant la structure d'une large gamme de polyesters aux propriétés des mélanges polyesters/PLLA, a ensuite été réalisée. Une forte dépendance de la résilience des mélanges polyesters/PLLA avec la cristallinité de l'additif polyester a été observée et quantifiée.

Une amélioration des propriétés mécaniques du PLLA a également été obtenue par polymérisation par ouverture de cycle du lactide amorcée par un poly(acide ricinoléique) di-hydroxy téléchélique. Les copolymères triblocs ainsi formés ont été caractérisés d'un point de vue morphologique et mécanique.

Enfin, un travail exploratoire utilisant l'ADMET comme méthode de polymérisation a été conduit, permettant la synthèse de nouveaux polymères prometteurs pour le renfort au choc du PLLA. Notamment, la copolymérisation de α,ω-diènes bio-sourcés a permis de mimer le polyéthylène basse densité linéaire, couramment employé pour le renfort au choc du PLLA.

Mots-clés : Poly(L-lactide), renfort au choc, copolymère à blocs, polycondensation, polymérisation par ouverture de cycle, ADMET, huiles végétales, acides gras, poly(ester-amide), polyester.

SUMMARY:

The objective of this thesis work, is to promote the use of fatty acid-based aliphatic polyesters as impact modifiers for poly(L-lactide) (PLLA).

Firstly, poly(ester-amide)s (PEAs) have been synthesized from castor oil derivatives. The structure-properties relationship of the PEAs so-formed was clearly established. The PEAs were then melt-blended with PLLA by extrusion, yielding blends with improved impact strength compared to neat PLLA.

A series of polyesters covering a wide range of thermo-mechanical properties was then employed to evaluate the influence of the polyester morphology on the properties of the blends with PLLA. A strong dependence of the impact strength of the blends was noticed with the crystallinity degree of the polyester additive.

An improvement of the mechanical properties of PLLA was also obtained by ring-opening polymerization of lactide initiated by a di-hydroxy telechelic poly(ricinoleic acid). The so-formed triblock copolymers were fully characterized in terms of morphology and mechanical properties.

Finally, an exploratory investigation related to the synthesis of PLLA impact modifiers by ADMET was carried out. Particularly, the copolymerization of two bio-based α,ω-dienes yielded a series of "LLDPE like" polyesters, LLDPE being a commonly used impact modifier for PLLA.

Keywords : Poly(L-lactide), rubber-toughening, block copolymer, polycondensation, ring-opening polymerization, ADMET, plant oils, fatty acids, poly(ester-amide), polyester.

Laboratoire de Chimie des Polymères Organiques
16 Avenue Pey-Berland
F-33607 Pessac
LCPO